Genetic Analysis of Two Structure-specific Endonucleases Hef and Fen1 in Archaeon *Haloferax volcanii*

Zhenhong Duan, MSc.

Thesis submitted to the University of Nottingham
for the degree of Doctor of Philosophy,
September 2008

Table of Contents

Abstract

Nucleotide excision repair (NER) is a versatile pathway of DNA repair that deals with a variety of DNA lesions, such as UV-induced DNA damage and interstrand crosslinks. In bacteria, the UvrABC system carries out NER. In human cells, XPF and XPG are two structure-specific endonucleases that act in NER. XPF is responsible for a 5' incision at the DNA lesion and XPG carries out the 3' incision. In Archaea, the third domain of life, most species have homologues of some eukaryal NER proteins. Interestingly, *Haloferax volcanii* encodes homologues of both the eukaryotic NER genes (*XPF*, *XPG*, *XPB* and *XPD*) and bacterial NER genes (*uvrA*, *uvrB*, *uvrC* and *uvrD*). In this study, the function of XPG, XPF and UvrA in *H. volcanii* is investigated.

XPG is related to FEN1, a structure-specific 5' flap endonuclease that acts in Okazaki fragment maturation. *H. volcanii* has a single gene homologous to both *XPG* and *FEN1*. The helicase/nuclease *hef* gene in *H. volcanii* is the archaeal homologue of human *XPF*, but also shows homology to Mus81 and FANCM. Mus81 has been found to resolve joint molecules in yeast, while FANCM is required for the repair of interstrand crosslinks in vertebrates. The *uvrA* gene in *H. volcanii* is the archaeal homologue of bacterial *uvrA*, which encodes a protein that plays a vital role in NER at the DNA damage recognition step.

This study demonstrates that in *H. volcanii*, UvrA is involved in the major pathway for repair of UV induced DNA damage. By contrast, Hef and UvrA are involved in two different pathways for the repair of mitomycin C induced DNA crosslinks. Fen1 and Hef have overlapping functions for the repair of DNA cross-links, but not oxidative damage. We also obtain a spontaneous suppressor *sfnA*, which can suppress the slow growth and MMC sensitivity, but not the UV sensitivity of *fen1* deletion mutants.

Using plasmid assays, it has been shown that the *hef* deletion mutant is deficient in accurate end-joining and homologous recombination, including both crossover and non-crossover recombination. In contrast, Fen1 has no significant role in accurate end-joining, but Fen1 may regulate the ratio of non-crossover recombination to crossover recombination.

Acknowledgements

First of all, I would like to thank Thorsten Allers for accepting my application to be a PhD student under his supervision and helping me to get scholarship. I would especially like to thank him for his politeness, patience, wisdom and support. He has always pointed me in the right direction at the right time. I feel so lucky to be his student.

Thank you to Lee, Sam, Michelle, Amy, Ed, Colin, and to the other members of the lab for their advice, assistance, and for making my time studying a pleasure. I would especially like to thank Stéphane and Bob, for their intriguing discussions and helpful suggestions.

I would like to thank my parents and sister for their generous support and encouragement. I always have their support, whenever I face difficulties and feel weak. They are really happy for my happiness. I have to mention my cute niece for her innocent love. I would also like to thank Paul's family for making me feel pampered all the time.

Finally, I would especially like to thank Paul for his love, patience, encouragement and generosity. I cannot imagine life without him, and without him I would not have been able to adapt to the environment so quickly and enjoy my life so much in a country with a culture so different from that of China. He leads my hands to explore a wonderful world beyond academic life. Maybe there is something called fate. I feel really lucky to meet Paul and look forward to the story "forever" with him.

Chapter I: Introduction

1.1 Archaea–the Third Domain

In the late 1970s an entirely new group of organisms - the archaea were recognised as a unique phylogenetic lineage based on 16S rRNA sequence analysis (Woese and Fox, 1977). Later, Archaea were assigned to be the third fundamental domain of life, in addition to Bacteria and Eukarya (Woese et al., 1990). In the last decade, the theory has been validated by comparative genomics as more and more DNA sequences of genomes become available.

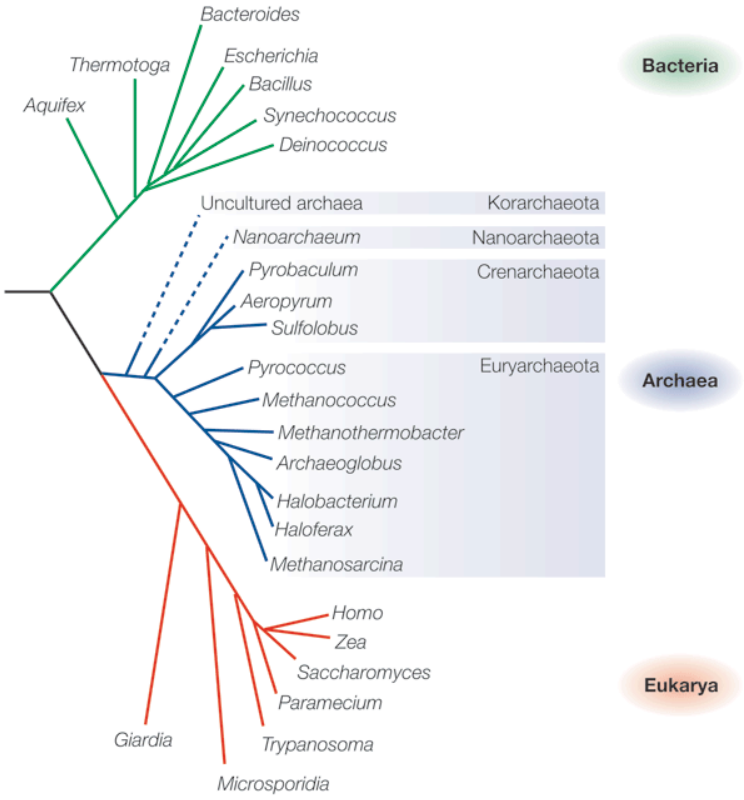

Figure 1.1 Archaeal taxonomy.

The rRNA tree reveals that the domain of Archaea comprises several phyla. Euryarchaeota is the most diverse group, including all known methanogens, halophiles and psychrophilic species, which can grow at permanently low temperatures, typically less than 10˚C. Members of Crenarchaeota are renowned as hyperthermophiles, but include the psychrophile *Crenarchaeum symbiosum.* Naoarchaeota has only one known member and Korarchaeota are identified only by environmental DNA sequences. Due to the paucity of identified species, the positions of Naoarchaeota and Korarchaeota on the rRNA tree are uncertain and indicated by dashed branches (Allers and Mevarech, 2005).

The archaeal domain is split into four kingdom-level phyla (Allers and Mevarech, 2005; Gribaldo and Brochier-Armanet, 2006): the Euryarchaeota, which contain the methanogenic and the halophilic archaea as well as the *Archaeoglobus* and *Pyrococcus* groups; the Crenarchaeota, which are dominated by thermophilic organisms such as *Sulfolobus* and *Thermoproteus*; the Korarchaeota, which have only been identified by environmental sequences but not cultured (Barns et al., 1996); and the Nanoarchaeota, of which only one example *Nanoarchaeum equitans* is known (Hohn et al., 2002; Huber et al., 2002). *N. equitans* harbors the smallest cellular genome presently known (480 kb). This hyperthermophile grows and divides at the surface of crenarchaeal *Ignicoccus* species and cannot be sultivated independently, indicating an obligate symbiotic, and possibly parasitic, life style. Recently, a group of mesophilic archaea has been proposed to be another phylum the Thaumarchaeota, based on the analysis of rRNA sequences, ribosomal proteins and genome sequence of *Cenarchaeum symbiosum* (Brochier-Armanet et al., 2008).

Archaea were initially renowned for being able to flourish and predominate in extreme environments, such as hot springs, salt lakes and submarine volcanic vents. This is true for high-temperature environments, since only archaea can thrive at temperatures above 95˚C and up to 113˚C (Huber et al., 2000). However, it is now clear that archaea are ubiquitous and constitute a significant portion of the global biomass (DeLong and Pace, 2001; Rothschild and Mancinelli, 2001).

Archaea have an unusual combination of bacterial and eukaryotic features. Morphologically they seem like bacteria, being unicellular and having circular chromosomes, but no defined nucleus. Archaea also have polycistronic transcription units and mostly have the Shine-Dalgarno sequences for the initiation of translation (Londei, 2005). With respect to metabolic enzymes such as those involved in energy production (Oren, 1999), nitrogen fixation (Belay et al., 1984) and polysaccharide synthesis (Moens and Vanderleyden, 1997), archaea are more closely related to bacteria than eukaryotes. Conversely, processes related to DNA replication, transcription and repair in archaea are more closely related to those of eukaryotes (Myllykallio et al., 2000; Bell and Jackson, 2001; Grabowski and Kelman, 2003).

Like bacteria, some archaea such as *Pyrococcus abyssi* have a single replication origin (*oriC*) (Myllykallio et al., 2000). Other archaea, more like eukaryotes, have multiple replication origins, for example, *Sulfolobus solfataricus*, and *H. volcanii* (Lundgren et al., 2004; Robinson et al., 2004; Norais et al., 2007a). Most strikingly, archaeal genomes encode homologues of almost all eukaryal DNA replication proteins such as archaeal/eukaryal primases (Lao-Sirieix et al., 2005), helicases and replicative

polymerases (Olsen and Woese, 1996; Forterre and Philippe, 1999; Leipe et al., 1999). The eukaryotic-like putative replication proteins identified in archaeal genomes are most likely involved in actual archaeal DNA replication, as indicated by the observation of direct interaction *in vivo* between the chromosomal origin (*oriC*) and the putative initiator protein Cdc6, which is homologous to both a subunit (Orc1) of eukaryotic ORC (origin recognition complex) and the helicase loader Cdc6 (Matsunaga et al., 2001). In addition, the size of Okazaki fragments found in archaea are approximately 100 nucleotides in length, which are similar to those of eukaryotes (Matsunaga et al., 2003).

Both positive and negative bacterial regulators of transcription have been identified and characterized in archaea (Ouhammouch, 2004). However, the central core components of the archaeal transcription machinery closely resemble those of eukaryotic RNA polymerase II (Kyrpides and Ouzounis, 1999; Kusser et al., 2008). In addition, although archaea also have small genomes like bacteria, archaea have histones and other nucleoid-organizing proteins that are involved in global aspects of transcriptional regulation, reminiscent of the transcription regulation in eukaryotes (Reeve, 2003; White, 2003).

Despite the similarities to both bacteria and eukaryotes, archaea also have some exclusive features, not present in either of the other two domains. The prime example of this is that their cell membranes have ether-linked isoprenoid lipids, rather than the fatty acid ester lipids composed in both bacteria and eukaryotes (Kates, 1993; van de Vossenberg et al., 1998). The absence of peptidoglycan cell walls has also been observed in archaea (Kandler and Konig, 1978). More importantly, around 40-50% of archaeal genes have no apparent homologue in the other two domains (Allers and Mevarech, 2005). Adaptation of some archaea to extreme environments necessarily requires unique proteins and enzymes that are stable under such conditions. The enzymes from extremophiles are now exploited as a source of high quality structure data (Ban et al., 2000; Shin et al., 2003; Gaudier et al., 2007). The application of archaeal enzymes is not limited to scientific research. One successful commercial example is the utilization of thermostable enzymes for DNA amplification by PCR, which are familiar to most scientists. While methane production by methanogenic archaea (all significant biological methane producers are Archaea) is relevant to the problem of global warming and production of fuel from biomaterials (Chapelle et al., 2002), which are hot topics in popular science as well as academic research.

Archaea have attracted great interests since the tripartite division of the living world. However, our knowledge about archaea has lagged far behind that of bacteria and eukaryotes. There are a variety of reasons, beginning with the fact that limited archaeal

species have been isolated and cultured in the laboratory. Another main problem is the lack of genetic techniques in the past. Therefore, great effort has been put into this field in the past thirty years. As a result, genetic systems have been developed for some thermophlic, methanogenic and halophilic archaea, including efficient transformation, shuttle vectors, multiple resistance markers and reporter gene systems (Allers and Mevarech, 2005; Rother and Metcalf, 2005; Soppa, 2006). Genetic tools applied to the study of archaea may reveal the fundamental differences and links between the three domains, complementing our knowledge of the whole living world.

1.2 *Haloferax volcanii*– a Model Organism for Archaeal Genetic Study

Haloferax volcanii was isolated from the Dead Sea (Mullakhanbhai and Larsen, 1975). It grows aerobically at 30-50˚C in medium containing 20% NaCl. *H. volcanii* has a multireplicon genome structure (a main chromosome of 2.9 Mb and four smaller replicons, including pHV1 86 kb, pHV2 6.4kb, pHV3 442 kb and pHV4 690 kb) with a G+C content of approximately 65% (Charlebois et al., 1991).

Compared to the strictly anaerobic requirement for methanogens and the extreme temperature requirement for themophiles in the laboratory, *H. volcanii* grows with ease in both complex and minimal media, either solid or liquid, in the laboratory (Mevarech and Werczberger, 1985). With a generation time of approximately 3 hr, they grow fast enough that they can be effectively studied.

H. volcanii is particularly suitable for genetic analysis in archaea as tools for its genetic manipulation are well developed. *H. volcanii* cells can be easily transformed with the use of PEG600 (Cline et al., 1989). Integrating and shuttle plasmid vectors are available (Allers and Mevarech, 2005; Soppa, 2006), with a number of antibiotic and auxotrophic selective markers (Allers and Mevarech, 2005). Recently, halophilic β-galactosidase genes have been developed as reporter genes. The expression of these genes can be easily identified by the blue color of the colonies in the presence of X-gal, as *H. volcanii* lacks the activity of β-galactosidase and produces a characteristic pink pigment in the laboratory (Holmes and Dyall-Smith, 2000a; Large et al., 2007). Constitutive and inducible promoters are also available (Gregor and Pfeifer, 2005; Large et al., 2007). More importantly, methods for constructing gene knockout mutants have been established and are developing quickly as more markers and promoters become available (Bitan-Banin et al., 2003; Allers et al., 2004; Allers and Mevarech, 2005; Large et al., 2007). Recently, a tryptophan inducible promoter has been successfully used in the analysis of one essential gene in *H. volcanii* (Large et al., 2007). More powerful genetic tools are promising by the application of this tightly controlled

promoter (See Chapter VII). In addition, sequencing of the genome is largely completed at TIGR (the Institute of Genome Research), with full annotation expected in the near future (Hartman *et al*, manuscript in preparation).

The natural habitat of *H. volcanii* is characterized by extremely high ionic strength, up to saturated salt water, by elevated temperature and by high levels of UV radiation (sunlight). All these features lead to DNA damage (Potts, 1994; Martin et al., 2000), while *H. volcanii* is an obligate halophile and thrives in such extreme conditions (Mullakhanbhai and Larsen, 1975). Therefore, *H. volcanii* must have effective DNA repair systems. These are the main interest of this project. The next few sections consist of a literature review of the current knowledge of major DNA repair pathways, mainly from the studies in bacteria and eukaryotes. DNA repair is commonly divided into five major pathways: direct damage reversal, nucleotide excision repair, base excision repair, mismatch repair and double strand break repair. Each pathway deals with specific types of lesion, except for some overlap.

1.3 Direct damage reversal

Direct damage reversal is the simplest method of preventing mutations. The best-studied method of damage reversal is photoreversal of cyclobutane pyrimidine dimers by the enzyme, CPD photolyase (Heelis et al., 1993). The reaction catalyzed by CPD photolyase, called 'photoreactivation', was the first DNA repair process to be discovered in bacteriophage in 1949. CPD photolyase contains two chromophores, which absorb light energy. This energy is used to split pyrimidine dimers.

Another example of direct damage reversal is performed by O^6-methylguanine-DNA methyltransferase (MGMT) (Drablos et al., 2004). The methyl group from the lesion is transferred to a specific cysteine residue within the methyltransferase itself (Daniels et al., 2004). Once the alkyl group has been transferred to the enzyme, the protein is permanently inactivated. Silencing of the human gene encoding this protein leads to elevated mutation frequency and increased susceptibility to cancer (Liu and Gerson, 2006; Mishina et al., 2006).

A third example is DNA dioxygenase AlkB in *E. coli* and its functional human homologues ABH2 and ABH3 (Duncan et al., 2002; Aas et al., 2003; Sedgwick, 2004). These enzymes are capable of release the methyl moiety as formadehyde, derectly reversing the damaged bases 1-methyladenine (1meA) and 3-methylcytosine (3meC) (Sedgwick et al., 2007).

1.4 Nucleotide Excision Repair

Nucleotide excision repair (NER) is a versatile pathway that deals with a variety of structurely unrelated lesions. NER repairs lesions that distort the DNA helix, interfere with base pairing and crosslink DNA double strands (Friedberg et al., 1995a; Costa et al., 2003). The impact of deficiencies in NER on human health has been best manifested by the existence of rare recessive human disorders, for example, xeroderma pigmentosum (XP), Cockayne's syndrome (CS) and trichothiodystrophy (TTD). Clinical features of these genetic disorders vary considerably, but the one common feature is a UV hypersensitivity phenotype (de Boer and Hoeijmakers, 2000; Lehmann, 2003).

NER works through a "cut and patch" mechanism by excising and removing a short stretch of nucleotides containing the lesion and subsequently filling the gap using the non-damaged strand as a template (Gillette et al., 2006). In both bacteria and eukaryotes, NER begins with the recognition of DNA damage, which is performed by two mechanisms, a global genome repair and a transcription coupled repair (Costa et al., 2003).

1.4.1 Global Genome Repair

Global genome repair (GGR) recognises DNA lesions throughout the genome, but its repair efficiency varies across the genome and is most likely influenced by chromatin environment (Van Houten et al., 2005; Gillette et al., 2006). Early studies in *E. coli* showed that cyclobutane pyrimidine dimers are repaired more slowly than 6-4 photoproducts, which cause greater helical distortion, even though the former occurs more frequently after UV irradiation (Van Houten, 1990). Using abasic (AP) sites with different modification as substrates, Van Houten and Snowden demonstrated that the larger the chemical substituents on the DNA, the higher the rate and extent of incision by the complete UvrABC nuclease system (Van Houten and Snowden, 1993). Studies by Hoare, using aromatic hydrocarbons further confirmed that the size of the chemical moiety greatly affected the extent and rate of incision (Hoare et al., 2000). In addition, Geacintov and his colleagues showed that the incision of the same DNA adduct varied depending on sequence context (Geacintov et al., 2002). Thus, both DNA modification and distortions to the duplex DNA structure are implied to affect damage recognition and incision.

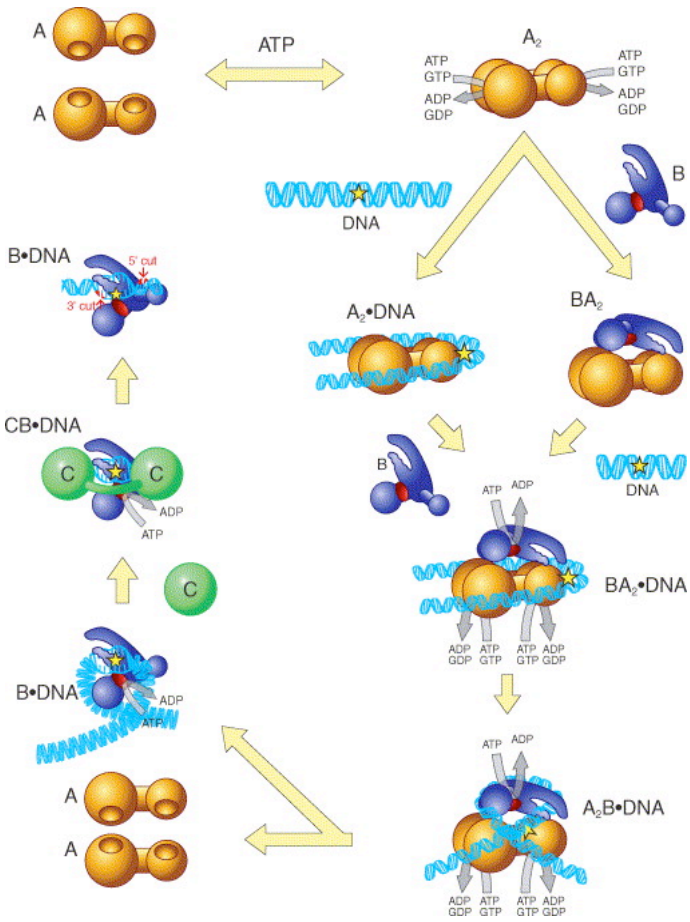

Figure 1.2 A model of UvrABC system in *E. coli*.

In solution, two molecules of UvrA form a dimer. The $UvrA_2$ complex possesses ATP/GTPase activity. UvrB can interact with this $UvrA_2$ dimer in solution or on DNA, creating the $UvrA_2B$ complex. Upon binding to DNA, the $UvrA_2B$:DNA complex undergoes conformational changes. The lesion remains in close contact with UvrA and then it is transferred to UvrB. UvrB is endowed with a cryptic ATPase activity (the red nodule on UvrB) that is activated in the context of $UvrA_2B$:DNA. In this complex, the DNA is unwound around the site of the lesion because UvrB has inserted its β-hairpin structure between the two strands of the DNA to facilitate damage verification. The DNA is also wrapped around UvrB. The UvrA molecules hydrolyze ATP and dissociate from the complex, thereby creating a stable UvrB:DNA complex. UvrC recognizes this UvrB:DNA complex. Before UvrC can make the 3' incision, UvrB must bind ATP, but not hydrolyze it. After the 3′ incision is generated, a second incision event on the 5' side of the DNA lesion is produced; thus, UvrC forms a dual incision approximately twelve nucleotides apart. After the incision events, the DNA remains stably bound to UvrB until UvrD, DNA pol I and ligase perform the repair synthesis reaction (Van Houten et al., 2005).

In *E. coli*, the UvrABC nuclease initiates GGR through a series of integrated steps, which culminate in cleavage of the damage-containing strand at two discrete sites (Van Houten et al., 2005). The UvrA protein forms a dimer that interacts with UvrB to form a heterotrimeric protein complex, $UvrA_2B$. Within this complex, UvrA initiates contact with the DNA and then load UvrB onto the damaged DNA site (DellaVecchia et al., 2004). The cryptic ATPase activity of UvrB is activated in the context of the UvrAB:DNA complex and is required for damage verification (Orren and Sancar, 1990). The interaction of $UvrA_2B$ with the lesion causes unwinding, denaturing and opening of the local DNA duplex at the lesion (Zou and Van Houten, 1999). The

conformational change leads to the self-dissociation of $UvrA_2$ with ATP hydrolysis and formation of a stable pre-incision UvrB–DNA complex (Oh and Grossman, 1986; Shi et al., 1992). After the release of UvrA, the UvrC protein interacts with the C-terminus of UvrB in the UvrB–DNA intermediate. Some research showed that this interaction would trigger an endonuclease activity in UvrB, which cleaves a phosphodiester bond four to seven bases 3' to the damage (Lin et al., 1992). Mutagenesis, biochemistry and structure studies have shown that UvrC catalyzes the sequential incisions with the first incision four-phosphodiester bonds 3' to the lesion, and the second, eight-phosphodiester bonds away from the DNA on the 5' side. Each of these incision reactions is performed by a distinct catalytic site, which can be inactivated independently (Lin and Sancar, 1992; Verhoeven et al., 2000). In addition, Cho (UvrC homologue), encoded by the SOS-inducible gene *ydjQ*, can incise the DNA at the 3' side of a lesion (Moolenaar et al., 2002). It has been suggested that most of the lesions in *E. coli* are initially repaired by UvrC alone, while the remaining damages that obstruct the 3' incisiong by UvrC will be repaired by the combined action of Cho (for 3' incision) and UvrC (for 5' incision). Following incision, DNA helicase II (UvrD) is required to release UvrC and the incised oligonucleotide, while DNA polymerase I is thought to remove UvrB from the non-damaged DNA strand during the repair synthesis (Caron et al., 1985; Husain et al., 1985). Finally DNA ligase joins the two ends of the nick, thus completing the NER pathway (Truglio et al., 2006).

In human cells, the UV-DDB (UV-damaged DNA binding protein, which is a heterodimeric protein with a small subunit encoded by the XPE/DDB2 gene) (Batty and Wood, 2000; Tang and Chu, 2002) and XPC-hHR23B complex are responsible for lesion recognition in GGR and act to recruit TFIIH, a multi protein complex containing XPB and XPD helicases, to the repair complex (Evans et al., 1997b). XPB and XPD carry out DNA dependent ATPase and helicase functions and have complementary activities: XPB unwinds the DNA in the 3'-5' direction, while XPD unwinds in the opposite direction (Weber et al., 1990; Drapkin et al., 1994). The combined action of XPC-hHR23B and TFIIH creates short stretches of single stranded DNA around the lesion that facilitates the recruitment of XPA and single strand DNA binding protein RPA to subsequently verify the damage, preventing gratuitous repair by aberrant NER complexes formed on undamaged DNA (Missura et al., 2001). XPG is also required for the full open-complex formation (Evans et al., 1997a). Once the preincision complex has formed, structure-specific endonucleases XPG and XPF-ERCC1 carry out the 3' incision and the 5' incision asymmetrically around the lesion, resulting in excision of 24-32-mer oligonucleotide containing the damage (Mu et al., 1996). PCNA and RFC arrival requires XPF 5' incision. Moreover, the positioning of RFC is facilitated by RPA

and induces XPF release. Concomitantly, XPG leads to PCNA recruitment and stabilization (Mocquet et al., 2008). Presumably, after the removal of oligonucleotide, PCNA is loaded onto DNA by RFC, as is the case in DNA replication (Kelman, 1997). XPG and RPA are released, as soon as Polδ is recruited by the RFC/PCNA complex (Mocquet et al., 2008). DNA polymerase δ or ε are capable of DNA repair synthesis across the gap using the undamaged strand as a template. The remaining nick can be sealed by DNA Ligase I and FEN1 (Mocquet et al., 2008). Recent research suggests that the XRCC1-Ligase III complex as the principal ligase involved in the ligation step of NER throughout the cell cycle in addition to DNA Ligase I that is mainly engaged in NER during the S phase (Moser et al., 2007).

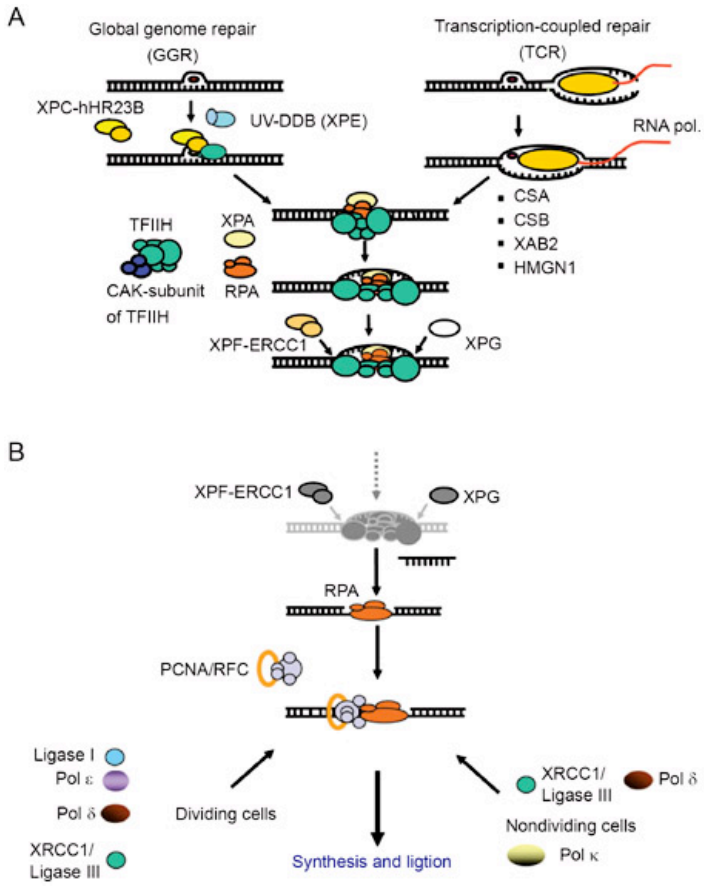

Figure 1.3 Two subpathways of mammalian NER.

(A) 1. Damage/distortion recognition in GGR and TCR. XPC-RAD23B and UV-DDB complexes recognize and bind to DNA damage-mediated helix distortion and initiate GGR. TCR is triggered by DNA damage-mediated blockage of RNAPIIo. 2. Lesion demarcation. In the next steps, the two sub-pathways converge. The lesion is verified and demarcated as a bona fide NER lesion by the concerted actions of helix opening and damage verification provided by TFIIH, XPA and RPA. 3. Dual incision. Within the pre-incision complex, ERCC1-XPF and XPG structure-specific endonucleases incise the damaged strand. (B) Gap filling and ligation. After dual incision around the lesion, the single strand gap is filled by DNA polymerase, PCNA and RFC, and sealed by DNA ligase III-XRCC1 in both dividing and non-dividing cells, whereas DNA polymerase and DNA ligase I are involved in dividing cells in addition to DNA polymerase and DNA ligase III-XRCC1. Although the involvement of these proteins has only been demonstrated for GG-NER, it is thought to hold for TC-NER as well (Fousteri and Mullenders, 2008).

Early studies identified a large number of yeast genes involved in NER (Reynolds and Friedberg, 1981; Wilcox and Prakash, 1981; Miller et al., 1982b; Miller et al., 1982a; Bankmann et al., 1992; Park et al., 1992)(Table 1.1). Homologues of all these genes, except for *RAD7*, *RAD16* and *MMS19* have been identified in humans. The Rad7-Rad16 complex displays a DNA-dependent ATPase activity and this activity is inhibited by the presence of UV damage in DNA. This observation has suggested a model in which the Rad7-Rad16 complex could track along DNA utilizing the energy from ATP hydrolysis, and inhibition of ATPase activity at the site of the DNA lesion would result in stable binding of the complex to the damage site. Thus the Rad7-Rad16 complex would be the first to arrive at the damage site in non-transcribed regions of the genome and the damage-bound Rad7-Rad16 complex would recruit other GGR proteins (Guzder et al., 1998). *MMS19* was initially identified in a screen for mutations that confer sensitivity to the alkylation agent MMS (Prakash and Prakash, 1977). Later a *mms19* mutant was also found to be sensitive to UV and DNA cross-linking agents with deficient removal of pyrimidine dimers and nicking of DNA containing interstrand cross-links (Prakash and Prakash, 1979). Thus, Mms19 also affects the initial step of NER.

	S. cerevisiae gene	Human gene	Biochemical activities
	RAD7	Not known	A DNA dependent ATPase binds UV-damaged DNA in an ATP dependent manner
	RAD16	Not known	
	RAD14	*XPA*	Damage binding protein
	RAD4	*XPC*	UV damaged DNA binding
	RAD23	*HR23B*	
TFIIH	*RAD3*	*XPD*	5' → 3' DNA helicase
TFIIH	*RAD25*	*XPB*	3' → 5' DNA helicase
TFIIH	*SSL1*	*P44*	-
TFIIH	*TFB1*	*P62*	-
TFIIH	*TFB2*	*P52*	-
TFIIH	*TFB3*	*MAT1*	-
	RAD1	*XPF*	Nuclease for 5' incision
	RAD10	*ERCC1*	
	RAD2	*XPG*	Nuclease for 3' incision
	MMS19	Not known	None detected
	RAD26	*CSB*	DNA dependent ATPase
	RAD28	*CSA*	-

Table 1.1 Budding yeast and human nucleotide excision repair proteins (Prakash and Prakash, 2000).

Mutations in human genes affect NER in a similar way to their homologous genes in yeast, except XPC, the human counterpart of yeast *RAD4*. Deletion of yeast *rad4* causes very high level of UV-sensitivity and *rad4* mutants are completely defective in incision (Reynolds and Friedberg, 1981; Wilcox and Prakash, 1981). By contrast, XPC is required for the repair of non-transcribed regions of the human genome but not for the repair of the transcribed DNA strand (Venema et al., 1990). Another difference between yeast and human NER is that both the Rad1-Rad10 endonuclease and the Rad2 endonuclease are indispensable for the incision reaction in yeast, while the human incision ensemble can generate normal levels of 3' incision in the absence of XPF-ERCC1 (Mu et al., 1996).

1.4.2 Transcription-Coupled Repair

The second mechanism of damage recognition in NER is through transcription-coupled repair (TCR) where DNA lesions are recognised during transcription. The outcome is that repair is faster in more frequently transcribed genes than in genes that are not transcribed often, and that DNA damage is preferentially repaired on the transcribed strand (Hanawalt, 2002; Fousteri and Mullenders, 2008).

In *E. coli*, a monomeric weak DNA independent ATPase encoded by the *mfd* (mutation frequency decline) gene is essential for TCR in UV-irradiated cells (Selby et al., 1991). The Mfd protein, also known as TRCF (transcription-repair coupling factor), recognises DNA damage during transcription of a damaged DNA molecule and releases the RNA polymerase, together with the truncated transcript, from the DNA in an ATP dependent manner. Subsequently, repair of the DNA damage is carried out by attracting NER factors particularly UvrA (Savery, 2007). In the yeast *S. cerevisiae*, TCR involves the Mfd counterpart encoded by the *rad26* gene (van Gool et al., 1994). Similar to the bacterial TCR, evidence has been presented in yeast that in some situations, a damage-arrested RNA polymerase might be released from the template by a mechanism that leads to its ubiquitylation and degradation (Woudstra et al., 2002).

In human cells, the hallmark of TCR is the accelerated repair of DNA lesions that efficiently block the elongating RNA polymerase II complex (RNAPIIo). For this repair, two proteins are required - CSA and CSB, named after the disease associated with defects in transcription coupled repair, Cockayne's syndrome (van Hoffen et al., 1993). CSB interacts with RNAPIIo and the interaction is stabilized by DNA damage (Tantin et al., 1997; van Gool et al., 1997). Upon UV-irradiation, CSA is recruited to RNA polymerase II in a CSB dependent way (Kamiuchi et al., 2002). All pre-incision NER core components are recruited to lesion-stalled RNAPIIo in a CSB-dependent manner (Fousteri et al., 2006). Incontrast to the release of RNA polymerase of TCR in

E. coli, the mammalian TCR complex is built up without the displacement of RNAPIIo (Tremeau-Bravard et al., 2004). Conformational change of RNAPIIo might be required to allow accessibility to repair proteins and such changes require the CSB protein (Tremeau-Bravard et al., 2004). Recent *in vitro* studies suggest that XPG might play an important role in the assembly of the TCR complex as XPG interacts with stalled RNAPIIo both independently and cooperatively with CSB (Sarker et al., 2005). Nonetheless in the context of chromatin, XPG appears to act downstream of CSB in TCR complex formation (Fousteri et al., 2006). *rad26* and *rad28* represent the yeast counterparts of *CSB* and *CSA*, respectively, and mutations in *rad26* (van Gool et al., 1994) but not *rad28* (Bhatia et al., 1996) affect TCR in yeast.

The NER in archaea is interesting because some species, mainly mesophilic methanogens and halophiles, have homologues for both the eukaryotic and bacterial NER genes (McCready and Marcello, 2003; White, 2003). It has been shown that dual incisions around UV-induced 6-4 photoproducts exist in *Methanobacterium thermoautotrophicum* by using its cell extract (Ogrunc et al., 1998). More recently, Crowley and colleagues found that the *uvrA*, *uvrB* and *uvrC* genes are required for the repair of UV induced DNA photoproducts in *Halobacterium sp. NRC-1*. However, the NER pathway is still not well defined in archaea.

1.5 Base Excision Repair

Base Excision Repair (BER), like NER, repairs DNA damage at the nucleotide level (Fortini et al., 2003). Unlike NER, however, BER is critical for the removal of oxidized and methylated bases from the DNA (David et al., 2007). The process of BER is essentially the same in eukaryotes and bacteria (Lindahl, 2001).

1.5.1 Glycosylase

As in all repair processes, the first step of BER is damage recognition. In the case of BER this is carried out by DNA glycosylases. Each glycosylase recognises certain types of lesion and then hydrolyses the *N*-glycosyl bond between the phosphate backbone and base, leaving an abasic or apurinic / apyrimidinic (AP) site. For example, 3-methyadenine-DNA glycosylases acts by recognising and subsequently removing methylated adenine from DNA (Karran et al., 1980) uracil-DNA glycosylases recognise and remove uracil, which is either incorporated mistakenly into DNA or has arisen through spontaneous cytosine deamination (Lindahl, 1974; Hatahet et al., 1994; Savva et al., 1995); PD-DNA glycosylase, often called UV-endonuclease, recognises pyrimidine dimers and cleaves the *N*-glycosylic bond of the 5' pyrimidine of the dimer (Hamilton et al., 1992).

1.5.2 AP Endonuclease and AP Lyase

Cells from all organisms possess strong AP endonuclease activities that cleave 5' to AP sites yielding single-stranded DNA breaks with 3'-OH and 5'-deoxyribosephosphate (5'-dRP) ends. Two major AP endonucleases have been identified in *E. coli*, exonuclease III (encoded by *xth*) and endonuclease IV (encoded by *nfo*) (Cunningham et al., 1986). Homologues of *xth* have been cloned from many different organisms, including yeast *PDEI*/*APN2* (Sander and Ramotar, 1997), *Drosophila Rrp1* (Gu et al., 1993) and human cells (*HAP*/*APE*) (Robson and Hickson, 1991), whereas the major yeast AP endonuclease Apn1 is an Nfo homologue (Popoff et al., 1990). Both classes of AP endonuclease possess 3'-phosphodiesterase and 3'- phospatase activities and some members of the Xth family also have strong 3'-5' exonuclease activity, for example *Drosophila* Rrp1 (Gu et al., 1993), *Streptococcus pneumoniae* ExoA (Puyet et al., 1989).

AP sites are also acted upon by AP lyases, which cleave 3' to the AP site by a β-elimination mechanism yielding SSBs with 3'-α, β-unsaturated aldehydic (3'-dRP) ends (Boiteux and Guillet, 2004). Such enzymatic activity is, in fact, associated with several of the DNA glycosylases, for example *E. coli* Fpg (Graves et al., 1992), human NTH1 (Prasad et al., 2007) and Nth1, Nth2 and ogg1 in yeast (Girard and Boiteux, 1997). 3'-dPR can be removed by the 3' phosphodiesterase activity of endonucleases (Johnson and Demple, 1988; Ramotar et al., 1991).

1.5.3 BER in Eukaryotes

In *S. cerevisiae*, genetic and biochemical data suggested a major role for Rad27 (homologue of human flap endonuclease 1 or FEN1) in the removal of the 5'-dRP (Wu and Wang, 1999), for Pol2 (Polε) in the DNA synthesis (Wang et al., 1993) and Cdc9 in the ligation step (Wu et al., 1999a).

In mammalian cells, there are two BER pathways (Krokan et al., 2000). In short-patch BER, AP endonuclease incises the DNA backbone 5' to the AP site. DNA polymerase beta (Polβ) catalyzes the excision of the 5'-dRP with its 5'-dRP lyase activity and fills in a single nucleotide gap using its DNA polymerase activity. The XRCC1-DNA ligaseIIIα (LigIIIα) complex then seals the nick, completing repair. In some cases, a bifunctional DNA glycosylase (glycosylase / AP lyase) removes the damaged base and incises the 3' to the AP site. Then AP endonuclease or another 3' repair diesterase removes the 3'-dRP to generate a 3'-OH group. Polβ fills in the gap and LigIIIα seals the nick. Long-patch BER is thought to have evolved to repair sites that are refractory to the dRP lyase activity of Polβ. This process results in a repair patch that is 2-12

nucleotides in length and involves other additional proteins including proliferating cell nuclear antigen (PCNA), replication factor C (RFC), flap endonuclease 1 (FEN1), the replication polymerases delta and epsilon (Polδ and ε), and DNA ligase I (LIGI).

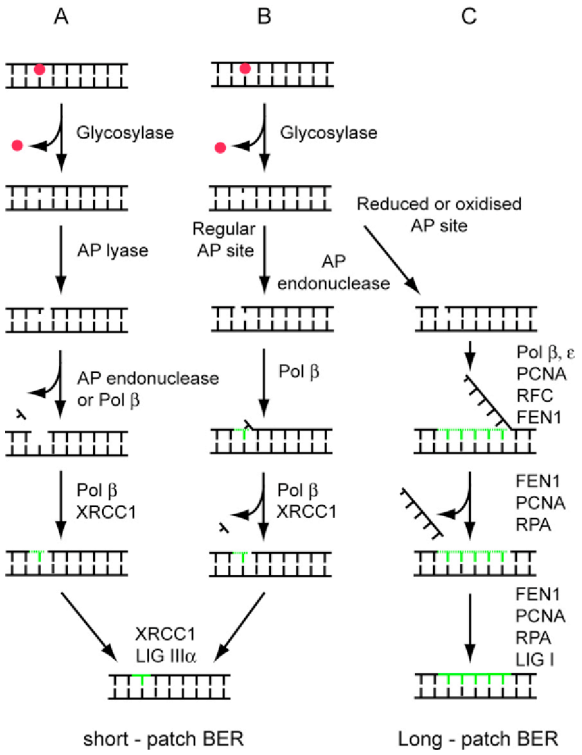

Figure 1.4 Alternative BER pathways in Mammalian cells.

A, B: Short-patch BER initiated by glycosylase then AP lyase or AP endonuclease, respectively. Unmodified AP sites result in a one-nucleotide repair patch generated by a common ligation step. C: Processing of reduced or oxidised AP sites proceeds via the PCNA-dependent pathway, and involves cleavage by FEN1 (Krokan et al., 2000).

1.6 Mismatch Repair

An associated form of BER is mismatch repair (MMR). MMR recognises misincorporated nucleotides during DNA synthesis that could become fixed as mutations during the next replicative cycle (Iyer et al., 2006). Nucleotide selection and proofreading associated with some DNA polymerases confer an error rate of ~10^{-7} per bp per replication (Kunkel, 2004). Genetic research shows that mistakes, which escape these fidelity devices, are corrected by mismatch repair, further elevating fidelity 50-1000 fold (Schofield and Hsieh, 2003).

Meselson and colleagues demonstrated that co-repair of closely linked mismatches usually occurs on the same DNA strand, an effect interpreted as an excision mode of repair with a tract size of several thousand nucleotides, when they transfected *E. coli* with phage λ heteroduplex DNA containing mismatched base pairs (Wildenberg and Meselson, 1975; Wagner and Meselson, 1976). Thus, the question of which base is the incorrect one or which strand of DNA is to be repaired is immediately raised. They suggested that this could be accomplished by exploitation of secondary signals within the helix such as the transient absence of methylation on newly synthesized DNA or via

a “special relation to the replication complex” (Wagner and Meselson, 1976). Methyl direction was confirmed in *E. coli*, when heteroduplex repair was shown to be controlled by the status of adenine modification at GATC sequences (Pukkila et al., 1983). Newly synthesized DNA is subject to be modified at this sequence by Dam methylase shortly after replication (Lyons and Schendel, 1984). The result is that for a short time after replication, the newly synthesised strand will be unmethylated and the template strand will be methylated. The mismatches must be repaired in this transient period.

1.6.1 MMR in *E. coli*

The best understood MMR is that in *E. coli*, which is carried out by MutS, MutH, MutL and helicase II (UvrD) proteins (Parker and Marinus, 1992). MutS homodimer protein recognizes mismatched base pairs and is responsible for initiation of MMR (Su and Modrich, 1986). MutL homodimer is recruited to the heteroduplex in a MutS- and ATP-dependent manner (Grilley et al., 1989). The assembly of MutS/MutL/heteroduplex ternary complex activates MutH, a latent endonuclease specific for unmodified GATC sequences. MutH cleaves the unmethylated strand of a hemimethylated GATC site 5' to the G (Welsh et al., 1987). The incision of MutH can occur either 3' or 5' to the mismatched pair on the unmodified strand, and the ensuing strand break serves as the actual signal that directs excision repair to the unmethylated strand (Figure 1.5). Formation of the MutS / MutL / heteroduplex complex also activates the activity of DNA helicase II, a unidirectional 3'-5' helicase (Matson, 1986). Evidence suggests that MutL can physically interact with DNA helicase II and load the helicase onto the appropriate DNA strand so that unwinding proceeds toward the mismatch in a manner consistent with heteroduplex orientation (Mechanic et al., 2000). After unwinding, the unmethylated DNA strand is degraded to the nearest methylated sequence on the opposing strand. When MutH incises 5' to the mismatch, excision depends on ExoVII or RecJ exconuclease both of which hydrolyze single-stranded DNA with 5'-3' polarity (Chase and Richardson, 1974; Lovett and Kolodner, 1989). When MutH cleaves 3' to the mismatch, excisions require ExoI, ExoVII or ExoX, all of which possess 3'-5' polarity (Lehman and Nussbaum, 1964; Chase and Richardson, 1974; Viswanathan and Lovett, 1999; Burdett et al., 2001; Viswanathan et al., 2001). The single-stranded gap produced by the action of helicase II and exonucleases is stabilized by SSB (Lahue et al., 1989). DNA polymerase III holoenzyme carries out the repair synthesis and DNA ligase restores the integrity of the DNA duplex (Lahue et al., 1989).

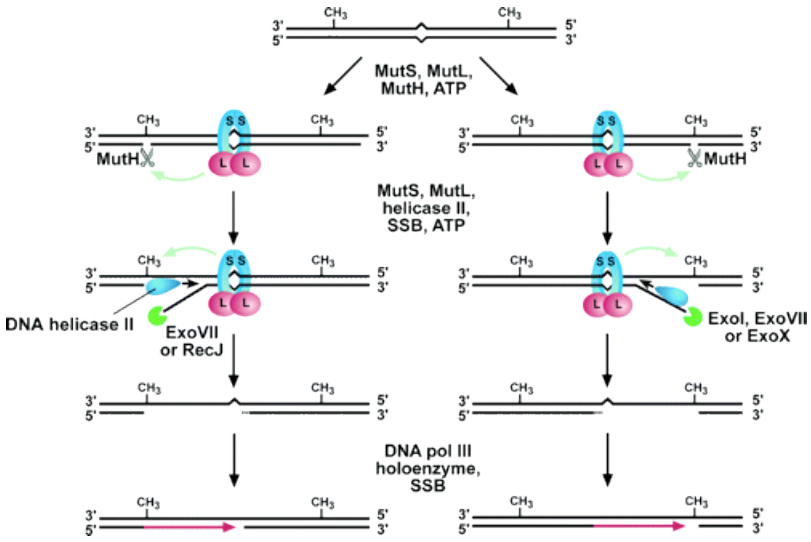

Figure 1.5 Mechanism of methyl-directed mismatch repair in *E. coli.*

MutS homodimer protein recognizes mismatched base pairs and recruits MutL homodimer to the lesion. The assembly of MutS/MutL/heteroduplex ternary complex activates MutH, which can cleaves either 3' or 5' to the mismatched pair on the unmodified strand. Formation of the MutS/MutL/heteroduplex complex activates the activity of DNA helicase II, a 3'-5' helicase. MutL can load the helicase onto the appropriate DNA strand. After unwinding toward the mismatch, the unmethylated DNA strand is degraded to the nearest methylated sequence on the opposing strand. ExoVII or RecJ exconuclease hydrolyzes ssDNA with 5'-3' polarity, while ExoI, ExoVII or ExoX are exonucleases with 3'-5' polarity. The ssDNA gap produced by helicase II and exonucleases is stabilized by SSB. DNA polymerase III holoenzyme carries out the repair synthesis and DNA ligase restores the integrity of the DNA duplex. Green arrows indicate MutS- and MutL-dependent signaling between the two DNA sites involved in the reaction (Iyer et al., 2006).

1.6.2 MMR in Eukaryotes

The current picture of MMR in eukaryotic cells resembles that of *E. coli* to a great extent, but with two important differences (Kolodner, 1996; Buermeyer et al., 1999; Kolodner and Marsischky, 1999; Marti et al., 2002; Augusto-Pinto et al., 2003). The first is related to strand discrimination. In eukaryotes, repair directed by methylation has not been directly demonstrated. In fact, the majority of organisms do not possess the modification enzyme like the Dam methyltranferase in *E. coli*, and no MutH homologue has been identified in the majority of organisms, including all eukaryotes (Eisen and Hanawalt, 1999). However, instead of DNA methylation, DNA replication processivity clamps have been suggested to provide the MMR machinery another mechanism of strand discrimination. MutS and MutL of *E. coli* both interact with β sliding clamp *in*

vitro (Lopez de Saro and O'Donnell, 2001; Lopez de Saro et al., 2006). Given the distinct orientation of β clamps on DNA, they could provide the MMR machinery with discrimination between parental DNA and the newly synthesized strands in bacteria (Kolodner, 1996). In eukaryotes, PCNA replication clamp interacts with several eukaryotic mismatch repair activities, for example, strong interaction with MutSα and MutSβ (Johnson et al., 1996; Clark et al., 2000), modulation of both 5' and 3' excisions (Guo et al., 2004) and involvement in the synthesis step in MMR through its interaction with Polδ (Gu et al., 1998). In addition, genetic studies in yeast have shown that a distinctive set of mutations in PCNA can result in MMR deficiency (Chen et al., 1999a; Lau et al., 2002). It has been suggested that PCNA might provide a physical link between repair and replication that would allow termini at the replication fork to function as strand signals (Umar et al., 1996). Another possibility is that non-covalent signals in the form of proteins that segregate with the individual strands during replication could conceivably provide a mechanism for discrimination of parents and nascent strands (Modrich and Lahue, 1996; Umar et al., 1996).

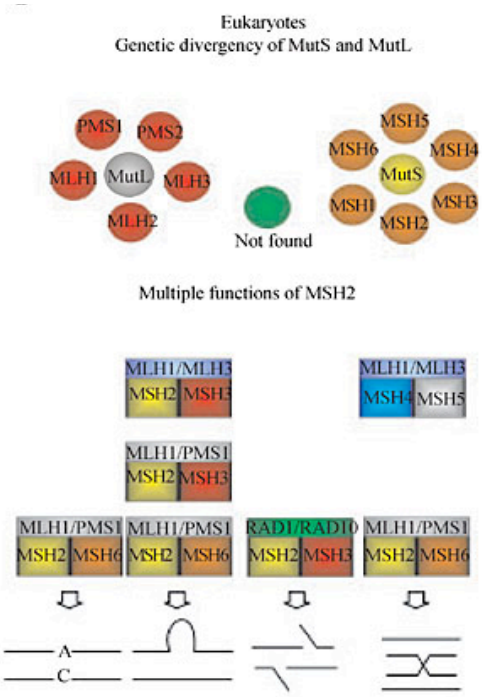

Figure 1.6 Schematic representation of the eukaryotic mismatch repair system.

The MutS proteins diverged into six homologues in eukaryotes, while MutL diverged into five other homologues; these are denominated MSH and MLH respectively. The MutH protein is not found in eukaryotes. The MSH and MLH proteins interact as a functional heterocomplex and repair several types of substrates, such as mismatches, single-strand loops generated during microsatellite replication, DNA double-strand breaks and Holliday junctions from meiotic crossing-over (Augusto-Pinto et al., 2003).

The second fundamental difference is that the MutS and MutL functional homologues are heterodimeric rather than homodimeric (Augusto-Pinto et al., 2003). At least six MutS homologues and five MutL homologues, referred to as MSH and MLH, respectively, have been identified in eukaryotes (Marti et al., 2002). The best characterized proteins of these homologues are MSH2, MSH3 and MSH6, which are involved in MMR in the nucleus and have been implied in mitotic genetic stability

where they participate in repair of base–base mismatches and insertion and deletion heterologies (Acharya et al., 1996). MSH2-MSH6 heterodimers recognize and repair base mismatches and loops of up to two bases, whereas MSH2-MSH3 heterodimers recognize loop-outs of different sizes (Strand et al., 1995; Palombo et al., 1996). MSH2 has also been implicated in meiotic gene conversion (Reenan and Kolodner, 1992). MSH4 and MSH5 proteins constitute another MSH heterodimer, which, however, does not participate in MMR, but instead is involved in meiotic crossing-over and chromosome segregation (Nakagawa et al., 1999; Kneitz et al., 2000; Snowden et al., 2004). In addition, MSH1 is found in yeast mitochondria and required for mitochondrial DNA stability in yeast, but has not been identified in mammalian cells (Reenan and Kolodner, 1992; Chi and Kolodner, 1994).

In addition, MLH1 and PMS1 (post-meiosis segregation 1, mammalian PMS2 corresponds to PMS1 in yeast, plants and nematodes) have been most extensively characterized. Yeast MLH1 and PMS1 form a heterodimer, which has been implicated in mitotic mutation avoidance and in postmeiotic segregation (PMS) (Prolla et al., 1994; Baker et al., 1996; Wang et al., 1999). MLH3, which has been identified in yeast and mammals (Flores-Rozas and Kolodner, 1998; Lipkin et al., 2000), plays an important role in meiotic crossing over (Wang et al., 1999; Santucci-Darmanin et al., 2002). MLH3 also contributes to mitotic genetic stabilization in yeast by preventing frameshift mutations (Flores-Rozas and Kolodner, 1998; Harfe et al., 2000), while its function in mammalian mitosis has been a subject of controversy (Lipkin et al., 2000; Wu et al., 2001; Hienonen et al., 2003; Liu et al., 2003; de Jong et al., 2004). Other MutL homologues have also been identified: MLH2 in yeast (Wang et al., 1999) and PMS1 in humans (Papadopoulos et al., 1994). The former protein may provide a function in meiosis (Wang et al., 1999).

Several reconstituted systems have been established by using purified human proteins (Genschel et al., 2002; Dzantiev et al., 2004; Zhang et al., 2005; Genschel and Modrich, 2006). The studies of these systems support mismatch-provoked excision *in vitro*, but much more details remain to be further explored (Iyer et al., 2006).

1.7 Homologous Recombination

1.7.1 Double-stranded Breaks

Double-stranded breaks (DSBs) are particularly dangerous kind of DNA lesion. It can interrupt the coding sequence of a gene, disrupt the linkage between coding and regulatory regions, alter chromosome organisation and perturb the systems that ensure

correct DNA replication, chromosome packaging and chromosome segregation (Helleday et al., 2007; Shrivastav et al., 2008). DSBs can be two-sided or one sided. Both types are a major threat to genomic stability.

DSBs can be induced by both endogenous and exogenous sources. Endogenous sources including transposition (Engels et al., 1990), immunoglobulin diversification (Dudley et al., 2005) and meiosis (Strom and Sjogren, 2007) involve the accidental or programmed generation of two-sided DSBs. One-sided DSBs are primarily related to DNA replication. Of particular interest is the induction of DSBs by exogenous sources in the context of cancer therapy. Ionizing radiation (IR) exhibits anti-tumour activity. IR-induced DSBs often contain modified bases at their 3' and 5' ends (Ward, 1988). Such ends with non-standard chemistry necessitate processing steps that are not needed when DSBs are introduced by nucleases, for example HO endonuclease, in experimental model systems (Paques and Haber, 1999). Intermediary metabolic products of *Streptomyces*, including bleomycin, neocarcinostatin and related compounds, have been effectively used in anti-tumour therapy (Povirk, 1996). They directly induce DSBs by attacking specific carbons in deoxyribose, leaving non-standard end-groups. A third class of DNA-based anti-tumour therapeutics is represented by topoisomerase inhibitors (Li and Liu, 2001). Topoisomerases are enzymes that open and close strands of DNA and involve a covalent DNA-protein bond in their catalytic cycle (Wang, 2002). The transition state can be stabilized by topoisomerase inhibitors leading to DSBs by type II inhibitors (e.g. etoposides) or single-stranded breaks by type I inhibitors (e.g. camptothecin), which may become one-sided DSBs during replication (Li and Liu, 2001).

Failure to repair DSBs or misrepair of them can lead to serious results, such as chromosome loss, chromosomal rearrangement, apoptosis or carcinogenesis (Hoeijmakers, 2001). Organisms have evolved several pathways for the repair of DSBs, mainly homologous recombination and non-homologous end joining and single strand annealing.

1.7.2 General Mechanism of Homologous Recombination

Homologous recombination (HR) is a ubiquitous DNA metabolic process that provides high-fidelity, template-dependent repair or tolerance of complex DNA damages including DNA gaps, DNA double-stranded breaks (DSBs) and DNA interstrand crosslinks (ICLs). In addition to its roles in normal DNA metabolism, HR occurs during specialized processes, such as meiotic recombination (which enables homologous chromosomes to repair and generate genetic diversity) (Li and Heyer, 2008).

There are three fundamental stages in homologous recombination: Presynapsis, synapsis and post-synapsis (Figure 1.7, reviewed in [Li and Heyer, 2008]). In the first stage (presynapsis) a blunt or approximately blunt duplex end must be converted into a 3'-OH ending single-stranded tail coated with a filament of RecA family members, which are strand exchange proteins. In the second stage (synapsis), this strand exchange filament initiates invasion of homologous DNA, linking the broken end to an undamaged DNA duplex in a three-way junction called D loop, where the invading 3' end primes DNA synthesis. In the third stage (postsynapsis), there are at least three options.

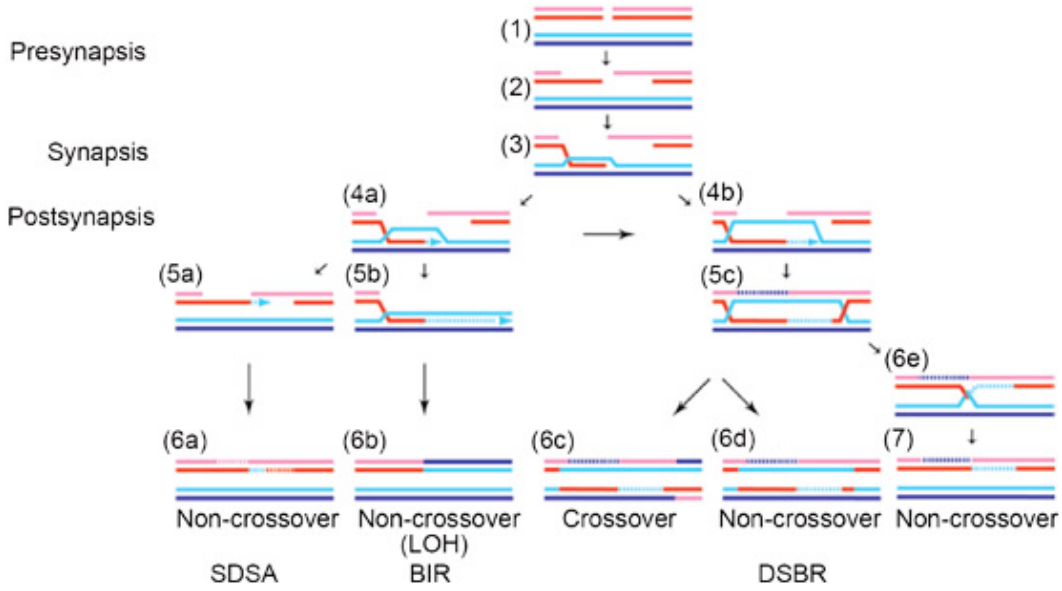

Figure1.7 Stages and pathways of recombination in DSB repair.

Homologous recombination can be conceptually divided into three stages: presynapsis, synapsis, and postsynapsis. During presynapsis, DSB ends are recognized and processed to a 3' overhang (steps 1-2). In synapsis, DNA strand invasion generates a D-loop (step 3). At least three different pathways are proposed after the D-loop intermediate. In SDSA (steps 4a - 5a - 6a), the invading strand is disengaged after DNA synthesis and annealed with the second end, leading to localized conversion without crossover. In BIR, (steps 4a - 5b - 6b), the D-loop is assembled into a full replication fork, copying the entire distal part of the chromosome to result in loss-of heterozygosity (LOH). In DSBR, (steps 4b - 5c - 6c-e - 7), both ends of the DSB are engaged, leading to double Holliday junction formation. The junction can be processed by either a resolvase into non-crossover or crossover products (steps 6c and d) or a mechanism involving BLM and TOPOIIIα (step 6e), leading exclusively to non-crossover products (step 7) (Li and Heyer, 2008).

Firstly, The invading strand in the D loop, after priming DNA synthesis, can be ejected from the invaded DNA and annealed with the second end. This process is called synthesis-dependent strand annealing (SDSA) (Nassif et al., 1994). SDSA process may involve multiple rounds of invasion, synthesis, and disengagement. Secondly, in break-induced replication (BIR), the D-loop is assembled into a full replication fork, copying the entire distal part of the chromosome to result in loss-of heterozygosity (LOH) (Kraus et al., 2001) (Formosa and Alberts, 1986). Thirdly, in double strand break repair (DSBR), both ends of the DSB are engaged after the second end capture, leading to the Holliday junction (HJ) formation. HJs can be moved along the DNA by a process called branch migration. The ligation after another round of invasion leads to a more complicated structure double Holliday junction (dHJ). The junction can be processed by either a resolvase into non-crossover or crossover products (West, 1997; Liu et al., 2004b) or a mechanism involving BLM-mediated branch migration and TOPOIIIα-catalyzed dissolution of a hemicatenane, leading exclusively to non-crossover products (Wu and Hickson, 2003; Plank et al., 2006; Wu et al., 2006)

1.7.3 HR in *E. coli*

RecBCD pathway

In *E. coli*, RecBCD pathway is the major route to process DSBs. RecBCD is multifunctional complex with highly processive helicase activity and nuclease activity, which nicks the strands separated by its helicase activity (Dillingham et al., 2003). It carries out the presynaptic end processing of recombination. Initially, the nuclease activity of RecBCD is preferentially targeted to the 3' strand. However this polarity of degradation is reversed when RecBCD encounters a specific sequence termed chi site (χ, 5'–GCTGGTGG-3') in a 3'-5' direction (Anderson and Kowalczykowski, 1997; Handa et al., 1997). The upregulated 5'-3' nulease activity, combined with the processive helicase activity, generates a 3' overhang for further process.

The strand exchange protein in *E. coli* is RecA, which consists of three domains: a large, central domain, surrounded by smaller amino and carboxy domains. The central domain is involved in DNA and ATP binding. The amino domain contains a large α-helix and short β-strand. This structure is important in the formation of the RecA polymer. The carboxyl domain facilitates interfilament associations (Story et al., 1992). However, RecA competes poorly with single-strand binding protein (SSB) for single strand DNA. RecBCD, after interaction with χ site, loads RecA onto the 3' single stranded DNA ends (Anderson and Kowalczykowski, 1997).

During synapsis, the single stranded DNA end invades a homologous DNA duplex and the RecA proteins 'search' for sequence homology (Voloshin et al., 1996). Unless homology is found, strand invasion is aborted. MMR controls HR by aborting strand exchange between divergent DNA sequences. For example, MMR has been shown to be the barrier to interspecies recombination between *E. coli* and *Salmonella typhimurium*. MutS and MutL mutants, but not MutH mutants, exhibit as much as a 100-fold increase in conjugational recombination frequencies (Rayssiguier et al., 1989).

In the postsynaptic stage of recombination, once significant homology has been found, DNA pairing is allowed and DNA synthesis is primed by the new D-loop structure and the invaded 3' ssDNA tail acts as a primer. The remainder of the postsynaptic stage in *E. coli* is carried out by RecG and RuvABC (Zerbib et al., 1998; Sharples et al., 1999). The RecG helicase can act on HJs and other branched structures including D loops and three-way junctions and is thought to be a good candidate for D-loop branch migration, which convert D loops to HJs (McGlynn et al., 2000). The RuvABC complex combines the branch migration activity of RuvAB with the resolvase activity of RuvC, a HJ-specific endonuclease, in one coordinated molecular machine (Zerbib et al., 1998). A tetramer of the RuvA protein binds to the four way HJ and two hexameric rings of the RuvB protein assemble on two of the arms (Parsons et al., 1995). The RuvB rings drive branch migration of the junction by pumping DNA through themselves, while a dimer of the RuvC endonuclease joins the complex to direct cleavage of opposite arms of the junction at certain preferred sequences (Shah et al., 1994), in an orientation determined by RuvB (van Gool et al., 1999). This resolves the HJ to two discrete nicked duplexes (Iwasaki et al., 1991). Finally, the nicks are prepared by DNA ligase.

RecFOR pathway

RecF, RecO and RecR proteins provide an alternative route for homologous recombination in the absence of RecBCD (Morimatsu and Kowalczykowski, 2003). In this pathway, the dsDNA ends resulting from a DSB are processed to ssDNA 3' tails by the helicase activity of RecQ in combination with the 5'-3' nuclease activity of RecJ (Kowalczykowski, 2000). The combined activity of RecFOR acts to displace SSB and load the RecA recombinase (Morimatsu and Kowalczykowski, 2003). RecR interacts with either RecO or RecF, forming either a RecFR or RecOR complex. The RecOR complex acts to facilitate the loading of RecA onto ssDNA, ensuring persistent binding to prevent the dissociation of the recombinase (Sandler and Clark, 1994; Bork et al., 2001). The RecFR complex prevents the RecA nucleoprotein filament extending into regions of dsDNA, where the filament would be inactive (Webb et al., 1997). Once the loading of RecA is complete, the homologous recombination process continues as in the RecBCD pathway.

RecFOR dependent homologous recombination is also active in *recBCD*$^{+}$ *E. coli* (Kowalczykowski, 2000). In the presence of RecBCD, RecFOR recognises and binds to ssDNA-dsDNA junctions and protects the nascent lagging strand of the arrested replication forks to maintain the fork structure (Hegde et al., 1996). Moreover, RecFOR can load RecA specifically onto gapped DNA and initiate recombination, which is important in the recovery of stalled replication forks (Morimatsu and Kowalczykowski, 2003).

1.7.4 HR in Eukaryotes

In eukaryotic organisms, the *RAD52* epistasis group of genes are required for the repair of DSBs by HR (Game and Mortimer, 1974). Many members of this group were first identified in *Saccahromyces cerevisiae* as mutants sensitive to ionizing radiation. So far, this group includes *RAD50*, *RAD51*, *RAD52*, *RAD54*, *RAD55*, *RAD57*, *RAD59*, *MRE11*, *XRS2*, BRCA2 and *RDH54/TID1* (Sung and Klein, 2006; Li and Heyer, 2008). Mutants in any of the *RAD52* group genes results in DNA damage sensitivity and defective HR.

All sub-pathways of HR (Figure 1.7) share the same initial steps in processing the DSB to a 3' overhanging tail, to which the assembly of the strand exchange protein filament is directed. Nucleolytic processing of DSBs involving non-standard chemistry, such as DSBs induced by IR or bleomycin, appears to specifically require the Mre11-Rad50-Xrs2 (MRX) complex in yeast or MRE11-RAD50-NBS1 (MRN) in human cells. Defects in these complexes lead to significant IR sensitivity, but the repair of a 'clean' DSB induced by the HO-endonuclease proceeds with no or little reduction in viability, involving only a minimal delay in repair kinetics (Ivanov et al., 1994; Krogh and Symington, 2004; Krishna et al., 2007). The 5'-3' exonuclease Exo1 (Fiorentini et al., 1997) and the product of the *SAE2* gene (Clerici et al., 2005) are also involved in 5'-end resection, probably acting in concert with the MRX complex.

Formation of Rad51 filament

In *S. cerevisiae* and human cells, Rad51 shows similarity to *E. coli* RecA protein, forming a very similar right-handed nucleoprotein filament on single strand DNA and promoting strand exchange between two homologous DNA molecules (Ogawa et al., 1993). Unlike RecA, which shows a kinetic delay in binding dsDNA relative to ssDNA, Rad51 exhibits only little preference of binding ssDNA over dsDNA (Bianco et al., 1998; Zaitseva et al., 1999). Moreover, Rad51 protein exhibits an approximately 100-fold lower ATPase activity than RecA on ssDNA or dsDNA (Sung, 1994; Bianco et al., 1998). These factors raise the question how Rad51 can specifically bind 3' ssDNA and fulfil its function as an invading protein.

RPA is the heterotrimeric ssDNA-binding protein in eukaryotes and is involved in all DNA metabolic processes involving ssDNA (Wold, 1997). RPA inhibits formation of the Rad51 filament on ssDNA, but it stimulates recombination by eliminating secondary structure in ssDNA and by binding to the displaced strand of the D loop *in vitro* (Sugiyama et al., 1997). The inhibition of Rad51 filament formation by RPA is overcome by Rad51 cofactors, collectively called mediator proteins (Beernink and Morrical, 1999). The Rad55-Rad57 complex and Rad52 have been identified as the key mediators of Rad51 filament formation in budding yeast (Gasior et al., 1998; Sugawara et al., 2003).

Rad55 and Rad57 are two Rad51 paralogs in *S. cerevisiae* that form a heterodimer with mediator activity, as they enable Rad51-mediated recombination in the presence of RPA-coated ssDNA *in vitro* (Sung, 1997b). Genetic studies have hinted that Rad55-Rad57 might stabilize the already assembled Rad51 presynaptic filament (Fortin and Symington, 2002). There are five human RAD51 paralogues ⎯ RAD51B, RAD51C, RAD511D, XRCC2 and XRCC3, but the limited sequence resemblance makes it difficult to assign which of the human RAD51 paralogues correspond to yeast Rad55-Rad57 (Thacker, 1999; Sung and Klein, 2006). Several complexes of the RAD51 paralogues have been reported, such as RAD51B-RAD51C, RAD51D-XRCC2, RAD51C-XRCC3 and RAD51B-RAD51C-RAD51D-XRCC2 (Schild et al., 2000; Masson et al., 2001). These protein complexes are related to Rad55 and Rad57 in structure (Paques and Haber, 1999; Symington, 2002) and probably in function, as deletion of any one of the Rad51 paralogues results in an inability to deliver RAD51 to recombination substrates in the cell (Gasior et al., 2001; Yonetani et al., 2005).

Rad52 forms multimeric ring structure that binds preferentially to ssDNA (Shinohara et al., 1998; Singleton et al., 2002). Rad52 interacts with Rad51 as well as with RPA (Shinohara et al., 1992). Rad52 accelerates the displacement of RPA from ssDNA by Rad51 and allows efficient Rad51-mediated recombiantion involving RPA coated ssDNA (Sung, 1997a; New et al., 1998; Shinohara and Ogawa, 1998). More importantly, Rad52 also exhibits the unique ability to anneal complementary DNA strands (Sugiyama et al., 1998). Such an activity is thought to be critical in second-end capture (Sugiyama et al., 2006) and promotes both crossover and noncrossover pathways of meiotic recombination in *S. cerevisiae* (Lao et al., 2008).

Although a Rad52 orthologue exists in vertebrates, its deletion only causes a mildly affected DNA recombination and repair phenotype in mouse and chicken DT40 cells (Rijkers et al., 1998; Yamaguchi-Iwai et al., 1998). However, combining the RAD52 mutation and XRCC3, which is one of the five RAD51 paralogues, results in lethality in

chicken DT40 cells (Fujimori et al., 2001). These observations indicate that in higher eukaryotic organisms, the promotion of Rad51 presynaptic filament assembly is primarily mediated by factors other than RAD52.

The tumour suppressor BRCA2 is of special interest among the mediator proteins. Heterozygous mutations in *BRCA2* predispose to breast, ovarian as well as other types of tumour (Jasin, 2002; Moynahan, 2002; West, 2003; Pellegrini and Venkitaraman, 2004). Moreover, bi-allelic loss of *BRCA2* function causes cancer-susceptibility syndrome Fanconi anaemia (West, 2003; Kennedy and D'Andrea, 2005). BRCA2 is required for IR-induced Rad51 focus formation *in vivo* (Moynahan et al., 2001; Xia et al., 2001; Tarsounas et al., 2003).

Experiments with the full-length *Ustilago maydis* BRH2 (homologue of BRCA2) and fragments of the human protein demonstrated that BRCA2 targets Rad51 filament formation to the ssDNA-dsDNA junction on RPA-coated ssDNA (Yang et al., 2002; Yang et al., 2005; Mazloum et al., 2007). The mechanism is likely to be complex, considering the size of BRCA2 (3, 418 amino acids), the multitude of Rad51-binding sites (8 BRC repeats and a C-terminal site), and the importance of its interaction partners. The structure of the BRC repeat has revealed a molecular mimicry of the Rad51 subunit-subunit interface, suggesting that BRCA2, through its BRC motif, might serve as a nucleation point of the Rad51 filament (Pellegrini et al., 2002). The C-terminal Rad51-binding site preferentially binds to the filament form of Rad51 (Esashi et al., 2005; Davies and Pellegrini, 2007). These results suggest that BRCA2 employs two mechanisms to favor Rad51 filament formation, nucleation and filament stabilization. The binding of the C-terminal site to Rad51 is negatively regulated by cyclin-dependent kinase (CDK) phosphorylation on S3291, suggesting that BRCA2 function in HR is regulated throughout the cell cycle (Esashi et al., 2005). Besides its critical interaction with hRad51, BRCA2 was also found to physically interact with a number of other proteins (Pellegrini and Venkitaraman, 2004). Genetic experiments have shown that depletion of DSS1 (Kojic et al., 2003; Gudmundsdottir et al., 2004), PALB2 (Xia et al., 2006), and BCCIP (Lu et al., 2005) affects HR, while the mechanistic function of these BRCA2-interacting proteins remains to be determined.

In yeast, Rad54 is a double strand DNA-dependent ATPase that interacts directly with Rad51 and assembles into higher order complexes in the presence of DNA (Petukhova et al., 1998). Rad54 is required for D loop and heteroduplex DNA formation (Petukhova et al., 2000; Smirnova et al., 2004).

Rad59 possesses sequence similarity to the N-terminal region of Rad52 (Bai and Symington, 1996) and is similarly capable of annealing complementary strands of

DNA. Rad59 is also believed to promote strand invasion, specially, in a RAD51- and RAD54-independent BIR pathway (Petukhova et al., 1999; Signon et al., 2001).

The meiotic recombinase Dmc1 and its associated factor

In addition to Rad51, *S. cerevisiae* and human cells also possess a meiotic-specific RecA homologue, Dmc1 (Bishop, 1994; Habu et al., 1996). Further genetic, cell biological and biochemistry analyses have unveiled protein factors that physically and functionally interact with Dmc1, such as Meis5-Sae3, Hop2-Mnd1 and Rdh54/Tid1 in yeast, HOP2-MND1, RAD54 and RAD54B in human cells (Sung and Klein, 2006). In yeast, Dmc1 is known to be required for normal levels of meiotic recombination (Bishop et al., 1992). In cells that lack Mei5 or Sae3, Dmc1 targeting to recombination site is impaired, whereas Rad51 targeting remains normal (Hayase et al., 2004; Tsubouchi and Roeder, 2004). It is thought that Mei5-Sae3 facilitates the assembly of the Dmc1 presynaptic filament. It is interesting to note that the formation of Dmc1 foci depends on Rad51, which indicates that Rad51 somehow facilitates the delivery of Dmc1 to the HR substrate or enhances the stability of the Dmc1 presynaptic filament (Bishop, 1994). Recent studies have shown a physical and a functional interaction between the *Arabidopsis thaliana* BRCA2 protein and DMC1. Depletion of BRCA2 by RNA-interference-mediated silencing results in defective meiosis (Siaud et al., 2004) and BRCA2 binds not only RAD51 but also DMC1 through its BRC repeats (Dray et al., 2006). Futher analyses have provided evidence that the BRCA2-DMC1 axis is indispensable for meiosis (Siaud et al., 2004). However, the mechanistic attributes of the Dmc1-associated HR machinery are not as well defined as the Rad51-accociated machinery.

Anti-recombinase function of the Srs2

The efficiency of HR is enhanced by mediator proteins, but attenuated by the Srs2 helicase that dismantles the Rad51-ssDNA complex. In yeast, Srs2 protein has a 3'-5' DNA helicase activity (Rong and Klein, 1993) and can dismantle the Rad51 presynaptic filament in a manner that requires ATP hydrolysis (Krejci et al., 2003; Veaute et al., 2003). The likely functional equivalent of Srs2 in other eukaryotes is FBH1 (Osman et al., 2005). Genetic evidence has implicated Srs2 in preventing the use of ssDNA gaps that arise during stalled replication as HR substrates and in specifically promoting post-replication DNA repair (Aboussekhra et al., 1992; Gangloff et al., 2000). In S phase, yeast PCNA (proliferating cell nuclear antigen, an essential component of the DNA replication apparatus that functions by tethering the DNA polymerase to the DNA template (Moldovan et al., 2007)), can be modified by the small ubiquitin-like modifier (SUMO) even in the absence of exogenous DNA damage (Hoege et al., 2002). The recruitment of Srs2 to the DNA replication fork has been reported to be dependent on

SUMO-modified PCNA and thought to promote translesion-synthesis gap repair and prevent unwanted recombination events of replicating chromosomes by removing Rad51 (Papouli et al., 2005; Pfander et al., 2005). During HR, the stages after strand invasion also seem to be regulated by Srs2. Specifically, DSBs in the *srs2* deletion mutant result in a prolonged DNA-damage-checkpoint-mediated cell-cycle arrest, which is dependent on Rad51 (Vaze et al., 2002; Aylon and Kupiec, 2003). It has been suggested that the capability of Srs2 to dissemble the Rad51 presynaptic filament prevents the accumulation of a Rad51-containing DNA intermediates that can trigger the DNA-damage-checkpoint-mediated arrest response.

Regulation of crossovers

After ssDNA invasion and generation of the D-loop intermediate, the DSB repair (DSBR) branch proceeds by engaging the second end of the DSB, by either second end capture through DNA annealing or a second invasion event (Figure 1.7 right). Annealing of the second end is catalyzed by the Rad52 protein, which exerts a unique function of being able to anneal complementary DNA strands (Lao et al., 2008). The resultant dHJ is a substrate either for dissolution into non-crossover products by BLM-TOPOIII or for resolution by a structure-specific endonuclease into crossover/non-crossover products (Figure 1.7 right). An endonuclease activity that exerts a similar specificity for HJs as the bacterial RuvC protein has been identified in mammalian cell extracts (Liu et al., 2004c). RAD51C was present in this cell extract and was required for resolvase activity.

The Mus81-Mms4 complex appears to be a replication context-specific cofactor of HR (Heyer et al., 2003; Hollingsworth and Brill, 2004) Cells deficient for the complex are not sensitive to DSBs induced by HO endonuclease or IR, but display sensitivity to fork-stalling agents like methylmethane sulfonate (MMS), UV, and the ribonucleotide reductase inhibitor hydroxyurea as well as the topoisomerase I inhibitor camptothecin (Boddy et al., 2000; Interthal and Heyer, 2000). The *mus81 mms4* mutants are epistatic with the RAD52 group for these phenotypes. Mus81-Mms4 is a structure-selective DNA endonuclease that cleaves a number of substrates *in vitro*, including replication fork-like substrates, nicked HJs, D-loops, and 3'-flaps (Heyer et al., 2003; Hollingsworth and Brill, 2004). A number of potential Mus81-Mms4 substrates are envisaged to arise during the processing of stalled replication forks. The *in vivo* substrate(s) of Mus81-Mms4 remain to be determined. However, *Schizosaccharomyces pombe* mutants in *mus81* and *eme1* are defective in meiotic recombination and can be complemented by the expression of RuvABC (Ciccia et al., 2003; Osman et al., 2003). In addition, Mus81-Mms4 has also been identified to be involved in ICL repair in mammalian cells (see below).

Alternative processing of dHJs is afforded by the combined action of the BLM DNA helicase with the type I topoisomerase TOPOIII and their cofactor BLAP75/Rmi1 (Wu and Hickson, 2003; Plank et al., 2006; Wu et al., 2006). In a process termed dissolution, BLM migrates the two junctions towards each other (Plank et al., 2006), and TOPOIII removes the hemi-catenanes that topologically link the two duplexes (Plank et al., 2006). Importantly, this mechanism leads to an obligatory non-crossover outcome, providing a satisfactory explanation for the increase in sister chromatid exchange in cells derived from Bloom's syndrome patients who are deficient for the BLM helicase (Chaganti et al., 1974). The corresponding budding yeast complex, Sgs1-Top3-Rmi1, has yet to be analyzed biochemically with dHJ substrates. Genetics studies have shown that the crossover but not the non-crossover recombination is increased in *sgs1* mutants (Ira et al., 2003; Rockmill et al., 2003). Surprisingly, crossover suppression by Sgs1 does not require its helicase activity during DSB repair (Lo et al., 2006), suggesting that Sgs1 may utilize other mechanisms than dHJ dissolution for crossover suppression, a notion that was also developed from analysis of crossover suppression by Sgs1 during meiotic recombination in *S. cerevisiae* (Oh et al., 2007).

Deletion of the yeast *MER3 gene*, which encodes a DNA helicase, affects the transition of DSBs to late HR intermediates and diminishes the level of meiotic crossovers several fold without affecting the formation of non-crossover (Nakagawa and Ogawa, 1999). The Mer3 protein can unwind different DNA substrates, including HJs (Nakagawa et al., 2001). Interestingly, the helicase activity of Mer3 extends the DNA joint that is made by Rad51 (Mazina et al., 2004). This attribute of Mer3 is thought to facilitate the formation of the double HJ during meiotic HR.

1.7.5 HR in Archaea

Some archaeal proteins proposed to be involved in HR have been characterised biochemically (see below). However, compared to the extensively studied HR in bacteria and eukaryotes, very little is known about the important DNA process HR in archaea.

RadA is the archaeal homologue of RecA and Rad51, and was discovered in both crenarchaeal and euryarchaeal genomes (Sandler et al., 1996). RadA shares greater sequence similarity to Rad51 than to RecA (~40% identity and ~20% identity, respectively). RadA from both crenarchaea and euryarchaea have DNA dependent ATPase activity, form nucleoprotein filaments and catalyses homologous pairing and strand exchange (Komori et al., 2000a; Seitz and Kowalczykowski, 2000). Polymerisation of archaeal RadA is principally the same as with eukaryotic Rad51 (Shin et al., 2003) and stoichiometry is the same as Rad51 and RecA, with one RadA

monomer per 3 nucleotides (Ariza et al., 2005). Structurally, Rad51 and RadA are strikingly similar (Shin et al., 2003). Deletion of *Haloferax volcanii radA* results in increased sensitivity to ethylmethane sulfonate and UV light, and cells are recombination deficient (Woods and Dyall-Smith, 1997).

Currently, no mediator of RadA catalysed recombination has been identified in archaea. However, homologues of the eukaryotic single strand binding protein RPA are present in archaea and RPA from *Pyrococcus furiosus* has been shown to interact with RadA and stimulate strand exchange *in vitro* (Komori and Ishino, 2001). This implies that mechanisms exist to overcome inhibition of RadA binding of DNA by RPA, analogous to Rad51/RPA and RecA/SSB (Kelly et al., 1998; Komori and Ishino, 2001; Wadsworth and White, 2001; Haseltine and Kowalczykowski, 2002). It is not elucidated what is responsible for overcoming inhibition of RadA ssDNA binding by RPA. However, RadB, a RadA paralogue has been shown to interact with RadA *in vitro*, and has been implicated in facilitating loading of RadA onto RPA coated ssDNA (Sandler et al., 1996; Sandler et al., 1999; Komori et al., 2000b). Recent genetic research in *H. volcanii* has shown some important results (Haldenby, 2007). Firstly, deletion mutants of *radB* are slow growing, sensitive to mitomycin C and UV irradiation, and deficient for both crossover and non-crossover recombination. Secondly, both RadA and RadB are involved in homologous recombination and RadA is epistatic to RadB. Thirdly, A suppressor of Δ*radB* was isolated and identified as a mutation in the polymerisation domain of RadA (RadA-A196V). All these data suggest a role for RadB as a recombination mediator.

One archaeal protein, Hjm/Hel308a, with homology to bacterial RecQ and eukaryotic Hel308, has recently been identified in the euryarchaeotes *P. furiosus* and *Methanothermobacter thermautotrophicus*, respectively (Fujikane et al., 2005; Guy and Bolt, 2005). Hjm of *P. furiosus* was proposed as a branch migration enzyme (Fujikane et al., 2005). However, it was later shown that Hel308a from *M. thermautotrophicus* preferentially binds to forked DNA structures (Guy and Bolt, 2005). More recent research demonstrated that Hjm of *Sulfolobus tokodaii* exhibites structure-specific single-stranded-DNA-annealing and fork regression activities *in vitro.* In addition, this Hjm physically interacts with Hjc, the Holliday junction-specific endonuclease in *S. tokodaii*. The unwinding activity of the Hjm is negatively regulated by the interaction *in vitro*. These results also suggest that Hjm/Hel 308 family helicases are involved in the processing of stalled replication forks (Li et al., 2008). Therefore, the branch migration protein in archaea is unclear.

Three Holliday junction resolvases have been identified and characterised. The first was discovered in *P. furiosus* and was named Hjc (Holliday junction cleavage) (Komori et al., 1999; Kvaratskhelia et al., 2001). Hjc was later confirmed as a resolvase as *M. thermautotrophicus* Hjc restores the DNA repair deficiency of *E. coli* RuvC mutants (Bolt et al., 2001). Hjc forms homodimer (Nishino et al., 2001a; Nishino et al., 2001b) and introduces symmetrical nicks into Holliday junctions, as observed with bacterial RuvC (Komori et al., 1999).

The crenarchaea possess an additional resolvase called Hje (Holliday junction endonulcease), discovered in *Sulfolobus solfataricus* (Kvaratskhelia et al., 2001). Hje cleaves independently of DNA sequence, like Hjc, but only nicks continuous strands of junctions in the stacked X-form. The euryarchaea also possess a second resolvase, Hjr (Holliday junction resolvase). Hjr was detected in *P. furiosus* (Kvaratskhelia et al., 2001) and introduces symmetrical nicks into Holliday junctions, as is characteristic of other resolvases. Both Hje and Hjr are thought to be viral in origin.

1.8 Non-homologous End Joining

Non-homologous end joining (NHEJ) is another principal mechanism for repairing DNA double-strand breaks (DSBs) in which the two DSB ends are directly rejoined (Hefferin and Tomkinson, 2005; van Gent and van der Burg, 2007). This pathway is mostly precise for simple breaks, such as blunt ends (van Heemst et al., 2004), but can lead to sequence alterations at the breakpoint when the ends are not compatible (Figure 1.8). Although the term "non-homologous" is used to describe this repair pathway, a tiny 1–6 bp region of sequence homology (microhomology) near the DNA end often facilitates rejoining (Pitcher et al., 2007).

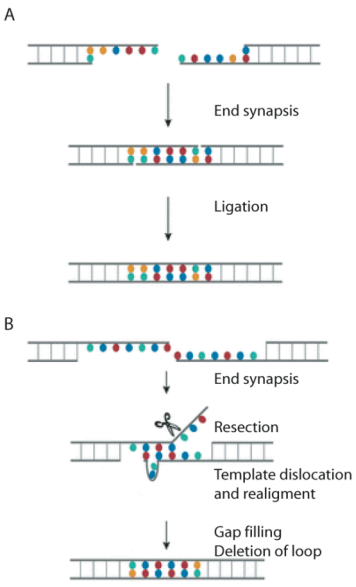

Figure 1.8 Microhomology-mediated NHEJ.

(A) DSBs with complementary undamaged overhangs can be aligned and relegated directly. (B) When the ends are not complementary, a synaptic complex is formed by searching for areas of microhomology. The alignment is followed by resection, gap-filling and ligation. (Pitcher et al., 2007).

NHEJ was initially identified in mammalian cells using a collection of X-ray sensitive rodent cell mutants (Botchan et al., 1980; Winocour and Keshet, 1980; Wilson et al., 1982). Subsequent studies have revealed the presence of functional homologous factors in yeasts (Dudasova et al., 2004; Daley et al., 2005b). Only recently a homologous NHEJ apparatus has been identified in prokaryotes (Aravind and Koonin, 2001; Doherty et al., 2001), suggesting that NHEJ has been conserved throughout evolution and operates from bacteria to human.

HR predominates in single cell eukaryotes such as *S. cerevisiae* (Dudasova et al., 2004). In contrast, NHEJ appears to be predominant in higher eukaryotes, probably as NHEJ is active throughout the cell-circle (Lieber et al., 2004), whereas HR only happens at late S and G2 phases when other intact sister chromotid is available as a template (Sonoda et al., 2006). In prokaryotes, it has been suggested that an NHEJ pathway may have evolved to repair DSBs that arise stationary phase, in which cells can be exposed for long periods of time to desiccation and other genotoxic agents with a reduction in the average number of chromosomes per cell (Weller et al., 2002; Wilson et al., 2003).

1.8.1 NHEJ in Mammalian Cells

Many proteins are required to efficiently perform NHEJ in mammalian cells (Lees-Miller and Meek, 2003; Pastwa and Blasiak, 2003; Sonoda et al., 2006; Helleday et al., 2007; Shrivastav et al., 2008). The core machinery consists of DNA-dependent protein kinase (DNA-PK) and the ligase IV/XRCC4/XLF complex (Figure 1.9). The Ku70/80 heterodimer, encoded by *XRCC6* and *XRCC5* respectively, is the DNA binding component of DNA-PK, which forms a ring that can specifically bind to DNA ends (Walker et al., 2001). This DNA–Ku complex then attracts and activates the catalytic subunit (DNA-PK_{CS}), a serine/threonine protein kinase encoded by *XRCC7/PRKDC* (Hartley et al., 1995; Fujimoto et al., 1997). The DNA-PK_{cs} protein is a member of the phosphatidylinositol-3 kinase related protein kinases (PIKK) family (Hartley et al., 1995; Poltoratsky et al., 1995), which also includes ATM (ataxia-telangiectasia mutated) and ATR (ATM-and Rad3-related) (Abraham, 2001). After juxtaposition of the two DNA ends, DNA-PK_{CS} is autophosphorylated (Ding et al., 2003; Reddy et al., 2004) and the ends become available for ligation by the ligase IV complex, which also contains the XRCC4 and XLF cofactors that are probably required for proper targeting of the ligase to DNA ends (Ahnesorg et al., 2006; Buck et al., 2006; Mari et al., 2006). The ligase IV complex is essential for the ligation step in NHEJ and may also be involved in alignment or gap-filling prior to ligation, since XRCC4 exists in a tight complex with DNA ligase IV (Lee et al., 2000) and can interact with DNA (Modesti et al., 1999), DNA-PK_{cs}, Ku (Nick McElhinny et al., 2000) and DNA polymerase μ (Mahajan et al., 2002).

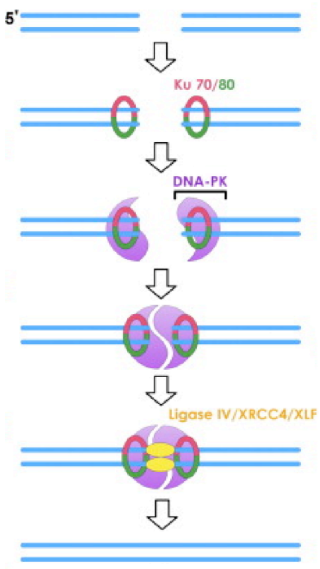

Figure 1.9 Model of the key steps required for mammalian NHEJ.

DNA ends are first bound by the Ku70/80 heterodimer, which then attracts DNA-PKcs to form the DNA-PK complex. DNA-PK then attracts the ligase IV complex (comprised of ligase IV, XRCC4 and XLF), which together seal the DNA ends. Note that in some cases the DNA ends require covalent modification prior to ligation, which is not shown in this model (Helleday et al., 2007).

Other factors involved in mammalian NHEJ

Mrell/Rad50/Nbs1

Rad50 is a split ABC-type ATPase with two heptad repeats in its centre, which fold into a long coiled-coil region bringing the two (N- and C-terminal) ATPase motifs Walker A and B into close proximity (Hopfner et al., 2000b; de Jager et al., 2001; van Noort et al., 2003). The apex of the Rad50 coiled coil contains a zinc hook that may facilitate the self-associates of Rad50 (Hopfner et al., 2000b; Anderson et al., 2001; Hopfner et al., 2002; Wiltzius et al., 2005). Mre11 is a nuclease of the SbcCD family with single-strand endonuclease activity, 3'-5' double strand exonuclease activity and weak DNA unwinding (stem-loop opening) activity (Paull and Gellert, 1998). Mre11 also contains two DNA-binding domains (one conserved in the centre and one less conserved in the C-terminus) and binds near the Rad50 ATPase to form a globular DNA-binding head (Hopfner et al., 2001). Whereas Mre11 and Rad50 are strongly conserved in all three life domains, the third member of the complex is less well conserved among species. Nevertheless, Nbs1 has a functional homologue Xrs2 in budding yeast *S. cerevisiae*. With Nbs1/Xrs2, these proteins form an integral complex capable of strong binding to DNA (Trujillo et al., 2003; Kobayashi et al., 2004). Nbs1 and Xrs2 share some common motifs, including an N-terminal FHA (forkhead-associated) domain, involved in binding to phosphorylated histone H2AX and phosphorylation sites of the checkpoint protein Atm (Tel1 in yeast), and a conserved C-terminal domain involved in interaction with Mre11 (Kobayashi et al., 2004; Shima et al., 2005). Mutantions in the central region of NBS1 are found to be accosiated with Nijmegen breakage syndrome (Thompson and Schild, 2002; De la Torre et al., 2003). The interaction of Nbs1/Xrs2 with Mre11 is crucial to all the functions of the Mre11 complex (Tauchi et al., 2002; Trujillo et al., 2003; Kobayashi et al., 2004; Tsukamoto et al., 2005).

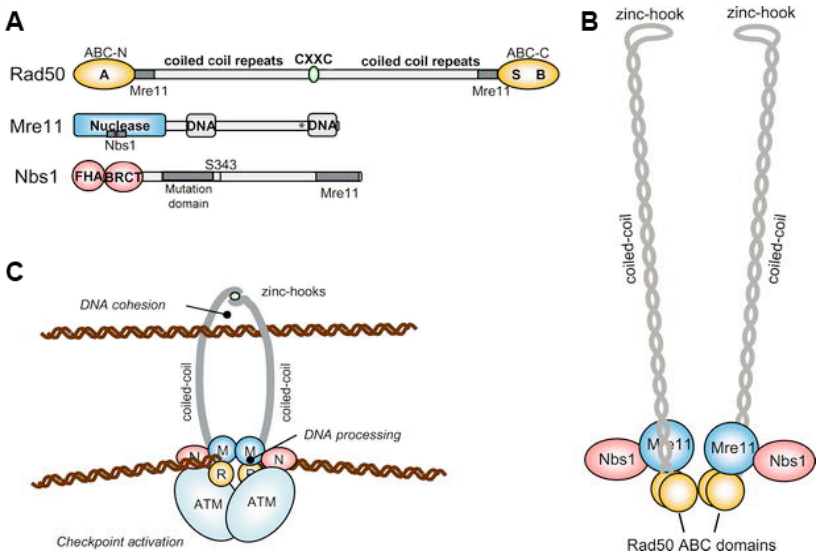

Figure 1.10 Functional domains and architecture of the Mre11 complex proteins.

(A) The domain structure and architecture of MRE11 and Rad50 are highly conserved in different organisms. The conserved motifs or domains are shown in different colours and labelled. (B) Structural model of the MRE112/RAD502/NBS12 complex architecture, using the colour code of A. MRE11 binds to the coiled-coil of RAD50, adjacent to the RAD50 ABC domains. The RAD50 antiparallel coiled-coil domains protrude from the ABC domains. The apex of the coiled-coil domains contains the zinc hook, implicated in metal-mediated intramolecular or intermolecular joining of Mre11 complexes via the RAD50 coiled-coils. The precise location of NBS1 (modeled in this illustration) has not been revealed. (C) Hypothetical model for the interaction of the Mre11 complex with an ATM dimer and DNA. In principle, a single $MRE11_2/RAD50_2/NBS1_2$ complex could link the sister chromatids to both DNA ends utilizing combined RAD50, MRE11 and NBS1 DNA-binding sites (Chen et al., 2001a). Alternatively, the Mre11 complex binds a single end, and tethering of ends proceeds by intermolecular joining of hook structures (Assenmacher and Hopfner, 2004).

The most striking feature of the Mre11 complex is the up to 60 nm long coiled-coil tail from Rad50, which would provide a flexible tether between sister chromotids and DSBs (Figure 1.10). It has been reported that the Mre11, Rad50, Nbs1 (MRN) complex stimulates DSB rejoining in assays using human cell extracts (Huang and Dynan, 2002). *In vivo*, the MRN complex may facilitate tethering of the opposing DNA ends of a DSB in proximity, or participate in processing DNA ends via its exonulease activity prior to ligation (D'Amours and Jackson, 2002). The MRN complex may be less critical under conditions where ends can be directly ligated than under conditions where ends require processing (de Jager et al., 2001; Hopfner et al., 2001).

In addition to NHEJ, the Mre11 complex has some other functions, such as telomere maintenance (Tsukamoto et al., 2001), regulation and progression of DNA replication (Maser et al., 2001), checkpoint and damage response (D'Amours and Jackson, 2002), and processing of DSBs during mitotic HR, as well as formation and end-resection of meiotic DSBs (Paques and Haber, 1999). Notably, the Mre11 complex is required for repair of hairpin-capped DSBs and prevention of chromosome rearrangements (Lobachev et al., 2002).

PNK

As a result of associated lesions, not all DNA ends are ready to be ligated. DNA ends can contain aberrant 3' phosphate groups, 5' hydroxyl groups, damaged backbone sugar residues and damaged DNA bases. Such DNA ends require processing before proper joining can proceed. DNA ends carrying 3' phosphates or 5' hydroxyl groups can be polished by polynucleotide kinase (PNK), which is a dual function enzyme that has both 5' DNA kinase and 3' DNA phosphatase activities (Jilani et al., 1999; Karimi-Busheri et al., 1999; Chappell et al., 2002). In addition, it has been shown to interact with XRCC4 (Koch et al., 2004).

hTdp1

Many IR-induced DNA breaks contain 3'-phosphoglycolate groups that must be removed prior to end joining. Human tyrosyl-DNA phosphodiesterase (hTdp1) removes protein moieties from camptothecin-induced topoisomerase I–DNA structures, and can also remove 3'-phosphoglycolate groups from dsDNA (Inamdar et al., 2002; Raymond et al., 2004; Raymond et al., 2005). It is, therefore, possible that hTdp1, in concert with PNK, could also play a role in processing of DNA ends during NHEJ.

53BP1

53BP1 was originally identified in a yeast two-hybrid screen as a protein that interacts with p53 (Iwabuchi et al., 1994). It is now recognized as an important player in the cellular response to DNA damage (Abraham, 2002; Wang et al., 2002). Mice defective for 53BP1 are radiosensitive, immune deficient and predisposed to cancer (Morales et al., 2003), suggesting a possible role in DNA DSB repair. Moreover, a fragment of 53BP1 stimulates DNA end joining *in vitro* (Iwabuchi et al., 2003) and 53BP1 partially co-localizes with autophosphorylated DNA-PKcs at nuclear foci (Chan et al., 2002) suggesting that 53BP1 could play a role in NHEJ. Recently a NHEJ subpathway dealing with ‘dirty’ ends has been reported. Although the mechanistic details of such a subpathway are not yet fully elucidated, it probably involves the ATM, 53BP1 and Mre11/Rad50/Nbs1 proteins and requires phosphorylation of histone H2AX (Riballo et al., 2004).

WRN

The Werner syndrome protein (WRN) is a member of the RecQ helicase family that has both ATP-dependent helicase activity and 3'–5' exonuclease activity (Hickson, 2003). WRN interacts with Ku (Li and Comai, 2001; Orren et al., 2001; Karmakar et al., 2002b) and the DNA-PK complex, and is phosphorylated by DNA-PK *in vitro* (Yannone et al., 2001; Karmakar et al., 2002a). Moreover, phosphorylation of WRN is abrogated in M059J cells, which lack DNA-PK_{cs} (Yannone et al., 2001; Karmakar et al., 2002a). WRN is, therefore, a physiological target of DNA-PK and a good candidate for a DNA processing enzyme that could be involved in NHEJ (Perry et al., 2006). WRN negative cells have a mildly radiosensitive phenotype (Yannone et al., 2001), which is consistent with such a role.

X family DNA polymerases

Several DNA polymerase X family members, including Pol μ and Pol λ, can fill in 5' single-stranded extensions (Nick McElhinny et al., 2005). DNA polymerase μ interacts with Ku and facilitates stable recruitment of XRCC4-DNA ligase IV to Ku-bound DNA, and DNA ligase IV-dependent end joining *in vitro* (Mahajan et al., 2002). After exposure to IR, the levels of DNA polymerase μ protein increase and the protein forms nuclear foci. In addition, Pol μ can align two ends without any homology, whereas Pol λ requires some microhomology (Daley et al., 2005a; Nick McElhinny et al., 2005).

Non-protein factors

Non-protein factors such as inositol hexaphosphate (IP6) and Mg–ATP are also required for NHEJ. IP6 binds to Ku and stimulates NHEJ *in vitro* (Hanakahi et al., 2000). Interestingly, inositol phosphates (including IP6), regulate chromatin remodeling in yeast (Shen et al., 2003; Steger et al., 2003), and it is tempting to speculate that they could regulate NHEJ *in vivo* in a similar manner. Mg–ATP is required for NHEJ *in vitro*, likely as a substrate for DNA-PK, and the catalytic activity of DNA-PKcs is essential for NHEJ *in vivo* (Kurimasa et al., 1999; Kienker et al., 2000), suggesting that DNA-PK-mediated phosphorylation is an essential part of NHEJ.

V(D)J recombination

The main players in NHEJ, DNA-PKcs, Ku, XRCC4, and DNA ligase IV, are also essential for V(D)J recombination. V(D)J recombination is the process whereby segments of the immunoglobulin genes and the T-cell receptor are rearranged during development of the vertebrate immune system (Figure 1.11). V(D)J recombination is initiated by the action of the lymphoid-specific recombinase activating factors, RAG1 and RAG2, that cleave specific regions of the T-cell receptor and immunoglobulin genes at two appropriate recombination signal sequences (RSS). RAG-mediated

cleavage results in the formation of DNA coding ends, each with a terminal DNA hairpin and a signal joint fragment containing blunt ended 5′-phosphorylated DNA ends. An endonuclease with DNA hairpin opening activity (likely Artemis, in complex with DNA-PKcs) opens the DNA hairpins at the coding ends to produce 3′-overhanging ends, which can be futher processed by polymerases, TdT and nucleases (Mansilla-Soto and Cortes, 2003). The NHEJ machinery (DNA-PKcs, Ku, DNA ligase IV and XRCC4) is required for completion of coding joints. Cells in which DNA-PKcs autophosphorylation sites have been mutated to alanine are capable of opening hairpins, but are defective in their ability to correctly form processed coding joints (Ding et al., 2003). Ku, DNA ligase IV and, in some cells, DNA-PKcs, are required for the formation of completed signal joints, which are subsequently lost from the cell (Pastink et al., 2001; Bassing et al., 2002; Gellert, 2002; Lees-Miller and Meek, 2003).

Mice harboring a naturally occurring mutation in *PRKDC* express a truncated, unstable form of the protein, and exhibit severe combined immunodeficiency (SCID) (Blunt et al., 1995; Kirchgessner et al., 1995; Miller et al., 1995; Blunt et al., 1996; Danska et al., 1996). Mutations in DNA-PKcs are also responsible for SCID in horses and dogs (Wiler et al., 1995; Meek et al., 2001; Ding et al., 2002).

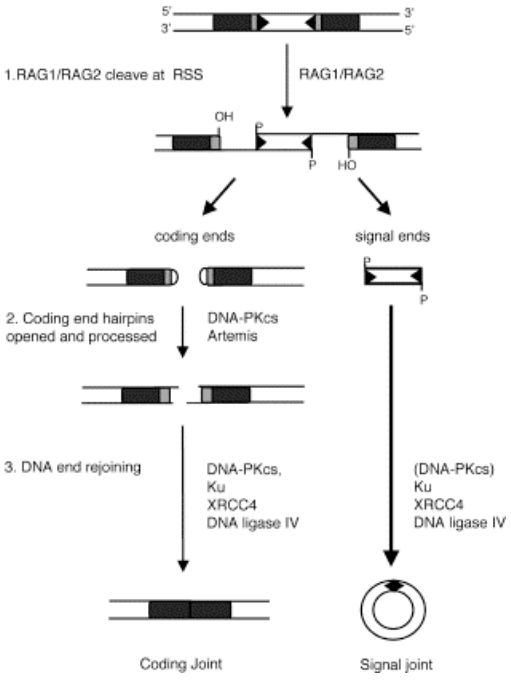

Figure 1.11 V(D)J recombination.

Step 1: V(D)J recombination is initiated by RAG1 and RAG2. Recombination signal sequences (RSS) are shown as dark triangles. RAG-mediated cleavage at RSS sites results in the formation of DNA coding ends (left) and a signal joint fragment (right). Step 2: An endonuclease with DNA hairpin opening activity opens the DNA hairpins at the coding ends to produce 3′-overhanging ends, which can be further processed. Regions of DNA that are subject to processing prior to rejoining are indicated by the lightly shaded segments. Step 3: DNA-PKcs, Ku, DNA ligase IV and XRCC4 are required for completion of coding joints. Ku, DNA ligase IV and, in some cells, DNA-PKcs, are required for the formation of completed signal joints, which are subsequently lost from the cell. From (Lees-Miller and Meek, 2003)

Mutations in DNA-PKcs have not been associated with human SCID, although a variation of human SCID that is characterized by radiosensitivity lacks another player in the V(D)J recombination pathway, Artemis (Moshous et al., 2001; Li et al., 2002; Kobayashi et al., 2003). Artemis has 5′–3′ exonuclease activity. However, interaction of Artemis with DNA-PKcs converts this to a DNA endonuclease with DNA hairpin-opening activity (Ma et al., 2002). This DNA-PKcs-dependent function of Artemis (Kirchgessner et al., 1995; Miller et al., 1995; Blunt et al., 1996) requires ATP, suggesting a requirement for DNA-PK-mediated phosphorylation; indeed, DNA-PK phosphorylates Artemis *in vitro* (Ma et al., 2002). As in murine SCID, lack of Artemis results in accumulation of DNA coding-ends with unopened hairpins (Figure 1.11). Thus, Artemis is a candidate for the DNA hairpin opening activity required for coding joint formation during V(D)J recombination (Schlissel, 2002; Mansilla-Soto and Cortes, 2003). In addition to the mild radiosensitivity phenotype, Artemis-deficient cells are highly sensitive to the DSB-inducing drug bleomycin; thus it is likely that Artemis is required to repair a subset of DSBs during NHEJ (Rooney et al., 2003).

Absence of Ku also confers defects in V(D)J recombination, however, in this case, neither coding ends nor signal ends are resolved (Figure 1.11) (Liang et al., 1996). The severity of the defects is more pronounced than in DNA-PKcs deficient mice, since Ku70 and Ku80 null mice are viable but show premature senescence while DNA-PKcs defective mice grow normally (Gao et al., 1998a). As with Ku deficiency, XRCC4 or ligase IV deficiency results in defects in both coding and signal joints, producing even more severe joining defects than Ku deficiency (Barnes et al., 1998; Frank et al., 1998; Gao et al., 1998b; Gu et al., 2000). Deletion of the Ligase IV or XRCC4 gene in mice leads to early embroyonic lethality (Barnes et al., 1998; Gao et al., 1998b).

Human terminal deoxytransferase (TdT) is another member of the DNA polymerase X family (Hubscher et al., 2000; Hubscher et al., 2002). TdT contributes to antibody diversity by catalyzing the addition of nucleotides to the junctions of coding ends during V(D)J recombination (Boule et al., 2001). TdT interacts with Ku and DNA-PKcs, and colocalizes with Ku at sites of DNA-damage (Mahajan et al., 1999; Mickelsen et al., 1999), suggesting a role in end-processing in both V(D)J recombination and DNA damage repair.

1.8.2 NHEJ in Yeast

In yeast, NHEJ is minor pathway of DSBs repair, while HR is the dominant repair pathway. NHEJ requires three protein complexes in *S. cerevisiae*: the Ku heterodimer (Yku70-Yku80), MRX (Mre11-Rad50-Xrs2), and DNA ligase IV (Dnl4-Lif1), as well as the ligase-associated protein Nej1 (Dudasova et al., 2004; Daley et al., 2005b).

Yku70 and Yku80 form the yeast Ku heterodimer, which by homology with human Ku is inferred to form a ring that binds DNA by sliding a DSB end through its opening (Walker et al., 2001). No homologue of mammalian DNA-PK_{cs} has been found in yeast, demonstrating that the role of yeast Ku is more general. Indeed, yeast Ku is involved in other cellular processes, including telomere maintenance and nuclear spatial organization (Boulton and Jackson, 1998; Taddei et al., 2004). Disruption of either the *YKU70* or *YKU80* gene affects mating-type switch and spontaneous mitotic recombination (Mages et al., 1996). In addition, it leads to sensitivity to bleomycin (Feldmann et al., 1996; Mages et al., 1996) and methyl methanesulfonate (MMS) (Feldmann et al., 1996; Milne et al., 1996), agents which lead directly or indirectly to the induction of DSB (Keszenman et al., 1992). Since yeast employs HR to repair DSB under most circumstances, loss of Yku70 and Yku80 activity significantly hypersensitizes yeast cells to ionising radiation (IR) only when the HR is debilitated (Boulton and Jackson, 1996; Siede et al., 1996).

Mre11, Rad50, and Xrs2 (functional homologue Nbs1 in mammalian cells) form the MRX complex (Usui et al., 1998), which also binds DNA but without a requirement for DSB ends as with Ku (Trujillo et al., 2003). Unlike other yeast NHEJ core proteins, MRX is also involved in HR, suggesting a role to regulate repair pathway utilization (Bressan et al., 1999). MRX also plays a role in telomere maintenance (Tsukamoto et al., 2001) and DNA damage checkpoints (D'Amours and Jackson, 2002). In *S. cerevisiae*, the MRX complex is also essential to NHEJ (Boulton and Jackson, 1996; Moore and Haber, 1996). Disruption of the *RAD50*, *MRE11* or *XRS2* genes impairs NHEJ to the same degree as disruption of *YKU70*, *YKU80* or *DNL4*. However, studies using the fission yeast *Schizosaccharomyces pombe* and vertebrates suggest that NHEJ may be independent of this complex and these proteins are not functionally conserved in all eukaryotes (Harfst et al., 2000; Mansilla-Soto and Cortes, 2003).

Yeast DNA ligase IV is composed of Dnl4 (homologous to human Lig4) (Wilson et al., 1997) and Lif1 (XRCC4 in humans) (Herrmann et al., 1998). Dnl4 is a typical ATP-dependent DNA ligase with tandem C-terminal BRCT domains that interact with a central coiled-coil region of Lif1 (Herrmann et al., 1998; Dore et al., 2006a). This interaction is strong and physically stabilizes Dnl4 (Herrmann et al., 1998), but further actions of Lif1 are enigmatic. Unlike Ku and MRX with multiple functions, the only known function of DNA ligase IV is NHEJ. A third ligase-associated protein is Nej1 (XLF in humans) (Revy et al., 2006), which plays a further poorly defined supporting role through less stable interactions with the amino terminal globular head of Lif1 (Frank-Vaillant and Marcand, 2001). Nej1 is required for efficient NHEJ, while yeast *nej1* mutants have partial residual function in a chromosomal assay (Wilson, 2002).

Nej1 has been suggested to promote nuclear import of Dnl4/Lif1 (Valencia et al., 2001), although Dnl4 has an apparent nuclear localization signal.

Several interactions between these protein complexes have been identified and characterized, specifically between Yku80-Dnl4, Xrs2-Lif1, Mre11-Yku80, and Lif1-Nej1 (Palmbos et al., 2005; Deshpande and Wilson, 2007). More recently, studies using chromatin immunoprecipitation revealed the *in vivo* assembly of the NHEJ repair complex. Ku and MRX assemble at a HO-endonuclease-induced DSB independently and rapidly after DSB formation. Ligase IV appears at the DSB later than Ku and MRX and in a strongly Ku-dependent manner. Ligase binding is extensive but slightly delayed in *rad50* yeast. Ligase IV binding occurs independently of Nej1, but instead it promotes loading of Nej1. Interestingly, dissociation of Ku and ligase from unrepaired DSBs depends on the presence of an intact MRX complex and ATP binding by Rad50, suggesting a possible role of MRX in terminating a NHEJ repair phase and in repair pathway switching (Wu et al., 2008).

Other factors in yeast NHEJ

Deletion of the *SIR2*, *SIR3* or *SIR4* genes, which are involved in transcription silencing and telomere maintenance in yeast, may reduce the level of NHEJ (Tsukanoto 1997)(Taddei et al., 2005). Sir proteins are present at DNA damage sites and interact with Ku, indicating that they might influence the accessibility of the broken ends to DNA processing enzymes and /or to the Ku complex in NHEJ (Martin et al., 1999; Mills et al., 1999; Pastwa and Blasiak, 2003).

End Processing mediated by the nucleases and DNA polymerases may also be required beyond simple ligation in yeast, particularly when the DNA termini are damaged or not fully compatible. In *S. cerevisiae*, the gap-filling polymerase is likely to be Pol4, a member the functionally diverse PolX family. It has been shown that the *pol4* mutant displays no obvious sensitivity to a variety of DNA damage agents, including UV, IR, MMS and H_2O_2 (Prasad et al., 1993; McInnis et al., 2002). In contrast, it confers increased levels of meiotic recombination, probably due to elevated levels of meiosis-specific DSB, and an increased frequency of illegitimate mating (Prasad et al., 1993; McInnis et al., 2002).

Pol4 possesses a similar domain structure (BRCA1 carboxyl terminus-BRCT, lyase and nucleiotidyl transferase domains) to the mammalian X family polymerases λ and μ, which have been implicated in mammalian NHEJ (Ma et al., 2004) and can partially complement a yeast pol4 mutation (Daley et al., 2005a). Pol4, like Pol λ and Pol μ, also has unusual catalytic properties that can be summarized as a reduced dependence on a stable primer-template pairing (Bebenek et al., 2005; Nick McElhinny et al., 2005). *In*

vivo, Pol4 is required for NHEJ only at 3' overhangs where the primer is the weakly reannealed overhang (Wilson and Lieber, 1999; Daley et al., 2005a). The NHEJ function of these polymerases lies in part in their amino-terminal BRCT domains, which in Pol4 interacts with Dnl4 (Tseng and Tomkinson, 2002). The interaction stimulates the DNA synthesis activity of Pol4 and the ligation activity of Lig4/Lif1 to a less extent. Thus, the interaction couples to steps of the microhomology-dependent NHEJ, gap-filling and ligation.

Another protein involved in the end-processing step of NHEJ in *S. cerevisiae* is Rad27 (the homologue of mammalian FEN-1), a structure-specific nuclease that possesses flap endonuclease and 5' to 3' exonuclease activities (Harrington and Lieber, 1994a). The *rad27* mutant is viable and shows no growth defects when NHEJ, but not HR, is debilitated (Symington, 1998; Debrauwere et al., 2001), suggesting that the DNA lesions accumulated in the *rad27* strain are processed by HR or that Rad27 could be an integral part of NHEJ, or its sub-pathway(s). Consistent with this, *rad27* cells display greatly inhibited completion of DSBs (Holmes and Haber, 1999). Rad27 has been shown to interact physically and functionally with Pol4 and Dnl4/Lif1 (Tseng and Tomkinson, 2004), and *rad27* strains show reduced joining of DSBs whose overhangs form 5' flaps (Wu et al., 1999b). The activities of Rad27 and the Pol4 polymerase and ligase are apparently coordinated to achieve optimal filling and 5' processing in NHEJ.

Artemis has been implicated in processing NHEJ in mammals (Ma et al., 2002), but its closest yeast homologue, Pso2/Snm1, appears to be exclusively associated with crosslink and hairpin repair (Li and Moses, 2003; Yu et al., 2004). The Mre11 3' exonuclease is frequently invoked, but its only established substrates *in vivo* are hairpins and Spo11-bound meiotic DSBs (Moreau et al., 1999; Lobachev et al., 2002). Mammalian PNK restores 3' phosphates and 5' hydroxyls to a ligatable form and acts in NHEJ by interaction with XRCC4 (Koch et al., 2004). Its yeast homologue, Tpp1, surprisingly lacks both the 5' kinase and fork-head associated (FHA) domains and is not required for NHEJ of DSBs with 3' phosphates (Daley et al., 2005a). However, other proteins probably exist for end processing in yeast NHEJ.

1.8.3 NHEJ in Prokaryotes

Only recently, homologues of eukaryotic NHEJ proteins have been identified in prokaryotes (Aravind and Koonin, 2001; Doherty et al., 2001). In contrast to eukaryotic NHEJ, prokaryotes have a much simplified version, which is composed of two repair factors — Ku and ligase (Bowater and Doherty, 2006; Pitcher et al., 2007). Bacterial Ku genes are most widely distributed in proteobacteria, firmicutes and actinobacteria. However, Ku genes are not present in all bacteria and are conspicuously absent from

many widely studied bacterial strains, such as *E. coli* K12 (enterobacteria) (Bowater and Doherty, 2006). Many of the *ku* genes are organized into operons containg ATP-dependent DNA ligases, including euryarchaeote *Archaeoglobus fulgidus* (Aravind and Koonin, 2001; Doherty et al., 2001; Weller and Doherty, 2001).

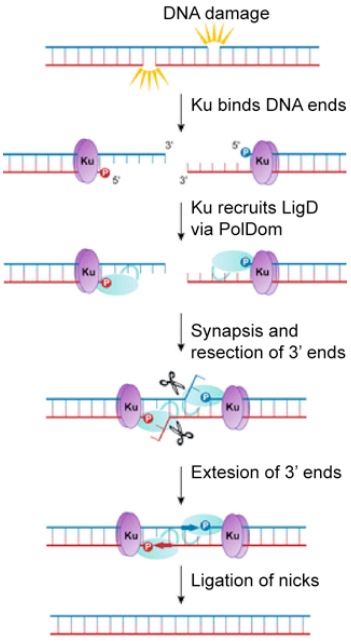

Figure 1.12 Mechanism of NHEJ repair in prokaryotes.

After the binding of Ku to 3'-protruding ends and further recruitment of LigD, it specifically recognizes the 5' phosphate (P) and directly mediates the synapsis event via a specific loop. After microhomology pairing, nonextenable 3' temini can be cleaved by the NucDom (nuclease domain) of LigD. Once the reqired nucleolysis has occurred, resynthesis by PolDom (primase/polymerisation domain) and ligation of nicks completes break repair (Pitcher et al., 2007).

The bacterial Ku proteins are approximately 30-40 kDa in size, much smaller than eukaryotic Ku complexes (70-80 kDa). In contrast to the heterodimeric Ku complex of eukaryotes, the bacterial Ku complexes are predominantly homodimeric in structure, forming dimers that also bind preferentially to the ends of DSBs (Weller et al., 2002).

Eukaryotes possess many proteins that are involved in DSB end processing to generate termini capable of being ligated. In contrast, prokaryotes have come up with a unique solution. In addition to a ligase domain, many of the prokaryotic Ku-associated ligase genes encode domains with end processing activities, including a polymerase that belongs to the PolX family, members of which include human Pol μ, Pol λ and TdT, implicated in gap-filling during NHEJ (Aravind and Koonin, 2001; Weller and Doherty, 2001). The NHEJ ligase Mt-LigD from *Mycobacteriun tuberculosis* possesses a remarkable variety of polymerase activities, including primase, terminal transferase and gap-filling polymerase activities (Della et al., 2004; Pitcher et al., 2005; Pitcher et al., 2007). A 3'-5' single-strand DNA exonuclease activitiy also resides in the Mt-ligase polypeptide that is capable of removing 3' overhangs (Della et al., 2004; Pitcher et al., 2005). Similar activities also reside in Pae-LigD, the homologue from *Pseudomonas aeruginosa* (Zhu and Shuman, 2005; Zhu et al., 2005).

In the two best-studied examples of the NHEJ ligases, Mt-LigD and Pae-LigD, the ancillary processing domains appear to be modular units (Gong et al., 2004; Gong et al., 2005; Pitcher et al., 2005; Zhu and Shuman, 2005; Zhu et al., 2005). Further analysis of genome sequence confirms this idea since homologous genes are organized in a variety of ways in different bacteria species (Bowater and Doherty, 2006). Additional complexity is observed in other organisms. For example, the genome of *Strepomyces coelicolor* encodes separate genes for nuclease, polymerase and ligase (Aravind and Koonin, 2001; Doherty et al., 2001; Bentley et al., 2002). Interestingly, Ku remains genetically associated with the polymerase in *Streptomyces coelicolor* and ligase in *Archaeoglobus fulgidus*, the only archaeal speices that is known to encode a Ku homologue so far (Aravind and Koonin, 2001; Doherty et al., 2001). Thus prokaryotes appear to have evolved a number of different solutions to provide a functional NHEJ pathway.

Reconstitution of bacterial NHEJ *in vitro*

The two-component NHEJ repair from *Mycobacterium tuberculosis* has been reconstituted *in vitro* (Weller et al., 2002; Della et al., 2004). Mt-Ku binds as a homodimer to the ends of dsDNA and specifically recruits the genetically associated LigD to the termini of DSBs, thereby stimulating the polymerase and end-joining activities of LigD (Weller et al., 2002; Pitcher et al., 2005). The NHEJ repair of complex DSBs can be fully reconstituted *in vitro* by the addition of Mt-Ku and Mt-LigD, and by Mt-LigD alone, if the ends of the break are annealed together. However, Mt-Ku is absolutely essential for the repair of discontinuous DSBs (Della et al., 2004).

The physical interaction between Ku and LigD (Pitcher et al., 2005) is mediated by PolDom (primase/polymerase domain) in mycobacteria *in vitro*; presumably this interaction is responsible for the sequestration of full-length LigD to Ku-bound DSBs *in vivo*. Most prokaryotic LigDs retain a PolDom, signifying that this mode of recruitment may be conserved. The PolDom-Ku subcomplex may serve a number of purposes in the NHEJ process, in addition to recruitment of LigD to DSBs. PolDom extension at the termini of breaks is enhanced by Ku (Pitcher et al., 2005). PolDom has a strong preference for binding to the terminal 5'-phosphate group at broken ends, suggesting that it may perform a direct role, together with Ku, in the synapsis process that brings DSB ends together. The Ku-PolDom subcomplex may also coordinate the order of processing and repair events at DSBs (Pitcher et al., 2005; Pitcher et al., 2007).

Reconstitution of bacterial NHEJ in Yeast

Some of the most compelling evidence that the Ku-LigD complex is solely responsible for bacterial NHEJ comes from genetic complementation experiments performed in *S. cerevisiae* (Della et al., 2004). Remarkably, ectopic coexpression of both Mt-LigD and Mt-Ku, but not the individual genes, resulted in complementation of yeast NHEJ-deficient strains (dnl4 and yku70), restoring NHEJ to 50% of wild-type yeast levels. Bacterial and yeast NHEJ could be differentiated on the basis of differing signature patterns of processed joints, with bacterial NHEJ preferentially forming a defined DSB repair joint, rarely observed in wild-type yeast, even when yeast NHEJ was active. The unique signature of bacterial processed joints confirmed that even in the absence of the yeast NHEJ apparatus, the bacterial proteins catalyzed the creation of intact chromosomes from two discontinuous DSB ends, suggesting that no other bacterial proteins are required for NHEJ.

1.9 Single Strand Annealing

Single strand annealing (SSA) is a minor repair pathway employed to repair double strand breaks (Ivanov et al., 1996; Paques and Haber, 1999). SSA was first proposed to explain results of intramolecular recombination in plasmid substrates introduced in *Xenopus laevis* oocytes or mammalian cells (Lin et al., 1984; Lin et al., 1990b; Lin et al., 1990a; Maryon and Carroll, 1991a; Maryon and Carroll, 1991b). Like non-homologous end joining (NHEJ), SSA is not a high fidelity repair pathway. Repeated sequences are required to be present either side of the break. The dsDNA ends of the DSB are then processed in the same manner as in other forms of HR to produce 3' ssDNA tails, and if these tails extend into the regions of homology, the formation of joint molecules is possible. After removal of the non-homologous ends and DNA synthesis, repair of the break is completed by DNA ligase. (Figure 1.13) The major disadvantage of this pathway of repair is that the sequence that is degraded between the two repeated sequences either side of the DSB is lost. If this sequence lies within a gene or other important region of DNA, the repair process itself can be mutagenic.

Studies in yeast indicated that the formation of deletions is delayed with increasing distance between the repeats, but is still possible at a distance of 15 kb and with repeats as small as 30 bp (Sugawara et al., 2000). Factors required for SSA have only been identified in *S. cerevisiae*. The removal of non-homologous 3'-single-stranded ends is dependent on the endonucleolytic activity of the Rad1/Rad10 complex and the presence of the Msh2 and Msh3 proteins (Ivanov and Haber, 1995; Saparbaev et al., 1996; Sugawara et al., 1997). When the length of the annealed region exceeds 1.2 kb, Msh2 and Msh3 are no longer required. Other known mismatch repair factors are not involved

in SSA. Another factor required for SSA is the Srs2 protein, which has 5'–3' helicase activity (Paques and Haber, 1997). An important role in SSA has been demonstrated for RAD52 and RAD59. In the absence of the Rad52 or Rad59 proteins, SSA is still possible, but at a drastically reduced level (Sugawara and Haber, 1992; Sugawara et al., 2000). The role of Rad52 annealing homologous ssDNA coated by RPA (Sugiyama et al., 1998) is in agreement with the SSA activity (Mortensen et al., 1996). In the absence of the MRX complex, SSA is possible but at a significantly reduced rate (Ivanov et al., 1996). Most likely this complex functions in the resection of the 5′-ends. In yeast, the SSA pathway has a minor role in the repair of X-ray-induced and bleomycin-induced DSBs, since *rad1* and *rad10* mutants are hardly sensitive to ionizing radiation or bleomycin (Moore, 1978). Similar results have been obtained in mammalian cells mutated in ERCC1 and XPF, the homologues of RAD10 and RAD1, respectively (Murray et al., 2002). However, mutations in the swi9 and swi10 genes in *Schizosaccharomyces pombe*, the homologues of RAD1 and RAD10, respectively, result in increased radiation sensitivity (Schmidt et al., 1989; Hang et al., 1996). The relative importance of SSA, therefore, differs between organisms.

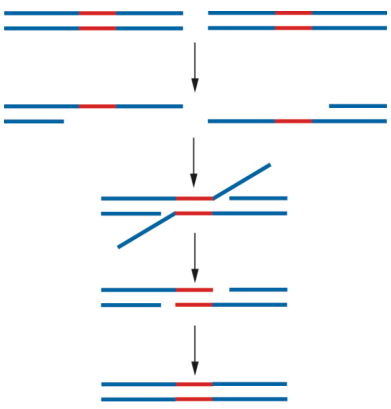

Figure 1.13 Schematic of the SSA.

Red boxes represent repeat sequences either side of the DSB. DNA ends at the break are resected to generate 3' ssDNA tails. exposure of regions of homology during resection of the 5'-ends allows formation of joint molecules. Repair of the DSB is completed by removal of non-homologous ends and ligation. As a consequence a deletion is introduced in the DNA.

1.10 Interstrand Crosslink Repair

1.10.1 Interstrand crosslinks

DNA interstrand crosslinks (ICLs) are one of the most deleterious DNA lesions. By covalently linking the Watson and Crick strands of the double helix, ICLs obstruct DNA replication and transcription (Dronkert and Kanaar, 2001; McHugh et al., 2001). ICL-inducing agents usually generate multiple types of DNA damage besides ICLs, such as DNA mono-adducts, intrastrand crosslinks, and DNA-protein crosslink. Although ICLs comprise only a small fraction of the induced damage, these are the

most cytotoxic and genotoxic lesions produced. Due to their high toxicity and selectivity against proliferating cells, a variety of ICL-inducing agents, including psoralens, cis-platinum and mitomycin C, are widely utilized in cancer chemotherapy (Dronkert and Kanaar, 2001; McHugh et al., 2001).

1.10.2 ICL repair in *E. coli*

ICL repair in *E. coli* has been characterized both genetically and biochemically. In the major pathway of ICL repair, nucleotide excision repair (NER) and homologous recombination (HR) work together to remove the ICL (Figure 1.14 A) (Van Houten, 1990). *In vitro*, repair starts with incisions by the NER enzymes UvrABC around the ICL in one DNA strand that 'unhook' and release the lesion in the form of an ologonucleotide still attached to the complementary strand by crosslinking agent (Van Houten et al., 1986). When a psoralen ICL is present, this is usually the strand with the furan ring. Incisions are at the ninth phosphodiester bond 5′ and the third bond 3′ to the ICL (Van Houten et al., 1986). Then, the 5′-exonuclease activity of DNA polymerase I generates a gap at the 3′ end of the ICL (Sladek et al., 1989). This yields an ssDNA region, which is necessary for RecA to initiate recombination. RecA performs strand exchange with intact homologous DNA resulting in heteroduplex DNA encompassing the region containing the cross-linked oligonucleotide (Sladek et al., 1989). As a result, a three-stranded region occurs with predominantly base pairing of the full-length strands. This enables UvrABC to incise the other DNA strand, containing the pyrone ring. Thereby, UvrABC enables release of the ICL-containing DNA fragment (Sladek et al., 1989). The resulting gap can be filled in by DNA polymerase I and ligated.

Repair in RecA-deficient strains is dependent on NER and DNA polymerase II (Figure 1.14 B) (Berardini et al., 1999). As in the major pathway, repair is initiated by the incision of UvrABC on one strand of the cross-linked DNA. DNA polymerase II synthesizes DNA across the region spanning the cross-linked oligonucleotide since recombination is impaired. Then, UvrABC removes the ICL by incisions in the complementary DNA strand. Thus, besides the major RecA-dependent recombination repair, a minor DNA polymerase II-dependent translesion repair pathway is capable of repairing ICLs.

Genetic studies have shown that bacteria deficient in NER protein UvrA and one of the recombination proteins, such as RecB, C, D, F, G, O, R are sensitive to ICL agents (Zdraveski et al., 2000). In addition, some ICL repair is seen in *uvr* mutants, which are unable to follow either of the pathways mentioned above. After replication is stalled due to the adduct, recombination repair or bypass may be induced without the need for UvrABC in the process, possibly using other nucleases (Vos, 1992).

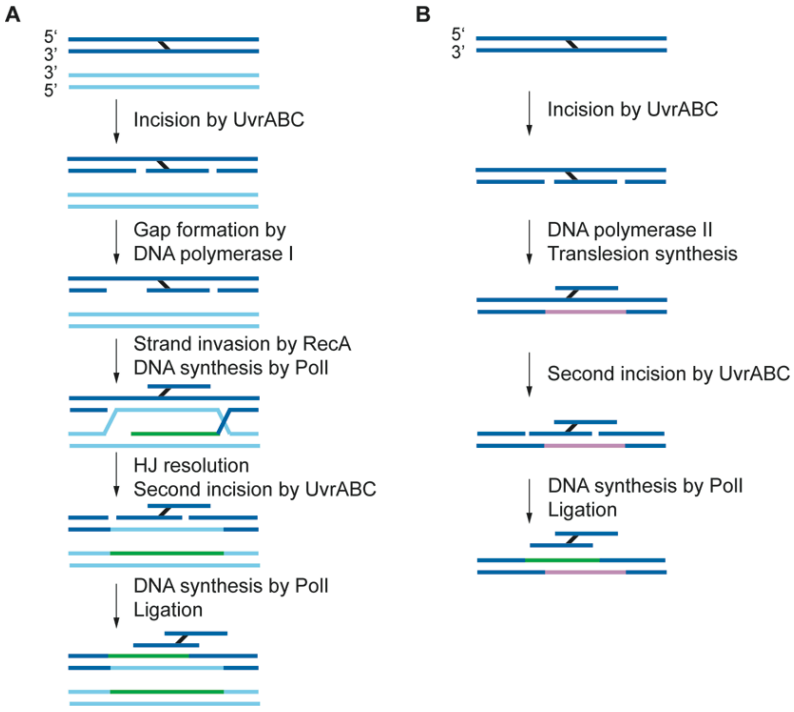

Figure 1. 14 ICL Repair in *E. coli.*

(A) Repair of the ICL by NER and HR. The NER enzymes UvrABC make incisions in one DNA strand both sides of the ICL lesion. The exonuclease activity of DNA polymerase I produces a ssDNA gap on the 3′ side of the ICL. This enables RecA to form a nucleoprotein filament on the ssDNA. The RecA nucleoprotein filament pairs with intact homologous dsDNA and performs strand exchange past the cross-linked oligonucleotide. Strand invasion of the damaged DNA into the homologous dsDNA initiates DNA synthesis. The resulting HJs are resolved to separate the two DNA molecules. To excise the cross-linked oligonucleotide, UvrABC incises the complementary DNA strand on both sides of the ICL. The remaining ssDNA gap in the chromosome is filled in by DNA polymerase I and ligated, resulting in the release of a cross-linked oligonucleotide. (B) Repair of the ICL by NER and TLS. First, UvrABC make incisions in one DNA strand both 5′ and 3′ to the ICL. Translesion DNA synthesis is performed by DNA polymerase II. A second round of NER releases the cross-linked oligonucleotide and restores the integrity of the DNA helix. The sister chromatids are shown in dark and light blue. The ICL is indicated by the black diagonal line connecting the DNA strands. Newly synthesized DNA by PolI is indicated in green. Translesion synthesized DNA by PolII is indicated in lavender.

1.10.3 ICL repair in *S. cerevisiae*

ICL repair in *S. cerevisiae* has not been characterized in as much detail as repair in *E. coli*. A large number of genes have been demonstrated to be involved in ICL repair. Most of these genes belong to one of the DNA repair pathways that process other types of lesions as well: NER, HR and post-replication/translesion repair (Dronkert and Kanaar, 2001; Grossmann et al., 2001; Saffran et al., 2004). Survival after treatment with ICL agents is also affected by mutations in BER (base excision repair) and MMR

(mismatch repair). BER can prevent the formation of ICLs by repair of precursor lesions (McHugh et al., 1999). Mismatch repair sensitizes cells to ICL agents as it interferes with translesion synthesis past monoadducts and intrastrand cross-links (Durant et al., 1999).

Apart from the genes that were already known to play a role in DNA repair, some genes involved in ICL repair have been identified by searching for mutations that sensitize yeast cells to ICL agents. For example, the *PSO* genes were identified in yeast mutants sensitive to photoactivated psoralens (Brendel et al., 2003). The *PSO2* gene has been well studied. Originally, the *SNM*1/*PSO*2 gene was identified independently in genetic screens for novel genes involved in the repair of ICLs produced by psoralen-UVA and nitrogen mustard (HN2), (Henriques and Moustacchi, 1980; Ruhland et al., 1981). The Pso2 protein is a member of the β-CASP metallo-β-lactamase superfamily of enzymes, which share a hydrolytic domain similar to that of the mRNA cleavage and polyadenylation specific factor, CPSF (Callebaut et al., 2002). Purified Pso2 is a 5'-3' dsDNA and ssDNA exonuclease (Li et al., 2005). One of the three human *PSO2/SNM1* paralogues, Artemis/hSNM1C is a ssDNA specific 5'-3' exonuclease involved in V(D)J recombination (Moshous et al., 2001). In addition, it has recently been reported that hSNM1A effectively suppresses the sensitivity of yeast *pso2* (*snm1*) disruptants to cross-linking agents (Hazrati et al., 2008)

S phase

In yeast, as with *E. coli*, NER is required for the 'unhooking' stage of ICL repair (Jachymczyk et al., 1981; Miller et al., 1982b). In contrast to bacteria, however, DSBs arise in the DNA of yeast cells treated with crosslinking agents. Both biochemical and cell biological evidence have shown that the DSB formation requires cell cycle progression into S phase, suggesting that DSBs are intermediates of ICL repair when replication forks are stalled at the unprocessed ICL or meet partially repaired (incised) ICL (Lehoczky et al., 2007). Yeast Mus81-Mms4, like mammalian Mus81-Eme1 is a structure-specific endonuclease with the preference of replication fork-like structures as the substrates *in vitro* (Bastin-Shanower et al., 2003) (See 1.11.1). Although human Mus81-Eme1 has been reported to be required for DSB formation after mitomycin C and cis-platin treatment (Ciccia et al., 2003), Mus81-Mms4 is not required for DSB formation during ICL repair in yeast (Lehoczky et al., 2007). There might be some redundancy in the processing of forks stalled by ICL.

In the exponential phase, *rad51* or *rad52* haploid cells are sensitive to ICL-inducing agents, such as cisplatin (Abe et al., 1994), HN2 and 8-Mop (McHugh et al., 2000), indicating the contribution of HR to ICL repair in cells passing through the S phase

(Figure 1.15). Ensuing repair of the one-sided DSBs near the ICL sites by HR may involve lesion processing by NER. A more complex scheme involves D-loop formation and DNA synthesis on the undamaged homologue prior to DNA strand invasion on the sister chromatid downstream of the blocking lesion, leading to damage tolerance (Li and Heyer, 2008).

In S phase cells, Pso2 has been demonstrated to be involved in ICL processing prior to DSB healing but downstream of NER incision (Barber et al., 2005). It has also been suggested that the 5'-3' exonuclease ExoI along with MMR factors (Msh2-Msh3 and Msh2-Msh6) are redundantly involved in the pathway that overlaps with Pso2. However, the substrates of these exonucleases are not clearly defined yet.

G_1 and G_2 phases

Post-replication repair (PRR) has been shown to be essential in the G_1 phase of the cell cycle (McHugh et al., 2000). PRR acts on damage in the context of DNA replication, allowing for bypass of replication fork-blocking lesions; this pathway, rather than removing lesions, permits replicating cells to tolerate the damage (Barbour and Xiao, 2003). Lesion bypass may be achieved by error-prone mechanisms, such as TLS by specialized DNA repair polymerase, or by error-free mechanisms, such as template switching (Figure 1.15). Strains lacking the PRR genes *RAD5*, *RAD6*, and *RAD18* did not have any crosslink-induced mutations but showed increased levels of recombination; *rad5* and *rad6* cells also had altered patterns of cross-link-induced gene conversion in comparison with repair-proficient yeast (Saffran et al., 2004). In addition, *rad6* and *rad18* cells have been observed to be highly sensitive to ICL-inducing agents throughout the cell cycle, suggesting that Rad6 and Rad18 play a central role to post-replication repair (PRR) in yeast (Barber et al., 2005). Rad6 is an E2 ubiquitin-conjugating enzyme and Rad18 is an E3 ubiquitin ligase, guiding substrate specificity. As a complex, Rad6-Rad18 regulates several distinct pathways of PRR and TLS via modification of PCNA (Friedberg et al., 2005; Ulrich, 2005). These include TLS by DNA polymerase ζ (Rev3 and Rev7) and /or Pol η (Rad30).

The absence of Rev3, which is the catalytic subunit of Pol ζ, decreases the survival fraction of stationary and G_1 phase cells, but not the exponential cells treated with HN2 (Sarkar et al., 2006). Unlike in mammalian cells, Rad30 (Pol η) cannot substitute for Rev3 in the ICL repair or tolerance in yeast (Grossmann et al., 2001; Shen et al., 2006).

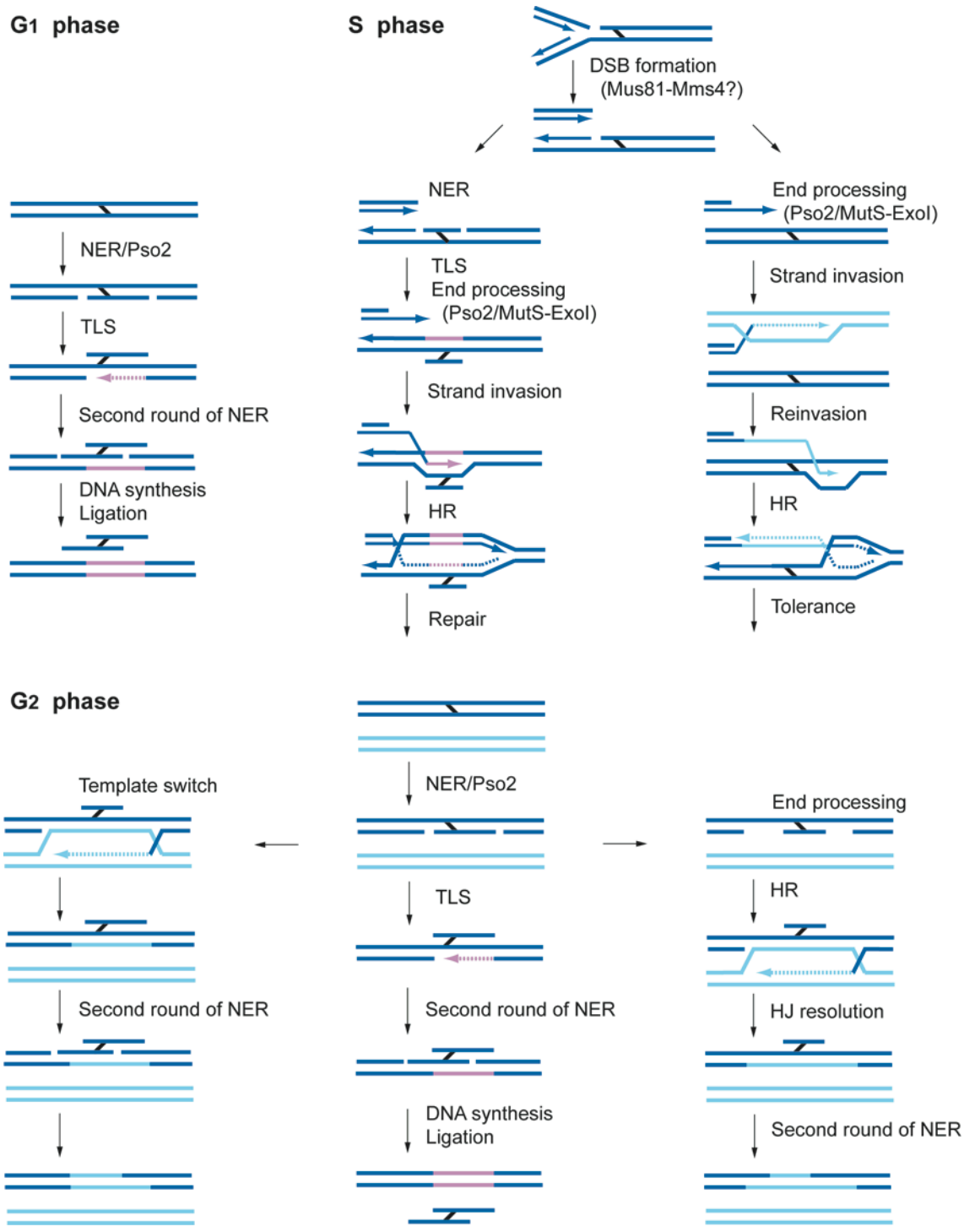

Figure1.15 Putative ICL repair pathways in *S. cerevisiae*.

Figure1.15 Putative ICL repair pathways in *S. cerevisiae*.

In the G_1 phase, NER introduces the incision on both sides of ICL lesion, followed by a Pso2 control step of end processing (Top left). Translesion DNA synthesis is performed by Pol ζ. A second round of NER releases the cross-linked oligonucleotide and restores the integrity of the DNA helix. In the S-phase, the presence of an ICL causes arrest of a replication fork. Incisions in the leading strand template next to the ICL produce a one-sided DSB. This step might be carried out by Mus81-Mms4. Introduction of a second incision on the other side of the ICL by NER allows the lesion to flip out and to be bypassed by TLS (Top middle). The DSB is processed (probably by Pso2 and MutS-Exo1) to form a 3'-OH ssDNA tail and to initiate strand invasion. The replication fork is restored and the lesion is bypassed by TLS. The lesion is eventually repaired, either after HR as drawn here or before the strand invasion. The DSB can also initiate DNA strand invasion using the homologue as a template. DNA is synthesized across the lesion, disengaged and reinvasion of the sister chromotid behind the lesion site can lead to restoration of the replication fork and tolerance of the ICL lesion (Top right). In the G_2 phase, the ICL lesion can be bypassed by NER and TLS as that in the G_1 phase (bottom middle). DNA can also be synthesized across the lesion by template switching. A second round of NER eventually repair the ICL lesion (bottom left). Alternatively, HR and a second round of NER repair the lesion after the 3' ssDNA invasion (bottom right). The ICL lesion is indicated by the black diagonal line connecting the DNA strands. The sister chromatids are shown in dark and light blue. Newly synthesized DNA is indicated by dashed line. Translesion synthesized DNA is indicated in lavender.

It has been suggested that following ICL incision, a 'classical' gap-filling reaction is attempted (by Pol δ) but blocked by the presence of the cross-linked moiety. This triggers the Rad6-Rad18-dependent monoubiquitination of PCNA at highly conserved K164, subsequently activates Rev1 and Pol ζ, leading to TLS past the incised ICL intermediate (Sarkar et al., 2006). Alternatively, an error-free pathway relying on another ubiquitin-conjugating complex Mms2-Ubc13, a further (putative) E3 ligase Rad5 and Rad18 might be involved (Wu et al., 2004).

In addition to PRR, yeast G_2 cells also carry out a recombination-dependent gap-filling step following ICL incision, analogous to the pathway established in *E. coli*, since an intact sister chromotid may be available. Instead, DNA can be synthesized across the lesion by template switching and NER can repair the ICL lesion eventually (Figure 1.15) (Dronkert and Kanaar, 2001; Barber et al., 2005).

Genetic studies have shown that NER genes and *PSO2* are epistatic with each other in yeast G_1 and G_2 cells (Barber et al., 2005; Friedberg et al., 2005; Ulrich, 2005). However, there is a clear ICL incision defect in NER mutants not observed in *pso2* mutants, suggesting a pathway consisting of NER incision followed by a Pso2-controlled step in this cell cycle phase (Magana-Schwencke et al., 1982; Grossmann et al., 2000). HR is not involved in yeast G_1-phase cells since *rad52* cells demonstrated no increase in HN2 sensitivity over that of the wild-type (McHugh et al., 2000). In contrast, an increased sensitivity of both NER-defective and *pso2* cells has been observed upon deletion of *rad52* in HN2 treated yeast G_2 cells (Barber et al., 2005). Therefore, a HR-dependent ICL repair does function when NER and Pso2 fail and the initial ICL incision or nucleolytic processing prior to HR can be NER independent.

1.10.4 ICL Repair in Mammalian Cells

As in yeast, mammalian ICL repair involves proteins from NER, HR and TLS pathways, although the pathways are incompletely understood at present (Dronkert and Kanaar, 2001; McHugh et al., 2001). A number of genes involved in mammalian ICL repair, for example, *RAD6* (Koken et al., 1991), *RAD18* (Tateishi et al., 2000; Xin et al., 2000), *RAD54* (Kanaar et al., 1996), *SNM1* (Grombacher et al., 1999), *REV3* (Gibbs et al., 1998; Xiao et al., 1998b) and *REV7* (Murakumo et al., 2000) have been identified by their sequence homology to yeast genes.

An important step, dual incision around the lesion (or unhooking of the lesion), has been proposed to be accomplished by the XPF-ERCC1 endonuclease (Kuraoka et al., 2000). A structure-specific endonuclease related to XPF-ERCC1, Mus81-Eme1 was recently identified to be required for DSB formation after mitomycin C and cis-platin

treatment (Ciccia et al., 2003). Mus81-Eme1 exhibits a high specificity for synthetic replication fork structures and 3'-flaps *in vitro* (Ciccia et al., 2003). A third nuclease with a specific function in ICL repair is Pso2/Smn1. The protein exhibits a 5'-3' DNA exonuclease activity, which is required after DSB formation (Bessho et al., 1997a; Li et al., 1999; Mu et al., 2000; Demuth et al., 2004). Unlike mammalian Mus81 or XPF-deficient cells that are sensitive to several ICL-inducing agents (De Silva et al., 2000; Chen et al., 2004; Niedernhofer et al., 2004; Hanada et al., 2006; Clingen et al., 2007), mouse *smn1*$^{-/-}$ cells were sensitive only to mitomycin C but not other ICL agents (Dronkert et al., 2000). In yeast, however, *pso2/smn1* mutants display sensitivity to a spectrum of ICL agents (Lehoczky et al., 2007).

There are some other differences between ICL repair in yeast and mammals. Yeast NER mutants all show a similar sensitivity to ICL agents (Friedberg et al., 1995b). In contrast, most NER mutant hamster cell lines show only a moderate sensitivity to ICL agents, while cell lines with a mutation in *ERCC1* and *XPF/ERCC4* (the mammalian homologues of *RAD10* and *RAD1*, respectively) are very sensitive to ICL agents (Damia et al., 1996). For example, severe symptoms like liver abnormalities, development delay, reduced lifespan and signs of premature senescence are typically observed with XPF or ERCC1 deficiency mice but are absent in NER-deficient XPA and XPC knockout mice (McWhir et al., 1993; Tian et al., 2004). A human deficiency in the ERCC1 gene was recently reported (Jaspers et al., 2007). The patient's cells show only mild repair defect to UV light and mitomycin C as compared to XP patient, while the clinic features are very severe. This discrepancy, in agreement with the observations of XPF and ERCC1 deficiency mice, suggests other functions for XPF-ERCC1 outside of NER (See 1.11.1).

Cell processes in mammals are often more complex than those in yeast, which is also reflected in the increased number of proteins involved mammalian ICL repair. Some yeast proteins, such as Rad6 (Koken et al., 1991), Rad23 (Masutani et al., 1994), Rad30 (McDonald et al., 1999), Rad51 (Thacker, 1999) and Snm1 (Dronkert et al., 2000), have more than one homologue/paralogue in mammalian cells. In addition, no homologues have been identified in yeast for some proteins involved in mammalian ICL repair, for example, the Fanconi anemia proteins (an exception being the FANCM homolog Mph1) (Patel and Joenje, 2007).

Fanconi Anemia

Fanconi anemia (FA) is a rare, recessive chromosomal-instability disorder and characterized by congenital abnormalities, bone marrow failure and a hypersensitivity to DNA interstrand cross-linking agents (Clarke et al., 1998). The genes for 13 known FA

complementation groups (called *FANC* genes) have now been identified (Patel and Joenje, 2007). A nuclear E3 mono-ubiquitin ligase core complex, including FANCA, B, C, E, F, G, L, M, and FAAP24, ubiquitylates the FANCD2-FANCI complex upon encountering stalled replication forks (Smogorzewska et al., 2007). This modification leads to colocalization of FANCD2-FANCI with HR proteins in DNA damage-induced foci together with BRCA2 (corresponding to FANCD1) possibly in conjunction with its interacting partner FANCN (PALB2). FANCJ has previously been identified as the DNA helicase BACH1/BRIP with a 5'-3' polarity and also functions downstream of FANCD2 ubiquitylation (Levitus et al., 2005). The role of BRCA2 in Rad51 filament formation (Chen et al., 1999b) (also see 1.6.4) and the physical interaction of FANCJ with RPA (Gupta et al., 2007), are consistent with a possible role in an early step in HR leading to the formation of the presynaptic Rad51 filament on ssDNA.

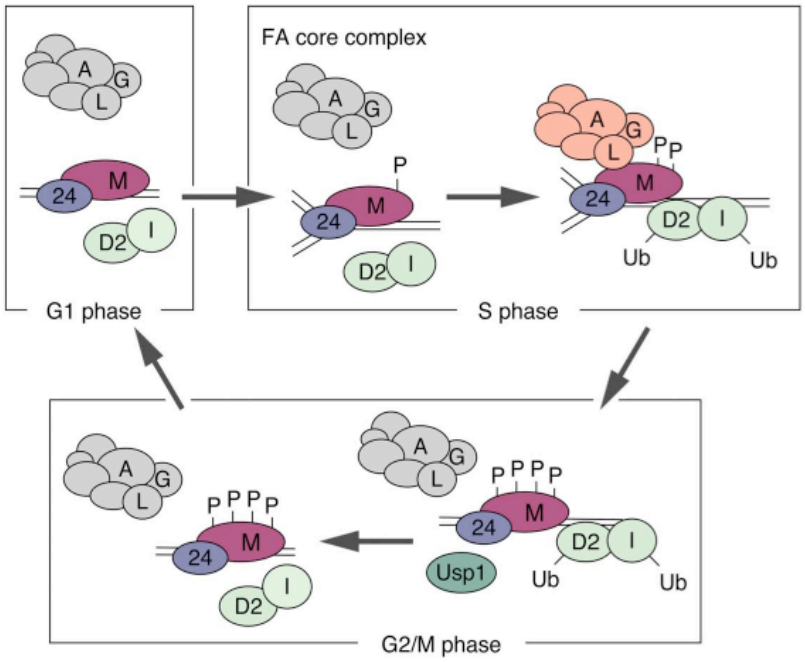

Figure 1.16 A model for the recruitment of the FA complex.

The FANCM/FAAP24 complex is associated with chromatin throughout the cell cycle. Early in the cell cycle (G_1 phase), the FA core (A/B/C/D/E/F/G/L complex) is assembled but does not associate with FANCM/FAAP24 complex in chromatin. In S phase, phorsphorylated FANCM can recruit the FA complex to chromatin, possibly to replication forks, and induce E3 ubiquitin ligase activity, resulting in monoubiquitination of FANCD2 and FACNI. In G_2/M phase, hyperphosphorylated FANCM may promote the release of the FA core complex, and USP1 may deubiquitinate FANCD2 and FANCI monoubiquitation (Kim et al., 2008).

FANCM is homologous to the archaeal protein Hef (helicase-assiciated endonuclease for fork-structured DNA) and is a member of XPF superfamily (see 1.10.1). FANCM and FAAP24 (Fanconi anemia-associated protein 24 kDa) form a heterodimer, which is required for activation of the FA core complex to ubiquitylate FANCD2-FANCI (Meetei et al., 2005; Ciccia et al., 2007; Xue et al., 2008). Although the N-terminal part of FANCM is homologous to the superfamily 2 DNA helicases, biochemical studies have shown that it is rather a dsDNA translocase (Meetei et al., 2005). Consistent with this, FANCM constitutively localizes to chromatin (Kim et al., 2008). Recent studies have shown that phosphorylation of FANCM is regulated during the cell cycle (Kim et al., 2008). FANCM is moderately phosphorylated during S phase, extensively phosphorylated during mitosis and dephosphorylated after mitotic exit. Interestingly, FANCM is also phosphorylated following DNA damage. It has been proposed that FANCM is a sensor for stalled forks, and this specificity could be provided by FAAP24 that preferentially binds to splayed DNA (Meetei et al., 2005; Ciccia et al., 2007). Chromatin localization of FA core complex is regulated by the phorsphorylation level of FANCM (Figure 1.16). Depletion of FAAP24 leads to the defective recruitment of the FA core complex to chromatin (Niedernhofer, 2007; Kim et al., 2008). Notably, FANCM and FAAP24 are the only two core complex factors that interact directly with DNA. Taken together, these data suggested that FANCM is an anchor required for recruitment of the FA core complex to chromatin, and the FANCM/FAAP24 interaction is essential or this chromatin–loading activity.

1.11 Structure-specific endonucleases

The purpose of this PhD project is to study the two structure-specific endonucleases Hef and Fen1 in *H. volcanii.* Structure-specific endonucleases play important roles for DNA processing. During DNA metabolism, double-stranded DNA inevitably forms three-way (replication fork) and four-way (Holliday) junctions, bubbles (melted base pairs), flaps (single-stranded branch), or broken ends with single-stranded extensions. These irregular structures must be correctly processed by helicases and nucleases to successfully complete DNA replication, recombination and repair (Friedberg et al., 1995b). Two different families of structure-specific endonucleases, the XPF/Rad1/Mus81/Hef family and the FEN1/Rad27/XPG family, have been identified. Each of these families processes DNA bubbles, flaps and single stranded extensions with unique polarity, 5' or 3' (Table 1.2).

Structure-specific endonuclease		3' polarity	5' polarity
Eukaryotes	*Homo sapiens*	XPF-ERCC1; MUS81-EME1	FEN1; XPG
	Saccharomyce scerevisiae	Rad1-Rad10; Mus81-Mms4	Rad27; Rad2
	Schizosaccharomyces pombe	Rad16-Swi10; Mus81-Eme1	Rad2; Rad13
Archaea	*Aeropyrum pernix*	XPF (homodimer)	FEN1 (XPG)
	Sulfolobus solfataricus	XPF (homodimer)	FEN1 (XPG)
	Pyrococcus furiosus	Hef (homodimer)	FEN1 (XPG)

Table 1.2 Structure-specific endonucleases in the principal organisms studied.

Eukaryotes have at least two 3' and two 5' structure-specific endonulceases. By contrast, archaea have only one 3' and one 5' structure-specific endonulceases. The non-catalytic partners of the eukaryotic 3' structure-specific endonucleases are shown in blue.

1.11.1 XPF/ /Mus81/Hef

XPF, Rad1, Mus81 and Hef are one group of structure-specific endonucleases that play important roles in the repair of DNA lesions caused by UV light or DNA cross-linking agents (Ciccia et al., 2008). Members of the XPF/Mus81/Hef protein family are present throughout the eukaryal and archaeal domains but are not found in bacteria. Most eukaryotes have four family members that assemble into two distinct heterodimeric complexes, XPF-ERCC1 and MUS81-EME1. Each complex contains one catalytic and one non-catalytic subunit (Figure 1.18) and exhibits endonuclease activity with a variety of DNA substrates (Figure 1.19). Eukaryotic XPF proteins cleave at the 5' side of bubbles around DNA lesions, while Mus81 proteins cleave at similar sites of fork, nicked Holliday junction and 3' flap structures. The catalytic subunits share a characteristic core containing an ERCC4 (excision repair cross cmplementary group 4) nuclease domain and a tandem helix-hairpin-helix $(HhH)_2$ domain. Diverged domains are present in the noncatalytic subunits and may be required for substrate targeting. Vertebrates possess two additional family members, FANCM and FAAP24, which possess inactive nuclease domains (See 1.10.4). Archaeal XPF/Mus81/Hef homologues are closer in sequence and structure to XPF-ERCC1 but are functionally akin to MUS81-EME1 in their preference for 3' flaps, forks and other branched structures. Despite their homodimeric quaternary structure, archaeal XPF/Mus81/Hef endonucleases require only a single active site for nuclease activity, consistent with their eukaryal counterparts.

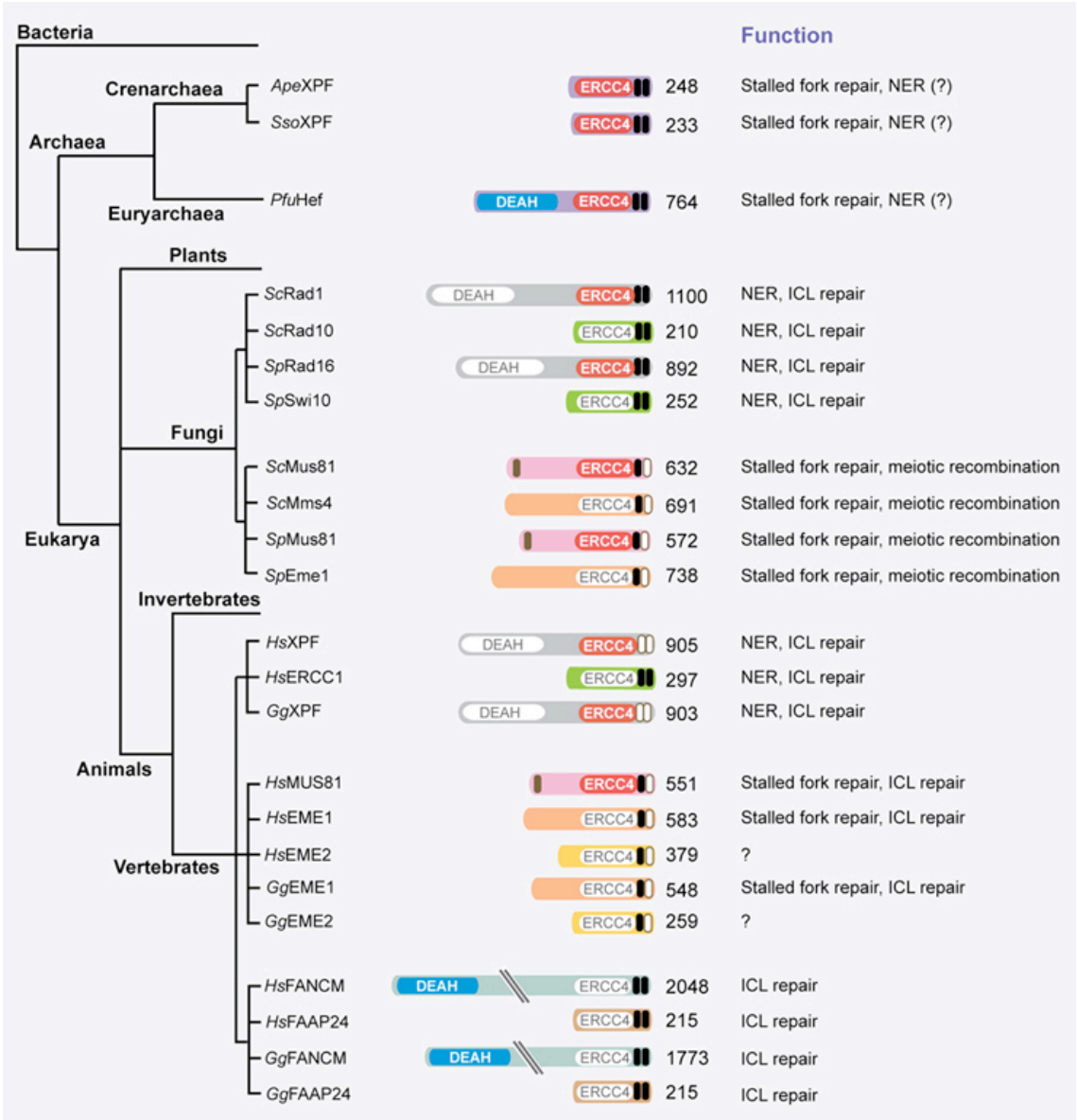

Figure 1.17 Evolutionary tree of the XPF and MUS81 family.

The domain organization and some functions of the archaeal and eukaryotic members of the XPF and MUS81 family are indicated. Orthologs are indicated with similar colors. Superfamily 2 DEAH helicase domains (*blue*), excision repair cross complementation group 4 (ERCC4) nuclease domains (*red*), and HhH motifs (*black ovals*) are indicated. Inactive DEAH and ERCC4 domains and pseudo-HhH motifs are labeled. Abbreviations: ICL, interstrand cross-link; NER, nucleotide excision repair (Ciccia et al., 2008).

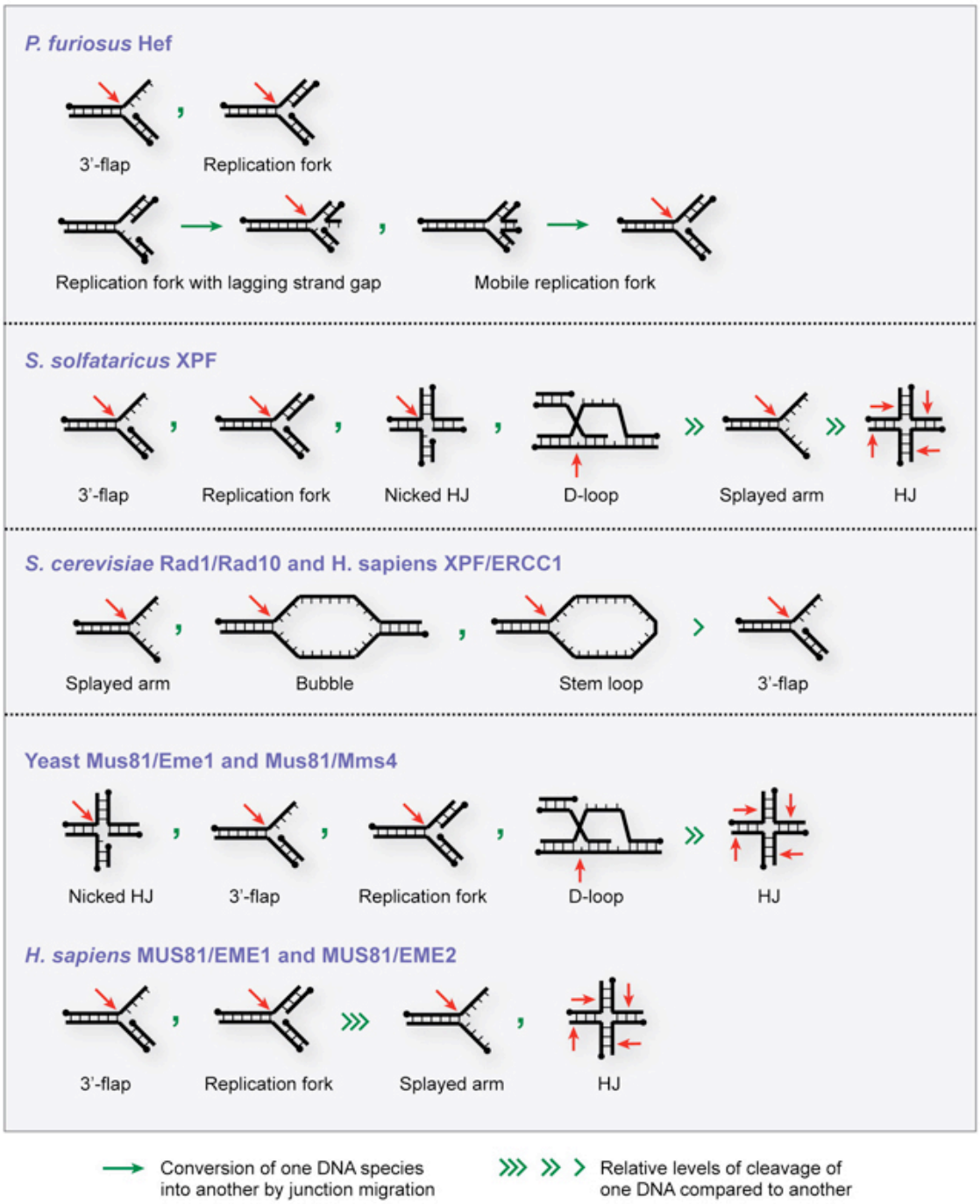

Figure 1.18 Substrate specificity of members of the XPF/MUS81 family.

Schematic representation of the substrates that are cleaved in vitro by various XPF/MUS81 family proteins. A red arrow indicates the approximate sites of cleavage within each DNA structure. Preferential cleavage of one particular substrate over another is indicated by > and >>. Substrates cleaved with equal efficiency are separated by commas. Black circles indicate 5' termini. Green arrows indicate conversion of one DNA species into another by junction migration. Abbreviations: HJ, Holliday junction; *H. sapiens*, *Homo sapiens*; *P. furiosus*, *Pyrococcus furiosus*; *S. cerevisiae*, *Saccharomyces cerevisiae*; *S. solfataricus*, *Sulfolobus solfataricus* (Ciccia et al., 2008).

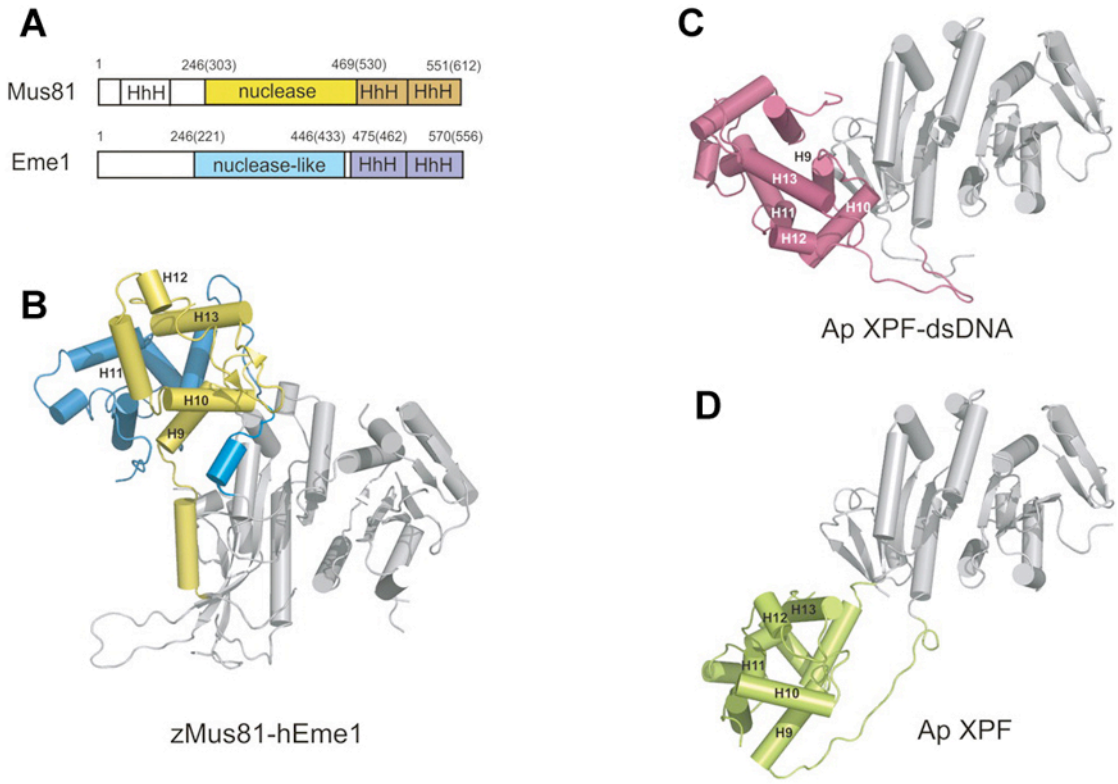

Figure 1.19 Structural comparison between cMUS81N and Ap XPF.

(A) Schematic representation of Mus81 an Eme1. Residue numbers of human and zebrafish (in parentheses) proteins are shown. The colored region represents the construct used for crystallization. Overall structures of the cMUS81N complex (B), the Ap XPF-dsDNA complex (C), and apo Ap XPF (D) are shown. The nuclease domains (gray) from three structures are in the same orientation, and the rest of the structures including the HhH2 domains of each structure are colored yellow and blue (zMus81N and hEme1N), pink (Ap XPF-dsDNA) and green (apo Ap XPF). Equivalent secondary structures among three structures are numbered from H9 to H13 (Chang et al., 2008).

XPF/RAD1

Eukaryotic XPF family members have an N-terminal SF2-like helicase domain and a C-terminal nuclease domain, followed by a DNA-binding domain containing two consecutive helix-hairpin-helix HhH motifs (McCutchen-Maloney et al., 1999; Shao and Grishin, 2000). The helicase domain apparently lacks essential catalytic residues for ATPase activity, such as KT in ATPase A motif and DE in ATPase B motif (Sgouros et al., 1999). The nuclease domain contains the active site motif GDXnERKX$_3$D related to prokaryotic endonucleases, which is thought to be involved in metal-dependent nuclease activities, as revealed by mutagenesis and biochemical analysis of XPF (Enzlin and Scharer, 2002). The two HhH motifs form a compact (HhH)$_2$ domain that has been

implicated in non-sequence specific DNA binding and was found to be present in many DNA break processing enzymes (Doherty et al., 1996; Sijbers et al., 1996), including the structure-specific DNA nucleases FEN1 and XPG (Harrington and Lieber, 1994b; Lieber, 1997).

Human XPF (xeroderma pigmentosa complementation group F, also known as ERCC4) associates with a noncatalytic partner ERCC1 (excision repair cross complementation group 1) to form a structure-specific endonuclease that preferentially cleaves DNA duplexes adjacent to a 3' single-stranded flap (Sijbers et al., 1996). DNA substrates containing ds/ssDNA junctions, such as bubbles, simple Y structures and hairpins, can be cleaved by ERCC1-XPF (de Laat et al., 1998a). The proper complex formation through the C-terminal binding domains of XPF (amino acid residues 814-905) and ERCC1 (amino acid residues 224-297) is required for the stability of the two proteins (de Laat et al., 1998b). The mammalian XPF-ERCC1 endonuclease, like its *S. cerevisiae* homologue Rad1-Rad10, is involved in nucleotide excision repair (NER) (Davies et al., 1995; Sijbers et al., 1996), gene targeting (Paques and Haber, 1999; Adair et al., 2000; Niedernhofer et al., 2001) and single strand annealing (SSA) (Sargent et al., 1997; Sargent et al., 2000; Al-Minawi et al., 2008). It has also been reported that XPF-ERCC1 is involved in telomere stability (TRF2 prevents NHEJ at telomeres through protection of the telomere overhang from XPF-ERCC1)(Zhu et al., 2003). Rad1-Rad10 has also been reported to process of blocked 3' termini in *S. cerevisiae* (Guzder et al., 2004). Further, Rad1-Rad10 together with mismatch repair proteins repair mismatched loops during meiosis recombination (Kirkpatrick, 1999). Similarly, XPF-ERCC1 homologues are involved in meiosic recombination in *Drosophila melanogaster* (Sekelsky et al., 1995) and in mating-type switching in *Schizosaccharomyces pombe* (Carr et al., 1994).

Compared to cells deficient in other NER proteins (XPA, XPG, CSB), XPF or ERCC1 deficient cells are highly sensitive to interstrand cross-linking agents, such as psoralen (Zhang et al., 2000), cispaltin (Damia et al., 1998) and mitomycin C (Kuraoka et al., 2000). XPF-ERCC1 can incise ICL containing DNA *in vitro* and has been suggested to carry out one essential step during ICL repair, converting ICLs to DSBs (Bessho et al., 1997b; Kuraoka et al., 2000). Deficiency of incision produced by XPF-ERCC1 has been observed in FA complementation group A, B, C, D_2, F and G cells, which are sensitive to interstrand cross-linking agents (Kumaresan and Lambert, 2000; Kumaresan et al., 2007). However, De Silva and colleagues showed that there is no clear relationship between initial incision at ICLs induced by cisplatin and cellular sensitivity, suggesting that the sensitivity of XPF and ERCC1 deficient cells probably results from a defect other than in excision repair (De Silva et al., 2002). Later Niedernhofer and colleagues

found that XPF-ERCC1 is required to resolve DNA ICL-induced double strand breaks (Niedernhofer et al., 2004).

Mus81

Mus81 (Methyl methansulfonate UV sensitive) is conserved in all eukaryotic organisms and shares sequence similarity with human XPF and yeast Rad1 endonucleases. Mus81 is a structure-specific endonuclease that works as a heterodimer with Eme1 (essential meiotic endonuclease 1, human and *Schizosaccharomyces pombe*) or Mms4 (*S. cerevisiae* (Mullen et al., 2001; Bastin-Shanower et al., 2003; Ciccia et al., 2003; Ogrunc and Sancar, 2003; Whitby et al., 2003). Sequence analysis suggests that Mus81 protein contains a nuclease domain, which is flanked by single HhH motifs (Interthal and Heyer, 2000). Thus, it was speculated that the Mus81 proteins might have different domain organization from crenarchaeal XPF family members, which possess a nuclease domain followed by two HhH motifs. However, the crystal structure of the hMus81ΔN (human Mus81ΔN) and cMus81ΔN-Eme1ΔN (chimeric complex of zebrafish Mus81ΔN and human Eme1ΔN) complex have revealed that both Mus81ΔN and Eme1ΔN contain nuclease and $(HhH)_2$ domains, displaying similar domain organization to that of XPF family members (Chang et al., 2008). When the nuclease domain of cMus81 is superimposed on the equivalent domain of DNA bound XPF of crenarcheaon *Aeropyrum pernix* (Ap XPF, (Newman et al., 2005)), the $(HhH)_2$ domain is rotated and twisted by 45° and 30°, respectively. Compared with that of apo Ap XPF, the $(HhH)_2$ domain of cMUS81 is rotated by 60° (Figure 1.19).

Two-hybrid experiments have revealed that Mus81 interacts with the checkpoint kinase Cds1 in *Schizosaccharomyces pombe* (Boddy et al., 2000) and the Rad54 recombination protein in *S. cerevisiae* (Interthal and Heyer, 2000), suggesting that the protein plays some roles in recombination and checkpoint signalling. Furthermore, yeasts, lacking both Mus81 and *E. coli* RecQ homologue Sgs1 (*S. cerevisiae*)/Rqh1 (*Schizosaccharomyces pombe*), are synthetic lethal, highlighting its importance in genome integrity and in the replication and recombination process (Boddy et al., 2000; Mullen et al., 2001). Recently, Sgs1 has been reported to limit the formation of aberrant joint molecule recombination intermediates that are otherwise resolved by Mus81-Mms4 (Jessop and Lichten, 2008; Oh et al., 2008).

The Mus81 complex, partially purified from yeast and human cells using the affinity tag, was shown to cleave synthetic Holliday junctions *in vitro* (Boddy et al., 2001; Chen et al., 2001b). However, the recombinant yeast Mus81 complex, expressed in *E. coli* or *S. cerevisiae*, preferred synthetic fork structures as cleavage substrates to the Holliday junction (Doe et al., 2002; Bastin-Shanower et al., 2003; Whitby et al., 2003; Ehmsen

and Heyer, 2008). Similar substrate preference was also observed in the partially purified and recombinant human Mus81-Eme1 complex (Constantinou et al., 2002; Ciccia et al., 2003). These data suggest that Mus81 cleaves stalled replication forks rather than HJs in mitotic cells and promotes meiosis recombination by removing 3' flaps during recombinant formation (Hollingsworth and Brill, 2004).

Yeast *mus81* mutants are sensitive to agents such as hydroxyurea, UV light, methylmethane sulfonate and camptothecin, which can stall replication forks, but not to ionizing radiation and bleomycin, which introduce DNA double strand breaks (Xiao et al., 1998a; Interthal and Heyer, 2000; Doe et al., 2002). Reduction in crossover recombinants has been observed in *mus81* mutant of *Schizosaccharomyces pombe* (7- to 25-fold) and in *mms4* mutant of *S. cerevisiae* (2-fold) (de los Santos et al., 2001). Mus81 has also been shown to be essential for sister chromatid recombination at broken replication forks in *Schizosaccharomyces pombe* (Roseaulin et al., 2008). These genetic analyses also support the function of the Mus81 complex in meiosis and stalled replication fork rescue.

Recently, Mus81 has been reported to be involved in generating the ICL-induced DSBs in mouse embryonic stem (ES) cells in S phase. In addition, *Mus81*$^{-/-}$ *Rad54*$^{-/-}$ ES cells were as hypersensitive to ICL agents as *Mus81*$^{-/-}$ cells, suggesting that Mus81-Eme1 and Rad54-mediated homologous recombination are involved in the same DNA replication-dependent ICL repair pathway (Hanada et al., 2006).

Archaeal XPF/Hef

The archaeal XPF homologues exhibit two distinct forms (Figure 1.17). In crenarchaea, the XPF gene encodes only the C-terminal nuclease and $(HhH)_2$ domains of approximately 240 amino acids, for example, the XPF homologue from *Sulfolobus solfataricus* (SsoXPF). However, SsoXPF has a pronounced preference for Mus81-type substrates such as 3' flaps, nicked four way junctions and D loops (Roberts and White, 2005a). Further biochemical studies have shown that SsXPF can digest a nicked DNA strand processively over at least 60 nt in a 3'-5' direction and can remove blocked 3' DNA termini and varied types of DNA lesions, such as CPD and fluorescein (Roberts and White, 2005b). Moreover, SsXPF displays a requirement for a functional interaction with the archaeal sliding clamp PCNA (Roberts et al., 2003) and an inhibition by ssDNA-binding protein SsoSSB (Roberts and White, 2005b). The XPF homologue from *Aeropyrum pernix* (ApeXPF) has a similar domain organization to SsoXPF. Both the nuclease and $(HhH)_2$ domains of ApeXPF form tightly associated dimer independently. Structural studies of ApeXPF in the presence and absence of dsDNA has revealed a large domain movement on binding dsDNA and suggested a model for XPF substrate recognition (Newman et al., 2005). In this model, the

downstream duplex is engaged by one $(HhH)_2$ domain and the upstream duplex by the other. The strand linking the two duplexes engages the hydrophobic strip in the nuclease domain, resulting in generation of a small stretch of unpaired ssDNA in the substrate strand, which is cleaved in the nuclease active site.

In euryarchaea, XPF is present as a helicase:nuclease fusion as in eukaryotes, with a polypeptide length of 700-800 amino acids. XPF from *Pyrococcus furiosus*, which is also known as Hef (helicase-associated endonuclease for fork-structured DNA), consists of two distinctive domains that are similar to DEAH helicase family and XPF nuclease superfamily, respectively (Komori et al., 2002; Nishino et al., 2003). The C-terminal nuclease domain is further divided into a compact catalytic nuclease subdomain and an $(HhH)_2$ subdomain, both of which are required for the homodimer formation and full cleavage activity for fork-structured DNA (Nishino et al., 2003; Nishino et al., 2005a). Biochemical characterization of each purified domains showed that these proteins have a specific affinity for branched DNA structures, with a strong preference of the forked structure (Komori et al., 2002). The N-terminal domain possesses an ATP-dependent helicase activity that specifically unwinds HJs and fork-structured DNA, while the Hef nuclease also does not act on HJs. However, the full length Hef can convert the HJ to the fork structure and introduce an incision dependent on the 5'-end of the nascent lagging strand (Komori et al., 2004). Further, structural and biochemical studies revealed that a positively charged extra region between the two conserved helicase regions, structurally similar to the "thumb" domain of DNA polymerase, plays critical roles in fork recognition (Nishino et al., 2005b).

1.11.2 FEN1//XPG

Another family of structure-specific nucleases is exemplified by the XPG and FEN1 homologues, which have remarkably different sequences from those of the XPF/Rad1/Mus81/Hef family and opposite cleavage polarity (Lieber, 1997).

XPG/Rad2

Human XPG (xeroderma pigmentosa complementation group G) belongs to the Fen1 family structure-specific nucleases and cleaves artificial DNA structures that contain ss/dsDNA junctions including bubbles, splayed arms, stem loops and flap substrates (O'Donovan et al., 1994; Cloud et al., 1995; Evans et al., 1997a). In *S. cerevisiae,* the homologue of human XPG is Rad2 (Habraken et al., 1996).

In mammalian NER, XPG cleaves on the 3' side of DNA lesions, while XPF-ERCC1 cleave on the 5' side (Evans et al., 1997a). Within NER, XPG also fulfil its roles that are independent from its nuclease activity in the opening of the DNA helix around the lesion and the formation of a stable damage recognition complex (Evans et al., 1997a;

Mu et al., 1997). The physical presence but not the catalytic activity of XPG is also required for the 5' incision by XPF-ERCC1 (Wakasugi et al., 1997). Moreover, XPG leads to PCNA recruitment and stabilization (Mocquet et al., 2008).

In addition to NER, XPG has been implied to function in the transcription-coupled repair of oxidative DNA damage and likely also in efficient RNA polymerase II-mediated transcription, which is independent of its nuclease activity (O'Donovan et al., 1994; Iyer et al., 1996; Klungland et al., 1999; Le Page et al., 2000; Shiomi et al., 2001; Lee et al., 2002). Two inherited human syndromes are associated with deficiencies in XPG: xeroderma pigmentosum (XP) and Cockayne syndrome (CS) (Clarkson, 2003; Lehmann, 2003). Studies on XPG mutants suggested that the nuclease activity of XPG is important for NER, whereas the involvement of XPG in transcription-coupled BER and transcription requires binding of XPG to specific DNA structures but not its nuclease activity (Nouspikel et al., 1997). Furthermore, NER is not essential for the viability of an organism, while complete loss of XPG function is lethal in mice (Shiomi et al., 2004).

Fen1/Rad27

Flap endonuclease 1 (FEN1) is a structure-specific endonuclease involved in DNA replication, recombination and repair (Liu et al., 2004a). It plays a critical role in maintaining human genome stability. Functional deficiency of FEN1 is predicted to cause genetic diseases and cancers (Shen et al., 2005; Zheng et al., 2007).

The best-known biochemical activity of FEN1 is its 5'-flap endonuclease (FEN) activity. Structural studies on euryarchaeal FEN1 from *Pyrococcus furiosus* (PfuFen1) have shown that the protein contains a helical clamp (Hosfield et al., 1998b). Upon binding to a substrate, PfuFen1 undergoes a conformational change that closes the clamp, effectively enclosing the single stranded flap. The substrate-induced conformational change identified in human FEN1 is consistent with this mechanism (Kim et al., 1999; Kim et al., 2001).

FEN1 cleaves on 5' DNA or RNA flaps efficiently and pseudo-Y at a lower rate (Harrington and Lieber, 1994b; Murante et al., 1994). Recent studies have shown that a double-flap structure, which has a 3' single nucleotide (nt), is the optimal substrates for FEN1 homologues in archaea (Kaiser et al., 1999), yeast (Kao et al., 2002), bacteria (Xu et al., 2000) and human (Storici et al., 2002; Friedrich-Heineken et al., 2003). FEN1 cuts this substrate on nucleotide into a duplex DNA downstream of the bifurcated junction, allowing the 3' tail to anneal to form a nick that can be ligated. This efficient flap endonuclease activity is crucial for FEN1 to fulfil its function in Okazaki fragment maturation and mammalian long patch NER (Bambara et al., 1997; Lieber, 1997; Kim et al., 1998).

Yeast genetic studies have suggested several pathways to resolve the accumulated flaps when Fen1 function is defective. The deletion of FEN1 homologues in yeast, such as *Schizosaccharomyces pombe RAD2* and *S. cerevisiae RAD27* causes lethality in combination with a deletion of either the *RAD51* (*RHP51* in *Schizosaccharomyces pombe*) or *RAD52* epistasis group of genes (Murray et al., 1994; Tishkoff et al., 1997b; Symington, 1998). These genes are important in homologous recombination, suggesting that HR is a backup for flap removal. Furthermore, a *rad27/pol3-exo* double mutant is synthetically lethal, which indicates that either the 3'-5' exonuclease decreases displacement synthesis and prevents further flap formation, or 5' flaps can equilibrate into 3' flaps that are the substrates for the 3'-5' exonuclease (Jin et al., 2001).

Defects in FEN1 increase the rate of spontaneous mutations. Detailed analysis of the mutation spectra has revealed that this mutator phenotype was almost entirely caused by accumulation of insertions or duplications, which were postulated to be caused by defects in Okazaki fragment processing (Tishkoff et al., 1997b; Gary et al., 1999; Xie et al., 2001). Two major repeat sequence expansions that are associated with human diseases have been identified. Dinucleotide repeat sequence expansion has been implicated in some human cancers (Ionov et al., 1993; Merlo et al., 1994) and trinuclotide repeat expansion is responsible for human neurodegenerative diseases, such as Huntington's disease and myotonic dystrophy (Bates and Lehrach, 1994; Paulson and Fischbeck, 1996). Although a linkage associating Huntinton's disease and a FEN1 function defect in human has not been established (Otto et al., 2001), Rad27 has been reported to maintain triplet repeat stability in *S. cerevisiae* (Liu et al., 2004d). Moreover, deficiency of Rad27 is directly related to destabilization of yeast micro- and minisatellite DNA sequence (Kokoska et al., 1998). Studies in both yeast and human cells have also shown that FEN1 contributes to telomere stability by ensuring efficient telomere replication of the lagging strand (Parenteau and Wellinger, 2002; Saharia et al., 2008).

The endonuclease activity of FEN1 is directly involved in restricting homologous recombination between short sequences, a process that causes genome rearrangement (Negritto et al., 2001). FEN1 disrupts the insertion of a short DNA fragment into its genome target by removing a short 5' flap resulting from unwinding of the short DNA fragment from its target genomic sequence. On the other hand, in chicken DT40 cells, FEN1 affects the efficiency of immunoglobulin gene conversion but not on that of the sister chromotid exchange. This observation suggests that FEN1 eliminates heterologous sequences at DNA damage site and facilitates DNA repair by homologous recombination (Kikuchi et al., 2005). FEN1 has also been implied in nonhomologous

end-joining by creating blunt ended double stranded DNA (Wu et al., 1999b; Liang et al., 2005).

In addition to its FEN activity, FEN1 is also known as an obligate dsDNA 5'-3' exonuclease (EXO) that cleaves nick, gap and 5'-resessive DNA and, to a lesser extent, blunt-ended DNA (Kaiser et al., 1999; Lee and Wilson, 1999). Recently, FEN1 was also known to possess a gap endonuclease (GEN) activity (Zheng et al., 2005). The EXO and GEN activity of FEN1 has been suggested in apoptotic DNA fragmentation and stalled DNA replication fork rescue (Parrish et al., 2003; Zheng et al., 2005).

The multiple functions of FEN1 are regulated via several mechanisms, including formation of complexes with different protein partners, nuclear localization in response to cell cycle or DNA damage and post-translational modification (Friedrich-Heineken et al., 2003; Henneke et al., 2003). For example, FEN1 has been found to interact physically and functionally with two RecQ-like helicases, WRN (Werner syndrome protein) and BLM (Bloom's syndrome protein). WRN has been demonstrated to unwind the chicken-foot HJ intermediates associated with a regressed replication fork and stimulates FEN1 to cleave the unwound product in a structure dependent manner (Sharma et al., 2004a). WRN can also stimulate the FEN and GEN activity. The stimulation is independent of the helicase or 3' exonulcease activity of WRN (Brosh et al., 2001; Zheng et al., 2005). BLM can stimulate both the FEN and EXO activity of FEN1. This function is independent of BLM catalytic activity (Sharma et al., 2004b). Another example is that two DNA clamps, proliferating cell nuclear antigen (PCNA) and Rad9/Rad1/Hus1 complex (9-1-1 complex), can independently bind to and activate FEN1 (Friedrich-Heineken et al., 2005). Acetylation of FEN1 was shown to abolish the stimulatory effect of the 9-1-1 complex but not that of PCNA. In addition, the binding and stimulation activity on FEN1 of WRN is not affected by the acetylation of FEN1, suggesting that WRN and PCNA might coordinatively regulate FEN1 (Sharma et al., 2005).

Eukaryotes have the 3' endonuclease of NER (XPG/Rad2) as well as the 5' flap endonuclease (FEN1/Rad27) responsible for the processing of Okazaki fragments. In contrast, archaea contain a single protein of FEN1/XPG family that shows nuclease activity *in vitro*, most similar to FEN1 (Hosfield et al., 1998a). The crystal structure studies have revealed that the *Sulfolobus solfataricus* PCNA1-PCNA2 heterodimer binds to a FEN1 monomer (Dore et al., 2006b). Moreover, biochemical studies have shown that the endonuclease activity of Fen1 is stimulated by the complex of PCNA2 and 3 or PCNA1, 2 and 3 in *Aeropyrum pernix* (Imamura et al., 2007). Therefore, as in eukaryotes, Fen1 interacts with PCNA and its endonuclease activity is regulated by the interaction in archaea.

Chapter II: Materials and Methods

2.1 Materials

2.1.1 *Haloferax volcanii* strains

Strain	Parent	Genotype	Notes
H26	H18	Δ*pyrE2*	Loss of pTA53 (Δ*pyrE2*, Nov^R) from *pyrE2* locus, leaving behind Δ*pyrE2*. Constructed by Thorsten Allers (Allers et al., 2004).
H53	H47	Δ*pyrE2* Δ*trpA*	Pop-out of pTA98 (Δ*trpA*, *pyrE2*+) from *trpA* locus, leaving behind Δ*trpA*. Constructed by Thorsten Allers (Allers et al., 2004).
H98	H90	Δ*pyrE2* Δ*hdrB*	Pop-out of p160 (Δ*hdrB*, *pyrE2*+) from *hdrB* locus, leaving behind Δ*hdrB*. Constructed by Thorsten Allers (Allers et al., 2004).
H115	H106	Δ*pyrE2 bgaHa-Kp*	Pop-out of pTA159 (*bgaHa-Kp*, *pyrE2*+) from *bgaHa* locus, leaving behind *bgaHa-Kp*. Constructed by Thorsten Allers.
H194	H180	Δ*pyrE2 bgaHa-Bb LeuB-Aa2* Δ*trpA* Δ*hdrB*	Pop-out of pTA160 (Δ*hdrB*, *pyrE2*+) from *hdrB* locus, leaving behind Δ*hdrB*. Constructed by Thorsten Allers.
H195	H181	Δ*pyrE2 bgaHa-Bb LeuB-Ag1* Δ*trpA* Δ*hdrB*	Pop-out of pTA160 (Δ*hdrB*, *pyrE2*+) from *hdrB* locus, leaving behind Δ*hdrB*. Constructed by Thorsten Allers (Guy et al., 2006).
H204	H200	Δ*pyrE2 bgaHa-Kp* Δ*mre11rad50*	Pop-out of pTA199 (Δ*mre11rad50*, *pyrE2*+) from *mre11rad50* locus, leaving behind Δ*mre11rad50*. Constructed by Thorsten Allers.
H280	H219	Δ*pyrE2 bgaHa-Bb LeuB-Aa2* Δ*trpA* Δ*hdrB* Δ*mre11rad50*	Pop-out of pTA199 (Δ*mre11rad50*, *pyrE2*+) from *mre11rad50* locus, leaving behind Δ*mre11rad50*. Constructed by Sam Haldenby.
H338	H26	*hef*+::[Δ*hef pyrE2*+] Δ*pyrE2*	Integration of pTA377 (Δ*hef*, *pyrE2*+) at *hef* locus by CO on left of deletion
H339	H26	*hef*+::[Δ*hef-hel pyrE2*+] Δ*pyrE2*	Integration of TAp378 (Δ*hef-hel*, *pyrE2*+) at *hef* locus by CO on left of deletion
H340	H26	*hef*+::[Δ*hef-nuc pyrE2*+] Δ*pyrE2*	Integration of pTA388 (Δ*hef-nuc*, *pyrE2*+) at *hef* locus by CO on left of deletion
H341	H194	*hef*+::[Δ*hef pyrE2*+] *bgaHa-Bb LeuB-Aa2* Δ*trpA* Δ*hdrB* Δ*pyrE2*	Integration of TAp377 (Δ*hef*, *pyrE2*+) at *hef* locus by CO on left of deletion
H342	H194	*hef*+::[Δ*hef-hel pyrE2*+] *bgaHa-Bb LeuB-Aa2* Δ*trpA* Δ*hdrB* Δ*pyrE2*	Integration of pTA378 (Δ*hef-hel*, *pyrE2*+) at *hef* locus by CO on left of deletion

H343	H194	*hef*+::[Δ*hef-nuc pyrE2*+] *bgaHa-Bb LeuB-Aa2* Δ*trpA* Δ*hdrB* Δ*pyrE2*	Integration of pTA388 (Δ*hef-nuc*, *pyrE2*+) at *hef* locus by CO on left of deletion
H344	H195	*hef*+::[Δ*hef pyrE2*+] *bgaHa-Bb LeuB-Ag1* Δ*trpA* Δ*hdrB* Δ*pyrE2*	Integration of pTA377 (Δ*hef*, *pyrE2*+) at *hef* locus by CO on left of deletion
H345	H195	*hef*+::[Δ*hef-hel pyrE2*+] *bgaHa-Bb LeuB-Ag1* Δ*trpA* Δ*hdrB* Δ*pyrE2*	Integration of pTA378 (Δ*hef-hel*, *pyrE2*+) at *hef* locus by CO on left of deletion
H346	H195	*hef*+::[Δ*hef-nuc pyrE2*+] *bgaHa-Bb LeuB-Ag1* Δ*trpA* Δ*hdrB* Δ*pyrE2*	Integration of pTA378 (Δ*hef-nuc*, *pyrE2*+) at *hef* locus by CO on left of deletion
H358	H338	Δ*hef* Δ*pyrE2*	Pop-out of pTA377 (Δ*hef*, *pyrE2*+) from *hef* locus, leaving behind Δ*hef*
H359	H339	Δ*hef-hel* Δ*pyrE2*	Pop-out of pTA378 (Δ*hef-hel*, *pyrE2*+) from *hef* locus, leaving behind Δ*hef-hel*
H360	H340	Δ*hef-nuc* Δ*pyrE2*	Pop-out of pTA388 (Δ*hef-nuc*, *pyrE2*+) from *hef* locus, leaving behind Δ*hef-nuc*
H361	H341	Δ*hef bgaHa-Bb LeuB-Aa2* Δ*trpA* Δ*hdrB* Δ*pyrE2*	Pop-out of pTA377 (Δ*hef*, *pyrE2*+) from *hef* locus, leaving behind Δ*hef*
H362	H342	Δ*hef-hel bgaHa-Bb LeuB-Aa2* Δ*trpA* Δ*hdrB* Δ*pyrE2*	Pop-out of pTA378 (Δ*hef-hel*, *pyrE2*+) from *hef* locus, leaving behind Δ*hef-hel*
H363	H343	Δ*hef-nuc bgaHa-Bb LeuB-Aa2* Δ*trpA* Δ*hdrB* Δ*pyrE2*	Pop-out of pTA388 (Δ*hef-nuc*, *pyrE2*+) from *hef* locus, leaving behind Δ*hef-nuc*
H364	H344	Δ*hef bgaHa-Bb LeuB-Ag1* Δ*trpA* Δ*hdrB* Δ*pyrE2*	Pop-out of pTA377 (Δ*hef*, *pyrE2*+) from *hef* locus, leaving behind Δ*hef*
H365	H345	Δ*hef-hel bgaHa-Bb LeuB-Ag1* Δ*trpA* Δ*hdrB* Δ*pyrE2*	Pop-out of pTA378 (Δ*hef-hel*, *pyrE2*+) from *hef* locus, leaving behind Δ*hef-hel*
H366	H346	Δ*hef-nuc bgaHa-Bb LeuB-Ag1* Δ*trpA* Δ*hdrB* Δ*pyrE2*	Pop-out of pTA388 (Δ*hef-nuc*, *pyrE2*+) from *hef* locus, leaving behind Δ*hef-nuc*
H367	H26	Δ*pyrE2 hel308a*+::[Δ*hel308a pyrE2*]	Integration of pTA424 (Δ*hel308*, *pyrE2*+) at *hel308a* locus by CO on left of deletion
H368	H194	Δ*pyrE2 bgaHa-Bb LeuB-Aa2* Δ*trpA* Δ*hdrB hel308a*+::[Δ*hel308a pyrE2*]	Integration of pTA424 (Δ*hel308*, *pyrE2*+) at *hel308a* locus by CO on left of deletion
H369	H195	Δ*pyrE2 bgaHa-Bb LeuB-Ag1* Δ*trpA* Δ*hdrB hel308a*+::[Δ*hel308a pyrE2*]	Integration of pTA424 (Δ*hel308*, *pyrE2*+) at *hel30a8* locus by CO on left of deletion
H477	H26	Δ*pyrE2 uvrA*+::[Δ*uvrA pyrE2*+]	Integration of pTA596 (Δ*uvrA*, *pyrE2*+) at *uvrA* locus by CO on left of deletion
H478	H358	Δ*hef* Δ*pyrE2 uvrA*+::[Δ*uvrA pyrE2*+]	Integration of pTA596 (Δ*uvrA*, *pyrE2*+) at *uvrA* locus by CO on left of deletion
H479	H359	Δ*hef-hel* Δ*pyrE2 uvrA*+::[Δ*uvrA pyrE2*+]	Integration of pTA596 (Δ*uvrA*, *pyrE2*+) at *uvrA* locus by CO on right of deletion
H480	H360	Δ*hef-nuc* Δ*pyrE2 uvrA*+::[Δ*uvrA pyrE2*+]	Integration of pTA596 (Δ*uvrA*, *pyrE2*+) at *uvrA* locus by CO on left of deletion

H481	H195	Δ*pyrE2 bgaHa-Bb LeuB-Ag1* Δ*trpA* Δ*hdrB uvrA*+::[Δ*uvrA pyrE2*+]	Integration of pTA596 (Δ*uvrA*, *pyrE2*+) at *uvrA* locus by CO on right of deletion
H482	H26	Δ*pyrE2 uvrD*+::[Δ*uvrD pyrE2*+]	Integration of pTA598 (Δ*uvrD*, *pyrE2*+) at *uvrD* locus by CO on right of deletion
H483	H358	Δ*hef* Δ*pyrE2 uvrD*+::[Δ*uvrD pyrE2*+]	Integration of pTA598 (Δ*uvrD*, *pyrE2*+) at *uvrD* locus by CO on left of deletion
H484	H359	Δ*hef-hel* Δ*pyrE2 uvrD*+::[Δ*uvrD pyrE2*+]	Integration of pTA598 (Δ*uvrD*, *pyrE2*+) at *uvrD* locus by CO on right of deletion
H485	H360	Δ*hef-nuc* Δ*pyrE2 uvrD*+::[Δ*uvrD pyrE2*+]	Integration of pTA598 (Δ*uvrD*, *pyrE2*+) at *uvrD* lo cus by CO on left of deletion
H486	H195	Δ*pyrE2 bgaHa-Bb LeuB-Ag1* Δ*trpA* Δ*hdrB uvrD*+::[Δ*uvrD pyrE2*+]	Integration of pTA598 (Δ*uvrD*, *pyrE2*+) at *uvrD* locus
H487	H195	Δ*pyrE2 bgaHa-Bb LeuB-Ag1* Δ*trpA* Δ*hdrB fen1*+::[Δ*fen1*::*trpA pyrE2*+]	Integration of pTA554 (Δ*fen1*::*trpA*, *pyrE2*+) at *fen1* locus by CO on right of deletion
H488	H364	Δ*hef bgaHa-Bb LeuB-Ag1* Δ*trpA* Δ*hdrB* Δ*pyrE2 fen1*+::[Δ*fen1*::*trpA pyrE2*+]	Integration of pTA554 (Δ*fen1*::*trpA*, *pyrE2*+) at *fen1* locus by CO on lef of deletion
H489	H365	Δ*hef-hel bgaHa-Bb LeuB-Ag1* Δ*trpA* Δ*hdrB* Δ*pyrE2 fen1*+::[Δ*fen1*::*trpA pyrE2*+]	Integration of pTA554 (Δ*fen1*::*trpA*, *pyrE2*+) at *fen1* locus by CO on left of deletion
H490	H366	Δ*hef-nuc bgaHa-Bb LeuB-Ag1* Δ*trpA* Δ*hdrB* Δ*pyrE2 fen1*+::[Δ*fen1*::*trpA pyrE2*+]	Integration of pTA554 (Δ*fen1*::*trpA*, *pyrE2*+) at *fen1* locus by CO on right of deletion
H509	H477	Δ*pyrE2* Δ*uvrA*	Pop-out of pTA596 (Δ*uvrA*, *pyrE2*+) from *uvrA* locus, leaving behind Δ*uvrA*
H510	H478	Δ*hef* Δ*pyrE2* Δ*uvrA*	Pop-out of pTA596 (Δ*uvrA*, *pyrE2*+) from *uvrA* locus, leaving behind Δ*uvrA*
H511	H479	Δ*hef-hel* Δ*pyrE2* Δ*uvrA*	Pop-out of pTA596 (Δ*uvrA*, *pyrE2*+) from *uvrA* locus, leaving behind Δ*uvrA*
H512	H480	Δ*hef-nuc* Δ*pyrE2* Δ*uvrA*	Pop-out of pTA596 (Δ*uvrA*, *pyrE2*+) from *uvrA* locus, leaving behind Δ*uvrA*
H513	H481	Δ*pyrE2 bgaHa-Bb LeuB-Ag1* Δ*trpA* Δ*hdrB* Δ*uvrA*	Pop-out of pTA596 (Δ*uvrA*, *pyrE2*+) from *uvrA* locus, leaving behind Δ*uvrA*
H514	H482	Δ*pyrE2* Δ*uvrD*	Pop-out of pTA598 (Δ*uvrD*, *pyrE2*+) from *uvrD* locus, leaving behind Δ*uvrD*
H515	H483	Δ*hef* Δ*pyrE2* Δ*uvrD*	Pop-out of pTA598 (Δ*uvrD*, *pyrE2*+) from *uvrD* locus, leaving behind Δ*uvrD*
H516	H484	Δ*hef-hel* Δ*pyrE2* Δ*uvrD*	Pop-out of pTA598 (Δ*uvrD*, *pyrE2*+) from *uvrD* locus, leaving behind Δ*uvrD*
H517	H485	Δ*hef-nuc* Δ*pyrE2* Δ*uvrD*	Pop-out of pTA598 (Δ*uvrD*, *pyrE2*+) from *uvrD* locus, leaving behind Δ*uvrD*
H518	H486	Δ*pyrE2 bgaHa-Bb LeuB-Ag1* Δ*trpA* Δ*hdrB* Δ*uvrD*	Pop-out of TAp598 (Δ*uvrD*, *pyrE2*+) from *uvrD* locus, leaving behind Δ*uvrD*

H522	H487	Δ*pyrE2 bgaHa-Bb LeuB-Ag1* Δ*trpA* Δ*hdrB* Δ*fen1*::*trpA*	Pop-out of pTA554 (Δ*fen1*::*trpA*+, *pyrE2*+) from *fen1* locus, leaving behind Δ*fen1*::*trpA*
H524	H489	Δ*hef-hel bgaHa-Bb LeuB-Ag1* Δ*trpA* Δ*hdrB* Δ*pyrE2* Δ*fen1*::*trpA*	Pop-out of pTA554 (Δ*fen1*::*trpA*+, *pyrE2*+) from *fen1* locus, leaving behind Δ*fen1*::*trpA*+
H525	H490	Δ*hef-nuc bgaHa-Bb LeuB-Ag1* Δ*trpA* Δ*hdrB* Δ*pyrE2* Δ*fen1*::*trpA*	Pop-out of pTA554 (Δ*fen1*::*trpA*+, *pyrE2*+) from *fen1* locus, leaving behind Δ*fen1*::*trpA*+
H537	H115	*uvrD*+::[Δ*uvrD pyrE2*+] *bgaHa-Kp* Δ*pyrE2*	Integration of pTA598 (Δ*uvrD*, *pyrE2*+) at *uvrD* locus by CO on left of deletion,
H538	H202	*uvrD*+::[Δ*uvrD pyrE2*+] *bgaHa-Kp* Δ*rad50* Δ*pyrE2*	Integration of pTA598 (Δ*uvrD*, *pyrE2*+) at *uvrD* locus by CO on right of deletion
H539	H203	*uvrD*+::[Δ*uvrD pyrE2*+] *bgaHa-Kp* Δ*mre11* Δ*pyrE2*	Integration of pTA598 (Δ*uvrD*, *pyrE2*+) at *uvrD* locus by CO on right of deletion,
H540	H204	*uvrD*+::[Δ*uvrD pyrE2*+] *bgaHa-Kp* Δ*mre11 rad50* Δ*pyrE2*	Integration of pTA598 (Δ*uvrD*, *pyrE2*+) at *uvrD* locus by CO on right of deletion
H559	H537	Δ*uvrD bgaHa-Kp* Δ*pyrE2*	Pop-out of pTA598 (Δ*uvrD*, *pyrE2*+) from *uvrD* locus, leaving behind Δ*uvrD*
H560	H538	Δ*uvrD bgaHa-Kp* Δ*rad50* Δ*pyrE2*	Pop-out of pTA598 (Δ*uvrD*, *pyrE2*+) from *uvrD* locus, leaving behind Δ*uvrD*
H561	H539	Δ*uvrD bgaHa-Kp* Δ*mre11* Δ*pyrE2*	Pop-out of pTA598 (Δ*uvrD*, *pyrE2*+) from *uvrD* locus, leaving behind Δ*uvrD*
H562	H540	Δ*uvrD bgaHa-Kp* Δ*mre11 rad50* Δ*pyrE2*	Pop-out of pTA598 (Δ*uvrD*, *pyrE2*+) from *uvrD* locus, leaving behind Δ*uvrD*
H572	H522	Δ*pyrE2 bgaHa-Bb LeuB-Ag1* Δ*trpA* Δ*hdrB* Δ*fen1*::*trpA* *hef*+::[Δ*hef pyrE2*+]	Integration of pTA377 (Δ*hef*, *pyrE2*+) at *hef* locus by CO on left of deletion
H598	H572	Δ*pyrE2 bgaHa-Bb LeuB-Ag1* Δ*trpA* Δ*hdrB* Δ*fen1*::*trpA* Δ*hef*	Pop-out of pTA377 (Δ*hef*, *pyrE2*+) from *hef* locus, leaving behind Δ*hef*
H632	H522	Δ*pyrE2 bgaHa-Bb LeuB-Ag1* Δ*trpA* Δ*hdrB* Δ*fen1*::*trpA* *uvrA*+::[Δ*uvrA pyrE2*+]	Integration of pTA596 (Δ*uvrA*, *pyrE2*+) at *uvrA* locus by CO on right of deletion
H633	H598	Δ*pyrE2 bgaHa-Bb LeuB-Ag1* Δ*trpA* Δ*hdrB* Δ*fen1*::*trpA* Δ*hef* *uvrA*+::[Δ*uvrA pyrE2*+]	Integration of pTA596 (Δ*uvrA*, *pyrE2*+) at *uvrA* locus by CO on right of deletion
H646	H632	Δ*pyrE2 bgaHa-Bb LeuB-Ag1* Δ*trpA* Δ*hdrB* Δ*fen1*::*trpA* Δ*uvrA*	Pop-out of pTA596 (Δ*uvrA*, *pyrE2*+) from *uvrA* locus, leaving behind Δ*uvrA*
H647	H633	Δ*pyrE2 bgaHa-Bb LeuB-Ag1* Δ*trpA* Δ*hdrB* Δ*fen1*::*trpA* Δ*hef* Δ*uvrA*	Pop-out of pTA596 (Δ*uvrA*, *pyrE2*+) from *uvrA* locus, leaving behind Δ*uvrA*
H648	H115	Δ*pyrE2 bgaHa-Kp* Δ*polX*	Pop-out of pTA714, Deletion of DNA polymerase X. Constructed by Stéphane Delmas.
H651	H204	Δ*pyrE2 bgaHa-Kp* Δ*mre11rad50* Δ*polX*	Pop-out of pTA714, Deletion of DNA polymerase X. Constructed by Stéphane Delmas.

H682	H115	Δ*pyrE2 bgaHa-Kp fen1*+::[Δ*fen1 pyrE2*+]	Integration of pTA535 (Δ*fen1*, *pyrE2*+) at *fen1* locus by CO on right of deletion
H683	H204	Δ*pyrE2 bgaHa-Kp* Δ*mre11 rad50 fen1*+::[Δ*fen1 pyrE2*+]	Integration of pTA535 (Δ*fen1*, *pyrE2*+) at *fen1* locus by CO on left of deletion
H684	H648	Δ*pyrE2 bgaHa-Kp* ΔpolX *fen1*+::[Δ*fen1 pyrE2*+]	Integration of pTA535 (Δ*fen1*, *pyrE2*+) at *fen1* locus by CO on right of deletion
H685	H651	Δ*pyrE2 bgaHa-Kp* Δ*mre11 rad50* ΔpolX *fen1*+::[Δ*fen1 pyrE2*+]	Integration of pTA535 (Δ*fen1*, *pyrE2*+) at *fen1* locus by CO on left of deletion
H720	H682	Δ*pyrE2 bgaHa-Kp* Δ*fen1*	Pop-out of pTA535 (Δ*fen1*, *pyrE2*+) from *fen1* locus, leaving behind Δ*fen1*
H721	H683	Δ*pyrE2 bgaHa-Kp* Δ*mre11 rad50* Δ*fen1*	Pop-out of pTA535 (Δ*fen1*, *pyrE2*+) from *fen1* locus, leaving behind Δ*fen1*
H722	H684	Δ*pyrE2 bgaHa-Kp* ΔpolX Δ*fen1*	Pop-out of pTA535 (Δ*fen1*, *pyrE2*+) from *fen1* locus, leaving behind Δ*fen1*
H723	H685	Δ*pyrE2 bgaHa-Kp* Δ*mre11 rad50* ΔpolX Δ*fen1*	Pop-out of pTA535 (Δ*fen1*, *pyrE2*+) from *fen1* locus, leaving behind Δ*fen1*
H734	H115	Δ*pyrE2 bgaHa-Kp* Δ*polY*	Constructed by Stéphane Delmas
H736	H648	Δ*pyrE2 bgaHa-Kp* Δ*polX* Δ*polY*	Constructed by Stéphane Delmas
H772	H280	Δ*pyrE2 bgaHa-Bb LeuB-Ag1* Δ*trpA* Δ*hdrB* Δ*mre11 rad50 hef*+::[Δ*hef pyrE2*+]	Integration of pTA377 (Δ*hef*, *pyrE2*+) at *hef* locus by CO on right of deletion
H782	H772	Δ*pyrE2 bgaHa-Bb LeuB-Ag1* Δ*trpA* Δ*hdrB* Δ*mre11 rad50* Δ*hef*	Pop-out of pTA377 (Δ*hef*, *pyrE2*+) from *hef* locus, leaving behind Δ*hef*
H818	H5859	Δ*pyrE2 bgaHa-Bb LeuB-Ag1* Δ*trpA* Δ*hdrB* Δ*fen1*::*trpA*::[Δ*fen1 pyrE2*] *sfnA*	Integration of pTA535 (Δ*fen1*, *pyrE2*+) at Δ*fen1*::*trpA* locus by CO on right of deletion. With an unknown Δ*fen1* suppressor *sfnA*
H823	H818	Δ*pyrE2 bgaHa-Bb LeuB-Ag1* Δ*trpA* Δ*hdrB* Δ*fen1 sfnA*	Pop-out of pTA535 (Δ*fen1*, *pyrE2*+) from *fen1* locus, leaving behind Δ*fen1* with an unknown Δ*fen1* suppressor *sfnA*
H859	H522	Δ*pyrE2 bgaHa-Bb LeuB-Ag1* Δ*trpA* Δ*hdrB* Δ*fen1*::*trpA sfnA*	A spontaneous mutant with an unknown Δ*fen1* suppressor *sfnA*

2.1.2 Escherichia coli strains

Strain	Genotype	Source
XL1-Blue	Δ*mcrA183* Δ*mcrCB-hsdSMR-mrr173 endA1 supE44 thi-1 recA1 gyrA96 relA1 lac* [F′ *proAB lacI*^{q}*Z*ΔM15 Tn*10*]	Stratagene
N2338	F^{-} *dam-3 dcm-6 ara-14 fhuA31 galK2 galT22 hdsR3 lacY1 leu-6 thi-1 thr-1 tsx-78*	RG Lloyd

2.1.3 Plasmids

Plasmid	Description
pTA35	pBluescript II SK+, standard *E. coli* vector.
pTA49	pBluescript II SK+ with *H. volcanii* 3.7 kb *Sau*3AI chromosomal fragment containing *trpA*, inserted at *Bam*HI site. Constructed by Thorsten Allers (Lam et al., 1990; Allers et al., 2004).
pTA52	pGB70, provided by Moshe Mevarech. *H. volcanii pyrE2* ORF under ferredoxin (*fdx*) promoter of *Halobacterium salinarium* inserted at the *Nco*I and *Xba*I sites pUC19 (Bitan-Banin et al., 2003).
pTA56	pIL11, provided by Moshe Mevarech. pUC19 with 130 bp *Bam*HI-*Nco*I *Halobacterium salinarum fdx* promoter fragment (*p.fdx*) inserted between *Bam*HI and *Xba*I sites (Bitan-Banin *et al*., 2003).
pTA128	pTA103 with 3.37 kb *Hin*dIII-*Age*I chromosomal fragment from *H. volcanii* strain H54 containing *bgaHa*, inserted at *Hin*dIII and *Xma*I sites. Constructed by Thorsten Allers.
pTA131	pBluescript II SK+ with 0.7 kb *Bam*HI/*Xba*I (both blunt-ended) *p.fdx::pyrE2* fragment from pGB70 inserted at *Psi*I site. Constructed by Thorsten Allers (Allers et al., 2004).
pTA137	pTA135 with 0.7 kb *Eco*RI-*Hin*dIII (both blunt-ended) *p.fdx::pyrE2* fragment from pGB70 inserted at *Psi*I site. Constructed by Greg Ngo.
pTA230	pTA131 with insertion of 3.75 kb *Nco*I-*Hin*dIII (both blunt-ended) fragment containing pHV2 origin from pWL-Nov, at *Pci*I site (blunt-ended). Constructed by Thorsten Allers (Allers et al., 2004).
pTA250	pTA131 with *H. volcanii* 1.10 kb *Aci*I chromosomal fragment (partial digest of 5.01 kb pTA194 *Xho*I-*Eco*RV fragment) containing possible *H. volcanii* replication origin from pHV4, inserted at *Cla*I site. Constructed by Thorsten Allers (Norais et al., 2007a).
pTA274	pTA230 shuttle vector with insertion of 3 kb *Sca*I-*Hin*dIII *bgaHa* fragment from p128 at Asp7I8-NotI sites (all sites except ScaI blunt-ended by Klenow). Constructed by Thorsten Allers.
pTA277	pTA230 shuttle vector with insertion of 3 kb *Sca*I-*Hin*dIII *bgaHa* fragment from p128 at Asp7I8-NotI sites (all sites except ScaI blunt-ended by Klenow). *dam*$^-$ version of pTA274. Constructed by Thorsten Allers.
pTA298	*H. volcanii trpA* ORF (*Pci*I-*Sph*I PCR fragment amplified from pTA49) in pIL11 between *Nco*I and *Sph*I sites, i.e. under *p.fdx* of *Halobacterium salinarium*. Constructed by Thorsten Allers (Lam et al., 1990).
pTA334	pBluescript II SK+ with *H. volcanii* 6.96 kb *Not*I chromosomal fragment containing *xpf/hef* nuclease gene, inserted at NotI sites. Constructed by Thorsten Allers.
pTA351	*trpA*-marked shuttle vector based on pTA132 with 948bp *Bmg*BI-*Eco*RV fragment from pTA250 (containing Hv oripHV1/4). Inserted at klenow blunted *Pci*I site. Constructed by Sam Haldenby.
pTA356	Shuttle vector based on pTA192 with 948bp *Bmg*BI-*Eco*RV fragment from pTA250 (containing Hv oripHV1/4). Inserted at klenow blunted PciI site. Constructed by Sam Haldenby (Norais et al., 2007a).
pTA360	Shuttle vector based on pTA192 with 948bp *Bmg*BI-*Eco*RV fragment from pTA250 (containing Hv oripHV1/4). Inserted at klenow blunted PciI site. *dam*$^-$ version of pTA356. Constructed by Sam Haldenby.
pTA369	pTA351 shuttle vector with 500 bp *Kpn*I-*Eco*RI *pyrE2* PCR product (without promoter) inserted at *Kpn*I and *Eco*RI sites.
pTA370	pTA131 with insertion of 1.6kb Δ*hef* PCR construct, made from pTA334 using internal primers with *Bam*HI sites and external primers with *Kpn*I and *Xba*I sites, inserted at *Kpn*I and *Xba*I sites.

pTA371	pTA131 with insertion of 2.3kb Δ*hef-hel* PCR construct, made from pTA334 using internal primers with *Bam*HI sites and external primers with *Kpn*I and *Xba*I sites, inserted at *Kpn*I and *Xba*I sites.
pTA377	pTA131 with insertion of 1.6kb Δ*hef* PCR construct, made from pTA334 using internal primers with *Bam*HI sites and external primers with *Kpn*I and *Xba*I sites, inserted at *Kpn*I and *Xba*I sites. *dam*$^-$ version of pTA370.
pTA378	pTA131 with insertion of 2.3kb Δ*hef-hel* PCR construct, made from pTA334 using internal primers with *Bam*HI sites and external primers with *Kpn*I and *Xba*I sites, inserted at *Kpn*I and *Xba*I sites. *dam*$^-$ version of pTA371.
pTA387	pTA131 with insertion of 3.5kb Δ*hef-nuc* PCR construct, made from pTA334 using internal primers with *Bam*HI sites and external primers with *Kpn*I and *Xba*I sites, inserted at *Kpn*I and *Xba*I sites.
pTA388	pTA131 with insertion of 3.5kb Δ*hef*-nuc *PCR* construct, made from pTA334 using internal primers with *Bam*HI sites and external primers with *Kpn*I and *Xba*I sites, inserted at *Kpn*I and *Xba*I sites. *dam*$^-$ version of pTA387.
pTA391	pTA351 shuttle vector with 500 bp *Kpn*I-*Eco*RI *pyrE2* PCR product (without promoter) inserted at *Kpn*I and *Eco*RI sites
pTA415	pBluescript II SK+ with *H. volcanii* 5.35kb *Mlu*I chromosomal fragment containing *hel308a* helicase gene, inserted at BssHII sites
pTA423	pTA131 with insertion of 1.6kb Δ*hel308a* PCR construct, made from pTA415 using internal primers with *Bam*HI sites and external primers with *Hin*dIII and *Xba*I sites, inserted at *Hin*dIII and *Xba*I sites.
pTA424	pTA131 with insertion of 1.6kb Δ*hel308a* PCR construct, made from pTA415 using internal primers with *Bam*HI sites and external primers with *Hin*dIII and *Xba*I sites, inserted at *Hin*dIII and *Xba*I sites. *dam*$^-$ version of pTA423.
pTA425	L11e terminator of H9 inserted in pTA369 at *Kpn*I site, upstream of promoter-less *pyrE2* gene (Large et al., 2007).
pTA426	L11e terminator of H9 inserted in pTA369 at *Kpn*I site, upstream of promoter-less *pyrE2* gene. *dam*$^-$ version of pTA425.
pTA427	Alias pRV1, provided by Mike Dyall-Smith. Shuttle vector with promoter-less *bgaH* gene, derived from pMDS133 by replacement of trpA' att terminator with L11e rRNA terminator of *H. volcanii* (Shimmin and Dennis, 1996)
pTA438	pTA131 with *H. volcanii* 1.10 kb *Aci*I chromosomal fragment (partial digest of 5.01 kb pTA194 *Xho*I-*Eco*RV fragment) containing possible *H. volcanii* replication origin from pHV4, inserted at *Cla*I site
pTA469	Succinic acid inducible promoter inserted at *Cla*I of pTA425. The inserted fragment includes the promoter of branched-chain amino acid ABC transporter gene and includes the promoter of branched-chain amino acid ABC transporter gene and the N-terminal part of the gene. The promoter is succinic acid inducible (Large *et al.*, 2007).
pTA480	pTA425 shuttle vector with the promoter of branched-chain amino acid ABC transporter gene inserted upstream of *pyrE2*, without the N terminal sequence of the transporter gene compared to pTA469 (Large et al., 2007)
pTA481	pTA425 shuttle vector with the promoter of branched-chain amino acid ABC transporter gene inserted upstream of *pyrE2*, without the N terminal sequence of the transporter gene compared to pTA469. *dam*$^-$ version of pTA480.
pTA486	Shuttle vector based on pTA351 with L11e terminator inserted upstream of MCS. Two *Bsp*HI sites have been blunted with Klenow and the direction of Amp has been changed.
pTA487	Shuttle vector based on pTA486 with *bgaHa* inserted in *Cla*I/*Spe*I sites. A *Bsp*HI site is just downstream of the *Cla*I site (Large et al., 2007).

pTA488	Shuttle vector based on pTA486 with *bgaHa* (amplified from pTA128) inserted in *Cla*I/SpeI sites. A *Bsp*HI site is just downstream of the *Cla*I site. *dam*⁻ version of pTA487.
pTA489	Shuttle vector based on pTA487 with *p.suc* from pTA469 inserted at *Bst*BI/*Bsp*HI sites (Large et al., 2007).
pTA491	Shuttle vector based on pTA487 with the promoter of branched-chain amino acid ABC transportergene inserted in *Bst*BI/*Bsp*HI sites (Large et al., 2007).
pTA492	Plasmid constructed for linear DNA, which contains *hel308a* franking sequence with *pyrE2* and *trpA* instead of *hel308a* gene.
pTA493	Shuttle vector based on pTA487 with *p.suc* from pTA469 inserted at *Bst*BI/*Bsp*HI sites. *dam*⁻ version of pTA489.
pTA495	Shuttle vector based on pTA487 with the promoter of branched-chain amino acid ABC transporter gene inserted at *Bst*BI/*Bsp*HI sites. *dam*⁻ version of pTA491.
pTA496	Plasmid constructed for linear DNA, which contains *hel308a* franking sequence with *pyrE2* and *trpA* instead of *hel308a* gene. *dam*⁻ version of pTA492.
pTA503	Insertion of *p.fdx::mre11RC* from pTA502 (*Bam*HI and *Xba*I, both ends blunted) in pTA357 at *Bsa*BI site. Constructed by Stéphane Delmas.
pTA519	pBluescript II SK+ with 0.8kb *Hin*dIII/*Bam*HI fragment from pTA424 containing the upstream of *hel308a* and 0.6kb *Bam*HI/*Xba*I fragment from pGB70 containing *p.fdx*::*pyrE2*
pTA520	pTA519 with 0.7kb *Bam*HI/*Xba*I (both blunted by Mung bean nuclease)fragment from pTA424 containing the downstream sequence of *hel308a* inserted at the *Xba*I site (blunted by Mung bean nuclease).
pTA521	pTA519 deleted the 137bp NspI (1353) /*Bam*HI (1490) fragment.
pTA522	pTA521 with 1.0kb *Eco*RV frament containing *trpA* from pTA49 inserted at the *Xba*I site (blunt-ended)
pTA523	pTA522 with 555bp *Not*I fragment containing the downstream of *hel308a* inserted at the *Not*I site.
pTA526	pTA360 shuttle vector with 1098 bp *Bst*BI-*Eco*RI (both blunt) fragment of pTA469, containing *pyrE2* under succintate-inducible promoter (*p.suc*), inserted at *Bsa*BI site. Constructed by Thorsten Allers.
pTA541	Shuttle vector based on pTA425 with 130bp PCR fragment of *p.fdx* from pGB70 inserted at *Cla*I site, upstream of *pyrE2*.
pTA543	Shuttle vector based on pTA425 with 42bp synthetic promoter inserted at *Cla*I site, upstream of *pyrE2* gene (Large et al., 2007).
pTA560	Shuttle vector based on p541 with 0.9kb PCR fragment of N-terminal of branched amino acid transporter gene and *pyrE2* from pTA469 inserted at *Cla*I/*Eco*RI site.
pTA561	Shuttle vector based on p541 with 0.9kb PCR fragment of N-terminal of branched amino acid transporter gene and *pyrE2* from pTA469 inserted at *Cla*I/*Eco*RI site.
pTA566	Shuttle vector based on pTA356 with 1.0kb *Kpn*I/*Nsp*I (both blunt-ended) *p.suc*::*pyrE2* fragment from pTA469 inserted at the *Sma*I site. The promoter is succinic acid inducible.
pTA567	Shuttle vector based on pTA425 with 130bp PCR fragment of *p.fdx* from pGB70 inserted at *Cla*I site, upstream of *pyrE2*.
pTA569	Shuttle vector based on pTA543 with 0.9kb PCR fragment of N-terminal of branched amino acid transporter gene and *pyrE2* from pTA469 inserted at *Cla*I/*Eco*RI site (Large *et al.*, 2007).
pTA570	Shuttle vector based on pTA543 with 0.9kb PCR fragment of N-terminal of branched amino acid transporter gene and *pyrE2* from pTA469 inserted at *Cla*I/*Eco*RI site.

pTA571	Shuttle vector based on pTA526 with 1.4kb *anti-mre11* fragment inserted at *Bst*BI (blunt) site. Constructed by Stéphane Delmas.
pTA575	Shuttle vector based on pTA566 with 1.4kb *anti-mre11* fragment inserted at *Bsa*BI site. Constructed by Stéphane Delmas.
pTA584	pBluescript II SK+ with *H. volcanii* 10.6kb *Sac*I chromosomal fragment containing *uvrA* gene, inserted at *Sac*I site.
pTA585	pBluescript II SK+ with Hf. volcanii 9.2kb *Cla*I chromosomal fragment containing *uvrD* gene, inserted at *Cla*I site.
pTA586	Shuttle vector based on pTA503 with 2.8kb *hel308a* gene from pTA415 inserted at *Eco*RV/*Not*I sites.
pTA587	Shuttle vector based on pTA503 with 2.8kb *hel308a* gene from pTA415 inserted at *Eco*RV/*Not*I sites. *dam*$^-$ version of pTA586.
pTA588	Shuttle vector based on pTA571 with 2.8kb *hel308a* gene from pTA415 inserted at *Eco*RV/*Not*I sites.
pTA589	Shuttle vector based on pTA571 with 2.8kb *hel308a* gene from pTA415 inserted at *Eco*RV/*Not*I sites. *dam*$^-$ version of pTA588.
pTA590	Shuttle vector based on pTA575 with 2.8kb *hel308a* gene from pTA415 inserted at *Eco*RV/*Not*I sites.
pTA591	Shuttle vector based on pTA575 with 2.8kb *hel308a* gene from pTA415 inserted at *Eco*RV/*Not*I sites. *dam*$^-$ version of pTA590.
pTA595	pTA131 with insertion of 1.5kb Δ*uvrA* PCR construct, made from pTA584 using internal primers with *Bam*HI sites and external primers with *Hin*dIII and *Xba*I sites, inserted at *Hin*dIII and *Xba*I sites.
pTA596	pTA131 with insertion of 1.5kb Δ*uvrA* PCR construct, made from pTA584 using internal primers with *Bam*HI sites and external primers with *Hin*dIII and *Xba*I sites, inserted at *Hin*dIII and *Xba*I sites. *dam*$^-$ version of pTA595.
pTA597	pTA131 with insertion of 1.6kb Δ*uvrD* PCR construct, made from pTA585 using internal primers with *Bam*HI sites and external primers with *Kpn*I and *Xba*I sites, inserted at *Kpn*I and *Xba*I sites.
pTA598	pTA131 with insertion of 1.6kb Δ*uvrD* PCR construct, made from pTA585 using internal primers with *Bam*HI sites and external primers with *Kpn*I and *Xba*I sites, inserted at *Kpn*I and *Xba*I sites. *dam*$^-$ version of pTA597.
pTA599	Shuttle vector based on pTA543 with 2.0kb fragment of *bgaHa* gene from pTA488 inserted at *Cla*I/SpeI site (Large et al., 2007).
pTA600	Shuttle vector based on pTA543 with 2.0kb fragment of *bgaHa* gene from p488 inserted at *Cla*I/SpeI site. *dam*$^-$ version of pTA599.
pTA601	Shuttle vector based on pTA570 with 2..3kb PCR product of N-terminal transporter (branched-chain amino acid ABC transporter gene)::*bgaHa* from pTA489 inserted at *Cla*I/SpeI site (Large et al., 2007).
pTA602	Shuttle vector based on pTA570 with 2.3kb PCR product of N-terminal transporter (branched-chain amino acid ABC transporter gene)::*bgaHa* from pTA489 inserted at *Cla*I/*Spe*I site. *dam*$^-$ version of pTA601.
pTA616	Succinic acid inducible promoter inserted at *Cla*I of pTA425. The inserted fragment includes the promoter of branched-chain amino acid ABC transporter gene and the N-terminal part of the gene. The promoter is succinic acid inducible. *dam*$^-$ version of pTA469.
pTA674	Insertion of *p.fdx*::*hel308a*RC in pTA356 at *Bam*HI/*Kpn*I site to construct a anti-*hel308a* shuttle vector. *p.fdx* prepared from p56/*Kpn*I+NcoI. *hel308a*RC prepared from PCR product/NcoI+*Bam*HI.

pTA675	Insertion of *p.syn*::*hel308a*RC in pTA356 at *Bam*HI/*Kpn*I site to construct a anti-*hel308a* shuttle vector. *p.syn*::*hel308a*RC prepared from pTA415/*Kpn*I+*Bam*HI.
pTA676	Insertion of *p.fdx*::*hel308a*RC in pTA356 at *Bam*HI/*Kpn*I site to construct a anti-*hel308a* shuttle vector. *p.fdx* prepared from pTA56/*Kpn*I+NcoI. *hel308a*RC prepared from PCR product/*Nco*I+*Bam*HI. *dam*$^-$ version of pTA674.
pTA677	Insertion of *p.syn*::*hel308a*RC in pTA356 at *Bam*HI/*Kpn*I site to construct a anti-*hel308a* shuttle vector. *p.syn*::*hel308a*RC amplified from pTA415/*Kpn*I+*Bam*HI. *dam*$^-$ version of pTA675.
pTA679	Insertion of *p.syn*::*hel308a*RC in pTA230 at *Bam*HI/*Kpn*I site to construct a anti-*hel308a* shuttle vector. *p.syn*::*hel308a*RC prepared from PCR product/*Kpn*I+*Bam*HI.
pTA680	Insertion of *p.syn*::*hel308a*RC in p230 at *Bam*HI/*Kpn*I site to construct a anti-*hel308a* shuttle vector. *p.syn*::*hel308a*RC prepared from PCR product/*Kpn*I+*Bam*HI. *dam*$^-$ version of pTA679.

2.1.4 Oligos

Oligo	Sequence	Discription
XPF IPR	CGTCCTCGGATCCCGACATCG GTG	Reverse PCR primer for upstream flanking region of *hef*, to generate *hef* deletion construct, contains *Bam*HI site
XPF EPF	GCGACCCGGTACCTCGGCGGA CTCG	Forward PCR primer for upstream flanking region of *hef*, to generate *hef* deletion construct, contains *Kpn*I site
XPF IPF	GTCGTCGGATCCGAGTACCGC TGAGC	Forward PCR primer for downstream flanking region of *hef*, to generate *hef* deletion construct, contains *Bam*HI site
XPF EPR	GGCGAACGCGATCTAGACGGC CGCC	Reverse PCR primer for downstream flanking region of *hef*, to generate *hef* deletion construct, contains *Xba*I site
XPF HDR	CACCTCGGATCCTTCTGCGTCC GACG	Reverse PCR primer for upstream flanking region of *hef* and helicase domain of *hef*, to generate nuclease domain deletion construct, contains *Bam*HI site
XPF NDF	GAAGGATCCGAGGTGGACGAC TCGGCC	Forward PCR primer for nuclease domain of *hef* and downstream flanking region of *hef*, to generate *hef* helicase domain deletion construct, contains *Bam*HI site
Fen1F	GCTATCTCACGACGACGGTCA AG	Forward PCR primer for *fen1*
Fen1R	GTCCATCAGTTCGGGGTTCC	Reverse PCR primer for *fen1*
uvrAF	GCGGTCCAAGGTGAGGTATTC	Forward PCR primer for *uvrA*
uvrAR	CGTTCTCGTTCAACAGCCC	Reverse PCR primer for *uvrA*
uvrDF	AGGTCATCGCCACGAGCCAG	Forward PCR primer for *uvrD*
uvrDR	GCTTGAGGTCCTTCTCCTGTC	Reverse PCR primer for *uvrD*
uvrA IPF	GCCGGATCCGCGACGTTTCGTT TTCAC	Forward PCR primer for downstream flanking sequence of *uvrA*, to generate *uvrA* deletion construct, contains *Bam*HI site

uvrA EPF	CCGAAGCTTTGCTGGTCGTCGCCG	Forward PCR primer for upstream flanking sequence of *uvrA*, to generate *uvrA* deletion construct, contains *Hin*dIII site
uvrA IPR	CTAGGATCCAGAGGACCGAATAGCCAT	Reverse PCR primer for upstream flanking sequence of *uvrA*, to generate *uvrA* deletion construct, contains *Bam*HI site
uvrA EPR	CGCTCTAGATTCGGTGCTCGCCGAGT	Reverse PCR primer for downstream flanking sequence of *uvrA*, to generate *uvrA* deletion construct, contains *Xba*I site
uvrD IPF	GTGGGATCCGCGCGGCGGC	Forward PCR primer for downstream flanking sequence of *uvrD*, to generate *uvrD* deletion construct, contains *Bam*HI site
uvrD EPF	GGAGGTACCGGAGGCGTGGAACG	Forward PCR primer for upstream flanking sequence of *uvrD*, to generate *uvrD* deletion construct, contains *Kpn*I site
uvrD IPR	GCAGGATCCCGGCCTTATCGGTGATA	Reverse PCR primer for upstream flanking sequence of *uvrD*, to generate *uvrD* deletion construct, contains *Bam*HII site
uvrD EPR	TCGTCTAGACTGACTTTTCTGGCGGC	Reverse PCR primer for downstream flanking sequence of *uvrD*, to generate *uvrD* deletion construct, contains *Xba*I site
ski2F	CCTCGCTCGTCTTCGTGAACTC	Forward PCR primer for *hel308a*
ski2R	CGACCCATCATCTGGTGGACTTC	Reverse PCR primer for *hel308a*
HQEPF	GCCGAAGCTTTTGGGGCGCGTCGTCC	Forward PCR primer for upstream flanking region of *hel308a*, to generate *hel308a* deletion construct, contains *Hin*dIII site
HQIPR	CGCATTGGATCCCCCTTGGACCGTCCC	Reverse PCR primer for upstream flanking region of *hel308a*, to generate *hel308a* deletion construct, contains *Bam*HI site
HQIPF	ATGAGGATCCTCGAAGCCGAGGCGACCG	Forward PCR primer for downstream flanking region of *hel308a*, to generate *hel308a* deletion construct, containing *Bam*HI site
HQEPR	CGGAATCTAGACGCAACGTTTACAAATACCCGCG	Reverse PCR primer for downstream flanking region of *hel308a*, to generate *hel308a* deletion construct, containing *Xba*I site
antiQF	GGGATCCCCGAGGCCCTCC	Used to amplify part of *hel308a* gene for anti-sense construct, containing *Bam*HI site.
antiQR	GACCATGGCGAGCAGGTGCGT	Used to amplify part of *hel308a* gene for anti-sense construct, containing NcoI site.
p.synQF	CTGGTACCGAGAATCGAAACGCTTATAAGTGCCCCCCGGCTAGAGAGCTGCATGTACCGCTCGAACAGTTCGTCGC	Used to amplify part of *hel308a* gene under the synthetic promoter for anti-sense construct, containing *Kpn*I site.
QU-p.synR	CGCCATGGAGCTCTCTAGCCGGGGGGCACTTATAAGCGTTTCGATTCTCCAGTGTGTCGACGAGTGGGAGGG	Reverse PCR primer for upstream flanking region of *hel308a* with p.syn, to generate *hel308a* insertion or deletion construct, contains *Nco*I site compatible with *Pci*I site.
TrpAR-*Eco*RI	CTGAATTCATGTATGAGAAAGGGTGGC	Reverse PCR primer for *trpA* gene, contains *Eco*RI site

QF-PstI	CCGCTGCAGGTGTCGCGGTCG TA	Forward primer for *hel308a* promoter region, containing *Pst*I site.
QR-*Xba*I	CCATCTAGAGGTCGATGGGTC GC	Reverse PCR primer for N-terminal of *hel308a* gene, containing *Xba*I site.
p.synF	CGAGAATCGAAACGCTTATAA GTGCCCCCCGGCTAGAGAGAT	Synthetic promoter
p.synR	CGATCTCTCTAGCCGGGGGGC ACTTATAAGCGTTTCGATTCT	Synthetic promoter
TERF	GACGGTACCGACTTCGACGAC TACTTCGACG	Forward PCR primer for L11e terminator with *Kpn*I site
TERR	GGCGGTACCGGGTCGAATCGG GTCGGTG	Reverse PCR primer for L11e terminator with *Kpn*I site
*pyrE2*MR	GTACTTGTCCACGTAGTAGCTC G	Sequencing primer designed wit*Hin pyrE2* gene.
pNo5SR	CGTGCCATCGATACATCGGCG GA	Primer designed to amplify the promoter of ABC transporter with *Cla*I site, then the PCR product from pTA469 can be digested with *Bst*BI/*Cla*I to insert in pTA425 digested with *Bst*BI/*Cla*I
E2FL	GAAGGTACCATCGATGGCGAA CGCAGCACTCATCGAGG	PCR primer for *pyrE2* with *Kpn*I site
E2ERI	GACCATGAATTCGCCAAGCTT GCATGCC	PCR primer for *pyrE2* with *Eco*RI site
*pyrE2*R	TCGACCTCTAGATTAGCCGTCG GCG	PCR primer for *pyrE2* with *Xba*I site.
mosaicF	ATGTATCGATGGCACGGGATA GCAAGC	PCR primer for N-terminal part of branched amino acid transporter gene with *Cla*I site
bgaF	GATCATCGATCATGACAGTTG GTGTCTGC	PCR primer for *bgaHa* with *Cla*I and *Bsp*HI
bgaR	GTTGACTAGTGGTCCCGTGCC GAC	PCR primer for *bgaHa* with *Spe*I site
PBSF2	TTAAGTTGGGTAACGCCAGGG	Primer for pBluescript
PBSR3	ACCCCAGGCTTTACACTTTATG C	Primer for pBluescript
p.trSR	GTGCCATGGACACATCGGCGG ATA	PCR primer for the promoter of the branched amino acid gene with *Nco*I site
p.trLR	TCGCCATGGCGAGCTGATAGG CTC	PCR primer for the *p.suc* (the promoter of branched amino acid transporter and the N-terminal part of the gene) with *Nco*I site
Hef RTF	AAACGGGGGCGTCGGCTAC	Forward primer for RT-PCR to detect *hef* transcipt
Hef RTR	GTGCGGGCGATGTTGGAG	Reverse primer for RT-PCR to detect *hef* transcript
rpoA RTF	CGGCGAGCACCTGATTGAC	Forward primer for RT-PCR to detect radB transcript
rpoA RTR	ACGGACGAGGAAGCAGACG	Reverse primer for RT-PCR to detect radB transcript

2.1.5 *H. volcanii* media

Sterilised by autoclaving, unless otherwise stated.

30% SW: 240 g NaCl, 30 g $MgCl_2 \cdot 6H_2O$, 35 g $MgSO_4 \cdot 7H_2O$, 7 g KCl, 20 ml 1 M Tris-HCl (pH 7.5), dH_2O to 1 L (not autoclaved)

18% SW: 200 ml 30% SW, 100ml dH_2O, 2 ml $CaCl_2$

Trace elements: 36 mg $MnCl_2 \cdot 4H_2O$, 44 mg $ZnSO_4 \cdot 7H_2O$, 230 mg $FeSO_4 \cdot 7H_2O$, $CuSO_4 \cdot 5H_2O$, dH_2O to 100ml

Hv-Min salts: 30 ml 1M NH_4Cl, 36 ml 0.5 M $CaCl_2$, 6 ml trace elements

Hv-Min carbon source: 41.7 ml 60% $_{DL}$-lactic acid Na_2 salt (Sigma), 37.5 g succinic acid Na_2 salt$\cdot 6H_2O$ (Sigma), 3.15 ml 80% glycerol, dH_2O to 250ml, pH 6.5

10x YPC: 50 g **Y**east extract (Difco), 10 g **P**eptone (Oxoid), 10 g **C**asamino acids, 17.6 ml 1M KOH, dH_2O to 1litre (Not autoclaved. Used immediately)

10x Ca: 50 g **C**asamino **a**cids, 23.5 ml 1M KOH, dH_2O to 1 litre (Not autoclaved. Used immediately)

Hv-YPC agar: 5 g Agar (Bacto), 100 ml dH_2O, 200 ml 30% SW, 33 ml 10x YPC, 2 ml 0.5 M $CaCl_2$. Microwaved without 10x YPC to dissolve agar. 10x YPC added, then autoclaved. $CaCl_2$ added prior to pouring.

Hv-Ca agar: 5 g Agar (Bacto), 100 ml dH_2O, 200 ml 30% SW, 33 ml 10x Ca, 2 ml 0.5 M $CaCl_2$, 36 µg tiotin (Sigma), 288 µg thiamine (Sigma). Microwaved without 10xCa to dissolve agar. 10x Ca added, then autoclaved. $CaCl_2$, thiamine and biotin added prior to pouring.

Hv-Min agar:5 g Agar (Bacto), 110 ml dH_2O, 200 ml 30% SW, 10 ml 1 M Tris-HCl (pH 7.5), 8.5 ml Hv-Min carbon source, 4 ml Hv-Min Salts, 650 µl 0.5 M KPO_4 buffer (pH 7.5), 36 µg biotin (Sigma), 288 µg thiamine (Sigma). Microwaved to dissolve agar. 1 M Tris-HCl (pH 7.5) added, then autoclaved.

Hv-YPC broth (Contains uracil, tryptophan and leucine)**:** 100 ml dH_2O, 200 ml 30% SW, 33 ml 10x YPC. Autoclaved and 2 ml 0.5 M $CaCl_2$ was added when the broth was cool.

***H. volcanii* media supplements:** The growth characteristics of *H. volcanii* mutants on different media are shown below. Depend on the aim of an experiment, supplements were selectively added. All media supplements were supplied by Sigma. Solutions were sterilised by filtration through a 0.2 µm filter.

Genotype	Growth on:		
	Hv-YPC	Hv-Ca	Hv-Min
Δ*leuB*	+	+	Leu$^-$
Δ*pyrE2*	+	Ura$^-$	Ura$^-$
Δ*trpA*	+	Trp$^-$	Trp$^-$
Δ*hdrB* [a]	Thy$^-$	Thy$^-$	Thy$^-$

[a] In addition to thymidine, Δ*hdrB* strain culture should be supplemented with hypoxanthine in Hv-Ca and with hypoxanthine, methionine, glycine and pantothenic acid in Hv-Min (Ortenberg et al., 2000).

Supplement	Abbreviation	Final concentration	Stock conc.
Leucine	Leu	50 µg/ml	10 mg/ml
Uracil	Ura	50 µg/ml	50 mg/ml
Thymidine [a]	Thy	50 µg/ml	4 mg/l
Tryptophan	Trp	50 µg/ml	10 mg/ml
5-FOA	5-FOA	50 µg/ml (and 10 µg/ml uracil)	50 mg/ml

[a] In addition to thymidine, hypoxanthine was added in Hv-Ca and Hv-Min media to a final concentration of 50 µg/ml. Methionine, glycine and pantothenic acid were also added in Hv-Min media to a final concentration of 50 µg/ml.

2.1.6 *E. coli* media

Sterilised by autoclaving, unless otherwise stated.

LB (agar): 10 g tryptone (Bacto), 5 g yeast extract (Difco), 10 g NaCl, 10 g agar (Bacto) when required, dH_2O to 1 litre

SOC: 20 g tryptone (Bacto), 5 g yeast extract (Difco), 0.58 g NaCl, 0.186 g KCl, 2.03 g $MgCl_2$, 2.46 g $MgSO_4$, dH_2O to 1 litre

E. coli media supplements

Supplement	Abbreviation	Final concentration
Ampicillin	Amp	50 µg/ml
Tetracycline	Tet	3.5 µg/ml
isopropyl-beta-D-thiogalactopyranoside	IPTG	0.15 mM
5-bromo-4-chloro-3-indolyl-β-D-galactopyranoside	X-gal	66.67 ug/ml

2.1.7 *H.volcanii* buffers and solutions

Buffered Spheroplasting Solution: 1 M NaCl, 27 mM KCl, 50 mM Tris-HCl (pH 8.5), 15% sucrose. Sterilised by filtration through a 0.2 µm filter.

Unbuffered Spheroplasting Solution: 1 M NaCl, 27 mM KCl, 15% sucrose, pH 7.5. Sterilised by filtration through a 0.2 µm filter.

Spheroplast Dilution Solution: 23% SW, 15% sucrose, 37.5 mM $CaCl_2$. Sterilised by filtration through a 0.2 µm filter.

Regeneration Solution: 18% SW, 1xYPC, 15% sucrose, 30 mM $CaCl_2$. Sterilised by filtration through a 0.2 µm filter.

Transformation Dilution Solution: 18% SW, 15% sucrose, 30 mM $CaCl_2$. Sterilised by filtration through a 0.2 µm filter.

ST Buffer: 1 M NaCl, 20 mM Tris-HCl (pH 7.5), autoclaved.

Lysis Solution: 100 mM EDTA (pH 8.0), 0.2% SDS.

Unbuffered Spheroplast solution for RNA work: 0.8 M NaCl, 27 mM KCl, 15% sucrose 15 g, ddH_2O to 100 ml, Adjust pH to ~7.5 with 1 M NaOH (~10 µl), 0.1% DEPC (diethylpyrocarbonate) 100 µl, Autoclave.

Agarose Plug Lysis Solution: 20 mM Tris-HCl (pH 8.8), 500 mM EDTA (pH 8.0), 1% sarkosyl, add RNase to 10 µg/ml if required, Add proteinase K (powder) to 0.5~1 mg/ml if required.

Agarose Plug Wash Solution: 25 mM Tris-HCl (pH 7.5), 100 mM EDTA (pH 8.0), add 0.5 mM PMSF (phenylmethanesulfonyl fluride, 100 mM in ethanol) if required.

2.1.8 Other buffers and solutions

20 × SSPE: 525.9 g NaCl, 82.8 g NaH_2PO_4, 28.2 g EDTA in 3 litres dH_2O, pH 7.4

TE: 10 mM Tris-HCl, 1 mM EDTA, pH 8.0

TBE: 89 mM Tris, 89 mM boric acid, 2 mM EDTA

TAE: 40 mM Tris-HCl, 20 mM acetic acid, 1 mM EDTA

Denaturing Solution: 1.5 M NaCl, 0.5 N NaOH

100 × Denhardt's Solution: 2% Ficoll 400, 2% PVP (poly vinyl pyrrolidone) 360, 2% BSA (bovine serum albumin)(Fraction V)

Prehybridisation Solution: 24 ml dH_2O, 12 ml 20 × SSPE, 2 ml 20% SDS, 2 ml 100 × Denhardt's solution

Hybridisation Solution: 1.5 g dextran sulphate, 9 ml 20x SSPE, 1.5 ml 20% SDS, 18 ml dH_2O

Low Stringency Wash Solution: 2 × SSPE, 0.5% SDS

High Stringency Wash Solution: 0.2 × SSPE, 0.5% SDS

Neutralising Buffer: 1.5 M NaCl, 0.5 M Tris-HCl, 1 mM EDTA

Gel Loading Dye (5x): 50 mM Tris-HCl, 100 mM EDTA, 15% Ficoll (w/v), 0.25% Bromophenol Blue (w/v), 0.25% Xylene Cyanol FF (w/v)

2.2 Methods

2.2.1 Computer Analyses

All primer design, sequence analysis and protein sequence analysis was carried out using MacVector 9.5.2 (Macvector Inc.). Sequence alignments were performed using Clustal W (Thompson et al., 1994) (Gonnet Series with an open gap penalty of 15.0, extended gap penalty of 0.2 and a Delay Divergent value of 40%).

2.2.2 Manipulation and analysis of nucleic acids

Restriction enzymes, Phusion polymerase, DyNAzyme polymerase, T4 DNA ligase, Antarctic phosphatase and Klenow (DNA polymerase I, large fragment) were supplied by New England Biolabs (NEB) unless otherwise stated. All reactions were carried out according to manufacturer's instruction.

PCR products were purified using QIAquick PCR Purification kit (QIAgen). Klenow-end filling, ligated, restriction digested and dephosphorylated DNA products were purified using QIAquick Nucleotide Removal kit (QIAgen). DNA was extracted from agarose gels using QIAquick Gel Extraction kit (QIAgen). Kits function to purify DNA by salt and pH dependent adsorption of DNA to a silica-gel membrane to separate from nucleotides and proteins, followed by elution in 30 to 50 µl volume of 10 mM Tris-HCl (pH 7.5). Other nucleic acids manipulation, for example, ethanol precipitation of DNA, agarose gel electrophoresis and gel extraction were carried out according to Molecular Cloning.

2.2.3 DNA sequencing and oligonucleotide synthesis

All sequencing reactions and analysis, and synthesis of oligonucleotides were carried out by the Biopolymer Synthesis and Analysis Unit (University of Nottingham). Sequencing was carried out using the dideoxy chain termination method (Sanger et al., 1977).

2.2.4 *H. volcanii* microbiology

Growth and storage of *H. volcanii*

Cultures on solid media were grown at 45°C in a static incubator (LEEC) in a plastic bag to prevent desiccation. Liquid cultures were grown in the same incubator with 8rpm rotation. For short-term storage, plates and cultures were stored at room temperature. For long-term storage, 20% glycerol (v/v) was added to cultures, mixed and flash frozen on dry ice. Frozen cultures were then stored at -80°C.

Extraction of genomic DNA from *H. volcanii*

1 ml of culture at $OD_{650} \approx 0.8$ was transferred to a 2 ml round bottom tube. Cells were pelleted at 3300 g for 8 min. The supernatant was removed and cells were resuspended in 200 µl of ST buffer. 200 µl of lysis buffer was then added and mixed by inversion. The cell lysate was overlaid with 1 ml of 100% ethanol to precipitate DNA at the interface. DNA was then spooled onto a capillary gel-loading tip by brisk stirring at the interface and allowed to dry briefly at room temperature. The pipette tip was then transferred to 500 µl of TE and the DNA resuspended. DNA was further purified by ethanol precipitation and resuspended in 100 µl of TE buffer by agitation using an Eppendorf Thermomixer Comfort shaking hot-block (45˚C, 600 rpm) for 1 hr. Completed resuspension of DNA was achieved by incubation at 4˚C overnight.

Extraction of plasmid DNA from *H. volcanii*

Plasmid DNA was extracted from *H. volcanii* using QIAquick mini prep kit (QIAgen). The procedure was the same as for *E. coli* except cells were initially resuspended in ST buffer instead of P1 buffer (NEB).

Pulsed-field gel electrophoresis

Intact *H. volcanii* DNA was prepared in agarose plugs. 2 ml of culture at $OD_{650} \approx 0.5$ was pelleted at 3300 g for 8 min, resuspended in 1 ml of cold buffered spheroplasting solution with 0.1% NaN_3 and pelleted again. The pellet was gently resuspended in 80 µl of buffered spheroplasting solution, transferred to 42°C water bath, mixed with 100 µl of pre-warmed 1.5% low-melt agarose (Seaplaque, 0.5 × buffered spheroplasting solution with 100 mM EDTA) and pipetted into plug moulds (Bio-Rad). The plugs were equilibrated in lysis solution with proteinase K at 50°C over night and transferred to fresh lysis solution supplemented with proteinase K and RNase for a further 4 hr equilibration. After 3 times 90 minutues wash, the plugs were equilibrated in 0.5 × TBE electrophoresis buffer for at least 1 hr before loaded onto a 1% agarose (Bio-Rad) 0.5 × TBE gel. Electrophoresis was performed at 14°C in a CHEF mapper (Bio-Rad) using 0.5 × TBE buffer, voltage gradient of 6 V/cm, switch angle of 120°, and switch times of 6.77 s (initial) to 17.35 s (final). Total run time was 31 hr 43 min.

Extraction of total RNA from *H. volcanii*

2 ml of culture at OD_{650} = 0.6-0.8 was transferred to a 2 ml round bottom tube. Cells were pelleted at 3300 g for 8 min. The supernatant was removed and cells were resuspended in 250 µl of unbuffered spheroplast solution. 500 µl of Trizol LS (invitrogen) was then added and incubated for 5 min at room temparature. Then 250 ul chloroform was added. The tube was vortexed for 30 seconds and further incubated for 3 min. Cell lysate was spined at 4°C 7000 g for 10 min. The top aqueous layer was transferred to a clean tube and overlaid with 0.5 ml isopropanol to precipitate RNA. The pellet was precipitated again with 1 ml 100% ethanol and then resuspended in 45 ul water. 5 µl 10 × Ambion TURBO DNase buffer and 1 µl TURBO DNase (Ambion) were added. The sample was incubated at 37°C for 30 min and then 1 µl TURBO DNase were added before a further incubation. The concentration and 260:280 nm ratio (should be around 2.0) of each RNA sample was measured using a Beckman Coulter DU530 spectrophotometer. Samples were separated into small aliquots and stored at -80˚C until required to minimise degradation.

Analysis of gene transcription

Primers were designed that would bind internal to the gene in question, to generate a PCR amplification product of 200 - 300 bp. 100 ng of RNA from each sample was used as a template for reverse transcription PCRs (RT-PCR) using a QIAgen One-Step RT-PCR kit. Reactions comprised of 1 × QIAGEN One-Step RT-PCR Buffer, 400 µM of each dNTP, 0.6 µM of each primer, 0.2 µl SUPERase-in (RNase inhibitor -Ambion), 100 ng RNA, 0.8 µl QIAGEN One-Step RT-PCR Enzyme Mix, in 20 µl total volume. Reaction conditions were titrated and optimal amplification was obtained with the following conditions.

Step	Time	Temperature
Reverse Transcription	30 min	50°C
DNA polymerase activation	15 min	95°C
Denaturation	0.5 min	94°C
Annealing	1 min	54°C
Extension	1 min	72°C
Cycles	25	
Final Extension	10 min	72°C

The resulting DNA amplification products were analysed by electrophoresis, ethidium bromide staining and comparison of band intensity using ImageGauge V4.22 (Fujifilm).

2.2.5 *E. coli* microbiology

Growth and storage of *E. coli*

Cultures on solid media were grown at 37°C in a static incubator (LEEC). Liquid cultures were grown in the same incubator with 8 rpm rotation. For short-term storage, plates and cultures were stored at 4°C. For long-term storage, 25% (v/v) glycerol was added to cultures and flash frozen on dry ice. Frozen cultures were then stored at -80°C.

Preparation of *E. coli* electrocompetent cells

An overnight culture of either strain XL-1 Blue or N2338 strain (*dam*$^+$ *and dam*$^-$ strains, respectively) was grown. Antibiotic selection was dependant on the strain: XL-1 Blue overnight cultures were supplemented with 50 µg/ml ampicillin and 3.5 µg/ml tetracycline, and N2338 overnight cultures were supplemented with 50 µg/ml ampicillin alone. Cells were diluted 1/100 in L broth, supplemented with appropriate antibiotics as described, and grown at 37˚C to A_{650} = 0.5-0.8. Cells were pelleted at 6000 g for 12 min at 4˚C and the supernatant was removed and the pellet resuspended in an equal volume of ice-cold sterile 1 mM HEPES (pH 7.5). This process was repeated using 0.5 volumes 1 mM HEPES, 0.25 volumes 1 mM HEPES + 10% glycerol, 0.1 volumes 1 mM HEPES + 10% glycerol, and finally 0.001 volumes 1 mM HEPES + 10% glycerol. Cells were flash frozen on dry ice and stored in 50 µl aliquots at -80°C.

Transformation of *E. coli* by electroporation

1 µg of DNA in 4 µl sterile dH_2O was added to 50 µl of electrocompetent cells, on ice. The mixed sample was added to a pre-chilled electroporation cuvette (1 mm electrode gap, GENEFLOW). The cuvette was placed in an *E. coli* gene pulser (BioRad) and subjected to a 1.8 kV pulse. 1 ml of SOC was added immediately and samples were incubated at 37°C with 8 rpm rotation for 1 hr. Cells were plated onto LB + Amp plates and incubated at 37°C overnight.

Mini/Midi scale purifications of *E. coli* plasmid DNA

QIAGEN QIAprep Spin Miniprep Kit or Plasmid Midi Kit was used to obtain circular plasmid DNA from *E. coli* strains by standard alkaline lysis, according to the manufacturer's guidelines. Plasmid purifications were carried out by miniprep when large yields of plasmid DNA were not required, e.g. for verification plasmids by restriction analysis and gel electrophoresis. The Plasmid Midi Kit was used when large, ultra-pure DNA yields were required, i.e. for frozen stocks of DNA and transformations of *H. volcanii*. DNA samples were frozen at -20°C.

Generation of unmethylated (*dam*$^-$) plasmid DNA

dam$^-$ (DNA adenine methylase) DNA was required for the transformation of *H. volcanii* as this organism possesses a restriction endonuclease that cleaves DNA at 5'-

$GA^{(CH3)}TC$-3' sequences. Therefore, unmethylated plasmid DNA was necessary to prevent degradation. This was achieved by transforming *dam*$^-$ *E. coli* strain N2338 with 10 ng of plasmid DNA extracted from XL1-Blue, followed by plating on LB + Amp and overnight incubation at 37°C. DNA was then extracted as usual, ready for transformation of *H. volcanii*.

2.2.6 Genetic manupulation of *H. volcanii*

The deletion of a chromosomal copy of a gene requires the identification of the gene in the genome, cloning of the gene onto a plasmid and the generation of a plasmid-borne deletion construct. The plasmid (usually pTA131) also requires *pyrE2* gene, which encodes orotate phosphoribosyl transferase and is involved in uracil biosynthesis (Bitan-Banin et al., 2003). The deletion construct is used to transform the desired *ura*$^-$ strain, where the plasmid integrates at the desired gene locus. Intramolecular recombinants that have lost the plasmid are counter selected using 5-fluoroorotic acid, which is converted to toxic 5-fluorouracil in *ura*$^+$ cells but not *ura*$^-$ cells (Figure 2.1). Colonies are then hybridised with a probe derived from an internal sequence of the gene to be deleted. Colonies that do not hybridise the probe are deleted for the gene. This is then confirmed by geomic DNA digestion and Southern blot analysis.

Generation of radiolabelled DNA probes by random priming

3 µl of template DNA (10 - 25 µg/ml), 2 µl of appropriate DNA ladder if required (1 µg/ml), and 10 µl of water were boiled for 5 min and then chilled on ice. 0.37 Mbq a-^{32}P dCTP (GE Healthcare, Amersham Redivue) was added along with 4 µl Hi Prime random priming mix (Roche). The mixture was incubated at 37˚C for 30 min and purified using a BioRad P30 column. The resulting probe was mixed with 450 µl of fish sperm DNA (10 mg/ml), boiled for 5 min then chilled on ice, ready for use.

Obtaining genomic clone of a gene

Predicted genes were identified using translated BLAST search (tBLASTx) (NCBI) on the *H. volcanii* genome (TIGR) using an appropriate query sequence, i.e. the desired gene from a related organism. The candidate gene in *H. volcanii* was mapped and restriction sites at least 500 bp upstream and downstream (but not present in between) were located. The sites were also present in the multiple cloning site of pBluescript II SK+. Genomic DNA was isolated from strain H26, as described in 'Isolation of *H. volcanii* genomic DNA' section, and digested with appropriate enzymes overnight to ensure complete digestion. Digested genomic DNA was then electrophoresed and a gel slice was extracted of the predicted fragment size. DNA was purified from agarose and ligated with cut and dephosphorylated pBluescript II SK+. Plasmid library DNA was

used to transform XL-1 Blue *E. coli* and plated at appropriate dilutions on LB + Amp. Plates were incubated overnight at 37˚C and colonies were patched onto LB plates with Amp and allowed a further overnight incubation at 37°C. PCR primers were designed complementary to a region of the desired gene to generate a product of about 500 bp. Colony lifts and blots were made of the patch plates. The PCR amplification product was used as a template for the radiolabelled probe. Colonies that hybridised with the probe contained the desired gene and were picked off the original plate and streaked on LB + Amp, and used to inoculate an LB + Amp overnight culture. Plasmid DNA was extracted from these cultures and sequenced using primers external to the gene, to confirm the desired clone.

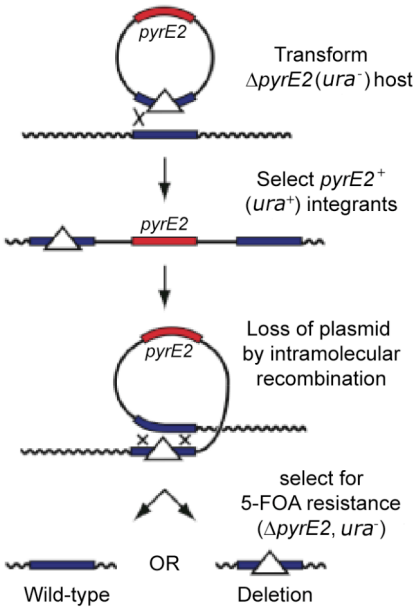

Figure 2.1 Chromosomal gene deletion by selection and counter-selection of an integrative plasmid.

A Δ*pyrE2* (*ura*$^-$) host is transformed with a *dam*$^-$ plasmid containing *pyrE2* marker and a deletion construct of the desired gene. The plasmid integrates at regions of homology to the locus of the gene to be deleted, conferring uracil prototrophy (*ura*$^+$). Once the integratant strain has been confirmed by genomic DNA digestion and Southern blot analysis, selection for uracil is relieved by serial growth in Hv-YPC (+ Thy if required). Intramolecular recombinats that have lost the plasmid are counter selected using 5-fluoroorotic acid, which is converted to toxic 5-fluorouracil in *ura*$^+$ cells but not *ura*$^-$ cells. Depending on the orientation of the second recombination event relative to the first, the resulting strain will be either deleted for the desired gene or remain as wild-type.

Generation of deletion constructs by PCR

Two pairs of primers were designed, based on the sequence of the plasmid-borne gene clone. One pair was used to amplify a region upstream of the targeted gene and the other pair was used to amplify downstream of the gene to be deleted. Novel restriction sites were introduced into the primers. For the two internal primers, the same restriction site was introduced so that both PCR products could be ligated. The external primers included restriction sites that are present in the polylinker region of pTA131 (Figure 2.2). A maximum of 3 bp were changed to introduce these novel restriction sites, which were introduced was unique and was not present anywhere else in the PCR products

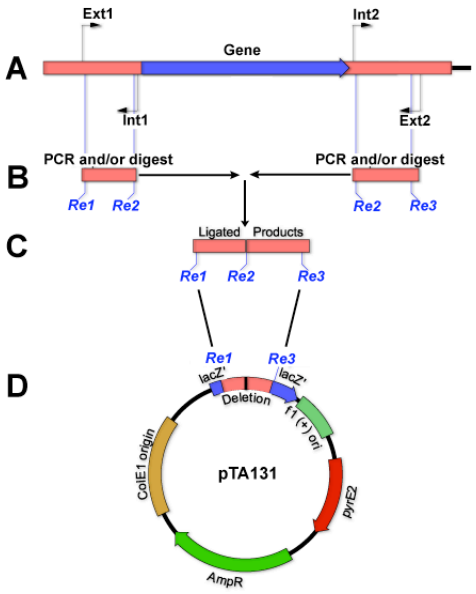

Figure 2.2 Schematic of generation of gene deletion constructs by PCR.

(A) Two pairs of PCR primers were designed to amplify flanking sequence of gene. (B) Amplification products are digested with *Re2* and ligated. (C) Ligated product is digested with *Re1* and *Re3*, and ligated into polylinker of pTA131. (D) Plasmid constructed for gene deletion.

Transformation of *H. volcanii*

H. volcanii has a restriction system that recognizes adenine-methylated GATC sites, resulting in DNA fragmentation followed by plasmid loss or chromosomal integration by recombination (Blaseio and Pfeifer, 1990). Therefore, DNA used to transform *H. volcanii* was prepared from *E. coli dam*$^-$ strain that is deficient in GATC methylation.

10 ml cultures were grown to OD_{650} = 0.6-0.8 and cells were pelleted by centrifugation in a 10 ml round-bottom tube at 3300 g for 10 min. The supernatant was removed and cells were resuspended in 2ml of buffered spheroplasting solution and transferred to a 2 ml round-bottom tube (Eppendorf). Cells were pelleted again and the supernatant removed as before. Cells were resuspended gently in 600 µl buffered spheroplasting solution. 200 µl of this was used per transformation and transferred to a fresh 2 ml tube. 20 µl 0.5 M EDTA (pH 8.0) was added, mixed by gentle inversion and incubated at room temperature for 10 min to allow removal of the *H. volcanii* S-layer (spheroplasting). A 30 µl DNA sample was prepared (15 µl unbuffered spheroplasting solution, 5 µl 0.5M EDTA pH 0.8, 1 µg plasmid DNA prepared from *dam*$^-$ *E. coli* host, and water to final volume of 30 µl), and added to the spheroplast cells and mixed as before. After five min, 250 µl of 60% polyethylene glycol 600 (PEG 600) (150 µl PEG 600 and 100 µl unbuffered spheroplasting solution) was added and mixed by gentle rocking 10 times. The mixture was incubated at room temperature for 30 min, then diluted with 1.5ml of spheroplast dilution solution and mixed by inversion. After 2 min the cells were pelleted at 3300 g for 8 min and the cell pellet was transferred to a sterile tube containing 1 ml of regeneration solution, supplemented with 60 µg/ml thymidine if required (Δ*hdrB* strains).

To allow recovery of cells, the tube was incubated for 90 min at 45˚C. The pellet was then resuspended by gently tapping the tube and incubated at 45˚C with 8 rpm rotation for 3 hr. Cells were transferred to a fresh 2ml round-bottom tube and centrifuged at 3300 g for 8 min. The cell pellet was resuspended gently in 1ml of transformation dilution solution. Appropriate dilutions were made and 100 µl of each dilution was plated on appropriate media lacking either uracil, leucine, tryptophan or thymidine, depending on the selectable marker present on the transformed plasmid (*pyrE2, leuB, trpA or hdrB*, respectively), and supplemented with appropriate additives where necessary. Plates were incubated for at least 5 days at 45˚C to allow colony growth.

Confirmation of integrated *H. volcanii* strain (Pop-in)

After transformation of pTA131 based deletion plasmid, integration of the plasmid onto the chromosome was verified by appropriate restriction digest of genomic DNA, electrophoresis of DNA on a 200 ml TAE 1% agarose gel and Southern blotting using an appropriate probe.

Loss of *pyrE2* marked plasmids from an integrant strain (Pop-out)

After verifying the genotype of a plasmid integrant strain, a second recombination event that would remove an integrated *pyrE2*-encoding plasmid from the chromosome was encouraged by relieving uracil selection. 5 ml of Hv-YPC broth was inoculated and incubated at 45°C with 8 rpm rotation. $OD_{650} \approx 0.6$ cultures were diluted 500-fold in fresh culture and grown again. This was repeated two more times, to encourage the integrated plasmid to recombine out of the chromosome of cells, thus becoming *ura*$^-$.

1 ml of culture at $OD_{650} \approx 0.6$ was pelleted at 3300 g for 8 min, and the cell pellet resuspended in 18% SW. Appropriate dilutions were made (10^0, 10^{-1} and 10^{-2} unless otherwise specified) and plated on Hv-Ca + 5FOA, in addition to other required additives. 5-FOA was necessary to counterselect against any remaining *pyrE2*$^+$ (plasmid integrant) cells, therefore only Δ*pyrE2* colonies with either the original chromosomal sequence or the gene deletion/mutant allele construct would form colonies. Plates were incubated at 45˚C for at least five days to allow colony formation, and colonies patched onto YPC plates (+Thy if Δ*hdrB*) (40 patches per plate).

Colony lift and hybridisation to identify Gene deletion strains

If the desired strain contained a deletion of a gene, 5-FOA resistant colonies were patched on YPC (+Thy if required) and grown at 45°C for about 5 days. Colony lifts and hybridisations were carried out using a probe homologous to the deleted fragment. Strains deleted for the gene could be identified, as they will not bind the probe and give a negative signal.

An 82 mm filter (Biorad) was rolled onto the surface of agar plates patched with colonies and left at room temperature for 1 min. The filter was then removed carefully

and placed colony side up on blotting paper soaked with 10% SDS and left for 2 min to allow cell lysis. The filter was then placed colony side up on blotting paper soaked in denaturing solution for 5 min, to denature the DNA. Following this, the filter was then transferred, colony side up, to blotting paper soaked in neutralising buffer and left for 3 min. A second neutralising step was carried out as before. The filter was then washed in 2 × SSPE briefly then allowed to dry thoroughly on fresh blotting paper.

DNA was then UV cross-linked to the filter, prehybridised, hybridised, washed, exposed and visualised in the same manner as described in the Southern Blotting methods, with the exclusion of marker ladder DNA from the probe template mixture. The DNA probe used was dependent on the procedure. If the aim were to hybridise potential clones, the probe would be a PCR amplification of a portion of the gene (> 400 bp in size). If detecting a gene deletion the probe would be a digest or amplification of a portion of the gene, not present in the deletion construct.

Southern blotting to confirm the genotype of deletion mutants

Agarose gels were stained in 1 litre of 0.5µg/ ml ethidium bromide solution for 30 min with gentle rocking. The gel was then visualised on a Geldoc (BioRad) to ensure that complete digestion of DNA had occurred. The gel was transferred to 1 litre of 0.25 M HCl for 20 min to depurinate DNA. The gel was then washed in 1 litre of water for 10 min and then denatured for 40 min in denaturing solution. A 15 × 25 cm Zeta-Probe GT positively charged membrane (BioRad) was soaked in water for 5 min then transferred to sufficient denaturing buffer to cover the membrane. The membrane and gel were positioned on a Vacugene XL gel blotter (Pharmacia Biotech). Sufficient denaturing solution was poured on the gel to cover it and the DNA was transferred to the membrane for 1 hr at 40 mBar vacuum, provided by a Vacugene Pump (Pharmacia Biotech). Immediately following transfer, the membrane was washed briefly in 2 × SSPE and allowed to dry on Whatman 3 mm blotting paper.

DNA was crosslinked to the membrane with 150 mJ/cm^2 UV light and placed in a hybridisation tube (Techne) with 40 ml of prehybridisation solution. 800 µl of fish sperm DNA (10 mg/ml, Roche) was boiled for 5 min, chilled on ice and added to the hybridisation tube. The membrane was incubated at 65˚C for 4 hr with rotation to allow prehybridisation. After 4 hr, the prehybridisation solution was replaced with 30ml hybridisation solution. A prepared radiolabelled DNA probe and fish sperm DNA were added and the membrane was hybridised overnight at 65˚C with rotation.

The following day, the hybridisation solution was replaced by 50 ml of low stringency wash solution and incubated for 5 min at 65˚C. The wash solution was then replaced by a further 50 ml and incubated at 65˚C. After 30 min, the wash solution was poured away and 50 ml of high stringency wash solution was added. The membrane was

incubated as before for 30 min before the wash solution was replaced by a further 50 ml and incubated for a further 30 min. After the final wash, the membrane was allowed to dry briefly on 3 mm Whatman blotting paper and wrapped in Saran wrap. The membrane was then allowed to expose using a phosphorimager screen (Fujifilm BAS Cassette 22325) for at least 12 hr. The screen was then scanned using a Molecular Dynamics STORM 840 scanner and the resulting graphical file was refined using L-Process and analysed using Image Quant (Fujifilm).

Genomic DNA libraries for promoter screen

H. volcanii H53 DNA was digested with *Aci*I for 30 min at the recommended temperature, using ~0.2 units/µg DNA in New England Biolabs buffer 1. Fragments of ~500 bp were excised from agarose gels and ligated with pTA425, which had previously been cut with *Cla*I and the DNA ends dephosphorylated. The plasmid library was used to transform *E. coli* N2338 and was subsequently plated on LB + Amp. DNA was prepared directly from colonies to avoid differential amplification and then was used to transform *H. volcanii* Δ*pyrE2* Δ*trpA* strain H53. Transformants were selected on Hv-Min plates containing 0.5% of either glucose, glycerol, succinic acid or lactic acid.

2.2.7 *H. volcanii* assays

Growth rate assays

Colonies were used to inoculate 6 ml of Hv-YPC broth (+ Thy if required) and incubated at 45˚C overnight. The fresh culture was diluted to $OD_{650} \approx 0.1$ and then put back at 45˚C till $OD_{650} \approx 0.5$. At this stage, 10 µl of the culture was added to 6ml fresh Hv-YPC broth (+Thy if required) and put back at 45˚C. The first sample was taken about 15 hr later and the OD_{650} of the culture were measured. Serial dilutions were made from 10^0 to 10^{-6} and duplicate 20 µl drops of culture were pipetted onto Hv-YPC agar (+Thy if required). At regular intervals, 50ul of culture were taken until $A_{650} \approx 1.0$ was reached.

UV survival assays

Colonies were used to inoculate 6 ml of Hv-YPC broth (+ Thy if required) and incubated at 45˚C overnight. The fresh culture was diluted to $OD_{650} \approx 0.1$ and then put back at 45˚C till $OD_{650} \approx 0.5$. Serial dilutions were made from 10^0 to 10^{-6} and duplicate 20 µl drops of culture were pipetted onto Hv-YPC agar (+Thy if required). Spots were allowed to dry at room temperature and plates were either exposed to ultraviolet light at a rate of 1 J/m^2/second (254 nm peak) or not exposed to UV light, as a control. Plates were shielded from visible light by use of a black plastic bag to prevent photo-reactivation of DNA, and incubated at 45°C until colonies were visible.

Gamma radiation survival assays

Colonies were used to inoculate 6 ml of Hv-YPC broth (+ Thy if required) and incubated at 45˚C overnight till $OD_{650} \approx 0.8$. Serial dilutions were made from 10^0 to 10^{-6} and duplicate 20 µl drops of culture were pipetted onto small Hv-YPC agar (+Thy if required). Plots were allowed to dry at room temperature. Plates were either exposed to gamma radiation (^{137}Cs as the source) at a rate of 6.6 Gy/min or not exposed to gamma radiation, as a control. Paltes were incubated at 45°C until colonies were visible.

Phleomycin sensitivity assays

Colonies were used to inoculate 6 ml of Hv-YPC broth (+ Thy if required) and incubated at 45˚C overnight. The fresh culture was diluted to OD650 ≈ 0.1 and then put back at 45˚C till OD650 ≈ 0.45. The culture was divided into several aliquots of 1ml and transferd to 1.5 ml cap tubes. 20 µl serial dilution of phleomycin in 18% SW were added to each tube to the final concentration of 0.5, 1 and 2 mg/ml or 20 µl 18% SW were added to the control tube. Then the tubes were incubated on Eppendorf thermomixer at 45°C 450 rpm for 1 hr. Serial dilutions were made from 10^0 to 10^{-6} and duplicate 20 µl drops of culture were pipetted onto Hv-YPC agar (+Thy if required). Plots were allowed to dry at room temperature. Plates were incubated at 45°C 3-4 days until colonies were visible.

H_2O_2 sensitivity essays

Colonies were used to inoculate 6 ml of Hv-YPC broth (+ Thy if required) and incubated at 45˚C overnight. The fresh culture was diluted to OD650 ≈ 0.1 and then put back at 45˚C till OD650 ≈ 0.45. The culture was divided into several aliquots of 1ml and transfered to 1.5 ml cap tubes. 20 µl serial dilution of H_2O_2 in 18% SW were added to each tube to the final concentration of 1, 2, 4, 6% or 20 µl 18% SW were added to the control tube. The tubes were incubated on Eppendorf thermomixer at 45°C for 1 hr. Serial dilutions were made from 10^0 to 10^{-6} and duplicate 20 µl drops of culture were pipetted onto Hv-YPC agar (+Thy if required). Plots were allowed to dry at room temperature. Plates were incubated at 45° until colonies were visible.

MMS sensitivity essays

Colonies were used to inoculate 6 ml of Hv-YPC broth (+ Thy if required) and incubated at 45˚C overnight. The fresh culture was diluted to OD650 ≈ 0.1 and then put back at 45˚C till $OD_{650} \approx 0.45$. The culture was divided into several aliquots of 1 ml and transfered to 1.5 ml cap tubes. 20 µl serial dilution of MMS in 18% SW were added to each tube to the final concentration of 0.02, 0.04, 0.06% or 20 µl 18% SW were added to the control tube. Then the tubes were incubated on Eppendorf thermomixer at 45°C 450 rpm for 1 hr. Serial dilutions were made from 10^0 to 10^{-6} and duplicate 20 µl drops of culture were pipetted onto Hv-YPC agar (+Thy if required). Plots were allowed to dry at room temperature. Plates were incubated at 45° until colonies were visible.

Mitomycin C sensitivity assays

Colonies were used to inoculate 6 ml of Hv-YPC broth (+ Thy if required) and incubated at 45˚C overnight. The fresh culture was diluted to $OD_{650} \approx 0.1$ and then put back at 45˚C till $OD_{650} \approx 0.5$. Serial dilutions were made from 10^0 to 10^{-6} and duplicate 20 µl drops of culture were pipetted onto Hv-YPC agar (+Thy if required) supplemented with mitomycin C to the final concentration of 0.02 ug/ml. MMC plates prepared in a single batch, within two weeks, were used for all the strains in an independent test. Cells were also pipetted onto YPC or YPC + Thy plates containing no mitomycin C as a control. Plates were allowed to dry at room temperature and then incubated at 45°C for 5-10 days until colonies formed.

Recombination assays

The following section describes several *H. volcanii* transformation assays designed to test the proficiency of recombination. Some aspects are common to all procedures and these will be outlined first.

Initial cell density

All cultures used for transformation were grown until $OD_{650} \approx 0.6$ so that cells were in late exponential phase. Liquid media used was Hv-YPC broth (+Thy if required), unless otherwise stated.

Plating of transformants

Transformants were plated on media to select for the appropriate marker(s) on the transforming plasmid, either containing no uracil and/or no leucine, as outlined in each protocol. Additional media supplements were added where necessary, e.g. if the strain being transformed was also *trpA*$^-$ but selection of tryptophan was not relevant to the assay, media was supplemented with tryptophan. Transformants were plated at dilutions ranging from 10^0 to 10^{-3}.

Viable cell count

It was essential to determine the total surviving cell for all transformation assays. This was obtained by plating dilutions of the transformations on non-selective media (Hv-YPC, + Thy if required) at dilutions from 10^{-4} to 10^{-6}.

Recovery phase and subsequent growth

All transformations were allowed to recover for 4.5 hr at 45˚C, 1.5 hr as a pellet with no agitation followed by 3 hr resuspended and with rotation. Following plating, transformants were incubated for 5 - 7 days at 45˚C.

Efficiency of circular plasmid restoration

pTA277 is a replicative plasmid containing a *pyrE2* marker and a functional β-galactosidase gene *bgaHa*, within which there is a *Bst*BI site. In *bgaHa-Bb* allele, an

oligonucleotide with an *Nco*I site was inserted at the *Bst*BI site of *bgaHa*. Cells from 0.5ml culture (OD_{650}=0.6, with *bgaHa-Bb* allele) were transformed with 100 ng pTA277 digested by *Bst*BI. Transformants were plated on Hv-Ca +Trp+Thy to select for Ura^+(*pyrE2*$^+$) cells containing pTA277. Following growth, plates were sprayed with Bluetech X-β-gal solution using an atomiser. Plates were then left overnight at room temperature. The following day, blue colonies and red colonies were counted. Then red colonies were patched out on HV-Ca+Thy+Thy. Only those cells had undergone accurate end-joining could give out the blue colour at the presence of X-β-gal. To distinguish the events that had happened in red cells, colony PCR were carried out to amplify the *bgaHa* region with primers PBSF2 and PBSR3. The primers specifically bind the polylinker regions of pTA277, which flank the *bgaHa* gene. Then PCR products were digested by *Nco*I. By analysing the size of the resulting restriction fragments, the genotype of the strain could be deduced. If the colony PCR product can be digested into expected fragements by *Nco*I, the cells used in the PCR were those had undergone homologous recombination, while the others had undergone inaccurate NHEJ.

Non-crossover vs. crossover recombination assay

Cells were transformed with pTA168 [*pyrE2*$^+$*, LeuB-Aa2*]. Transformants were plated on Hv-Min +Trp+Thy+Ura to select for cells that had undergone a r*eco*mbination event between plasmid-borne *LeuB-Aa2* allele and chromosomal *LeuB-Ag1* allele (generating a wildtype *leu*$^+$ allele), whether crossover or non-crossover. Colonies were patched on Hv-Min +Trp+Thy, to select for crossover recombination events in cells that had integrated the plasmid and become *pyrE2*$^+$ *leu*$^+$, and on Hv-Min +Trp+Thy+Ura as a control to ensure that all colonies patched were *leu*$^+$. From these data, a percentage of crossover events (*leuB*$^+$ *pyrE2*$^+$) vs total recombination events (*leuB*$^+$) could be derived, therefore the remaining recombination events (*leuB*$^+$*, pyrE2*$^-$) were non-crossover recombination events. Transformation was also carried out using water instead of DNA, to control for reversion of the mutant chromosomal *LeuB-Ag1* allele to wild-type. The rate of reversion of the chromosomal *leu*B-*Ag2* allele was calculated by dividing the number of colonies present on water control plates by the viable count. This value was then used as a weighting index and multiplied by the viable count for the pTA168 transformation. The resulting value was the expected number of colonies present that were l*euB*+ through reversion and not by recombination with pTA168. However, no reversions were observed in any of the trials.

Chapter III: Construction of deletion mutants

3.1 Construction of hef deletion mutants

Cloning of the *H. volcanii hef* gene and its flanking region of the gene was carried out by Thorsten Allers, prior to the commencement of this PhD study. The sequence of the *H. volcanii hef* ORF, as annotated by the Institute for Genomic Research (TIGR), was obtained. *hef* was annotated as ORF01969 on the chromosome at position 2841653–2844229 bp, close to the main chromosome replication origin *oriC1* (Figure 3.1)(Norais et al., 2007a). *Not*I restriction sites were present 2645 bp upstream and 1743 bp downstream of ORF01969 that would generate a fragment of 6964 bp upon digestion. Genomic DNA from wild-type strain WR340 (Bitan-Banin et al., 2003) was digested with *Not*I, electrophoresed and fragments of approximately 7 kb were extracted and purified. The DNA fragments were then ligated to the *Not*I site of pBluescript II SK+ and used to transform XL1-Blue strain *E. coli*. Transformants were screened by colony lift with the *hef* cloning probe prepared by PCR. The binding sites of the PCR primers, xpf-F and xpf-R, are within the coding region of *hef*. A clone containing pBluescript II SK+ with *hef* was successfully obtained. The plasmid was designed as pTA334 (Figure 3.3).

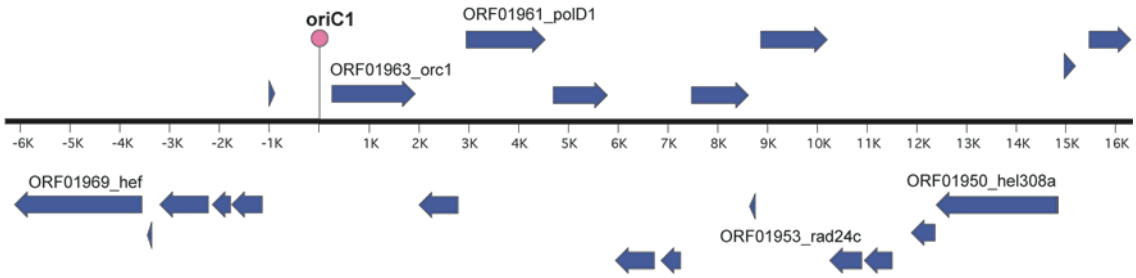

Figure 3.1 Open reading frames near Hv *oriC1*.

ORF01969_Hef and ORF_01950_Hel308a are close to the main chromosome replication origin *oriC1* in *H. volcanii.* Within this region, other ORFs annotated as DNA metabolism genes are ORF01963_orc1, ORF01961_polD1 and ORF01953_rad24c.

3.1.1 Design of Primers for the *hef* deletion plasmids

Sequence alignment analysis suggests that Hef from *H. volcanii* is a homologue of human XPF and FANCM. All these proteins have a helicase:nuclease fusion

arrangement. Human XPF and FANCM have only one functional domain since the conserved motifs in the other domain have been disturbed (McCutchen-Maloney et al., 1999; Meetei et al., 2005). In contrast, Hef from *H. volcanii* has two domains with intact essential motifs (Figure 3.2).

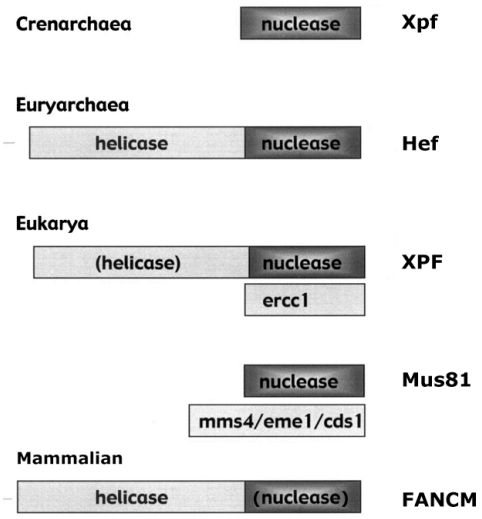

Figure 3.2 Structure of Hef homologues.

The archaea Hef homologues come in two different forms: in Crenarchaea, the *xpf* gene encodes only the C-terminal nuclease domain, like eukaryotic *Mus81*; in Euryarchaea, Hef is presented as a helicase:nuclease fusion as in Eukarya. Howerver, the helicase domains of eukaryotic XPFs lack essential (catalytic) residues for ATPase activity. The Hef in euryarchaea is also a homologue of human FANCM, which has a similar structure but the conserved motifs in the nuclease domain have been disturbed (White, 2003).

Primer	Primer Sequence
XPF-EPR	GCGACCC**GGTACC**TCGGCGGACTCG *Kpn*I
XPF-IPR	C GTC CTC **GGA TCC** CGA CAT CGGTG D E S G S M *Bam*HI
XPF-IPF	GTC GTC **GGA TCC** GAG TAC CGC TGA GC V V G S E Y R * *Bam*HI
XPF-EPR	GGCGAACGCGA**TCTAGA**CGGCCGCC *Xba*I
XPF-NDF	GAA **GGA TCC** GAG GTG GAC GAC TCG GCC E G S E V D D S A *Bam*HI
XPF-HDR	CAC CTC **GGA TCC** TTC TGC GTC CGA CG V E S G E A D S *Bam*HI

Table 3.1. PCR primers for *hef* deletion mutants.

The start code and stop code of the *hef* gene are underlined. The oligos within the helicase or nuclease domains are highlighted in blue and dark yellow, respectively. Restriction sites are shown as bold.

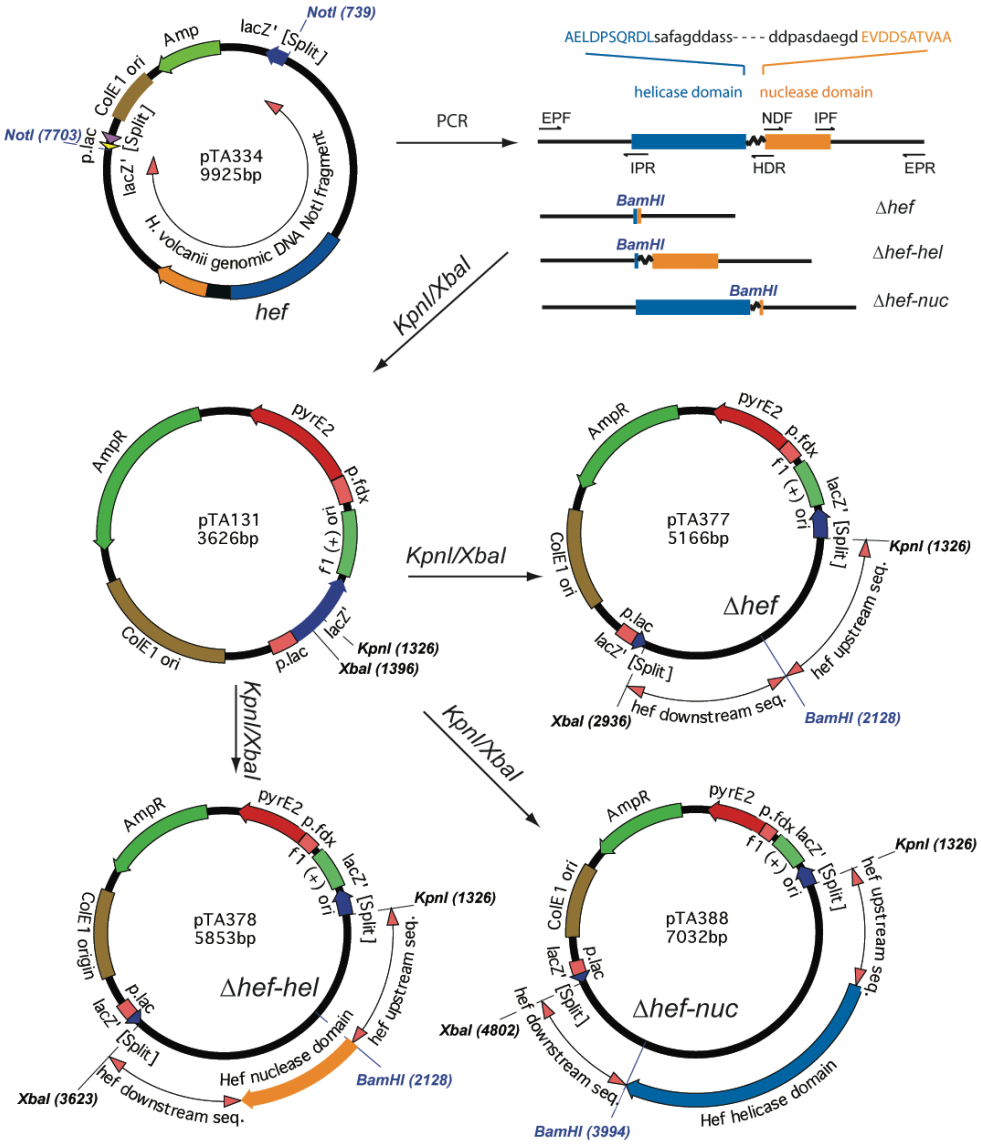

Figure 3.3 Primers design and plasmids constructed for *hef* deletion mutants.

The helicase domain, nuclease domain and the disordered region between the two domains are shown in blue, golden and black colours respectively. The helicase and nuclease domain sequences around the boundary of the disordered region are shown in capital letters. The N-terminal and C-terminal protein sequence of the disordered region are shown in lower case. PCR fragments by using two pairs of primers EPF/IPR and IPF/EPR were digested by *Bam*HI and ligated. The ligation products were digested by *Kpn*I/*Xba*I and then inserted at the *Kpn*I/*Xba*I sites of pTA131 to generate *hef* deletion plasmid pTA370 (dam^+) and pTA377 (dam^-). PCR fragments by using two pairs of primers EPF/IPR and NPF/EPR were digested by *Bam*HI, ligated and then inserted at the *Kpn*I/*Xba*I site of pTA131 to generate *hef* helicase domain deletion plasmid pTA371 (dam^+) and pTA378 (dam^-). PCR fragments by using two pairs of primers EPF/HDR and IPF/EPR were digested by *Bam*HI, ligated and then inserted at the *Kpn*I/*Xba*I site of pTA131 to generate *hef* nulease domain deletion plasmid pTA387 (dam^+) and pTA388 (dam^-).

Mutant constructions for entire and partial *hef* deletion were carried out. For entire deletion, internal primers (XPF-IPF and XPF-IPR) immediately flanking *hef* were designed to incorporate a novel *Bam*HI restriction site. The external primers upstream and downstream of *hef* were designed to contain *Kpn*I and *Xba*I respectively, which are part of the multiple cloning site of the *pyrE2*-marked integrative vector pTA131 (Allers et al., 2004). Globplot, a program used to analyse the domain boundary (Linding et al., 2003), predicts a disordered region between the *hef* helicase and nuclease domains. Therefore two other primers (XPF-HDR and XPF-NDF) for *hef* partial deletion were designed within the disordered region (See Table 3.1 and Figure 3.3).

3.1.2 Construction of plasmids for *hef* deletion mutants

PCR products were gel purified, digested, ligated and inserted into *pyrE2*-marked integrative plasmid pTA131. Three plasmids, pTA370 with construction of entire *hef* deletion, pTA371 with constuction of *hef* helicase domain deletion and pTA387 with constuction of *hef* nuclease domain deletion, were constructed in *E. coli* XL-1 Blue and then used to transform *E. coli* N2338 to prepare *dam*$^-$ DNA of the plasmids pTA377, pTA378 and pTA388 (Figure 3.3). *H. volcanii* has a restriction system that recognizes adenine-methylated GATC sites, resulting in DNA fragmentation followed by plasmid loss or chromosomal integration by recombination (Blaseio and Pfeifer, 1990). Thus, DNA used to transform *H. volcanii* needs to be prepared from *E. coli dam*$^-$ strain that is deficient in GATC methylation.

3.1.3 Pop-in and pop-out for *hef* deletion

The *pyrE2*-marked pop-in pop-out system is highly efficient to knockout non-essential genes in *H. volcanii* (Allers and Mevarech, 2005). The *pyrE2* gene encodes orotate phosphoribosyl transferase and is involved in uracil biosynthesis (Bitan-Banin et al., 2003). This system first uses circular DNA to transform *ura*$^-$ strain and selects for uracil prototrophy transformants (pop-in). Intramolecular recombinats that have lost the plasmid are counter selected using 5-fluoroorotic acid, which is converted to toxic 5-fluorouracil in *ura*$^+$ cells but not *ura*$^-$ cells (pop-out). The deletion mutant must be verified by Southern blotting later, unless the mutant has a readily screened phenotype. Since the deletion mutant is *ura*$^-$, the pop-in pop-out system can be re-used (Figure 3.4).

pTA377, pTA378 and pTA388 for *hef* deletion constructions were used to transform *ura*$^-$ strains H26 and H195. H26 is a *pyrE2* deletion strain, which can be used as a

parent strain for deletion mutant construction by using *pyrE2* counter selecting system Pop-in and pop-out (Allers et al., 2004). H194 and H195 are triple deletion strains (Δ*pyrE2* Δ*trpA* Δ*hdrB*) with different *leuB* and *bgaHa* alleles (Guy et al., 2006). H194 and H195 can also be used as parent strains to construct deletion mutants and their daughter strains can be used in recombination assays. Integrants (*ura*$^{+}$) were successfully obtained on Hv-Ca (Thy) plates and verified by genomic DNA digestion and Southern blotting (Figure 3.5 and 3.6). Integrants were cultured in non-selective liquid medium Hv-YPC (Thy) for about 30 generations and then *ura*$^{-}$ colonies were selected on 5-FOA plates. 5-FOA^{R} (*ura*$^{-}$) pop-out strains were screened by colony lift (Figure 3.7) and verified by genomic DNA digestion and Southern blotting (Figure 3.8).

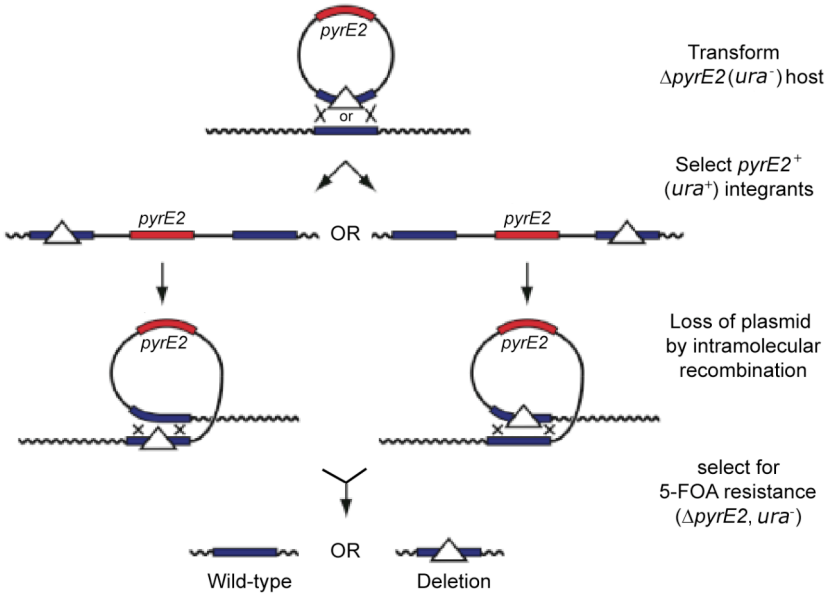

Figure 3.4 Pop-in pop-out gene deletion system.

A Δ*pyrE2* (*ura*$^{-}$) host is transformed with a plasmid containing the *pyrE2* marker and a deletion construct of the desired gene. To avoid being cleaved by a restriction system in *H. volcanii*, the plasmid DNA is prepared from an *E. coli dam*$^{-}$ strain. The plasmid integrates at regions of homology to the locus of the gene to be deleted, conferring uracil prototrophy (*ura*$^{+}$). Once the integratant strain has been confirmed by genomic DNA digestion and Southern blot analysis, selection for uracil is relieved by serial growth in Hv-YPC (+ Thy if required). Intramolecular recombinats that have lost the plasmid are counter selected using 5-fluoroorotic acid, which is converted to toxic 5-fluorouracil in *ura*$^{+}$ cells but not *ura*$^{-}$ cells. Depending on the orientation of the second recombination event relative to the first, the resulting strain will be either deleted for the desired gene or remain as wild-type.

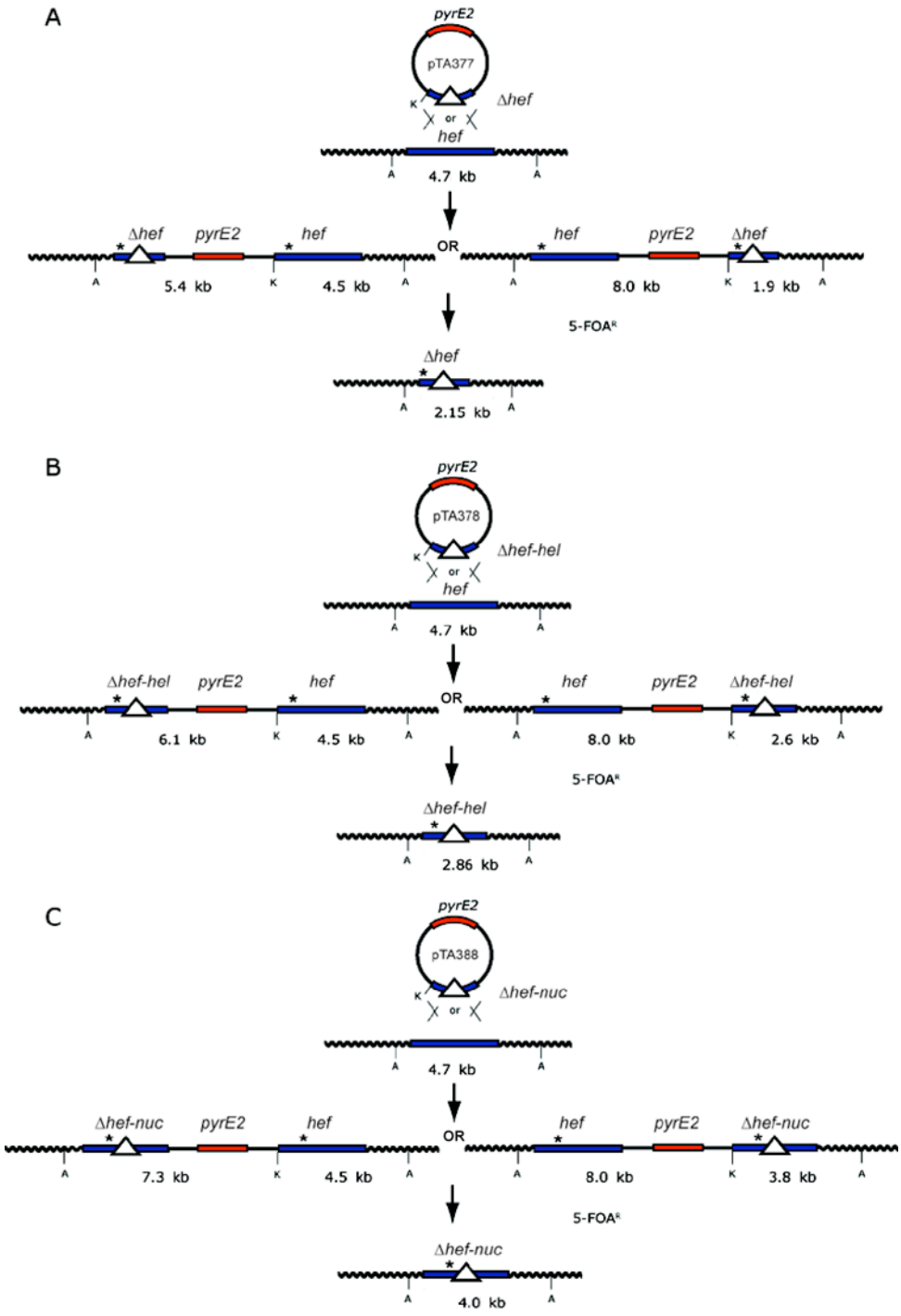

Figure 3.5 Schematic diagram of *hef* deletion mutant construction.

Plasmids pTA377 pTA378 and pTA388 were used to transform *ura*$^-$ strains. The plasmids may be inserted into the genome by homologous recombination in two possible orientations. Restriction sites used for genomic DNA digestions and the expected fragments resulting from these digestions are shown (A, *Age*I; K, *Kpn*I). * indicates the region homologous to the probe. Loss of the plasmid by intrachromosomal recombination resulted in the *hef* deletion strains. A. Deletion of *hef*; B. Deletion of the helicase domain of *hef* (Δ*hef-hel*); C. Deletion of the nuclease domain of *hef* (Δ*hef-nuc*).

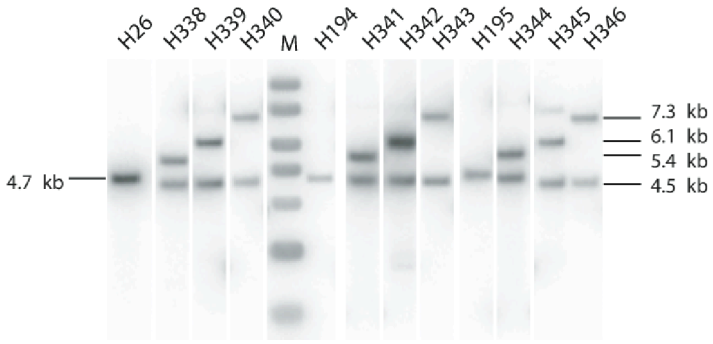

Figure 3.6 Southern blot analysis of integrated strain construction.

Lane M, size marker (from top to bottom): 10, 8, 6, 5, 4, 3 and 2 kb. Genomic DNA were digested with *Age*I/*Kpn*I and probed with the flanking regions of *hef*. H26, H194 and H195 genomic DNA digested with *Age*I/*Kpn*I were used as wild-type control. H338, H341 and H344 were generated by pTA377 integrated upstream of the *hef* gene in H26, H194 and H195, respectively. H339, H342 and H345 were generated by pTA378 integrated upstream of the *hef* gene in H26, H194 and H195, respectively. H340, H343 and H346 were generated by pTA388 integrated upstream of the *hef* gene in H26, H194 and H195, respectively.

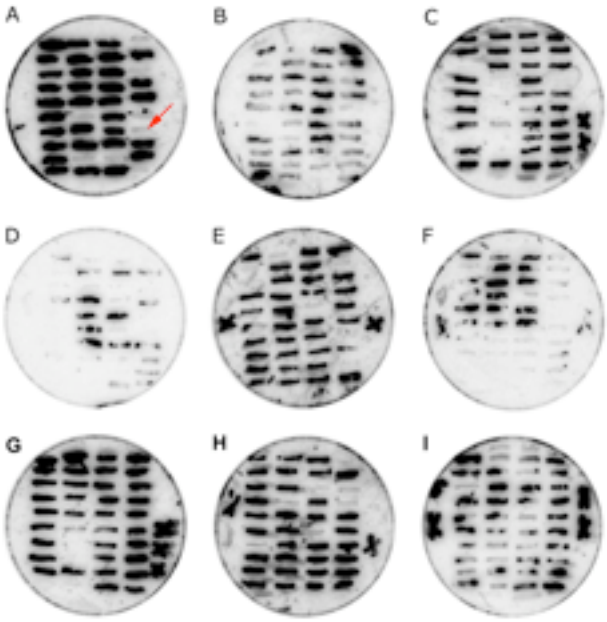

Figure 3.7 Colony lift and Southern blotting to screen for *hef* deletion mutants.

5-FOA^R colonies selected on Hv-Ca (Thy, 5-FOA) plates were patched out on Hv-YPC (Thy) plates, transferred to Biorad filter and probed with *hef* coding region (gel purified 0.7 kb *Bam*HI/*Blp*I fragment of pTA371 and 0.7 kb *Bam*HI/*Eco*RV fragment of pTA387). Colonies gave out negative signals were detected. One pop-out candidate is shown by the red arrow. A, B and C indicate pTA377 pop-out of H338, H341 and H344, respectively. D, E and F indicate pTA378 pop-out of H339, H342 and H345, respectively. G, H and I indicate pTA388 pop-out of H340, H343 and H346, respectively.

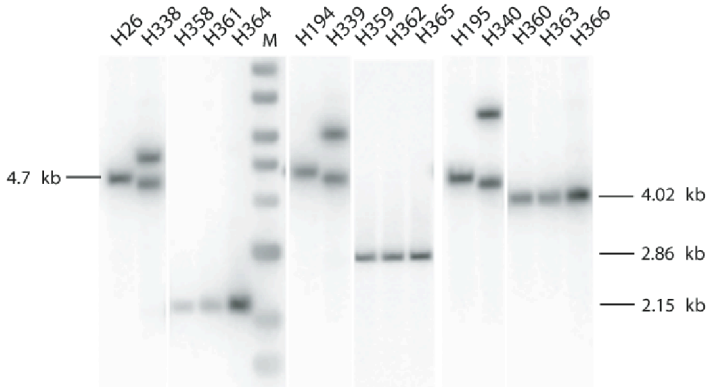

Figure 3.8 Southern blot analysis of Δ*hef* strains construction.

Lane M, size marker (from top to bottom): 10, 8, 6, 5, 4, 3, 2 and 1.5 kb. Genomic DNA were digested with *Age*I and probed with the flanking regions of *hef*. Genomic DNA of H26, H194 and H195 digested with *Age*I were used as wild-type control. Genomic DNA of H338, H339 and H340 digested with *Age*I were used as pop-in strain control. Δ*hef* strains H358, H361 and H364 were generated by pTA377 pop-out of H338, H341 and H344, respectively. Δ*hef-hel* strains H359, H362 and H365 were generated by pTA378 pop-out H339, H342 and H345, respectively. Δ*hef-nuc* strains H360, H363 and H366 were generated by pTA388 pop-out H340, H343 and H346, respectively.

3.1.4 Construction of *mre11 rad50* and *hef* double deletion mutant H782

Mre11 and Rad50 are well conserved (Aravind et al., 1999). These two proteins form a complex that is a key player in most aspects of the cellular response to DNA double-strand breaks, including homologous recombination (HR), nonhomologous end joining (NHEJ), telomere maintainance and DNA damage checkpoint activation (Assenmacher and Hopfner, 2004). The eukaryotic homologues of Hef are also involved in HR, NHEJ and telomere maintainance (See 1.11.1). To study the functional relationship between Hef and the Mre11/Rad50 complex in *H. volcanii*, a deletion mutant of these genes was constructed.

pTA377 for *hef* entire deletion were used to transform *ura*$^-$ strain H280 (Δ*mre11 rad50*, constructed by Thorsten Allers). Integrants were successfully obtained on Hv-Ca (Thy) plates and verified by genomic DNA digestion and Southern blotting. H772 was cultured in non-selective liquid medium Hv-YPC (Thy) for about 30 generations and then *ura*$^-$ colonies were selected on 5-FOA plates. 5-FOA^R (*ura*$^-$) pop-out strains were screened by colony lift and verified by genomic DNA digestion and Southern blotting (Figure 3.9).

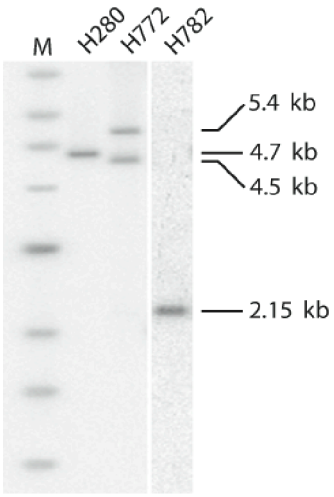

Figure 3.9 Southern blot analysis of pTA377 pop-in and pop-out of H280.

Lane M, size marker (from top to bottom): 10, 8, 6, 5, 4, 3, 2 1.5 and 1 kb. Genomic DNA were digested with *Kpn*I/*Age*I and probed with flanking region of *hef*. H280 genomic DNA digested with *Kpn*I/*Age*I was used as wild-type control. pTA377 integrated upstream of the *hef* gene in H280 and yielded strain H772. pTA377 pop-out of H772 and yielded Δ*mre11 rad50* Δ*hef* strain H782.

3.2 Construction of *fen1* deletion mutants

FEN1 family members are structure-specific endonucleases and have been widely identified, such as from bacteria, archaea, yeast, plants, Xenopus and mammals (Liu et al., 2004a). This important family of proteins is involved in DNA replication, recombination, repair and transcription (See 1.11.2).

3.2.1 Construct of plasmids for Δ*fen1::trpA*$^+$ mutants

The sequence of the *H. volcanii fen1* ORF, as annotated by the Institute for Genomic Research was obtained. *fen1* was annotated as ORF02107 on the chromosome at position 2710411–2711391 bp. In fact, beside human *FEN1*, sequence alignments show that the gene of this open reading frame is also a homologue of human *XPG*, another structure-specific endonuclease belonging to the FEN1 family. Both *FEN1* and *XPG* are essential in mammals (Kucherlapati et al., 2002; Shiomi et al., 2004).

For entire deletion of the *fen1* gene in *H. volcanii*, Cédric Norais, a PhD student in Hannu Myllykallio's laboratory (University of Paris, Orsay), constructed pTA535 (Figure 3.9). Internal primers immediately flanking *fen1* were designed to incorporate a novel *Bam*HI restriction site. The external primers upstream and downstream of *fen1* were designed to contain *Eco*RI and *Xba*I sites respectively, which are part of the multiple cloning site of the *pyrE2*-marked integrative vector pTA131. Then the 971 bp *p.fdx::trpA*$^+$ *Bam*HI fragment from pTA298 was inserted at the *Bam*HI site of pTA535 by Thorsten Allers, to generate the plasmid pTA544 with the Δ*fen1*::*trpA*$^+$ construct in *E. coli* XL-1 Blue and then used to transform *E. coli* N2338 to prepare *dam*$^-$ DNA of plasmid pTA554 (Figure 3.10).

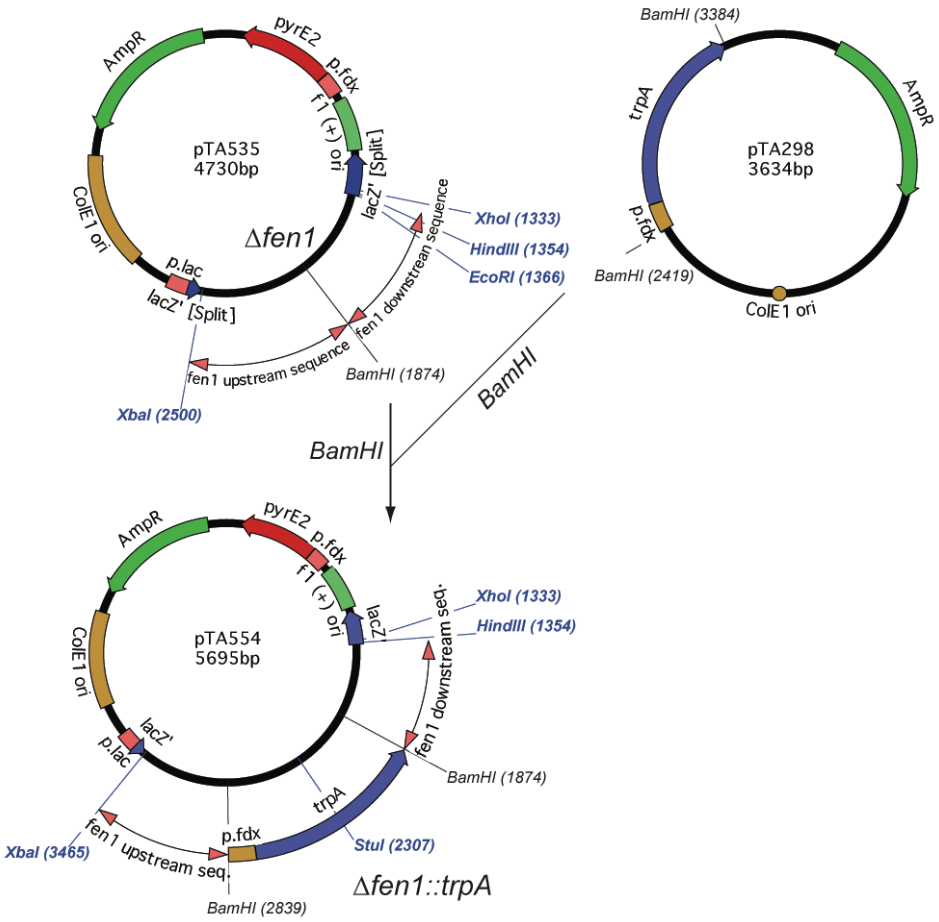

Figure 3.10 Construction of Δ*fen1::trpA* plasmid pTA554.

pTA535 is a *fen1* deletion plasmid construced on pTA131. The *Bam*HI fragment containing *p.fdx::trpA*$^+$ from pTA298 was inserted at the *Bam*HI site of pTA535 to generate the Δ*fen::trpA*$^+$ plasmid pTA544 (*dam*$^+$) and pTA554 (*dam*$^-$).

3.2.2 Construction of Δ*fen1::trpA*$^+$ in the background of *hef* partial deletion

pTA554 for *fen1* deletion was used to transform *ura*$^-$ *trp*$^-$ strains H195 (used as wild-type), H365 (Δ*hef-hel*) and H366 (Δ*hef-nuc*) (Figure 3.9). Integrants were successfully obtained on Hv-Ca (Thy) plates and verified by genomic DNA digestion and Southern blotting (Figure 3.11, Figure 3.12 A and B). H487, H489 and H490 were cultured in non-selective liquid medium Hv-YPC (Thy) for about 30 generations and then *ura*$^-$ colonies were selected on 5-FOA plates. 5-FOA^R (*ura*$^-$) pop-out strains were screened by colony lift and verified by genomic DNA digestion and Southern blotting (Figure 3.12 C). Deletion mutants H522 (Δ*fen1::trpA*$^+$), H524 (Δ*hef-hel* Δ*fen1::trpA*$^+$) and H525 (Δ*hef-nuc* Δ*fen1::trpA*$^+$) were constructed successfully.

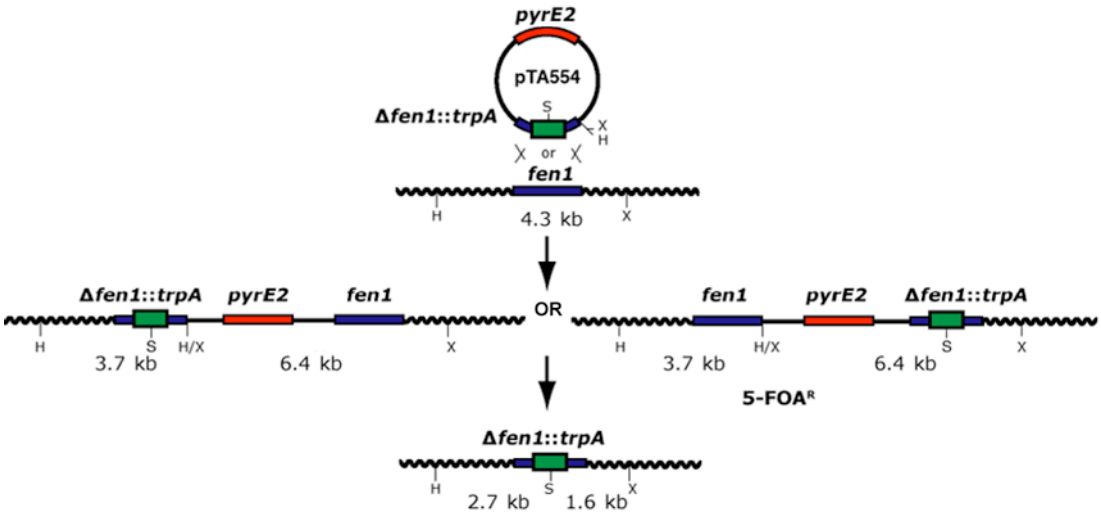

Figure 3.11 Schematic diagram of Δ*fen1*::*trpA* mutant Construction.

Plasmid pTA554 was constructed as described in the legend of Figure 3.7. There are two possible orientations of pTA554 insertion into the genome by homologous recombination. Restriction sites used for genomic DNA digestions and the expected fragments resulting from these digestions are shown (H, *Hin*dIII; S, *Stu*I; X, *Xho*I). Loss of the plasmid by intrachromosomal recombination resulted in the Δ*fen1*::*trpA* strain.

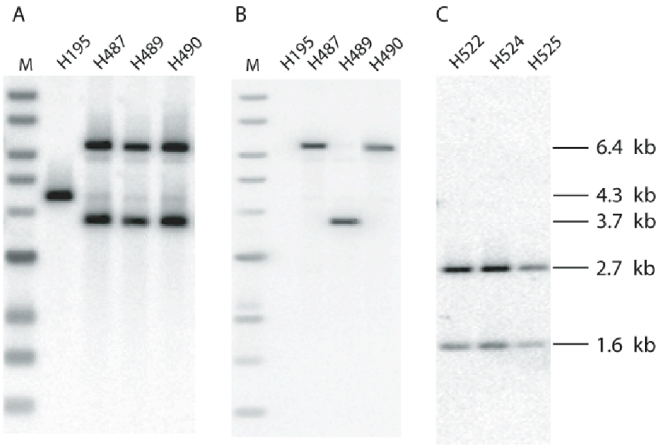

Figure 3.12 Southern blot analysis of pTA554 pop-in and pop-out.

Lane M, size marker (from top to bottom): 10, 8, 6, 5, 4, 3, 2, 1.5 and 1 kb. (A) Genomic DNA were digested with *Hin*dIII/*Xho*I and probed with the flanking regions of *fen1*. (B) Genomic DNA were digested with *Hin*dIII/*Xho*I and probed with *trpA*. Genomic DNA of H195 digested with *Hin*dIII /*Xho*I was used as wild-type control. H487 and H490 were generated by pTA554 integrated downstream of the *fen1* gene in H195 and H366, respectively. pTA554 integrated upstream of the *fen1* gene in H365 and yielded strain H489. (C) Genomic DNA were digested with *Hin*dIII/*Xho*I/*Stu*I and probed with the flanking regions of *fen1*. Δ*fen1*::*trpA*$^{+}$ strains H522, H524 and H525 were generated by pTA554 pop-out of H487, H489 and H490, respectively.

3.2.3 Construction of Δ*fen1*::*trpA*$^+$ Δ*hef* double deletion mutant H598

Human FEN1 and XPF are two structure-specific endonucleases with opposite polarity (Friedberg et al., 1995b). To determine if the homologues of these two proteins in *H. volcanii* have overlapping functions, a double deletion mutant was constructed. pTA377 for *hef* entire deletion were used to transform *ura*$^-$ strains H522 (Δ*fen1*::*trpA*$^+$). Integrants were successfully obtained on Hv-Ca (Thy) plates and verified by genomic DNA digestion and Southern blotting (Figure 3.13). H572 was cultured in non-selective liquid medium Hv-YPC (Thy) for about 30 generations and then *ura*$^-$ colonies were selected on 5-FOA plates. 5-FOA^R (*ura*$^-$) pop-out strains were screened by colony lift and verified by genomic DNA digestion and Southern blotting (Figure 3.13).

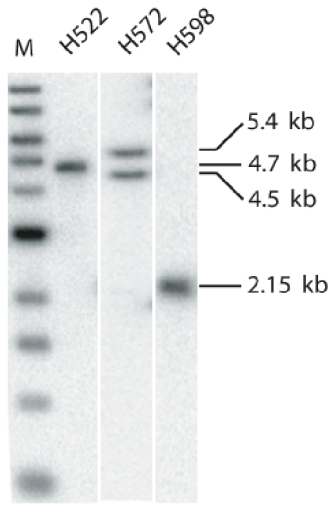

Figure 3.13 Southern blot analysis of pTA377 pop-in and pop-out of H522.

Lane M, size marker (from top to bottom): 10, 8, 6, 5, 4, 3, 2, 1.5, 1 and 0.5 kb. Genomic DNA were digested with *Kpn*I/*Age*I and probed with the flanking regions of *hef*. H522 genomic DNA digested with *Kpn*I/*Age*I was used as the wild-type control. pTA377 integrated upstream of *hef* gene in H522 and yielded strain H572; p377 pop-out of H572 and yielded Δ*fen1*::*trpA*$^+$ Δ*hef* strain H598.

3.2.4 Construction of *fen1* deletion mutant H823

H522, the *fen1* deletion strain with *trpA*$^+$ marker was easily selected and grows well at normal growth condition. Therefore an unmarked *fen1* deletion construction was planned to make the background of the mutant strain as simple as possible (Figure 3.14). pTA535 for *fen1* deletion were used to transform *ura*$^-$ strains H522 (Δ*fen1*::*trpA*+). Integrants were successfully obtained on Hv-Ca (Thy) plates and verified by genomic DNA digestion and Southern blotting (Figure 3.15 A). H818 was cultured in non-selective liquid medium Hv-YPC (Thy) for about 30 generations and then selected on Trp$^-$ plates (Figure 3.15 B). Pop-out strains were verified by genomic DNA digestion and subsequenctly Southern blotting (Figure 3.15 A).

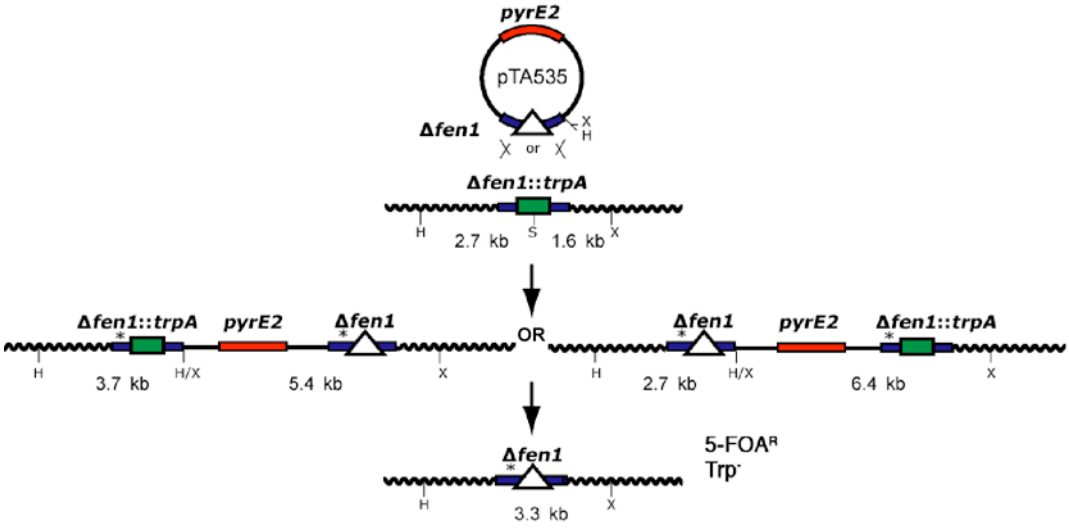

Figure 3.14 Schematic diagram of *fen1* deletion mutant Construction.

Plasmid pTA535 was constructed as described in 3.2.1 (Figure 3.7). There are two possible orientations of pTA535 insertion into the genome by homologous recombination. Restriction sites used for genomic DNA digestions and the expected fragments resulting from these digestions are shown (H, *Hin*dIII; X, *Xho*I). Loss of the plasmid by intrachromosomal recombination resulted in the Δ*fen1* strain.

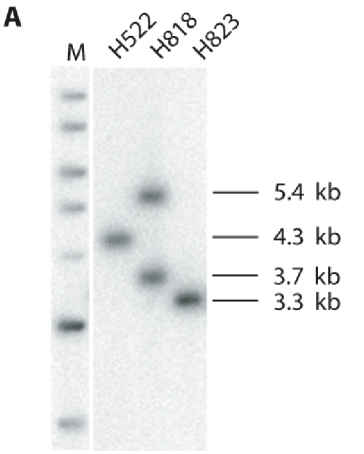

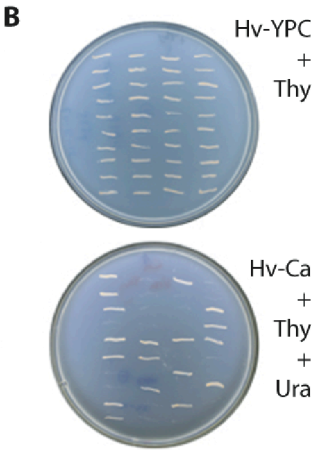

Figure 3.15 Construction of Δ*fen1* mutant without *trpA* marker

(A) Southern blot analysis of pTA535 pop-in and pop-out H522. Lane M, size marker (from top to bottom): 10, 8, 6, 5, 4, 3 and 2 kb. Genomic DNA were digested with *Hin*dIII/*Xho*I and probed with the flanking regions of *fen1*. H195 genomic DNA digested with *Hin*dIII/*Xho*I was used as wild-type control. pTA535 integrated downstream of the *hef* gene in H522 and yielded strain H818. pTA535 pop-out H818 and generated Δ*fen1* strain H823. (B) Screen for *trpA*$^-$ colonies on selective plates. H818 was cultured in complex medium Hv-YPC (Thy) for about 30 generations and then spreaded on Hv-YPC (Thy) plates. Single colonies were patched out on Hv-YPC (Thy) and Trp$^-$ plates Hv-Ca (Thy Ura) to selecte pTA535 pop-out strains (*trpA*$^-$).

3.2.5 Construction of *fen1* deletion mutant in the background of H115

H115 is a *pyrE2* deletion strain with *bgaHa-kp* allele, which can be used as parent strain to construct deletion mutants and its daughter strains can also be used in recombination assay. pTA535 for *fen1* deletion were used to transform *ura*$^-$ strains H115 (used as wild-type), H204 (Δ*mre11 rad50*), H648 (Δ*polX*) and H651 (Δ*polX* Δ*mre11 rad50*). Integrants were successfully obtained on Hv-Ca plates and verified by genomic DNA digestion and Southern blotting (Figure 3.16). H682, H683, H684 and H685 were cultured in non-selective liquid medium Hv-YPC for about 30 generations and then *ura*$^-$ colonies were selected on 5-FOA plates. 5-FOA^R (*ura*$^-$) pop-out strains were verified by genomic DNA digestion and then Southern blotting (Figure 3.16).

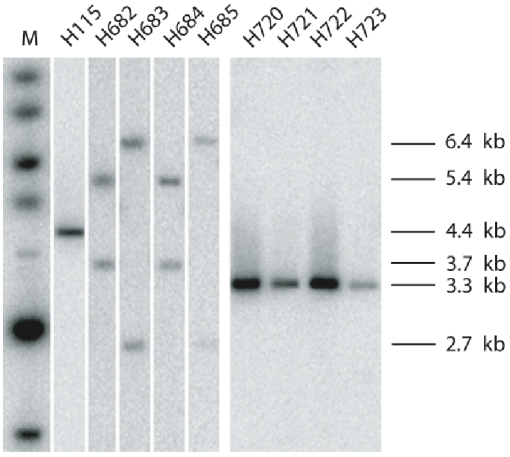

Figure 3.16 Southern blot analysis of pTA554 pop-in and pop-out of H115 background strains.

Lane M, size marker (from top to bottom): 10, 8, 6, 5, 4, 3 and 2 kb. Genomic DNA were digested with *Hin*dIII/*Xho*I and probed with the flanking regions of *fen1*. H115 genomic DNA digested with *Hin*dIII /*Xho*I was used as wild-type control. H682 and H684 were generated by pTA535 integrated upstream of the *fen1* gene in H115 and H648, respectively. H683, H685 were generated by pTA535 integrated downstream of *fen1* gene in H204 and H651, respectively. Δ*fen1* strains H720, H721, H722 and H723 were generated by pTA535 pop-out of H682, H683, H684 and H685, respectively.

3.3 Construction of *uvrA* deletion mutants

Most archaea have genes encoding homologues of the eukaryal NER nucleases XPF (Rad1) and XPG (Rad2)/FEN1 (Rad27), and helicases XPB (Rad25) and XPD (Rad3). Intriguingly, homologues of bacterial NER genes have been found in some archaea species, mainly mesophilic methanogens and halophiles (McCready and Marcello, 2003; White, 2003). In *E. coli*, the UvrA protein plays a vitally important role in nucleotide excision repair due to the fact that UvrA is the first component to recognize

DNA damage in NER (Truglio et al., 2006). It would be interesting to explore the overlapping function of the two NER machineries in *H. volcanii.*

3.3.1 Cloning of *uvrA* and its flanking regions

The sequence of the *H. volcanii uvrA* ORF was obtained and submitted to the EMBL nucleotide sequence database with the accession number AM989993. *uvrA* was annotated as ORF01566 on the main chromosome at position 347502–350453 bp by the Institute for Genomic Research (TIGR). *Sac*I restriction sites were present 4910 bp upstream and 2865 bp downstream of ORF01566 that would generate a fragment of 10626 bp upon digestion. Genomic DNA from wild-type *H. volcanii* was digested with *Sac*I, electrophoresed and fragments of approximately 10.6kb were extracted and purified. The DNA fragments were then ligated to the *Sac*I site of pBluescript II SK+ and used to transform XL1-Blue strain *E. coli*. Transformants were screened by colony lift with the *uvrA* cloning probe prepared by PCR. The binding sites of the PCR primers, uvrAF and uvrAR, are within the coding region of *uvrA*. A clone containing pBluescript II SK+ with *uvrA* was successfully obtained. The plasmid was designed as pTA584 (Figure 3.17 and 3.18).

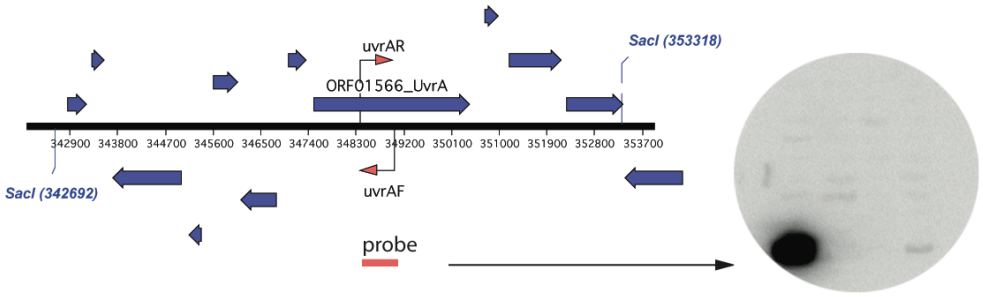

Figure 3.17 Cloning of *uvrA.*

Colony hybridisation of *E. coli* patches containing *H.volcanii* ~10.5 kb *Sac*I digested DNA, plasmid-borne fragments, potentially containing *uvrA*. The probe template was generated by amplification of a fragment of chromosomal *uvrA*. Colonies giving positive signals contained pBluescript II SK+ with the *Sac*I fragment containing *uvrA*.

3.3.2 Design of primers for *uvrA* deletion plasmid

Four primers were designed based on the *uvrA* gene cloned in pTA584. For entire deletion of the *uvrA* gene, internal primers (uvrA-IPF and uvrA-IPR) immediately flanking *uvrA* were designed to incorporate a novel *Bam*HI restriction site. The external primers upstream and downstream of *uvrA* were designed to contain *Hin*dIII and *Xba*I respectively, which are part of the multiple cloning site of the *pyrE2*-marked integrate vector pTA131 (Figure 3.18).

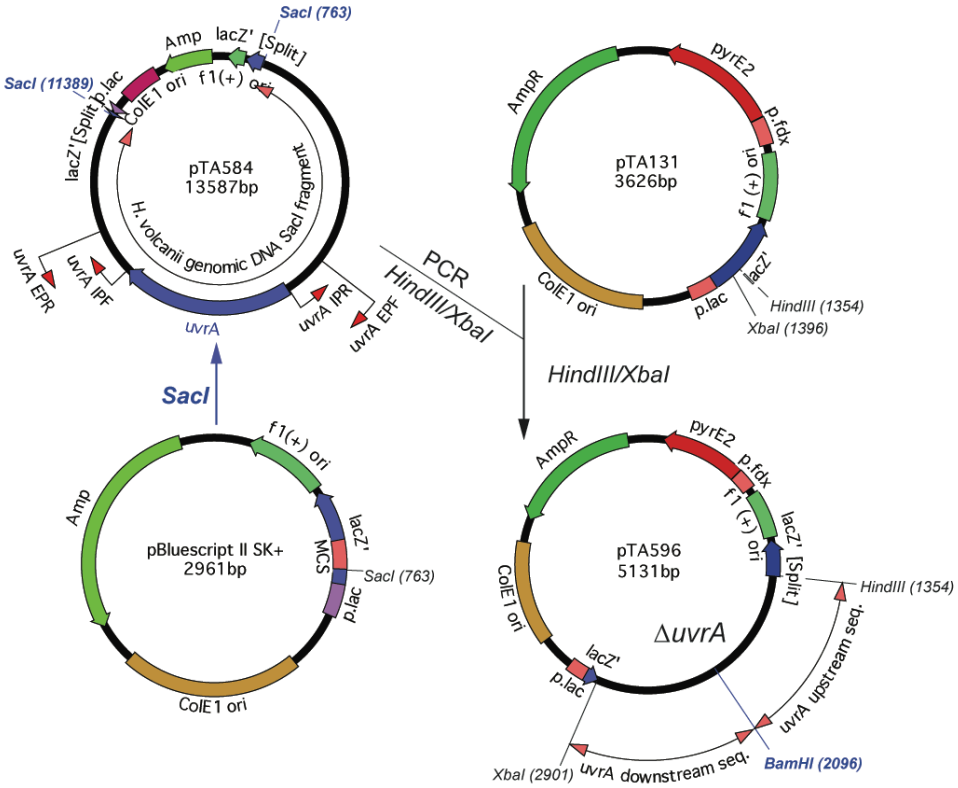

Figure 3.18 Primers design and plasmids constructed for *uvrA* deletion mutants.

A 10.6 kb *Sac*I fragment containing *uvrA* gene and its flanking sequence was cloned into pBluescript II SK+ to generate pTA584. Two pairs of PCR primer *uvrA* EPF/*uvrA* IPR and *uvrA* IPF/*uvrA* EPR were used to amplify the flanking regions of *uvrA* from pTA584. The PCR products were digested by *Bam*HI and ligated. The ligation product were then digested by *Hin*dIII/*Xba*I and inserted at the *Hin*dIII/*Xba*I sites of pTA131 to generate *uvrA* deletion plasmid pTA595 (dam^+) and pTA596 (dam^-).

3.3.3 Plasmid constructed for *uvrA* deletion mutants

PCR products of *uvrA* flanking regions were gel purified, digested, ligated and inserted

into *pyrE2*-marked integrative plasmid pTA131. pTA595 was constructed in *E. coli* XL-1 Blue and then used to transform *E. coli* N2338 to prepare *dam*$^-$ DNA of plasmid pTA596 (Figure 3.18).

3.3.4 Construction of Δ*uvrA* mutants in the background of *hef* deletion

pTA596 for *uvrA* deletion were used to transform *ura*$^-$ strains H26 (used as wild-type), H358 (Δ*hef*), H359 (Δ*hef-hel*), H360 (Δ*hef-nuc*) and H195 (used as wild-type) (Figure 3.19). Integrants were successfully obtained on Hv-Ca (Thy) plates and verified by genomic DNA digestion and Southern blotting (Figure 3.20 A). Integrants were cultured in non-selective liquid medium Hv-YPC (Thy) for about 30 generations and then *ura*$^-$ colonies were selected on 5-FOA plates. 5-FOA^R (*ura*$^-$) pop-out strains were screened by colony lift and verified by genomic DNA digestion and Southern blotting (Figure 3.20 B).

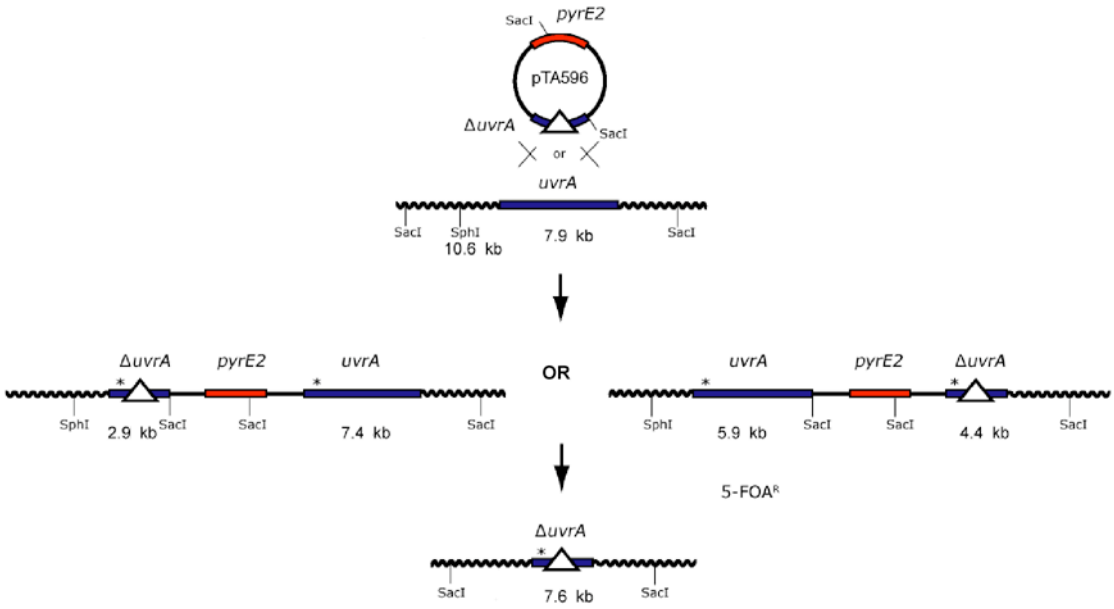

Figure 3.19 Schematic diagram of *uvrA* deletion mutant construction.

Plasmid pTA596 was constructed as described in the legend of Figure 3.18. There are two possible orientations of pTA596 insertion into the genome by homologous recombination. Restriction sites used for genomic DNA digestions and the expected fragments resulting from these digestions are shown. * indicates the region homologous to the probe. Loss of the plasmid by intrachromosomal recombination resulted in the Δ*uvrA* strain.

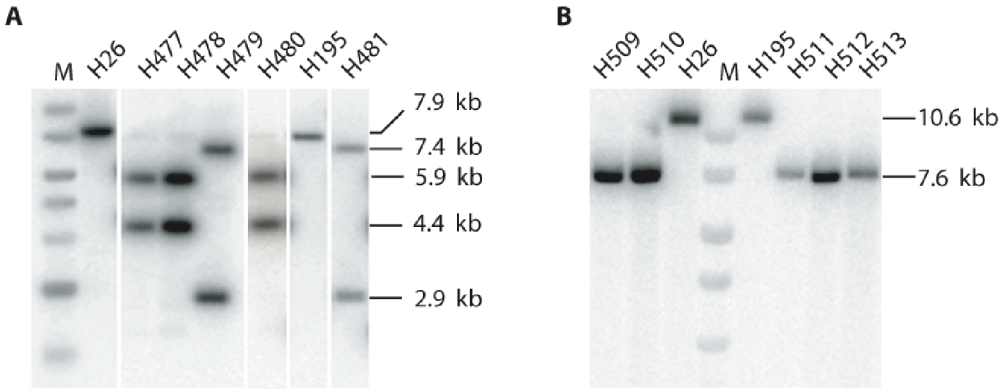

Figure 3.20 Southern blot analysis of pTA596 pop-in and pop-out of H26 and H195.

(A) Lane M, size marker (from top to bottom): 10, 8, 6, 5, 4, 3 and 2 kb. Genomic DNA were digested with *Sac*I/*Sph*I and probed with the flanking regions of *uvrA*. H26 and H195 genomic DNA digested with *Sac*I/*Sph*I were used as wild-type control. H477, H478 and H480 were generated by pTA596 integrated downstream of the *uvrA* gene in H26, H358 and H360, respectively. H481 and H479 were generated by pTA596 integrated upstream of the *uvrA* gene in H195and H359, respectively. (B) Lane M, size marker (from top to bottom): 10, 8, 6, 5 and 4 kb. Genomic DNA were digested with *Sac*I and probed with flanking regions of *uvrA*. H26 and H195 genomic DNA digested with *Sac*I were used as wild-type control. Δ*uvrA* strains H509, H510, H511, H512 and H513 were generated by pTA596 pop-out of H477, H478, H479, H480 and H481, respectively.

3.3.5 Construction of Δ*fen1::trpA*$^+$ Δ*uvrA* double deletion mutant H646

pTA596 for *uvrA* deletion were used to transform *ura*$^-$ strains H522 (Δ*fen1::trpA*$^+$). Integrants were successfully obtained on Hv-Ca (Thy) plates and verified by genomic DNA digestion and Southern blotting (Figure 3.21 A). H632 was cultured in non-selective liquid medium Hv-YPC (Thy) for about 30 generations and then *ura*$^-$ colonies were selected on 5-FOA plates. 5-FOA^R (*ura*$^-$) pop-out strains were screened by colony lift and verified by genomic DNA digestion and Southern blotting (Figure 3.21 B).

3.3.6 Construction of Δ*fen1::trpA*$^+$ Δ*hef* Δ*uvrA* triple mutant H647

pTA596 for *uvrA* deletion were used to transform *ura*$^-$ strains H598 (Δ*fen1::trpA*$^+$ Δ*hef*). Integrants were successfully obtained on Hv-Ca (Thy) plates and verified by genomic DNA digestion and Southern blotting (Figure 3.21 A). H633 was cultured in non-selective liquid medium Hv-YPC (Thy) for about 30 generations and then *ura*$^-$

colonies were selected on 5-FOA plates. 5-FOA^R (*ura*$^-$) pop-out strains were screened by colony lift and verified by genomic DNA digestion and Southern blotting (See Figure 3.21 B).

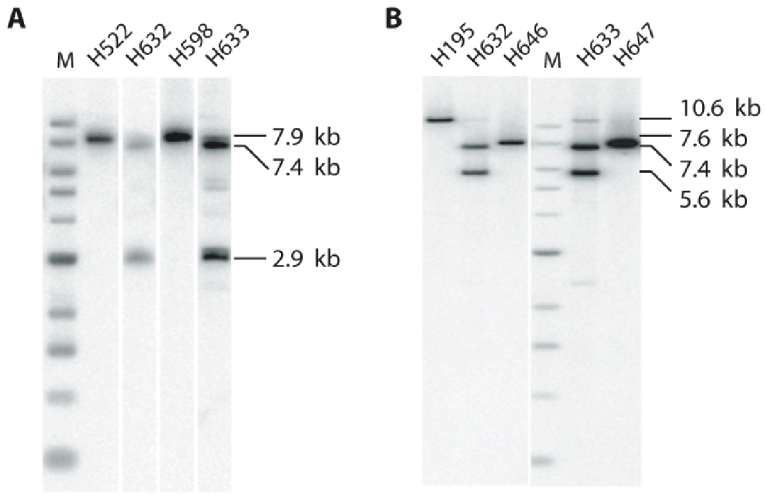

Figure 3.21 Construction of strains H646 and H647.

Lane M, size marker (from top to bottom): 10, 8, 6, 5, 4, 3, 2, 1.5, 1and 0.5 kb. (A) Southern blot analysis of pTA596 integrated strain construction. Genomic DNA were digested with *Sac*I/*Sph*I and probed with the flanking regions of *uvrA*. Genomic DNA of H522 and H598 digested with *Sac*I/*Sph*I were used as wild-type control. H632 and H633 were generated by pTA596 integrated upstream of the *uvrA* gene in H522 and H598, respectively. (B) Southern blot analysis of pTA596 pop-out of H632 and H633. Genomic DNA were digested with *Sac*I and probed with the flanking regions of *uvrA*. Genomic DNA of H195 digested with *Sac*I was used as wild-type control. Genomic DNA of H632 and H633 digested with *Sac*I were used as pop-in control. Δ*fen1*::*trpA*$^+$ Δ*uvrA* strain H646 and Δ*fen1*::*trpA*$^+$ Δ*hef* Δ*uvrA* strain H647 were generated by pTA596 pop-out of H632 and H633, respectively.

3.4 Construction of uvrD deletion mutants

The DNA helicase UvrD (helicase II) protein plays an important role in nucleotide excision repair, mismatch repair, rolling circular plasmid replication and recombination (Modrich, 1989; Sancar, 1996; Veaute et al., 2005; Lestini and Michel, 2007). Like other bacterial NER proteins, homologues of UvrD have been found in some archaeal species, mainly mesophilic methanogens and halophiles (McCready and Marcello, 2003; White, 2003).

3.4.1 Cloning of *uvrD* and its flanking regions

The sequence of the *H. volcanii uvrD* ORF, as annotated by the Institute for Genomic Research was obtained. *uvrD* was annotated as ORF01543 on contig270 at position 369241–371091 bp. *Cla*I restriction sites were present 2781 bp upstream and 4553 bp downstream of ORF01543 that would generate a fragment of 9184 bp upon digestion. Genomic DNA from wild-type *H. volcanii* was digested with *Cla*I, electrophoresed and fragments of approximately 9.2 kb were extracted and purified. The DNA fragments were then ligated to the *Cla*I site of pBluescript II SK+ and used to transform XL1-Blue strain *E. coli*. Transformants were screened by colony lift with the *uvrD* cloning probe prepared by PCR. The binding sites of the PCR primers, uvrDF and uvrDR, are within the coding region of *uvrD*. A clone containing pBluescript II SK+ with *uvrD* was successfully obtained. The plasmid was designed as pTA585 (Figure 3.22).

3.4.2 Design of primers for *uvrD* deletion plasmid

Four primers were designed based on the *uvrD* gene cloned in pTA585. For entire deletion of *uvrD* gene, internal primers (uvrD-IPF and uvrD-IPR) immediately flanking *uvrD* were designed to incorporate a novel *Bam*HI restriction site. The external primers upstream and downstream of *uvrD* were designed to contain *Kpn*I and *Xba*I respectively, which are part of the multiple cloning site of the *pyrE2*-marked integrate vector pTA131 (Figure 3.22).

3.4.3 Plasmid constructed for *uvrD* deletion mutants

PCR products of *uvrD* flaning regions were gel purified, digested, ligated and inserted into *pyrE2*-marked integrative plasmid pTA131. pTA597 was constructed in *E. coli* XL-1 Blue and then used to transform *E. coli* N2338 to prepare *dam*$^-$ DNA of plasmid pTA598 (Figure 3.22).

3.4.4 Construction of Δ*uvrD* mutants in the background of *hef* deletion

pTA598 for *uvrD* deletion were used to transform *ura*$^-$ strains H26 (used as wild-type), H358 (Δ*hef*), H359 (Δ*hef-hel*), H360 (Δ*hef-nuc*) and H195 (used as wild-type) (Figure 3.23). Integrants (*ura*$^+$) were successfully obtained on Hv-Ca (Thy) plates and verified by genomic DNA digestion and Southern blotting (Figure 3.24). Integrants were cultured in non-selective liquid medium Hv-YPC (Thy) for about 30 generations and then *ura*$^-$ colonies were selected on 5-FOA plates. 5-FOA^R (*ura*$^-$) pop-out strains were

screened by colony lift and verified by genomic DNA digestion and Southern blotting (Figure 3.25).

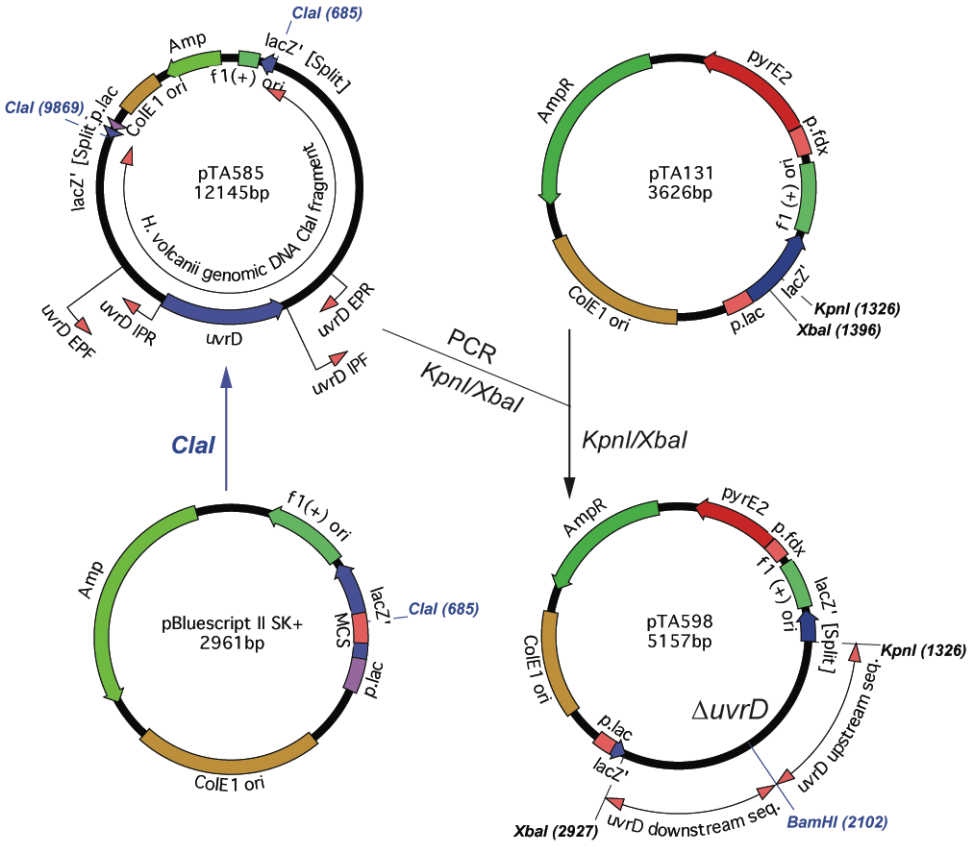

Figure 3.22 Primers design and plasmids constructed for *uvrD* deletion mutants.

A 9.2 kb *Cla*I fragment containing *uvrD* gene and its flanking sequence was cloned into pBluescript II SK+ to generate pTA585. Two pairs of PCR primer *uvrD* EPF/*uvrD* IPR and *uvrD* IPF/*uvrD* EPR were used to amplify the flanking regions of *uvrD* from pTA585. The PCR products were digested by *Bam*HI and ligated. The ligation product were then digested by *Kpn*I/*Xba*I and inserted at the *Kpn*I/*Xba*I sites of pTA131 to generate *uvrD* deletion plasmid pTA597 (dam^+) and pTA598 (dam^-).

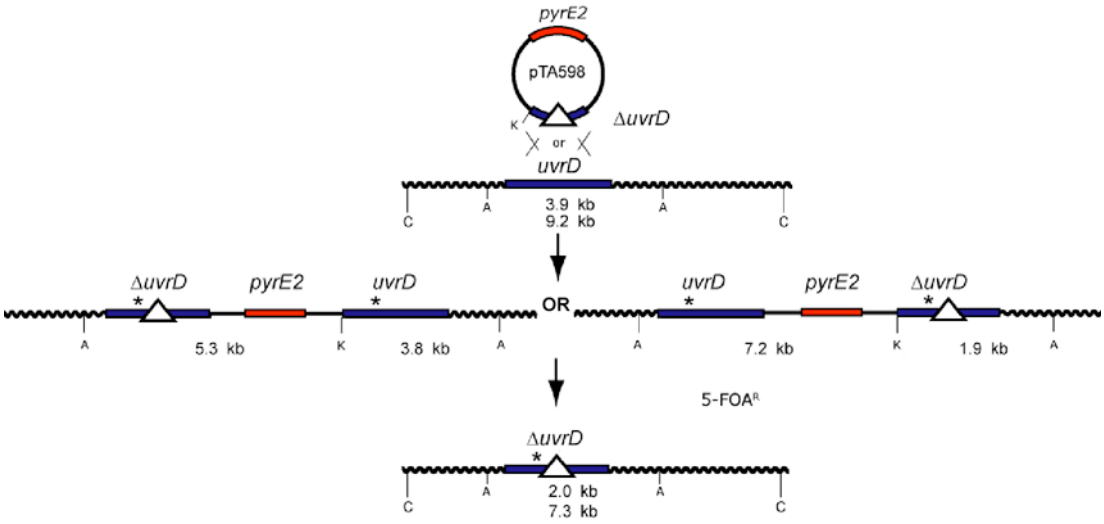

Figure 3.23 Schematic diagram of *uvrD* deletion construction.

Plasmid pTA598 was constructed as described in the legend of Figure 3.22. There are two possible orientations of pTA598 insertion into the genome by homologous recombination. Restriction sites used for genomic DNA digestions and the expected fragments resulting from these digestions are shown (A, *Age*I; K, *Kpn*I; C, *Cla*I). * indicates the region homologous to the probe. Loss of the plasmid by intrachromosomal recombination resulted in the Δ*uvrD* strain.

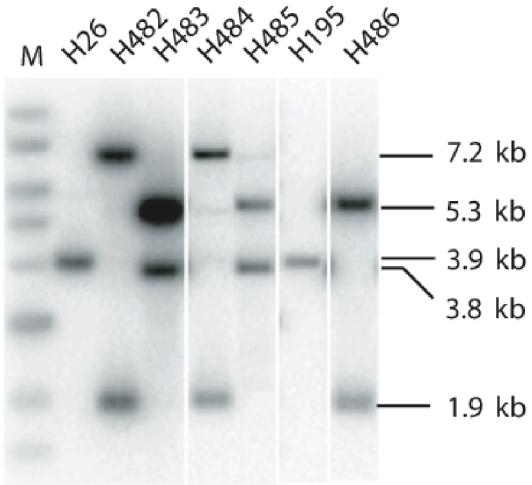

Figure 3.24 Southern blot analysis of pTA598 pop-in.

(A) Lane M, size marker (from top to bottom): 10, 8, 6, 5, 4, 3, 2 and 1.5 kb. Genomic DNA were digested with *Age*I/*Kpn*I and probed with the flanking regions of *uvrD*. Genomic DNA of H26 and H195 digested with *Age*I/*Kpn*I were used as wild-type control. pTA598 integrated downstream of the *uvrD* gene in H26 and H359 then yielded strains H482, and H484, respectively. H483 and H485 were generated by pTA598 integrated upstream of the *uvrD* gene in H358 and H360, respectively. pTA598 integrated in H195 and then generated strain and H486.

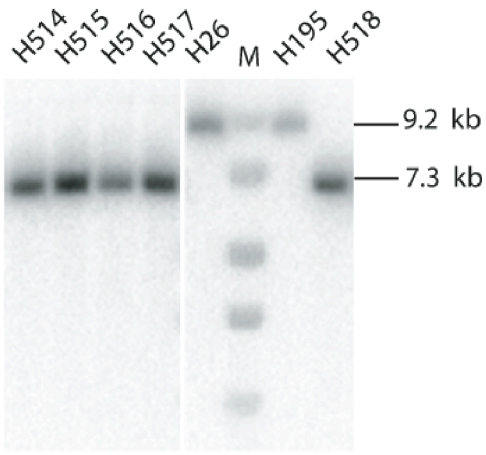

Figure 3.25 Southern blotting of pTA598 pop-out.

Lane M, size marker (from top to bottom): 10, 8, 6, 5 and 4 kb. Genomic DNA were digested with *Cla*I and probed with the flanking regions of *uvrD*. Genomic DNA of H26 and H195 digested with *Cla*I were used as wild-type control. H514, H515, H516, H517 and H518 were generated by pTA598 pop-out of H482, H483, H484, H485 and H486, respectively

3.5 Construction of *hel308a* deletion mutant

Hel308 is a superfamily 2 helicase conserved in eukaryotes and archaea. The homologous helicase constitutes the N-terminal domain of Mus308 from *Drosophila melanogaster*. The *MUS308* gene was first identified as a gene required for resistance to DNA-damaging agents (Henderson et al., 1987). *Mus308* mutants are hypersensitive to DNA interstrand cross-linking agents, such as photoactivated psoralen and nitrogen mustard, without marked sensitivity to the monofunctional alkylating agent methyl methanesulfonate (MMS), suggesting a function specific for ICLs repair (Boyd et al., 1990). MUS308 consists of an N-terminal SF2 helicase domain and a C-terminal DNA polymerase domain, which shares over 55% sequence similarity with the polymerases in the A family such as *E. coli* PolI (Harris et al., 1996). The human orthologue of Mus308, POLQ or POLθ, has the same organization (Seki et al., 2003) and can exceptionally perform translesion DNA synthesis (TLS) bypass AP sites and thymine glycol adducts (Seki et al., 2004). Consistently, studies in chicken DT40 cells have demonstrated that POLQ and POLβ share an overlapping function in the base excision repair of oxidative damage (Yoshimura et al., 2006). Mouse PolQ plays a role in somatic hypermutation of the immunoglobulin genes (Seki et al., 2005; Masuda et al., 2007).

In addition to this helicase-polymerase fusion protein, metazoans also encode an orthologue of the helicase alone. Human HEL308 is a ssDNA-dependent ATPase and 3'-5' DNA helicase with limited processivity (Marini and Wood, 2002). The orthologue

from *D. melanogaster*, Mus301, has been implicated to play a role in double strand break repair and meiotic recombination (McCaffrey et al., 2006). Mutants of *mus301* are sensitive to MMS and HN2 (Laurencon et al., 2004).

Mus308 proteins are absent from bacteria and yeast. Intriguingly, the N-terminal sequence of Mus308 is highly conserved in Archaea. Euryarchaeal Hel308 proteins from *Pyrococcus furiosus* (also known as Hjm, Holliday junction migration) and *Methanothermobacter thermautotrophicus* (Hel308a/Mth810) have been cloned and studied biochemically (Fujikane et al., 2005; Guy and Bolt, 2005). Both proteins have RecQ-like activities *in vitro*, targeting branched DNA substrates that are models for replication forks and unwinding lagging strands. The crystal structures of crenarchaeal Hel308 from *Archaeoglubus fulgidus* and *Sulfolobus solfataricus* are very similar (Buttner et al., 2007; Richards et al., 2008). Further, structural and biochemical studies on Hel308 from *S. solfataricus* have suggested that in addition to its helicase activity, one function of the protein may be in the removal of bound proteins at stalled replication forks and recombination intermediates (Richards et al., 2008). These data suggests that Hel308 proteins in archaea, like their homologues in metazoans, are important for the maintenance of genome stability.

3.5.1 Cloning of *hel308a* and its flanking regions

The sequences of the *H. volcanii hel308* ORF, as annotated by the Institute for Genomic Research (TIGR) was obtained. *hel308a* was annotated as ORF01950 on the main chromosome at position 12388–14871 bp. *hel308b* was annotated as ORF00981 on the main chromosome at position 880821–882740 bp. Deletion of *hel308a* was attempted since OFR01950 is close to the main chromosome replication origin *oriC1* (Norais et al., 2007a) and on the other side of ORF01969_hef (Figure 3.1). *Mlu*I restriction sites were present 820 bp upstream and 2047 bp downstream of ORF01950 that would generate a fragment of 5350 bp upon digestion. Genomic DNA from wild-type *H. volcanii* was digested with *Mlu*I, electrophoresed and fragments of approximately 5.4 kb were extracted and purified. The fragments of DNA were then ligated to the *Bss*HII site of pBluescript II SK+ and used to transform XL1-Blue strain *E. coli*. Transformants were screened by colony lift with the *hel308a* cloning probe prepared by PCR. The binding sites of the PCR primers, ski2F and ski2R, are within the coding region of *hel308a*. A clone containing pBluescript II SK+ with *hel308a* was successfully obtained. The plasmid was designed as pTA415. (Figure 3.26)

3.5.2 Pop-in and pop-out to construct *hel308a* deletion mutant

Design of primers for *hel308a* deletion plasmid

Four primers were designed based on the *hel308a* gene cloned in pTA415. For entire deletion of the *hel308a* gene, internal primers (HQIPF and HQIPR) immediately flanking *hel308a* were designed to incorporate a novel *Bam*HI restriction site. The external primers upstream and downstream of *hel308a* were designed to contain *Hin*dIII and *Xba*I respectively, which are part of the multiple cloning site of the *pyrE2*-marked integrative vector pTA131 (Figure 3.26).

Plasmids constructed for *hel308a* deletion mutants

PCR products of *hel308a* flanking regions were gel purified, digested, ligated and inserted into *pyrE2*-marked integrative plasmid pTA131. pTA423 was constructed in *E. coli* XL-1 Blue and then used to transform *E. coli* N2338 to prepare *dam*$^-$ DNA of plasmid pTA424 (Figure 3.26).

Pop-in and pop-out

pTA424 for *hel308a* deletion was used to transform *ura*$^-$ strains H26, H194 and H195 (Figure 3.27). *ura*$^+$ integrants H367, H368 and H369 were successfully obtained and verified by genomic DNA digestion and Southern blotting (Figure 3.28). Integrants (*ura*$^+$) were cultured in non-selective liquid medium Hv-YPC (Thy) for about 30 generations and then *ura*$^-$ colonies were selected on 5-FOA plates. Pop-out candidates screened by colony lift were not so obvious (Figure 3.28). Only four ambiguous colonies from H369 were picked up but Southern blotting analysis showed all the strains are wild type (Figure 3.29).

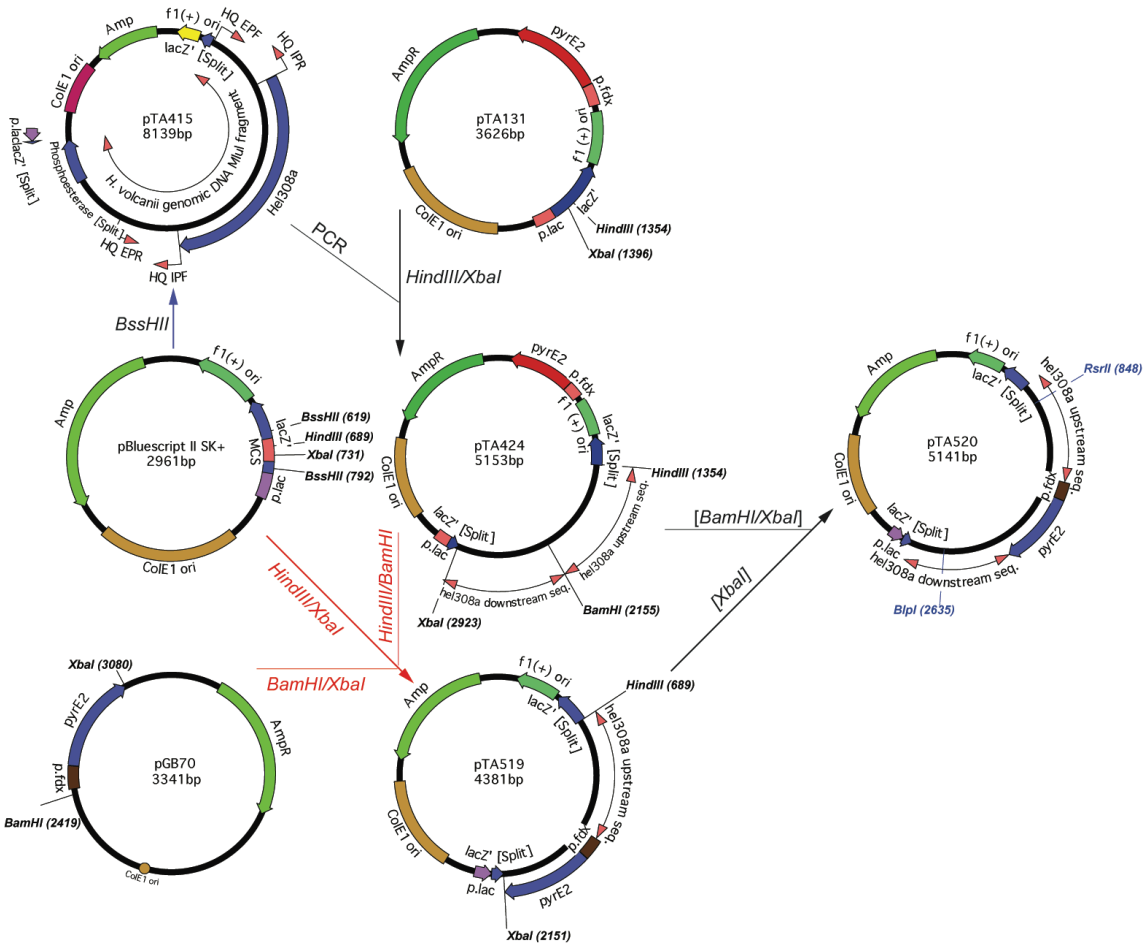

Figure 3.26 Cloning of *hel308a* and construction of pTA424, pTA519 and pTA520.

A 5.35 kb *mlu*I fragment containing *hel308a* gene and its flanking sequence was cloned into pBluescript II SK+ to generate pTA415. Two pairs of PCR primer HQ EPF/HQ IPR and HQ IPF/HQ EPR were used to amplify the flanking regions of *uvrD* from pTA415. The PCR products were digested by *Bam*HI and ligated. The ligation product were then digested by *Hin*dIII/*Xba*I and inserted at the *Hin*dIII/*Xba*I sites of pTA131 to generate *hel308a* deletion plasmid pTA423 (dam^+) and pTA424 (dam^-). The *Hin*dIII/*Bam*HI fragment containing the upstream sequence of *hel308a* from pTA424 and the *Bam*HI/*Xba*I fragment containing *p.fdx::pyrE2* from pGB70 (Bitan-Banin et al., 2003) were inserted at the *Hin*dIII/*Xba*I sites of pBluescript II SK+ to generate pTA519. Then the *Bam*HI/*Xba*I fragment containing the downstream sequence of *hel308a* from pTA424 was blunted by Mung bean nuclease and inserted at the *XbaI* site of pTA519, which was also blunted by mung bean nuclease to generate pTA520. The *Rsr*II/*Blp*I fragment of pTA520 was used in linear DNA transformation.

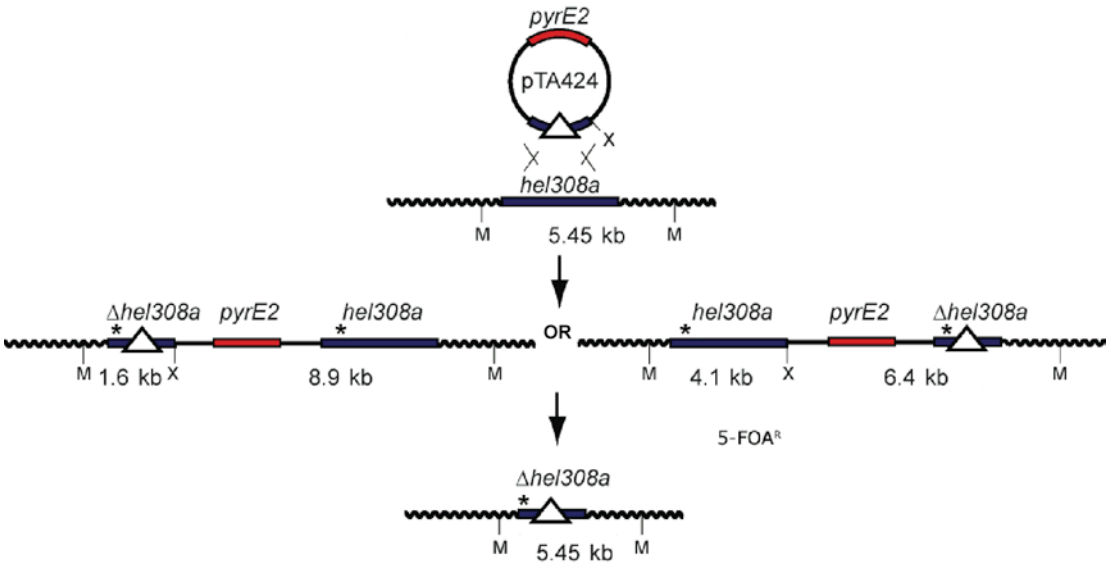

Figure 3.27 Schematic diagram of *hel308a* deletion construction.

There are two possible orientations of pTA424 insertion into the genome by homologous recombination. Restriction sites used for genomic DNA digestions and the expected fragments resulting from these digestions are shown (M, *Mlu*I; X, *Xba*I). * indicates the region homologous to the probe. Loss of the plasmid by intrachromosomal recombination would result in the Δ*hel308a* strain.

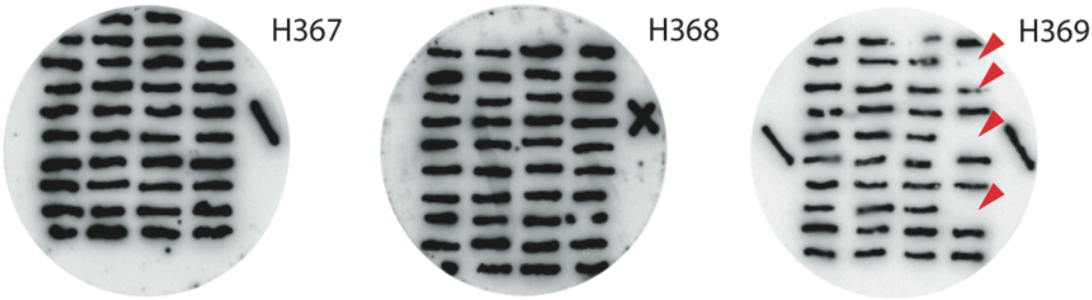

Figure 3.28 Colony lift and Southern blot of pTA424 pop-out strains.

ura$^-$ colonies selected on 5-FOA plates were patched out on Hv-YPC (Thy) plates. Pop-out candidates screened by colony lift were not so obvious. Four pTA424 pop-out candidates from H369 were highlighted by red arrows.

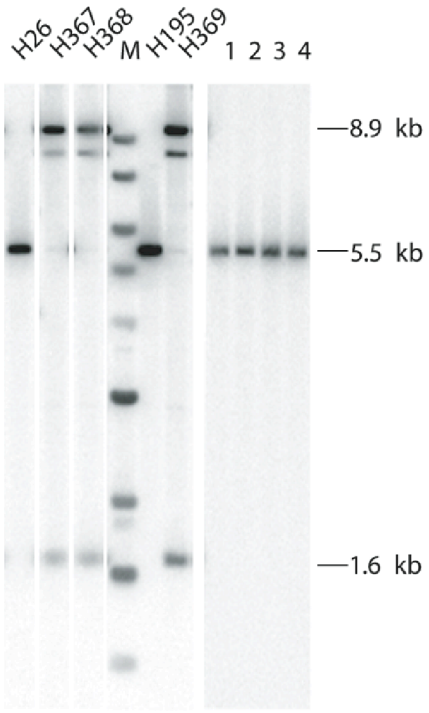

Figure 3.29 Southern analysis of pTA424 pop-in and pop-out of H26, H194 and H195.

Lane M, size marker (from top to bottom): 10, 8, 6, 5, 4, 3, 2 1.5 and 1 kb. Genomic DNA were digested with *Mlu*I/*Xba*I and probed with the flanking regions of *hel308a*. Genomic DNA of H26 and H195 digested with *Mlu*I/*Xba*I were used as wild-type control. H367, H368 and H369 were generated by pTA424 integrated upstream of the *hel308a* gene in H26, H194 and H195, respectively. Genomic DNA of Lane 1-4 were prepared from four pTA424 pop-out candidates from H369, respectively.

3.5.3 Linear transformation attempt to delete *hel308a*

In the *pyrE2* counter-selectable marker system (Pop-in and pop-out), integration of a non-replicating plasmid transforms the *ura*$^-$ mutant cell to *ura*$^+$ (pop-in). Subsequent growth on media containing 5-FOA is used to select for loss of the *pyrE2* gene by intrachromosomal recombination. However, 5-FOA selects for both deletion mutants and wild-type strains (Figure 3.4). Instead of the two-step counter selection, a one step direct selection was carried out (Figure 3.30 A). For *hel308a* deletion, a linear DNA fragment containing *hel308a* flanking sequences and *pyrE2*-marker replacing *hel308a* was used to transform *ura*$^-$ strains. Transformants were directly selected on Hv-Ca (Thy+Trp) plates.

To construct the linear DNA, the *Hin*dIII/*Bam*HI fragment from pTA424 containing the upstream of *hel308a* and the *Bam*HI/*Xba*I fragment containing *p.fdx::pyrE2* from pGB70 (Bitan-Banin et al., 2003) were ligated and inserted at the *Hin*dIII/*Xba*I sites of pBluescript II SK+ to construct pTA519. Then the *Bam*HI/*Xba*I fragment from pTA424 containing the downstream of *hel308a* was blunted by Mung bean nuclease and then inserted at the *Xba*I site of pTA519, also blunted by Mung bean nuclease, to construct pTA520 (Figure 3.31). The *Rsr*II/*Blp*I fragment of pTA520, containing *pyrE2* marker and homologous to *hel308a* flanking sequence, was used to transform *ura*$^-$ strain H194 and H195. Colonies on selective plates Hv-Ca (Thy+Trp) were patched out on Hv-YPC

(Thy) plates and colony lift was carried out. Candidates of *hel308a* deletion from the result of colony lift were further analysed by genomic DNA digestion and Southern blotting. However, all the strains still carried *hel308a* (Figure 3.30 C).

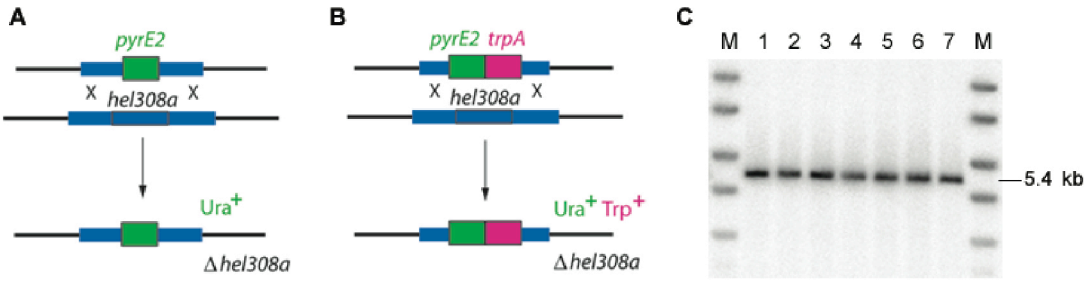

Figure 3.30 Linear DNA transformation for *hel308a* deletion.

(A) Schematic of linear DNA transformation with *pyrE2* marker for *hel308a* deletion. (B) Schematic of linear DNA transformation with *pyrE2* and *trpA* markers for *hel308a* deletion. (C) Southern blot analysis of linear DNA transformation for *hel308a* deletion in strains H194 and H195. Lane M, size marker (from top to bottom): 10, 8, 6, 5 and 4kb. Genomic DNA were digested with *Mlu*I and probed with the flanking regions of *hel308a*. H194 and H195 genomic DNA digested with *Mlu*I were used as wild-type control (lanes 1 and 3). One candidate from H194 (lane 2) and four candidates from H195 (lanes 4-7) were checked by Southern blotting.

To enhance the chance of *hel308a* deletion, a *trpA* marker was also introduced downstream of the *pyrE2* marker (Figure 3.30 B). The *Eco*RV frament containing *trpA* from pTA49 (Allers et al., 2004) was inserted at the *Xba*I site of pTA521, blunted by Klenow. pTA521 is a plasmid based on pTA519 and with the deletion of *hel308a* promoter region (*Nsp*I/*Bam*HI fragment). Then the *Not*I fragment from pTA424 containing the downstream of *hel308a* was inserted at the *Not*I site of pTA521 to construct pTA496 (Figure 3.31). The *Bsa*BI/*Msc*I fragment of pTA496, which contains *hel308a* flanking sequence together with *pyrE2* and *trpA* markers, was used to transform *ura*$^-$*trpA*$^-$ strain H195. Colonies on selective plates Hv-Ca (Thy) were patched out on Hv-YPC (Thy) plates and colony lift was carried out. Candidates of *hel308a* deletion from the result of colony lift were further analysed by Southern blotting. Again, all the strains still carried *hel308a* (Data not shown).

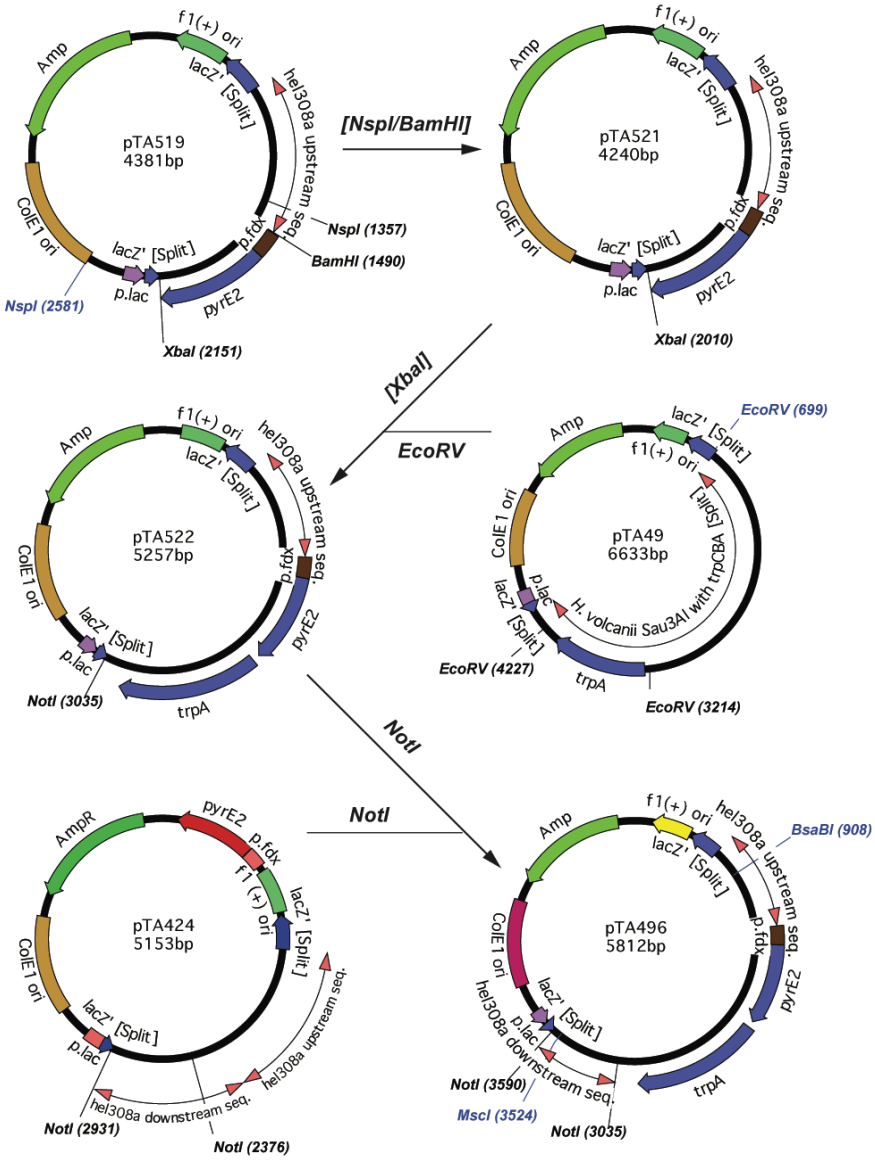

Figure 3.31 Construction of pTA496.

pTA519 was digested with *Nsp*I/*Bam*HI and blunted by Klewnow. The large fragment purified from agarose gel was ligated and used to transformed *E. coli* XL1-Blue. Thus the promoter region of *hel308a* was omitted from pTA519 to generate pTA521. The *Eco*RV fragment from pTA49 (Allers et al., 2004) containing the *trpA* marker was inserted at the *Xba*I site of pTA521, which was blunted by Klenow enzyme, to generate pTA522. The *Not*I fragment containing downstream sequence of *hel308a* from pTA424 was inserted at the *Not*I site of pTA522 to generate pTA496. The direction of the insertion was verified by sequencing. The *Bss*BI /*Msc*I fragment of pTA496 was used in linear transformation.

3.5.4 *hel308a* knockout using plasmid-based gene complementation

It appears that *hel308a* is an essential gene in *H. volcanii* since both *pyrE2*-marked counter selection and linear DNA transformation failed to obtain a *hel308a* deletion mutant. A third way, using plasmid based gene complementation was carried out (Figure 3.32). Different from before, linear transformation was carried out in the presence of a replicative plasmid, which contains the entire *hel308a* coding region and its own promoter. After the replacement of *hel308a* with *pyrE2* and *trpA* markers, the plasmid would be cured in Hv-YPC (Thy) media (non-selective for *pyrE2*), leaving behind the *hel308a* deletion structure on the chromosome.

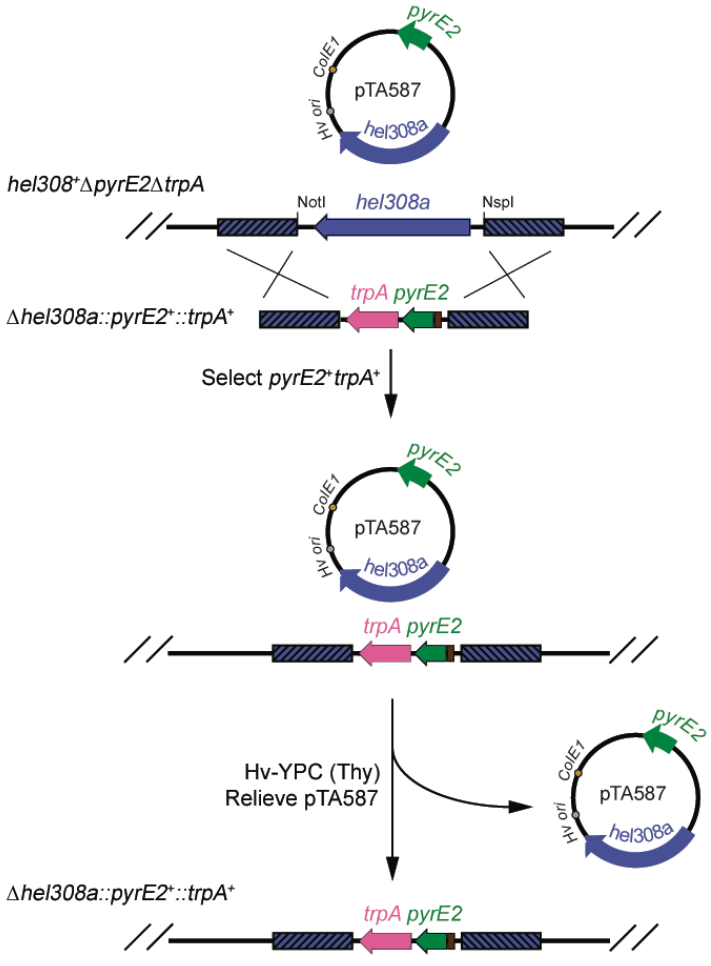

Figure 3.32 Schematic diagram of *hel308a* knockout using plasmid-based gene complementation.

pTA587 is a shuttle vector with *hel308a* gene and used to transformed Δ*pyrE2* Δ*trpA* host strain. *pyrE2*$^+$ transformants, which contain pTA587 are selected on Hv-Ca (Trp) plates. Then the *Bsa*BI/*Msc*I fragment from pTA496, which contains the flanking regions of *hel308a*, *pyrE2* and *trpA* markers, is transformed into the cells with pTA587. The integration of *pyrE2* and *trpA* markers at the *hel308a* locus can be selected on Hv-Ca plates. Once the genotype of transformants are verified by genomic DNA digestion and Southern blotting, pTA587 can be cured in complex medium and Δ*hel308a::pyrE2*$^+$ *trpA*+ mutant will be constructed.

Archaeal promoters have a TATA-box and basal-regulation element (BRE) positioned 25-30 bp upstream of the translational initiation site (Reeve, 2003), with the BRE being located upstream of the TATA-box. The TATA-box of promoters is the site of DNA melting prior to transcriptional initiation and is bound by a TATA binding protein (TBP). Melting of DNA is facilitated by the high A+T% of the TATA box, as base pairing between adenine and thymine is weaker than between cytosine and guanine. The BRE is the site of binding for transcription factor B (TFB), a protein that stabilises the binding of TBPs to the TATA box (Reeve, 2003). Mutagenesis of these elements has shown that their sequences contribute directly to the strength of the promoter (Soppa, 2001). Different consensus sequences have been established for the TATA-box in different archaeal species, with halophilic TATA-boxes having a consensus sequence of NTTTWWWN (W = A or T; N = any nucleotide), whereas the BRE is generally defined as being purine rich (Soppa, 2001).

Figure 3.33 Schematic of the proposed *hel308a* promoter.

The BRE and TATA-box are highlighted in light blue and orange, respectively. The consensus sequence for haloarchaeal TATA-boxes is displayed under the TATA-box: Nucleotides in black conform to the haloarchaeal TATA-box consensus sequence, whereas those in red do not. The start codon of *hel308a* is shown in blue.

Figure 3.33 shows the position of the proposed promoter elements of *hel308a.* A TATA box was identified that corresponds almost perfectly with the haloarchaeal TATA-box consensus. In addition, a BRE appears immediately upstream of the TATA-box. As discussed above, archaeal promoters are typically 25 - 30 bp upstream of the start codon. The predicted *hel308a* promoter lays 26 bp upstream of the proposed ATG start codon of *hel308a*, as expected.

pTA586 was constructed by inserting the 2.8 kb *Nsp*I (blunt)/*Not*I fragment from pTA415 at *Eco*RV/*Not*I sites of shuttle vector pTA503. The *Nsp*I site is 140 bp upstream of *hel308a* strart codon and the *Not*I site is 222 bp downstream of *hel308a*

stop codon. Thus the subcloned fragment contains the entire *hel308a* gene and its original promoter region, pTA586 was constructed in *E. coli* XL-1 Blue and then used to transform *E. coli* N2338 to prepare *dam*$^-$ plasmid DNA pTA587 (Figure 3.34).

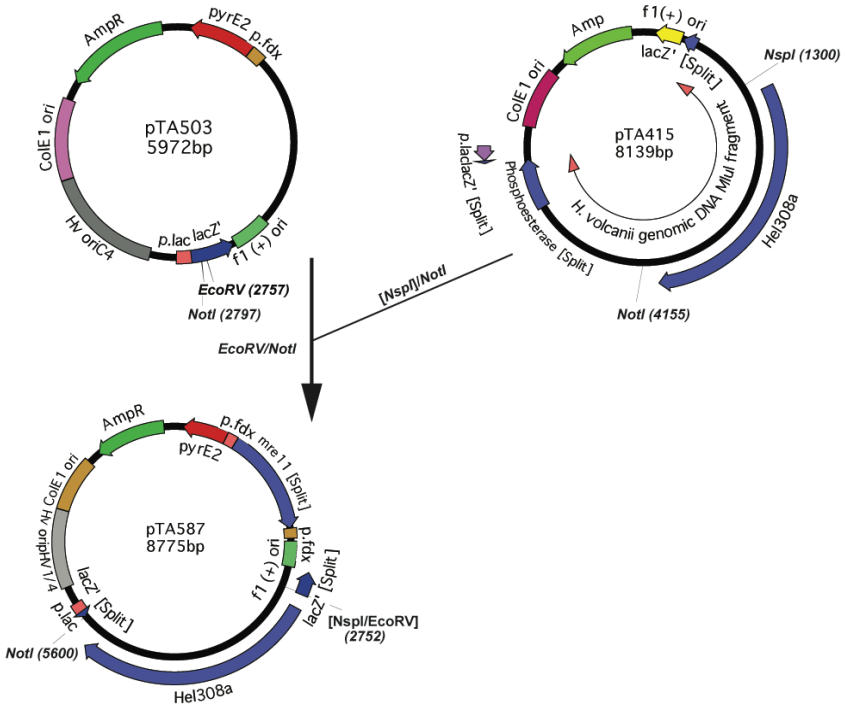

Figure 3.34 Construction of pTA587.

pTA415 was digested by *Nsp*I and blunted by Klenow. Then the linearized plasmid was digested by *Not*I. The *Nsp*I (blunt)/*Not*I fragment containing *hel308a* and its promoter was gel purified and inserted at *Eco*RV/*Not*I site of pTA503, a shuttle vector with replication origin *ori-pHV1/4* of *H. volcanii* (Norais et al., 2007a), to generate pTA586 (*dam*$^+$) and pTA587 (*dam*$^-$).

pTA587 was used as a *hel308a* complementation plasmid to transform Δ*pyrE2* Δ*trpA* Δ*hdrB* stain H195. A single colony maintaining pTA587 (*pyrE2*$^+$) was selected on Hv-Ca (Thy Trp) plates and then transformed with the *Bsa*BI/*Msc*I fragment of pTA496. pTA587 does not contain sequences homologous to the *hel308a* flanking regions on pTA496. This would avoid the recombination between pTA587 and the linear fragment from pTA496. *pyrE2*$^+$ *trpA*$^+$ transformants were selected on Hv-Ca (Thy) and restreaked twice on the same selective plates. Candidates of *hel308a* deletion from the result were further analysed by Southern blotting. Unfortunately, all the strains still carried *hel308a* (Data not shown).

3.5.5 Knockdown of *hel308a* with anti-sense RNA

All data clearly showed that *hel308a* is an essential gene in *H. volcanii* since three different strategies failed to obtain a *hel308a* deletion mutant. Instead of knockout of *hel308a* from the chromosome, down regulation of *hel308a* expression was attempted.

RNA interference has been applied extensively to direct gene expression in eukaryotes (Guo and Kemphues, 1995; Pederson, 2004). Dicer, a member of the Ribonuclease III (RNase III) family, plays an important role in RNA interference (Ji, 2008). It functions as a dsRNA-processing enzyme, producing small interfering RNA (siRNA). One strand of the siRNA, the antisense or guide strand, is loaded into the RNA induced silencing complex (RISC) and targets RISC to mRNA with complementary sequences, triggering mRNA cleavage or translational inhibition. However, there is no homologue of the dicer in *H. volcanii.*

Biological control by naturally occurring antisense RNAs has been found in many bacteria (Simons, 1988; Carpousis, 2003), and also been well studied in several eukaryotic systems (Werner, 2005; Mazo et al., 2007). Artificial antisense RNA has been wildly used to regulate gene expression (Sczakiel, 1997). Therefore, translational interference with plasmid-based antisense-*hel308a* was also attempted by using antisense-*hel308a*. With a limited amount of Hel308a, cells might be viable and exhibit some phenotype.

A 1.28 kb *anti-hel308a* fragment, containing a complementary sequence to N-terminal of *hel308a*, was amplified with primers antiQF/antiQR from pTA415 and then digested with *Bam*HI and *Nco*I. The *Kpn*I/*Nco*I fragment from pIL11 contains *p.fdx*, a constitute promoter of ferredoxin gene (Bitan-Banin et al., 2003). The *Bam*HI/*Nco*I *anti-hel308a* fragment, together with the *p.fdx* fragment, was ligated and inserted at the *Bam*HI/*Kpn*I sites in the shuttle vector pTA356 to construct pTA674. Instead of *p.fdx*, a stronger promoter *p.syn* based on the *H. volcanii* consensus tRNA promoter sequence (C. Daniels, personal communication.) was put upstream of *anti-hel308a* to construct pTA675 and pTA679, based on shuttle vector pTA356 and pTA230 (Allers et al., 2004), respectively. pTA674, pTA675 and pTA679 were constructed in *E. coli* XL-1 Blue and then used to transform *E. coli* N2338 to prepare *dam*$^-$ DNA of plasmids pTA676, pTA677 and pTA680 (Figure 3.35). pTA676 and pTA677 carry the chromosome replication origin Hv oripHV1/4 and maintain at low copy number (Norais et al., 2007a), while pTA680 is maintained at approximately six copies per genome equivalent since it carries plasmid pHV2 origin (Charlebois et al., 1987).

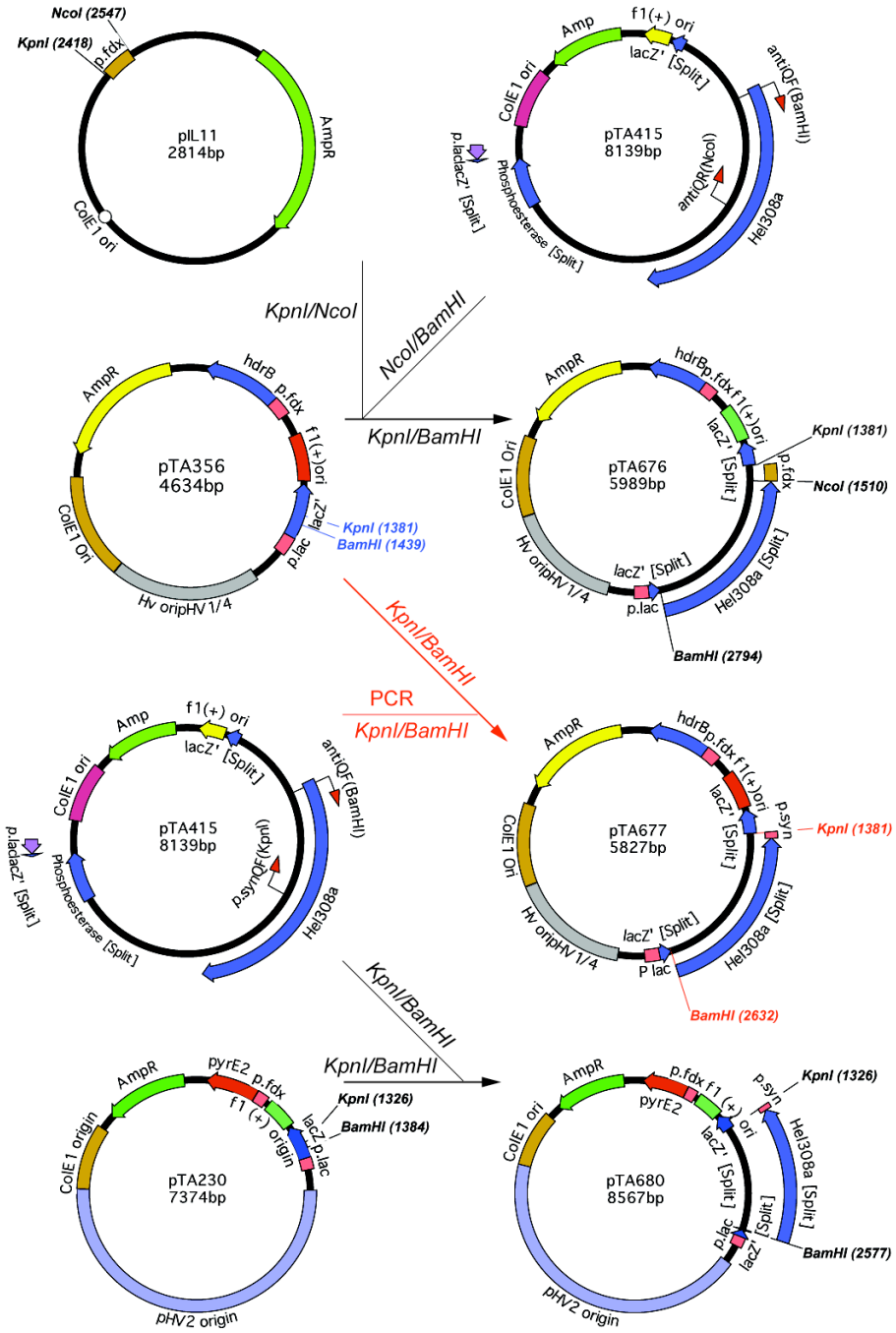

Figure 3.35 Schematic diagram of *anti-hel308a* construction.

The *Kpn*I/*Nco*I fragment containing *p.fdx* from pIL11 (Bitan-Banin et al., 2003) and the fragment amplified with primers antiQF/antiQR from pTA415 and then digested with *Bam*HI and *Nco*I were ligated and inserted at the *Bam*HI/*Kpn*I sites in shuttle vector pTA356 to construct pTA674 (*dam*$^+$) and pTA676 (*dam*$^-$). Instead, the fragment amplified with primers antiQF/p.synQF from pTA415 and then digested with *Kpn*I and *Bam*HI was inserted at the *Kpn*I/*Bam*HI sites in shuttle vector vector pTA356 to generate pTA675 (*dam*$^+$) and pTA677 (*dam*$^-$), or in shuttle vector pTA230 (Allers et al., 2004) to generate pTA679 (*dam*$^+$) and pTA680 (*dam*$^-$).

pTA676 and pTA677 were used to transform Δ*pyrE2* Δ*hdrB* stains H98 (Allers et al., 2004) and selected on Hv-Ca (Ura) plates. pTA360, the *dam*$^-$ version of pTA356 was used as a control. pTA680 was also used to transform H98 but selected on Hv-Ca (Thy) plates. pTA245, the *dam*$^-$ version of pTA230 (Allers et al., 2004) was used as the control. However, all transformation showed similar efficiency and transformants grew normally, which implied that these three *anti-hel308* construction failed to knockdown the transcription of *hel308a*.

3.6 Generation time

The growth rates of the mutants were examined under normal growing conditions (Table 3.2).

Strain	Genotype	Generation time (hr)	Viable cell number		
			OD_{650} = 0.2	OD_{650} = 0.4	OD_{650} = 0.6
H195	WT	1.9	5.0E7	1.6E8	2.8E8
H280	Δ*mre11rad50*	2.4	6.0E7	1.6E8	3.3E8
H364	Δ*hef*	2.2	4.0E7	1.6E8	2.7E8
H513	Δ*uvrA*	1.9	5.0E7	1.6E8	3.0E8
H518	ΔuvrD	1.9	4.0E7	1.6E8	3.0E8
H522	Δ*fen1*::*trpA*	2.3	3.0E7	1.3E8	2.6E8
H859	Δ*fen1*::*trpA sfnA*	2.0	5.0E7	1.4E8	2.8E8
H823	Δ*fen1 sfnA*	2.0	6.0E7	1.6E8	3.0E8
H598	Δ*hef* Δ*fen1*	3.9	2.0E7	5.0E7	8.0E7
H782	Δ*hef* Δ*mre11rad50*	4.2	2.0E7	4.0E7	1.0E8
H26	WT	1.9	5.0E7	1.6E8	3.6E8
H358	Δ*hef*	2.4	4.0E7	1.6E8	3.0E8
H359	Δ*hef-hel*	2.4	4.0E7	1.5E8	2.9E8
H360	Δ*hef-nuc*	2.0	5.0E7	1.7E8	3.8E8
H115	WT	2.2	5.0E7	1.5E8	2.8E8
H204	Δ*mre11rad50*	2.4	5.0E7	1.3E8	2.9E8
H720	Δ*fen1*	2.5	4.0E7	8.0E7	2.4E8
H721	Δ*fen1* Δ*mre11rad50*	3.5	2.0E7	8.0E7	1.6E8

Table 3.2 Generation time of principal strains used in this project.

Strains are shown in isogenic groups. Only relevant genotypes are shown. Generation time was estimated by the doubling time of viable cell numbers during the phase of exponential growth. The data were from two independent experiments.

The generation time of Δ*uvrA* strain H513 and Δ*uvrD* strain H518 was the same as the generation time of the wild-type strain H195. Strains H280, H522 and H364 with single deletion of *mre11 rad50*, *fen1* or *hef* showed slightly increased generation time. The generation time of H721 with double deletion of *fen1* and *mre11 rad50* was shown to increase by more than 50%. More significantly, the generation times of H598 and H782, strains with double deletion of *hef* and *fen1* or *mre11 rad50*, were more than doubled compared to the wild-type strain H195. Moreover, the viable cell numbers of the double deletion mutants H598, H782 and H721 were decreased noticeably throughout the exponential phase, which implicated great portion of cell death or filament. These data strongly suggested that *hef*, *fen1* and *mre11 rad50* have overlapped functions that are important for normal growth in *H. volcanii.*

The generation time of Δ*hef-nuc* strain H360 was very similar to the generation time of the wild-type strain H26 (2.0 and 1.9 hr, respectively). However, generation times of both Δ*hef* strain H358 and Δ*hef-hel* strain H359 increased to 2.4 hr. This suggested that the Hef helicase domain, rather than the Hef nuclease domain, is involved in the normal growth of *H. volcanii.*

H823 is a mutant constructed with unmarked *fen1*deletion (See 3.2.4). Once restreaked on complex media, H823 appeared to grow faster than the supposed parent strain H522, a *trpA* marked *fen1* deletion mutant. Indeed, the generation time of H823 (2.0 hr) turned out to be closer to that of the wild-type strain H195 (1.9 hr) than that of H522 (2.3 hr). The original strain used to construct H823 was named H859, a spontaneous mutant from H522. H859 appeared to contain a suppressor capable of at least suppressing the slow growth phenotype characteristic of Δ*fen1* strains. This suppressor of *fen1* was named *sfnA*.

3.7 Discussion

The results presented in this chapter showed that *hef*, *fen1* and *uvrA* single deletion mutants, together with pairwise double deletion mutants and triple deletion mutants were successfully constructed. In addition, *uvrD* single deletion mutant and double deletion mutants in the background of entire or partial deletion of *hef* were also obtained. Deletion mutants were observed with different growth rate, which might be related to the different function of specific gene in *H. volcanii.*

fen1 deletion mutant is viable in *H. volcanii*

Fen1 has been implicated in cellular metabolism in many ways. Fen1 is believed to play an important role in Okazaki fragment processing, since it was identified as a factor

responsible for the completion of replication *in vitro* (Ishimi et al., 1988; Turchi and Bambara, 1993; Waga et al., 1994). Deletion of both copies of FEN1 genes leads to mouse embryonic lethality (Kucherlapati et al., 2002). Mouse FEN1 null blastocysts ($Fen1^{-/-}$) cannot enter S phase to carry out normal DNA synthesis and are arrested in the endocycle (Larsen et al., 2003). However, yeast cells lacking the *fen1* gene (*RAD27* in *S. cerevisiae*) have been shown to be viable (Reagan et al., 1995). More surprisingly, homozygous mutant ($FEN1^{-/-}$) of vertebrate chicken DT40 cells are also viable (Matsuzaki et al., 2002). However, yeast double mutant of *rad27* and exonuclease 1 (*exo1*) is lethal (Budd and Campbell, 1997; Tishkoff et al., 1997a).

Human EXO1 has also been reported to possess 5' flap endonuclease activity (Lee and Wilson, 1999) as well as 5'-3' exonuclease activity (Tishkoff et al., 1997a). Therefore a similar nuclease could compensate for the Rad27/FEN1 deficiency. Alternatively, another nuclease activity may contribute to Okazaki fragment processing. In yeast, Dna2, which can interact with Rad27, has been shown to display not only 5'-3' DNA helicase activity but also single-strand-specific endonuclease activity (Lee and Wilson, 1999; Bae and Seo, 2000). It has been reported that in conjunction with Rad27, Dna2 acts sequentially or in a parallel pathway (Kao et al., 2004) to facilitate the complete removal of RNA primers in Okazaki fragments. A *DNA2* homolog has been identified in human cells (Eki et al., 1996; Masuda-Sasa et al., 2006); such a homologue could substitute for at least the function of FEN1 in DNA replication. Although there is no Exo1 homologue, ORF02212 encodes a DNA2-like helicase in *H. volcanii*. Deletion of the helicase gene alone does not confer the cells any phenotype (Thorsten Allers, unpublished data). However, the DNA2-like helicase might be a backup of Fen1 and mainly functions at the absence of Fen1. It would be interesting to find out the overlapping function of these two proteins by construct a double deletion mutant.

Fen1, Hef and Mre11Rad50 are involved in normal growth maintenance

The slow growth observed with *fen1* deletion mutants suggests that Fen1 is probably also involved in the maturation of lagging strand in *H.* volcanii. The generation time of *hef* helicase domain and entire *hef* deletion mutants (but not the *hef* nuclease domain deletion mutant) are increased, suggesting that Hef helicase domain is involved in the normal growth of *H. volcanii*.

Double deletion strains of *hef*, *fen1* and *mre11rad50* are growing much more slowly than single deletion mutants. These double deletion mutants also showed decreased viable cell numbers. Both Fen1 and hef are structure-specific endonuclease with opposite polarity (Liu et al., 2004a; Ciccia et al., 2008). Mre11Rad50 complex is a

nuclease of SbcCD family with single-strand endonuclease activity, 3'-5' double strand exonuclease activity and weak DNA unwinding (stem-loop opening) activity (Paull and Gellert, 1998; Usui et al., 1998; Trujillo et al., 2003). These nucleases might have overlapping functions that are important to maintain normal growth in *H. volcanii.*

Fen1 and Hef might partially overlap the function of RadA

Deletion of *mre11 rad50* slightly increases the generation time (by about 20%) but does not affect the viable cell count. The strain with single deletion of *radA* is obviously sick, with prolonged generation time and less viable cells (Thorsten Allers, unpublished data). The growth is severely impaired in the strain with deletion of *mre11rad50* and *radA* (Thorsten Allers, unpublished data). Deletion of *mre11rad50* and *hef* or *fen1* also leads to slower growth and a decreased viable cell count, while the phenotypes are not as severe as those of *mre11rad50* and *radA* double mutants. In *H. volcanii*, RadA is a vital factor for homologous recombination (Woods and Dyall-Smith, 1997). Therefore, Hef and Fen1 might have functions that partially overlap the function of RadA in HR.

Deletion of *uvrA* or *uvrD* does not affect the normal growth

Bacterial UvrA is a DNA repair protein involved in the UvrABC pathway, which is responsible for bacterial nucleotide excision repair (Van Houten and McCullough, 1994). Like its homologue in bacteria, *H. volcanii* UvrA might also mainly be a DNA repair protein since the generation time and viable cell numbers of deletion mutants show not much difference from wild-type control.

UvrD is a helicase with 3'-5' polarity (Matson, 1986) and required for the displacement of DNA strands cleaved during both nucleotide excision repair (Van Houten and McCullough, 1994) and mismatch repair (Lahue et al., 1989). UvrD also plays a role in rolling circular plasmid replication (Bruand and Ehrlich, 2000; Cadman et al., 2006). In addition, UvrD is implicated to be involved in replication, either by acting at replication forks, at recombination intermediates formed as a result of replication blockage or at the gaps between Okazaki fragments (Moolenaar et al., 2000; Lestini and Michel, 2007). However, *uvrD* deletion mutant of *H. volcanii* is viable and grows normally without DNA damage treatment. This suggests that UvrD in *H. volcanii* might be a DNA repair protein and not directly involved in DNA replication, or UvrD and some other proteins have redundant functions in DNA repair since there are a number of open reading frames have been annotated as helicases.

hel308a* is an essential gene in *H. volcanii

Studies have suggested that Hel308 family proteins are important for the maintenance

of genome stability. For example, Mus308 from *D. melanogaster* and POLQ from vertiberates are involved in DNA repair (Boyd et al., 1990; Seki et al., 2004; Yoshimura et al., 2006). Mus301 from *D. melanogaster* has been implicated to play a role in both DNA repair and recombination (Laurencon et al., 2004; McCaffrey et al., 2006). Euryarchaeal Hel308 proteins from *Pyrococcus furiosus* (Hjm) and *Methanothermobacter thermautotrophicus* (Hel308a/Mth810) have been shown to target replication forks and unwinding lagging strands (Fujikane et al., 2005; Guy and Bolt, 2005). Hel308 from crenarchaeon *S. solfataricus* has been implicated a role in the removal of bound proteins at stalled replication forks and recombination intermediates (Richards et al., 2008).

Hel308a from *H. volcanii*, like its homologues in other archaea or metazoans, might have some important function for the maintenance of genome stability. Several methods were tried to construct *hel308* deletion mutant but all failed. The results strongly suggested that *hel308* is an essential gene in *H. volcanii.* Therefore, instead of trying to knockout *hel308a* from the chromosome, translational interference was also attempted by using antisense-*hel308a*. However, this trial was not effective too.

The antisense-*hel308a* were constructed by inserting the complementary sequence of *N*-terminal coding region of *hel308a* downstream of a constitute promoter *p.fdx* or *p.syn* on replicative plasmids. Antisense RNAs in prokaryotic systems often inhibit translation of mRNA. In some cases, antisense RNAs overlapping Shine-Dalgarno (SD) sequences (Shine and Dalgarno, 1974; Kozak, 1986) and start codons of the target gene are more effective than those only containing complementary sequence to the coding region (Hirashima et al., 1986; Ma and Simons, 1990). The former antisense RNA can form duplex region around the SD sequence of the target gene and prevent recruitment of the translation initiation complex (Ma and Simons, 1990). In other cases, antisense/target RNA duplexes are formed upstream of SD sequences or start codons (Nordstrom et al., 1988; Malmgren et al., 1996). Stable secondary structures have been reported to be important for the efficiency of antisense RNAs (Simons, 1988; Malmgren et al., 1996; Sczakiel, 1997). Thus, redesign of antisense *hel308a* might bring about successful knockdown of *hel308a.*

In addition, great efforts have been made to screen inducible promoters that can improve the current genetic tools in *H. volcanii.* A new system with a tightly controlled promoter that can be induced by tryptophan, is more promising to knockout *hel308a* (see Chapter VI)(Large et al., 2007).

Chapter IV: DNA damage tests

DNA damage agents and radiation have been utilized for decades to uncover and explore pathways of DNA repair, DNA damage response and mutagenesis, for example, the discoveries of the UvrABC system in *E. coli* and the Rad proteins in yeast (Shuster and Boyce, 1964; Howard-Flanders et al., 1966; Game and Mortimer, 1974; Prakash, 1977; Van Houten and McCullough, 1994; Bennett et al., 2001). The experiments described in this chapter mainly aim to elucidate the roles of the two structure-specific endonucleases Hef and Fen1 in DNA repair. Additionally, multiple repair pathways for different types of DNA damage are explored.

4.1 UV radiation test

4.1.1 Introduction

Radiation of cells with UV light induces DNA lesions that can be classified into two major groups, *cis-syn* cyclobutane-pyrimidine dimers (CPDs) and pyrimidine (6-4) pyrimidone photoproducts (6-4PPs). 6-4PPs are formed at 20-30% of the yields of CPDs (Friedberg et al., 1995b; Cadet et al., 2005). Both classes of lesions distort the DNA helix and arrest replication forks (Setlow et al., 1963). Direct photoreactivation was found in many prokaryotic and eukaryotic organisms, but not in mammals, while nucleotide excision repair (NER) seems to be universally distributed (Sancar, 1996; Thoma, 1999; Todo, 1999). In *E. coli*, the recovery of replication in the dark after UV-induced arrest depends largely on lesion removal by the NER repair enzymes (Setlow et al., 1963; Courcelle et al., 1999). In humans, defects in NER genes cause the sun-sensitive, cancer prone genetic disorders xeroderma pigmentosum (XP), Cockayne's syndrome (CS) and trichothiodystrophy (TTD) (Friedberg et al., 1995a; Fuss and Cooper, 2006). Intriguingly, *H. volcanii* possesses both eukaryotic (*rad1*/*XPF*, *rad2*/*XPG*, r*ad3*/*XPD* and *rad25*/*XPB*) and bacterial (*uvrA*, *uvrB*, *uvrC* and *uvrD*) NER homologues. Groups of strains with isogenic backgrounds were used to investigate UV induced DNA damage repair in *H. volcanii*.

4.1.2 Results

Hef and Fen1

H358 (Δ*hef*), H359 (Δ*hef-hel*) and H360 (Δ*hef-nuc*) are not more sensitive to UV irradiation than H26 (*hef*+) (Figure 4.1 A). H522 (Δ*fen1*::*trpA*) and *fen1* deletion

mutants in the background of entire or partial *hef* deletion (H598 (Δ*fen1*::*trpA* Δ*hef*), H524 (Δ*fen1*::*trpA* Δ*hef-hel*) and H525 (Δ*fen1*::*trpA* Δ*hef-nuc*)) are all moderately sensitive to UV irradiation (Figure 4.1 B). These data suggest that Fen1 is involved in the repair of UV induced DNA damage to a limited degree, but Hef is not.

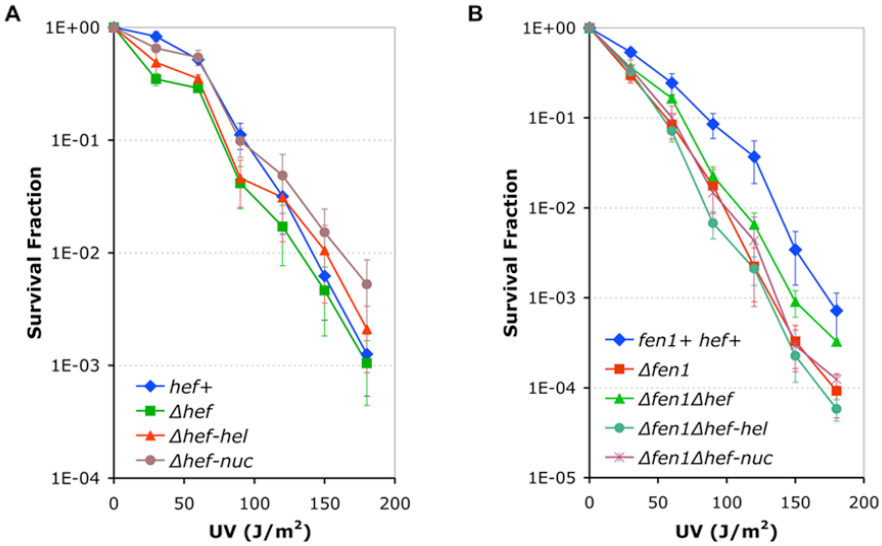

Figure 4.1 UV sensitivity of *hef* and *fen1* deletion mutants.

(A) Comparison of survival fractions of H26 (*hef*+), H358 (Δ*hef*), H359 (Δ*hef-hel*) and H360 (Δ*hef-nuc*) following UV irradiation. (B) Comparison of survival fractions of H195 (*fen1*+ *hef*+), H522 (Δ*fen1*::*trpA*), H598 (Δ*fen1*::*trpA* Δ*hef*), H524 (Δ*fen1*::*trpA* Δ*hef-hel*) and H525 (Δ*fen1*::*trpA* Δ*hef-nuc*) following UV irradiation. All data points are calculated as the mean value of three trials. Error bars are based on standard error. Only relevant genotypes are shown.

UvrA, Hef and Fen1

H509 (Δ*uvrA*) is extremely sensitive to UV irradiation (Figure 4.2 A). At the UV doses of 30 J/m^2, the survival fraction of H509 (Δ*uvrA*, in the background of H26) decreased to 10^{-5}, while the survival fraction of H26 (*uvrA*+) was around 10^{-3} at UV doses as high as 180 J/m^2 (Figure 4.1 A). H509 (Δ*uvrA*), H510 (Δ*uvrA* Δ*hef*), H511 (Δ*uvrA* Δ*hef-hel*) and H512 (Δ*uvrA* Δ*hef-nuc*) are all very sensitive and showed similar sensitivity (Figure 4.2 A). H513 (Δ*uvrA*, in the background of H195) is also very sensitive and H646 (Δ*uvrA* Δ*fen1*::*trpA*) is slightly more sensitive than H513 (Δ*uvrA*) (Figure 4.2 B). These data strongly suggest that UvrA is involved in the major repair of UV induced DNA damage and Fen1 is involved in a minor repair pathway.

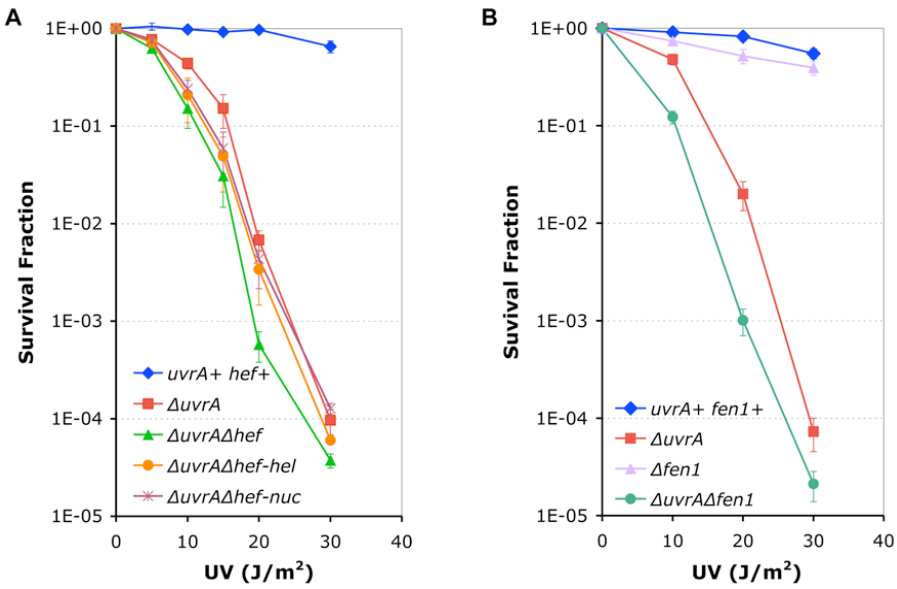

Figure 4.2 UV sensitivity of *uvrA*, *hef* and *fen1* deletion mutants.

(A) Comparison of survival fractions of H26 (*uvrA*+ *hef*+), H509 (Δ*uvrA*), H510 (Δ*uvrA* Δ*hef*), H511 (Δ*uvrA* Δ*hef-hel*) and H512 (Δ*uvrA* Δ*hef-nuc*) following UV irradiation. (B) Comparison of survival fractions of H195 (*uvrA*+ *fen1*+), H513 (Δ*uvrA*), H522 (Δ*fen1*::*trpA*) and H646 (Δ*fen1*::*trpA* Δ*uvrA*) following UV irradiation. All data points are calculated as the mean value of three trials. Error bars are based on standard error. Only relevant genotypes are shown.

UvrD

H514 (Δ*uvrD*) is not more sensitive to UV irradiation than H26 (*uvrD*+ *hef*+) (Figure 4.3 A). Double mutants H515 (Δ*uvrD* Δ*hef*), H516 (Δ*uvrD* Δ*hef-hel*) and H517 (Δ*uvrD* Δ*hef-nuc*) are also not more sensitive than H26 (*uvrD*+ *hef*+). Therefore, unlike in *E. coli*, the deletion of *uvrD* does not confer UV sensitive phenotype in *H. volcanii.*

Fen1 and Mre11Rad50

H720 (Δ*fen1*) is moderately sensitive to UV irradiation but H204 (Δ*mre11rad50*) is more resistant to UV irradiation (Figure 4.3 B). The survival fraction of H721 (Δ*fen1* Δ*mre11rad50*) was between those of H204 (Δ*mre11rad50*) and H720 (Δ*fen1*). These data shown here suggest that Fen1 and Mre11Rad50 are involved in different repair pathways for UV induced DNA damage.

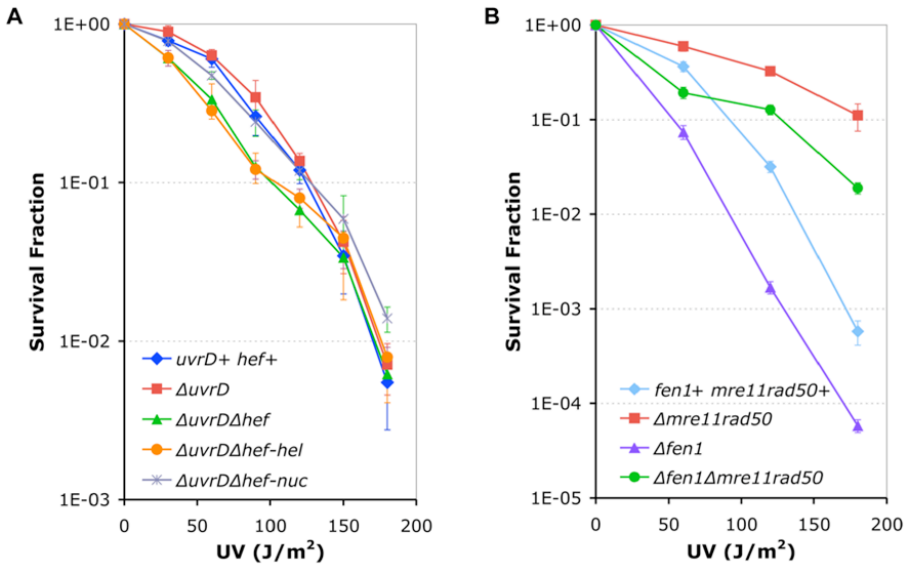

Figure 4.3 UV sensitivity of *uvrD*, *hef*, *fen1* and *mre11rad50* deleion mutants.

(A) Comparison of survival fractions of H26 (*uvrD*+ *hef*+), H514 (Δ*uvrD*), H515 (Δ*uvrD* Δ*hef*), H516 (Δ*uvrD* Δ*hef-hel*) and H517 (Δ*uvrD* Δ*hef-nuc*) following UV irradiation. (B) Comparison of survival fractions of H115 (*fen1*+ *mre11rad50*+), H204 (Δ*mre11rad50*), H720 (Δ*fen1*) and H721 (Δ*fen1* Δ*mre11rad50*) following UV irradiation. All data points are calculated as the mean value of three trials. Error bars are based on standard error. Only relevant genotypes are shown.

4.1.3 Discussion

UvrA is vital in UV-induced DNA damage repair

Homologues of all bacterial NER genes (including *uvrA*, *uvrB*, *uvrC* and *uvrD*) and homologues of some eukaryal NER genes (including *XPF*/*RAD1*, *XPG*/*RAD27*, *XPB*/*RAD25* and *XPD*/*RAD3*) are found in *H. volcanii*. It has been demonstrated that the *uvrA* gene in *H. volcanii* is a functional homologue of the bacterial *uvrA* gene. In the absence of this gene, cells were extremely sensitive to UV light (Figure 4.2). In contrast, the *hef* deletion mutant was as resistant to UV as wild-type strain (Figure 4.1 A). The entire or partial deletion of *hef* in the background of *uvrA* deletion strain had no significant effect on survival rate after UV radiation. In addition, mutants with *xpb* deletion also appeared to be not sensitive to UV (Michelle Hawkins and Thorsten Allers, unpublished data). Therefore, UvrA is a crucial factor for repair of UV induced DNA damage and the UvrABC system most likely carries out the functional NER in *H. volcanii.*

Fen1 is involved in a minor repair pathway distinct from UvrABC

Studies have shown that the fission yeast *Schizosaccharomyces pombe* and the filamentous fungus *Neurospora crassa* have an extra pathway (UVDE) for excision of UV photoproducts in addition to NER (Yajima et al., 1995; Yonemasu et al., 1997). UVDE (UV damage endonuclease) can recognise UV induced cyclobutane pyrimidine dimers and pyrimidine and pyrimidine (6-4) photoproducts and incise at the 5' sites, leaving 3'-hydroxyl and 5'-phosphoryl groups at the site of cleavage. Rad2, the homologue of Fen1 from *Schizosaccharomyces pombe*, is involved in processing UVDE-nicked DNA, in a very similar way to long-patch base excision repair (McCready et al., 2000). Interestingly, the expression of UVDE from *N. crassa* has been demonstrated to stimulate the repair process in mammalian cells by introducing a single strand break immediately 5' to UV induced photoproducts (Okano et al., 2000). Moreover, the single strand break introduced by UVDE was shown to be a substrate for FEN1 homologues from human, *S. cerevisiae* and *Schizosaccharomyces pombe in vitro* (Yoon et al., 1999).

UVDE has been found only in some eukaryotic microorganisms, some bacteria (including *Bacillus subtilis* and *Deinococcus radiodurans*) and some archaea (for example, *Haloquadratum walsbyi*, *Sulfolobus acidocaldarius*, *Methanoculleus marisnigri*) (Takao et al., 1996; White et al., 1999). However, *Micrococcus luteus* and phage T4-infected *E. coli* contain a DNA glycosylase/AP lyase that specifically recognizes CDPs and catalyzes a two-step DNA incision process at the site of these dimers (Demple and Linn, 1980; Haseltine et al., 1980; Radany and Friedberg, 1980). A similar activity was found in *S. cerevisiae* (Hamilton et al., 1992). These enzymatic activities are considered to be part of a base excision repair pathway. In addition, UV radiation also induces lesions that are subject to BER, for example thymine glycol and 5-formyluracil (Seeberg et al., 1995). Although no homologue of UVDE has been annotated in *H. volcanii*, it is possible that some endonuclease or glycosylase has a similar activity to nick at the 5' site of UV lesions. Subsequently, Fen1 might be required to process the 5' flap after DNA synthesis and involved in a BER like pathway. On the other hand, human FEN1 has been reported a gap endonuclease (GEN) activity, which is critical in resolving stalled replication forks (Zheng et al., 2005). UV irradiation has been known to cause several types of DNA damage and stall the DNA replication fork (Altshuler, 1993; Limoli et al., 2002). Human FEN1, but not the GEN-

deficient mutant, E178A, has been shown to rescue the defect in resistance to UV in a yeast Fen1 null mutant. Interestingly, sequence alignments show that the glutamic acid mutated in the GEN-deficient mutant is also conserved in Fen1 from *H. volcanii* (Figure 4.4). It is possible that this archaeal Fen1 can also cleave stalled replication fork by its GEN activity to initiate the recombination repair pathway.

H. sapiens	FEN1	176	ATEDMDCLTFGSP	188
C. elegans	CRN-1	176	VTEDMDALTFGST	188
S. cerevisiae	Rad27	174	ASEDMDTLCYRTP	186
H. volcanii	Fen1	172	GSEDYDTLLFGAP	184
	Consensus		--ED-D-L-----	

Figure 4.4 Alignments about a motif related to GEN activity of Fen1 homologues from human, nematode, yeast and *H. volcanii.*

Role of the Mre11Rad50 complex

The strain with the deletion of *mre11 rad50* appears to be more resistant to UV. The UV sensitivity of the *fen1* deletion strain could be masked by the deletion of *mre11* and *rad50* at high doses of UV exposure (Figure 4.3 B). The Mre11/Rad50 complex is involved in many essential DNA processes dealing with DNA ends and conserved in bacteria, archaea and eukaryotes (Usui et al., 1998; Assenmacher and Hopfner, 2004). DSBs may result from the replication of a UV damaged template (Galli and Schiestl, 1998). In most thermophilic archaea, the *mre11* and *rad50* genes cluster with a bipolar helicase gene *herA* and a 5' to 3' exonuclease gene *nurA* (Constantinesco et al., 2004). Mre11 from *S. acidocaldarius* and *S. tokadaii* have been shown to interact with HerA *in vivo* (Quaiser et al., 2008; Zhang et al., 2008). Purified Mre11 and Rad50 from *Pyrococcus furiosus* act cooperateively with HerA and NurA to resect the 5' strand at a DNA end. The 3' single-stranded DNA end generated by these proteins can be utilized by the archaeal RecA homologue RadA to catlyze strand exchange (Hopkins and Paull, 2008). However, no homologue of *herA* or *nurA* has been found in *H. volcanii* yet. Other studies in the lab suggest that the repair of DSBs by homologous recombination is restrained by the Mre11Rad50 complex and the use of homologous recombination in *mre11 rad50* mutants enhances cell survival (Stéphane Delmas and Thorsten Allers, unpublished data).

4.2 Gamma radiation and phleomycin test

4.2.1 Introduction

DNA damage by ionizing radiation has been studied for many years (Corry and Cole, 1968; Ulmer et al., 1979; Henner et al., 1982). Among the many types of damage induced by ionizing radiation, one of the most serious lesions is DNA double strand break (DSB). The amount of radiation-induced DNA breakage is linearly dose-dependent, and strand incision events occur uniformly at all nucleotide sites, regardless of sequence. The 5'-terminal group at points of breakage is a simple phosphoryl moiety. By contrast, two types of 3' terminus exist. One is a simple phosphoryl group and the other is neither hydroxyl nor a phosphoryl group (Henner et al., 1982). More than 100 genes have been found to be sensitive to gamma radiation in *S. cerevisiae*, including the *rad1* and *rad27* genes (Bennett et al., 2001).

In the laboratory, it is more convenient and economical to produce DNA double strand breaks with phleomycin than gamma radiation. Pleomycin is a glycopeptide antibiotic, structurely related to bleomycin (Huang et al., 1981). Phleomycin is freely soluble in water and has a broad spectrum of toxicity, exhibiting *in vivo* activity against bacteria, eukaryotic organisms, and plant and animal cells. Most cells growing aerobically are killed by phleomycin in the concentration range of 0.1 to 50 μg/ml. For example, phleomycin is used at 5 μg/ml in media to select resistant transformants in bacteria (Sleigh and Grigg, 1977). It is also used at 5-50 μg/ml for eukaryotic microorganisms (Mulsant et al., 1988), at 10 μg/ml for yeasts (Gatignol et al., 1990), at 10-50 μg/ml for fungi, and at 5-25 μg/ml for plants (Perez et al., 1989). It is generally believed that pleomycin can bind DNA by intercalation of its planar bithiazole-containing moiety. The DNA is degraded by the metal ion-chelating portion of the molecule, which forms an active complex with iron II and molecular oxygen (Povirk et al., 1981).

4.2.2 Results

Strains H26 (*hef*+), H358 (Δ*hef*), H359 (Δ*hef-hel*) and H360 (Δ*hef-nuc*) were used to test gamma radiation sensitivity. Even at doses as high as 1000 Gy, all mutants showed similar survival fraction to the control strain H26 (Data not shown). These data suggest that Hef is not involved in the major repair of gamma radiation induced DNA double strand breaks.

Strains H195 (*hef*+ *uvrA*+ *fen1*+), H364 (Δ*hef*), H513 (Δ*uvrA*) and H522 (Δ*fen1*::*trpA*) were used to test phleomycin sensitivity. Consistent with the results of the gamma radiation test, H364 (Δ*hef*) is not more sensitive to phleomycin than H195 (wild-type). H513 (Δ*uvrA*) is as resistant as H195 (wild-type) (Figure 4.5 A and B). Interestingly, H364 (Δ*hef*) and H522 (Δ*fen1*::*trpA*) are more resistant to phleomycin at the high concentration (2 mg/ml), as the survival fraction of H364 (Δ*hef*) and H522 (Δ*fen1*::*trpA*) are about 10 times higher than that of the wild-type strain H195.

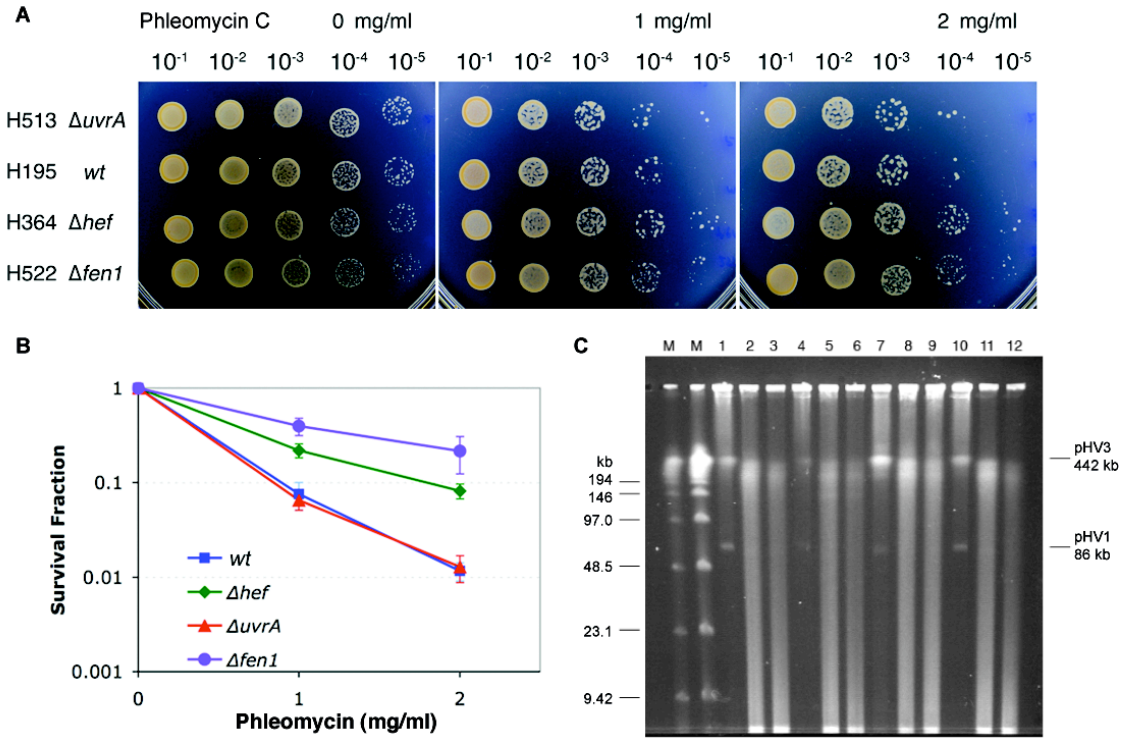

Figure 4.5 Phleomycin sensitivity of *hef*, *fen1* and *uvrA* deletion mutants.

(A) Plate assay of phleomycin sensitivity. (B) Comparison of survival fractions of H195 (*hef*+ *uvrA*+ *fen1*+), H364 (Δ*hef*), H513 (Δ*uvrA*) and H522 (Δ*fen1*::*trpA*) following phleomycin treatment. All data points are calculated as the mean value of three trials. Error bars are based on standard error. Only relevant genotypes are shown. (C) Pulsed-field gel of genomic DNA after treatment with phleomycin. Lane M, Low range PFG Marker (from top to bottom): 194, 146, 97.0, 48.5, 23.1 and 9.42 kb. Lane 1-3, Lane 4-6, Lane 7-9 and Lane 10-12 are genomic DNA of H195 (*hef*+ *uvrA*+ *fen1*+), H364 (Δ*hef*), H513 (Δ*uvrA*) and H522 (Δ*fen1*::*trpA*) treated with phleomycin for 1 hr at concentrations of 0, 1 and 2 mg/ml, respectively.

Intracellular salts such as KCl and NaCl have previously been found to mitigate the effects of oxidative free radicals produced by radiation *in vivo* and *in vitro* (Raaphorst

and Kruuv, 1977; Shahmohammadi et al., 1998). In addition, membrane pigments have been reported to offer protection against cellular damage induced by gamma radiation in *Halobacteriun* sp. NRC1 (Kottemann et al., 2005). To investigate if the high concentration of salt or membrane pigments in *H. volcanii* would mitigate the effect of phleomycin, pulsed-field gel electrophoresis was carried out. The results clearly showed that genomic DNA samples from all the strains tested were degraded to a similar extent (Figure 4.5 C). It suggests that the resistance of H364 (Δ*hef*) and H522 (Δ*fen1*::*trpA*) to phleomycin is not principally due to the protection of genomic DNA from double strand breaks in the presence of salt, but because of the existence of efficient DNA repair.

The Mre11/Rad50 complex plays an important role in DSB repair (Assenmacher and Hopfner, 2004). Strains H115 (*fen1*+ *mre11rad50*+), H204 (Δ*mre11rad50*), H720 (Δ*fen1*) and H721 (Δ*fen1*Δ*mre11rad50*) were used to study further the DSB repair. H204 (Δ*mre11rad50*) and H720 (Δ*fen1*) showed a similar resistance to phleomycin (Figure 4.6). The deletion of *fen1* and *mre11rad50* has an additive effect, as H721 (Δ*fen1*Δ*mre11rad50*) showed higher survival fraction than either H204 (Δ*mre11rad50*) or H720 (Δ*fen1*). Therefore, Fen1 and Mre11Rad50 are involved in different pathways of DSB repair.

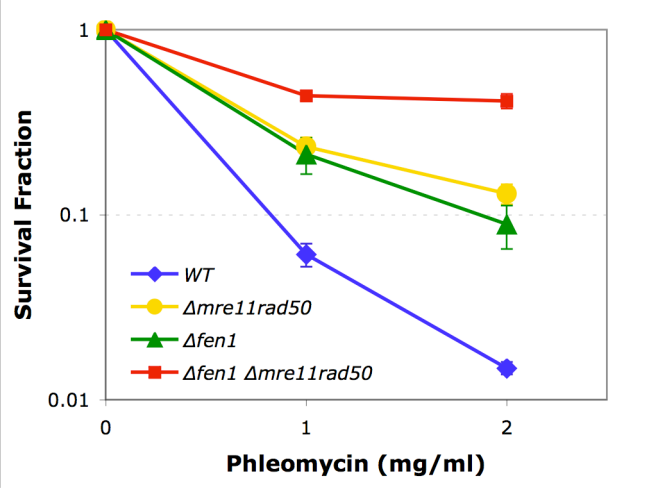

Figure 4.6 Phleomycin sensitivity of *fen1* and *mre11rad50* deletion mutants.

Comparison of survival fractions of H115 (*fen1*+ *mre11rad50*+), H204 (Δ*mre11rad50*), H720 (Δ*fen1*) and H721 (Δ*fen1*Δ*mre11rad50*) following phleomycin treatment. All data points are calculated as the mean value of two trials. Error bars are based on standard error. Only relevant genotypes are shown.

4.2.3 Discussion

DSB repair is highly efficient in *H. volcanii*

Both gamma radiation and phleomycin treatment lead to double-stranded DNA breaks with 'dirty' ends. Although some studies have suggested that membrane pigments and intracellular salts can provide protection from radiation (Raaphorst and Kruuv, 1977; Shahmohammadi et al., 1998; Kottemann et al., 2005), the pulsed-field gel electrophoresis clearly demonstrated that extensive DSBs were generated after acute treatment of phleomycin in *H. volcanii.* Normally phleomycin is used to treat other organisms at the doses up to 50 μg/ml. For *H. volcanii*, the wild-type strain still had 1% cell survival at doses as high as 2 mg/ml.

Desiccation is known to induce DSBs (Mattimore and Battista, 1996; DiRuggiero et al., 1999; Kottemann et al., 2005; Franca et al., 2007). Natural habitats of *H. volcanii* are characterized by high temperatures and a high intensity of sunlight, where cells are always in danger of desiccation. Mechanisms like sporulation (Setlow, 1995; Nicholson et al., 2000), production of extra–cellular polysaccharides (Ophir and Gutnick, 1994; Tamaru et al., 2005) and cellular accumulation of trehalose and sucrose have been reported to confer desiccation–tolerant phenotypes in many prokaryotes (Kempf and Bremer, 1998). However, neither of these mechanisms is utilized by *H. volcanii.* Instead, genome analysis shows that *H. volcanii* possesses homologues of DNA repair proteins for all major pathways. Therefore, efficient DNA repair systems might be evolved in this organism, which can survive in extreme conditions that lead to DSBs.

HR is the major pathway to repair DSBs in *H. volcanii*

Homologous recombination (HR), non-homologous end joining (NHEJ) and single strand annealing (SSA) are known to be involved in DSB repair (Shrivastav et al., 2008). Considering that UvrA is a NER factor, it is not surprising that the *uvrA* deletion mutant was not sensitive to phleomycin.

Single strand annealing (SSA) is a minor repair pathway for DSBs in eukaryotes and requires Rad1, the Hef homologue, for the removal of non-homologous 3'-single-stranded ends (Ivanov et al., 1996; Paques and Haber, 1999). In the absence of Hef, cells were not more sensitive to gamma radiation or phleomycin. Therefore, SSA is not a significant repair pathway for DSBs in *H. volcanii*, or SSA in *H. volcanii* may be carried out by some other protein(s) instead of Hef.

The mutant with *hef* deletion was as resistant as the wild-type strain to gamma radiation at the tested doses. More interestingly, cells with *hef* or *fen1* deletion appeared to be

more resistant to phleomycin at the doses where DSBs were extensively generated. Eukaryotic cells mutated in *hef* homologues (i.e. *rad1* in budding yeast and *XPF* in mammals) are not sensitive to ionizing radiation or bleomycin (Moore, 1978; Murray et al., 2002). Similarly, eukaryotic cells mutated in *fen1* homologues (i.e. *rad27* in budding yeast and *FEN1* in mammals) are not sensitive to ionizing radiation (Reagan et al., 1995; Shibata and Nakamura, 2002). In addition, it has been demonstrated that Chicken *KU70*$^{-/-}$ DT40 cells are less sensitive to high doses of ionizing radiation than wild-type cells (Takata et al., 1998). Similarly, yeast cells that are defective in NHEJ by inactivating of *KU*, *DNL4* or *LIF1* have shown an enhanced resistance to high doses of phleomycin (Zhang et al., 2007b).

HR and NHEJ are the two major pathways for DSB repair in eukaryotes (Shrivastav et al., 2008). HR predominates in single cell eukaryotes such as *S. cerevisiae* (Dudasova et al., 2004). In contrast, NHEJ appears to be predominant in higher eukaryotes, probably as NHEJ is active throughout the cell-cycle (Lieber et al., 2004), whereas HR only happens at late S and G2 phases when an intact sister chromatid is available as a template (Sonoda et al., 2006). HR alone can repair DSBs very efficiently in DT40 cells and *S. cerevisiae*, whereas NHEJ may actually result in an increase in lethal mutation following phleomycin treatment because of its lower fidelity than HR.

Rad1 (Hef homologue in yeast), a component of the structure-specific endonuclease Rad1/Rad10, plays a role in microhomology-mediated end joining by 3' flap removal (Ma et al., 2003; Lee and Lee, 2007). Genetic studies indicate that the Rad1/Rad10 endonuclease is also involved in removing nonhomologous 3' ends during HR (Ivanov and Haber, 1995). However, a Rad1-independent pathway has also been reported (Colaiacovo et al., 1999). Rad27 (Fen1 homologue in yeast) is responsible for removing 5' flap NHEJ intermediates (Wu et al., 1999b). In addition, Rad27 has been shown to interact physically and functionally with other NHEJ factors Pol4 and Dnl4/Lif1 (Tseng and Tomkinson, 2004). Therefore, the deletion of *hef* or *fen1* in *H. volcanii* might inhibit the completion of DSB repair by NHEJ, leaving DSBs to be repaired mainly by HR and subsequently, lead to an increase in the survival fraction. Consistent with this hypothesis, the *radA* deletion strain is extremely sensitive to gamma radiation (Thorsten Allers, unpublished data). At the doses that show no harm to the wild-type strain, the survival fraction of the mutant is only about 10^{-3}.

In addition, Fen1 and Mre11Rad50 are involved in two different pathways for phleomycin-induced DSB repair. Using a plasmid assay, Mre11Rad50 has been found to restrain HR for the repair of DSBs with “clean” ends (Stéphane Delmas and Thorsten

Allers, unpublished data). *H. volcanii* is an organism with multicopy chromosomes per cell. Therefore, an intact chromosome might be available to be used as a template in HR throughout the cell cycle (Breuert et al., 2006). The use of homologous recombination in *mre11 rad50* mutants enhances cell survival. Using a similar plasmid assay, Fen1 has been found no significant role in this type of HR (See 5.2.3), but Fen1 might be required for the processing of "dirty" ends to facilitate further repair of DSBs. In the absence of Fen1, other nucleases may be involved and cooperate with Mre11Rad50.

4.3 H_2O_2 and MMS test

4.3.1 Introduction

Hydrogen peroxide (H_2O_2) is a potent oxidant of lipids, proteins and nucleic acids (Fridovich, 1978; Marnett, 2000). Different strategies have been developed to protect cell from oxidative damage. On one hand, cells produce scavengers of activated oxygen species such as catalase (Loewen and Triggs, 1984), superoxide dismutase (Carlioz and Touati, 1986) and peroxidase (Fridovich, 1995; Park et al., 2000; Veenhuis et al., 2000; Lushchak, 2006). On the other hand, DNA repair enzymes involved in base excision repair (BER), translesion synthesis (TLS) and homologous recombination (HR) (David et al., 2007; Ragu et al., 2007) appear to be important in repairing oxidative DNA lesions (Slupphaug et al., 2003).

Methyl methanesulfonate (MMS) is a monofunctional DNA alkalyting agent and a known carcinogen (Lawley, 1989; Beranek, 1990). DNA damage caused by alkylating agents is predominantly repaired by DNA alkyltransferases and base excision repair (Lindahl and Wood, 1999). The sensitivity of cells to MMS is also increased when other DNA repair pathways are compromised. For example, the disruption of the homologous recombination pathway by mutating genes in the *rad52* epistasis group significantly increases the sensitivity to MMS in *S. cerevisiae* (Xiao et al., 1996; Krogh and Symington, 2004).

4.3.2 Results

H_2O_2 Test Results

UvrA

The survival fractions of H513 (Δ*uvrA*) and H509 (Δ*uvrA*) are similar to that of their parental strains H195 (*uvrA*+) and H513, respectively (Figure 4.7 A and C). These data strongly suggest that UvrA is not involved in the repair of H_2O_2 induced DNA damage.

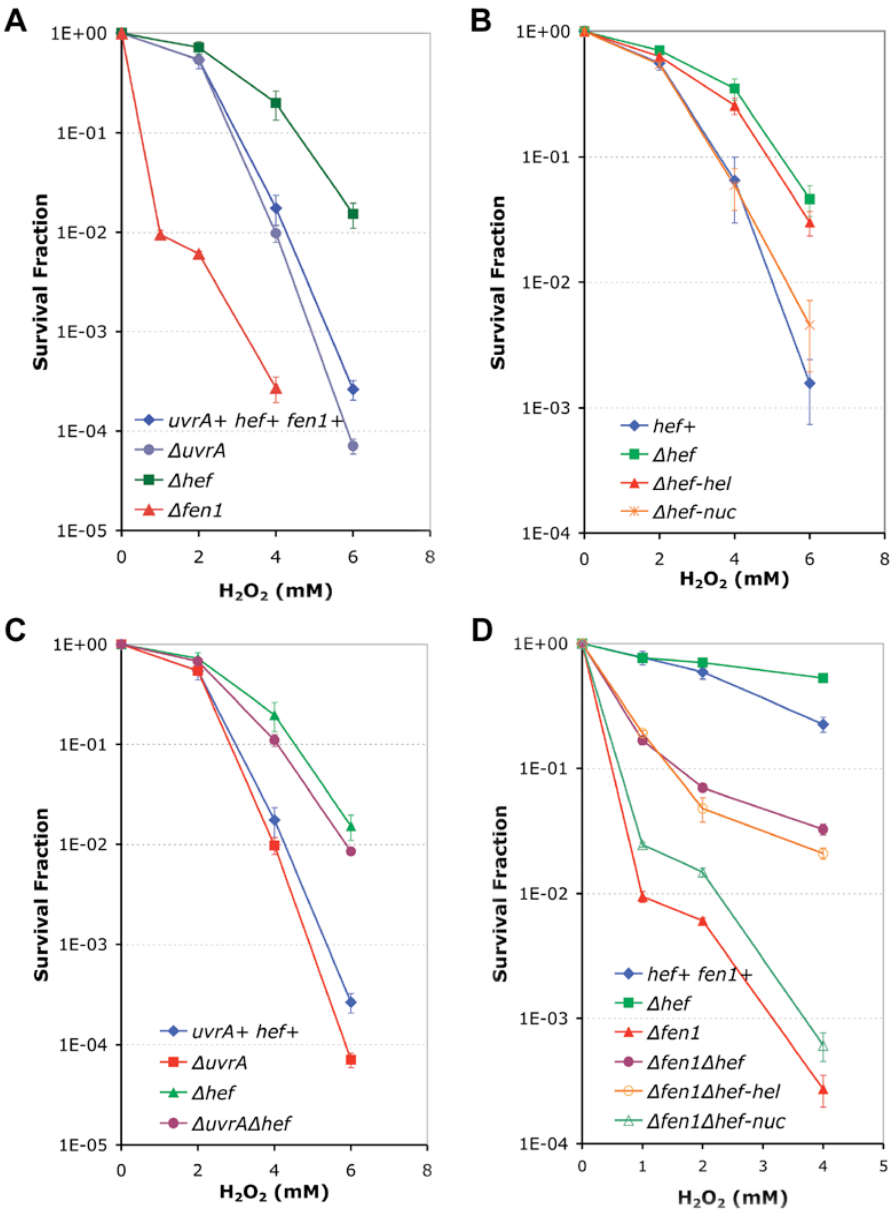

Figure 4.7 H_2O_2 sensitivity of Δ*uvrA*, Δ*hef* and Δ*fen1* mutants.

(A) Comparison of survival fractions of H195 (*hef*+ *fen1*+ *uvrA*+), H364 (Δ*hef*), H513 (Δ*uvrA*) and H522 (Δ*fen1*::*trpA*) following H_2O_2 treatment. (B) Comparison of survival fractions of H26 (*hef*+), H358 (Δ*hef*), H359 (Δ*hef-hel*) and H360 (Δ*hef-nuc*) following H_2O_2 treatment. (C) Comparison of survival fractions of H26 (*uvrA*+ *hef*+), H358 (Δ*hef*), H509 (Δ*uvrA*) and H510 (Δ*uvrA* Δ*hef*) following H_2O_2 treatment. (D) Comparison of survival fractions of H195 (*fen1*+ *hef*+), H364 (Δ*hef*), H522 (Δ*fen1*::*trpA*), H598 (Δ*fen1*::*trpA* Δ*hef*), H524 (Δ*fen1*::*trpA* Δ*hef-hel*) and H525 (Δ*fen1*::*trpA* Δ*hef-nuc*) following H_2O_2 treatment. All data points are calculated as the mean value of three trials. Error bars are based on standard error. Only relevant genotypes are shown.

Hef and Fen1

H522 (Δ*fen1*::*trpA*) is very sensitive to H_2O_2 (Figure 4.7 A). After 1 hr treatment of 6 mM H_2O_2, H522 (Δ*fen1*::*trpA*) could not survive. In contrast, H364 (Δ*hef*) is more resistant than H195 (*hef*+). In addition, H358 (Δ*hef*) and H359 (Δ*hef-hel*) are also more resistant than H26 (*hef*+), while H360 (Δ*hef-nuc*) has a similar sensitivity to that of H26 (*hef*+) (Figure 4.7 B). More interestingly, H522 (Δ*fen1*::*trpA*) and H525 (Δ*fen1*::*trpA* Δ*hef-nuc*) are both very sensitive, while H598 (Δ*fen1*::*trpA* Δ*hef*) and H524 (Δ*fen1*::*trpA* Δ*hef-hel*) are less sensitive than H522 (Δ*fen1*::*trpA*) and H525 (Δ*fen1*::*trpA* Δ*hef-nuc*) (Figure 4.7 D). These data suggest that Fen1 is involved in the major repair of H_2O_2 induced DNA damage and the Hef helicase domain is involved in a minor pathway, which counteracts the major pathway.

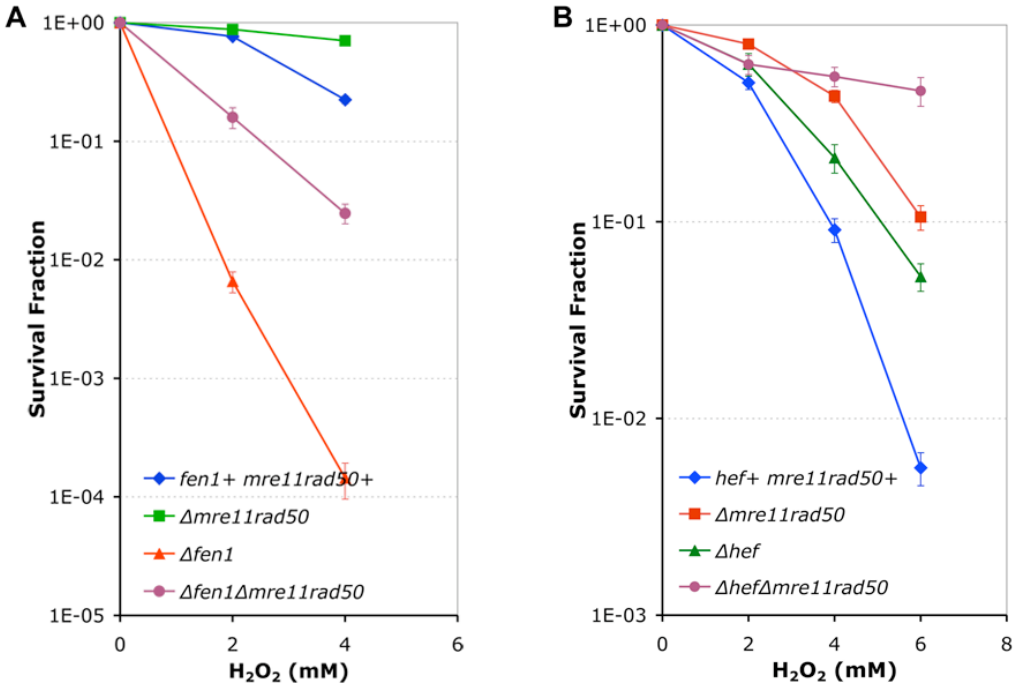

Figure 4.8 H_2O_2 sensitivity of *hef*, *fen1* and *mre11rad50* mutants.

(A) Comparison of survival fractions of H115 (*fen1*+ *mre11rad50*+), H204 (Δ*mre11rad50*), H720 (Δ*fen1*) and H721 (Δ*fen1* Δ*mre11rad50*) following H_2O_2 treatment. (B) Comparison of survival fractions of H195 (*hef*+ *mre11rad50*+), H280 (Δ*mre11rad50*), H364 (Δ*hef*) and H782 (Δ*hef* Δ*mre11rad50*) following H_2O_2 treatment. All data points are calculated as the mean value of three trials. Error bars are based on standard error. Only relevant genotypes are shown.

Fen1, Hef and Mre11Rad50

At a concentration of 4 mM, H204 (Δ*mre11rad50*) is slightly more resistant than H115 (*fen1*+ *mre11rad50*+), and the survival fraction of H721 (Δ*fen1* Δ*mre11rad50*) is between those of H720 (Δ*fen1*) and H115 (*fen1*+ *mre11rad50*+) (Figure 4.8 A). Therefore deletion of *mre11rad50*, like deletion of *hef-hel*, partially rescues the H_2O_2 sensitivity of *fen1* deletion strains. In addition, H782 (Δ*hef* Δ*mre11rad50*) is more resistant than both H280 (Δ*mre11rad50*) and H364 (Δ*hef*) (Figure 4.8 B). These data suggest that the Hef helicase domain and Mre11Rad50 are involved in two different minor pathways, which counteract the Fen1 dependent major repair pathway for H_2O_2 induced DNA damage.

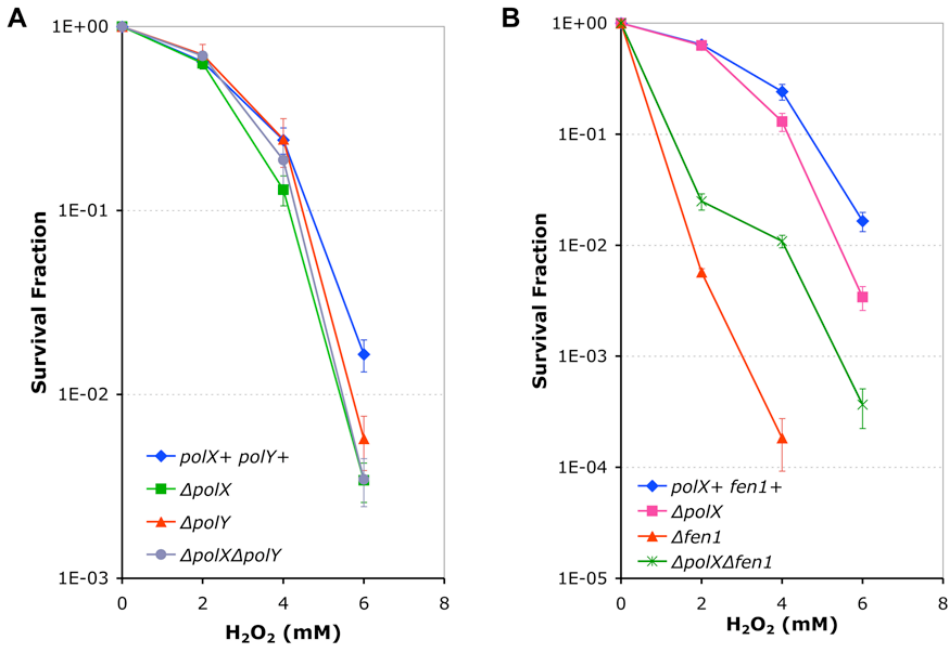

Figure 4.9 H_2O_2 sensitivity of *fen1*, *polX* and *polY* mutants.

(A) Comparison of survival fractions of H115 (*fen1*+ *polX*+), H648 (Δ*polX*), H720 (Δ*fen1*) and H723 (Δ*fen1* Δ*polX*) following H_2O_2 treatment. (B) Comparison of survival fractions of H115 (*polX*+ *polY*+), H648 (Δ*polX*), H734 (Δ*polY*) and H736 (Δ*polX* Δ*polY*) following H_2O_2 treatment. All data points are calculated as the mean value of three trials. Error bars are bases on standard error. Only relevant genotypes are shown.

PolX and PolY

DNA polymerases carry out DNA synthesis, one common step among a variety of DNA repair mechanisms. DNA polymerases are classified into different families (A, B, C, D,

X and Y) according to their biochemical properties. *H. volcanii* possesses at least four DNA polymerases, PolB, PolD, PolX and PolY. Previous genetic studies have shown that the putative replication polymerases, PolB and PolD, are essential in *H. volcanii* (Thorsten Allers, unpublished data).

At high concentration of H_2O_2 (6mM), H648 (Δ*polX*) and H734 (Δ*polY*) are slightly more sensitive than H115 (*polX*+ *polY*+) (Figure 4.9 A). H736 (Δ*polX* Δ*polY*) is not more sensitive than H648 (Δ*polX*) and H734 (Δ*polY*) even after 1 hr treatment of 6mM H_2O_2, which will kill almost all the cells with *fen1* deletion. These data suggest that neither PolX nor PolY is the major polymerase that cooperates with Fen1 in the repair of high concentration H_2O_2 induced DNA damage.

Fen1 and PolX

H648 (Δ*polX*) is only slightly sensitive to high concentration treatment of H_2O_2 (above 2 mM), while H720 (Δ*fen1*) is very sensitive and could not survive after the treatment with 6 mM H_2O_2. The survival fraction of H723 (Δ*fen1* Δ*polX*) was between that of H115 (*fen1*+ *polX*+) and H720 (Δ*fen1*) (Figure 4.9 B). Notably, the deletion of *polX* can partially rescue the lethality of *fen1* deletion at high concentration of H_2O_2 (6 mM).

MMS Test Results

Strains H195 (*hef*+ *uvrA*+ *fen1*+), H364 (Δ*hef*), H513 (Δ*uvrA*) and H522 (Δ*fen1*::*trpA*) were used to test MMS sensitivity. H364 (Δ*hef*) and H513 (Δ*uvrA*) have a similar sensitivity to MMS to that of the wild-type strain H195 (Figure 4.10). In contrast, H522 (Δ*fen1*::*trpA*) is about 100 times more sensitive to MMS than other strains at the concentration of 0.04%. These data suggest that Fen1 is involved in MMS induced DNA damage repair, while Hef and UvrA are not.

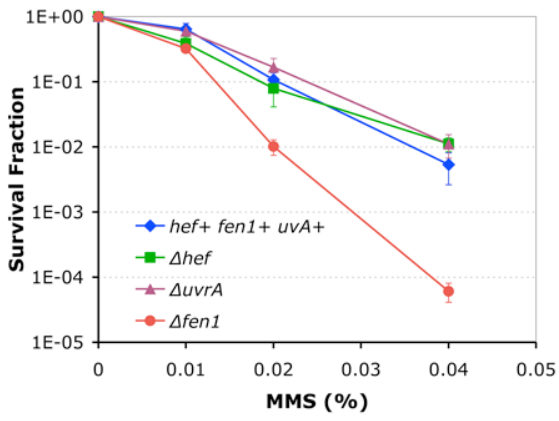

Figure 4.10 MMS sensitivity test.

Comparison of survival fractions of H195 (*hef*+ *fen1*+ *uvrA*+), H364 (Δ*hef*), H513 (Δ*uvrA*) and H522 (Δ*fen1*) following MMS treatment. All data points are calculated as the mean value of three trials. Error bars are based on standard error. Only relevant genotypes are shown.

4.3.3 Discussion

Fen1 is involved in the major repair of MMS and H_2O_2 induced DNA damage

The base excision repair pathway has evolved to protect cells from deleterious effects of endogenous DNA damage and is also important for the repair of exogenous DNA lesions induced by strong alkylating and oxidative agents, such as MMS and H_2O_2 respectively (Seeberg et al., 1995; Lindahl and Wood, 1999). As expected, cells with *uvrA* deletion were not sensitive to MMS and H_2O_2, suggesting no significant role of NER for the repair of MMS or H_2O_2 induced DNA damage. In contrast, mutants with *fen1* deletion were much more sensitive to MMS and H_2O_2 than the wild-type strains, suggesting that Fen1 is involved in the repair of MMS and H_2O_2 induced DNA damage.

In *S. cerevisiae*, Rad27 (homologue of FEN1) plays a major role in BER by removing the 5'-dRP (Wu and Wang, 1999). In mammalian cells, FEN1 is responsible for removing the 5' flap after DNA synthesis in long-patch BER (Krokan et al., 2000). Archaeal FEN1 proteins (from *Archaeglobus fulgidus*, *Methanococcus jannaschii* and *Pyrococcus furiosus*) have similar nuclease activity to that of the homologues in eukaryotes (Hosfield et al., 1998a). In addition to Fen1, several other open reading frames of *H. volcanii* encode homologues of BER proteins, for example, ORF01386_apn1, ORF01726_udg1, ORF_00253_ogg etc. Therefore, base excision repair might be the Fen1 dependent repair pathway for MMS or H_2O_2 induced DNA damage in *H. volcanii.*

Role of PolX and PolY

In the presence of Fen1, deletion mutants of *polX* and/or *polY* appeared to be as resistant as wild-type strain to H_2O_2, suggesting these two polymerases are not involved in the BER with Fen1 in *H. volcanii*.

Abasic sites can be formed by the removal of damaged bases, which can arise by oxidation, methylation and deamination of normal bases. In eukaryotes, although most abasic sites are removed by BER prior to DNA synthesis, a small number of lesions may escape from repair or occur during S phase and pose a serious challenge to DNA replication (Freisinger et al., 2004; Hogg et al., 2004). During replication, abasic sites can be either bypassed by specialized, but error-prone, DNA polymerases from the Y and X families, or by an error-free mechanism-either by homologous recombination or by template slippage (Boiteux and Guillet, 2004).

All X family polymerases are single-subunit enzymes, lacking the 3'-5' exonuclease (proofreading) activity and display very low processivity (Bebenek and Kunkel, 2004). Pol β, the paradigm of X family polymerases and the polymerase involved in eukaryotic BER, is moderately accurate (Kunkel and Loeb, 1981; Kunkel, 1985). It has been reported that the expression of mRNA of two X family polymerases Pol λ and Pol μ is both down-regulated upon the treatment of UV, gamma radiation or H_2O_2 in mammalian cells (Aoufouchi et al., 2000). Y family polymerase members also lack 3'-5' exonuclease activity and exhibit error-prone behaviour (Goodman, 2002). Therefore, PolX and PolY from *H. volcanii* may also have low fidelity and carry out translesion syntheses as a minor pathway to tolerate ICLs. However, the reliance of translesion synthesis may increase lethal mutations. Consistent with this, at high concentration of H_2O_2, deletion of *polX* partially rescued the lethality of *fen1* deletion.

Both Hef helicase and Mre11Rad50 counteract Fen1-involved excision repair but in two different pathways

Deletion of *hef-hel* or *mre11rad50* conferred moderate H_2O_2 resistance to the cell, and partially rescued the severe sensitivity of *fen1* deletion. Moreover, deletion of *hef-hel* and *mre11rad50* appeared to have additive effect on H_2O_2 resistance, suggesting that Hef helicase and Mre11Rad50 counteract Fen1-dependent BER, but in two different pathways.

A double-flap structure, which has a 3' single nucleotide (nt), has been shown to be the optimal substrates for FEN1 homologues in archaea (Kaiser et al., 1999), yeast (Kao et al., 2002), bacteria (Xu et al., 2000) and humans (Storici et al., 2002; Friedrich-Heineken et al., 2003). Meanwhile, biochemical studies have suggested that the helicase activity of Hef from euryarchaeon *Pyrococcus furiosus* may unwind and migrate the branch point of the stalled replication fork to a suitable position for incision by the C-terminal nuclease, probably the 5' nascent lagging strand end near the branch point (Komori et al., 2004). Therefore, the helicase activity of Hef might affect the efficient BER induced DNA damage by impeding the 5'-flap endonuclease activity of Fen1.

The Mre11/Rad50 complex exhibits single-stranded endonuclease (Connelly et al., 1997; Furuse et al., 1998; Trujillo et al., 1998; Hopfner et al., 2000a) and ATP-stimulated 3'-5' exonuclease activities (Paull and Gellert, 1998; Trujillo et al., 1998; Connelly et al., 1999; Hopfner et al., 2001). These nuclease activities might also affect the substrates for the 5'-flap endonuclease activity of Fen1.

In addition, bacteria and eukaryotes have been known to utilize multiple mechanisms to counteract the deleterious action of abasic sites, which can be formed after oxidative DNA damage (Friedberg, 2003). Besides BER, the repair of chromosomal abasic sites involves NER, HR and TLS in both *E. coli* and eukaryotic cells (Otterlei et al., 2000; Boiteux and Guillet, 2004). Our data suggest that oxidative DNA damage might be converted into DSBs by some nucleases other than Fen1. Subsequently, DSBs could be repaired by HR, which has been found to be restrained by the Mre11Rad50 complex in *H. volcanii* (Stéphane Delmas and Thorsten Allers, unpublished data). The use of homologous recombination in *mre11 rad50* mutants enhances cell survival.

4.4 MMC test

4.4.1 Introduction

Mitomycin C (MMC) is a bifunctional alkylating agent used as an antibiotic or antitumor drug. MMC reacts covalently with DNA *in vivo* and *in vitro*, forming cross-links with guanine residues of 5'-CG-3' sequences through the minor groove of DNA. This interaction prevents the separation of the complementary DNA strand, thus inhibiting essential DNA processes like replication and transcription (Ueda and Komano, 1984; Tomasz et al., 1987).

The ICL repair in *E. coli* has been characterized both genetically and biochemically. In the major pathway, nucleotide excision repair (NER) and homologous recombination (HR) work together to remove the ICLs. NER and DNA polymerase II carry out a minor repair pathway, translesion synthesis (TLS). Likewise, it is believed that NER, HR and TLS are involved in the repair of ICLs in yeast. The repair of ICLs in mammalian cells has not been characterized in as much detail as that in *E. coli* and yeast. The repair involves some proteins from NER, HR and TSL pathways, along with other proteins (Noll et al., 2006).

4.4.2 Results

To examine the ICL repair in *H. volcanii*, isogenic groups of mutant strains were analyzed in parallel with a wild-type strain. *H. volcanii* appears to be very sensitive to MMC. For the optimal results, plates containing 0.02 μg/ml MMC were used to distinguish the sensitivity of different strains.

Hef

H358 (Δ*hef*) and H359 (Δ*hef-hel*) showed a similar sensitivity to MMC (See Figure 4.11). Both strains are more sensitive to MMC than H26 (*hef*+). H360 (Δ*hef-nuc*) is also sensitive to MMC, but less sensitive than H358 (Δ*hef*) or H359 (Δ*hef-hel*). These data suggest that the helicase and nuclease domains of Hef are both involved in MMC induced ICLs repair, but might be involved at different steps.

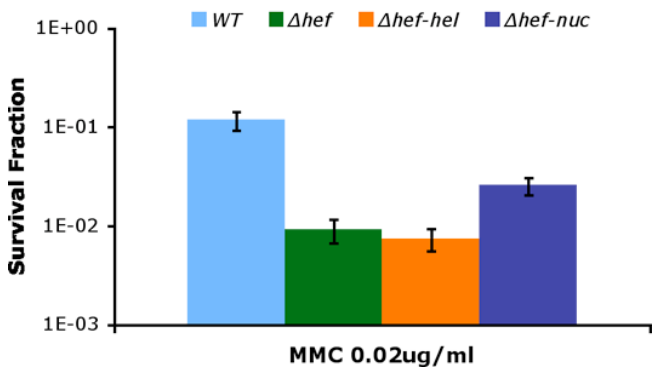

Figure 4.11 MMC sensitivity of *hef* deletion mutants.

Survival fractions of H26 (wild-type), H358 (Δ*hef*), H359 (Δ*hef-hel*) and H360 (Δ*hef-nuc*) following MMC treatment are compared. All data points are calculated as the mean value of three trials. Error bars are based on standard error. Only relevant genotypes are shown.

Hef and Fen1

H522 (Δ*fen1*::*trpA*) and H364 (Δ*hef*) showed a similar sensitivity to MMC (Figure 4.12). Double deletion strain H598 (Δ*fen1*::*trpA* Δ*hef*) was more sensitive than single deletion mutants H522 (Δ*fen1*::*trpA*) and H364 (Δ*hef*). These data suggest that both Hef and Fen1 are responsible for MMC induced ICL repair. In addition, H525 (Δ*fen1*::*trpA* Δ*hef-nuc*) and H598 (Δ*fen1*::*trpA* Δ*hef*) showed similar sensitivity, while H524 (Δ*fen1*::*trpA* Δ*hef-hel*) was even more sensitive than H598 (Δ*fen1*::*trpA* Δ*hef*). These data suggest that in the absence of the Hef helicase domain and Fen1, the expression of the Hef nuclease domain further decreases cell survival.

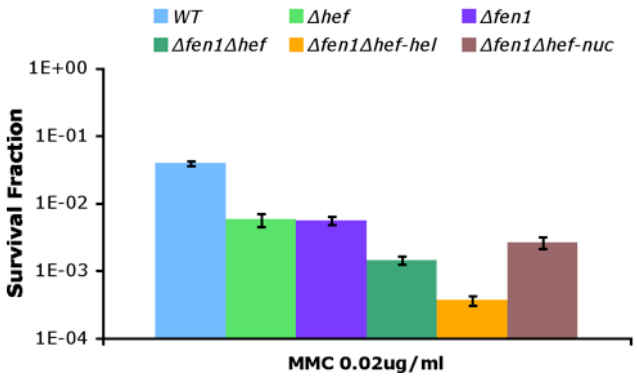

Figure 4.12 MMC sensitivity of *hef* and *fen1* deletion mutants.

Survival fractions of H195 (*hef*+ *fen1*+), H364 (Δ*hef*), H522 (Δ*fen1*::*trpA*), H598 (Δ*hef* Δ*fen1*::*trpA*), H524 (Δ*hef-hel* Δ*fen1*::*trpA*) and H525 (Δ*hef-nuc* Δ*fen1*::*trpA*) following MMC treatment are compared. All data points are calculated as the mean value of three trials. Error bars are based on standard error. Only relevant genotypes are shown.

Hef and UvrA

H513 (Δ*uvrA*) and H358 (Δ*hef*) have a similar sensitivity to MMC (Figure 4.13). H510 (Δ*uvrA* Δ*hef*) is about 100 times more sensitive than H358 (Δ*hef*) or H513 (Δ*uvrA*). These data suggest that UvrA is also involved in MMC induced ICL repair and UvrA and Hef are involved in two different pathways.

H511 (Δ*uvrA* Δ*hef-hel*) and H512 (Δ*uvrA* Δ*hef-nuc*) showed similar survival fractions to that of H510 (Δ*uvrA* Δ*hef*). Due to the limited differences and variation of values, paired *t*-tests were carried out to test the hypothesis that the survival fraction of H511 (Δ*uvrA* Δ*hef-hel*) is lower than that of H510 (Δ*uvrA* Δ*hef*) and the survival fraction of H512 (Δ*uvrA* Δ*hef-nuc*) is lower than that of H510 (Δ*uvrA* Δ*hef*). Both *p* values are more than 0.05. Therefore, H510 (Δ*uvrA* Δ*hef*), H511 (Δ*uvrA* Δ*hef-hel*) and H512 (Δ*uvrA* Δ*hef-nuc*) were concluded to have a similar sensitivity to MMC.

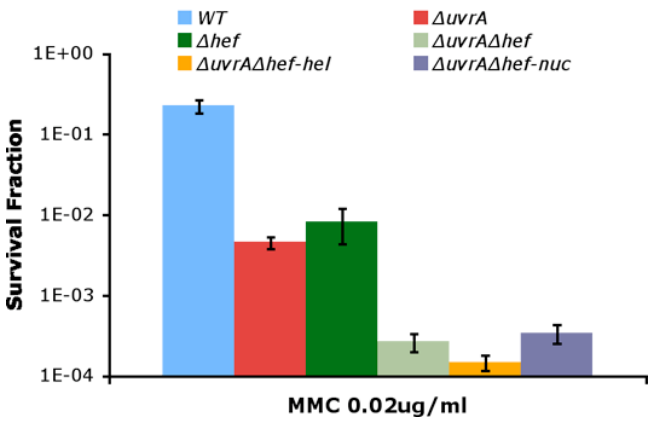

Figure 4.13 MMC sensitivity of *hef* and *uvrA* deletion mutants.

Survival fractions of H26 (*uvrA*+ *hef*+), H358 (Δ*hef*), H509 (Δ*uvrA*), H510 (Δ*uvrA* Δ*hef*), H511 (Δ*uvrA* Δ*hef-hel*) and H512 (Δ*uvrA* Δ*hef-nuc*) following MMC treatment are compared. All data points are calculated as the mean value of three trials. Error bars are based on standard error. Only relevant genotypes are shown.

Hef, Fen1 and UvrA

H646 (Δ*uvrA* Δ*fen1*::*trpA*) is about 100 times more sensitive than H513 (Δ*uvrA*) or H522 (Δ*fen1*::*trpA*), suggesting that UvrA and Fen1 are involved in two different ICL repair pathways (Figure 4.14). The triple deletion mutant H647 (Δ*hef* Δ*fen1*::*trpA* Δ*uvrA*) is 10 times more resistant than the double deletion mutant H647 (Δ*fen1*::*trpA* Δ*uvrA*). This result implies that in the background of *uvrA* deletion, Hef without Fen1 cannot increase the chance of survival. This confirms the overlapping function of Hef and Fen1 in MMC induced ICL repair.

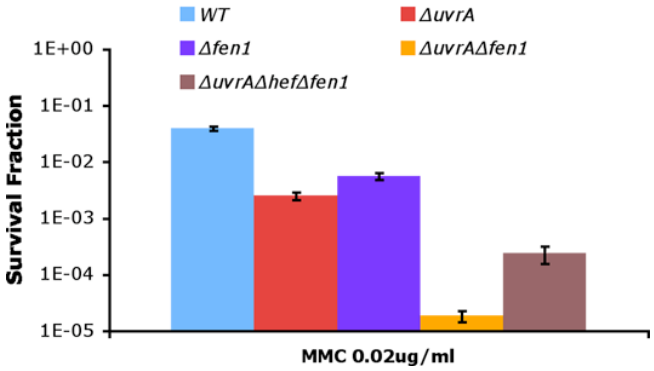

Figure 4.14 MMC sensitivity of mutants with *hef*, *fen1* and *uvrA* deletion.

Survival fractions of H195 (*hef*+ *fen1*+ *uvrA*+), H513 (Δ*uvrA*), H522 (Δ*fen1*::*trpA*), H646 (Δ*fen1*::*trpA* Δ*uvrA*) and H647 (Δ*hef* Δ*fen1*::*trpA* Δ*uvrA*) following MMC treatment are compared. All data points are calculated as the mean value of three trials. Error bars are based on standard error. Only relevant genotypes are shown.

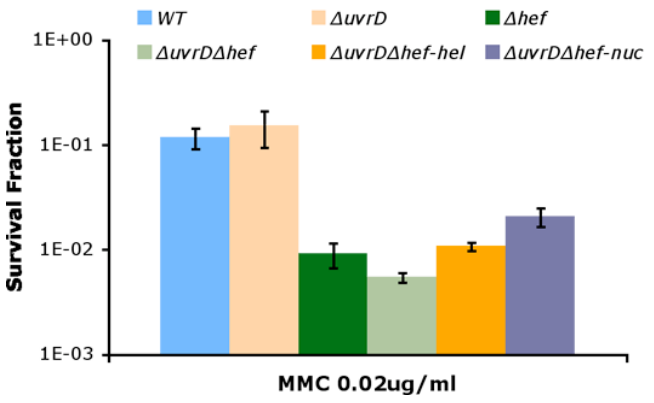

Figure 4.15 MMC sensitivity of *hef* and *uvrD* deletion mutants.

Survival fractions of H26 (*uvrD*+ *hef*+), H358 (Δ*hef*), H514 (Δ*uvrD*), H515 (Δ*uvrD* Δ*hef*), H516 (Δ*uvrD* Δ*hef-hel*) and H517 (Δ*uvrD* Δ*hef-nuc*) following MMC treatment are compared. All data points are calculated as the mean value of three trials. Error bars are based on standard error. Only relevant genotypes are shown.

Hef and UvrD

H514 (Δ*uvrD*) is no more sensitive than H26 (*uvrD*+ *hef*+), suggesting that UvrD is not involved in ICL repair or another protein can fulfil its function (Figure 4.15). H515 (Δ*uvrD* Δ*hef*) and H516 (Δ*uvrD* Δ*hef-hel*) are slightly more sensitive than H517 (Δ*uvrD* Δ*hef-nuc*). Thus, the Hef helicase domain and UvrD may have partially overlapping functions in ICL repair.

Hef, Fen1 and Mre11Rad50

H280 (Δ*mre11rad50*) has a similar sensitivity to that of H364 (Δ*hef*) (Figure 4.16 A). Moreover, H782 (Δ*hef* Δ*mre11rad50*) is at least 25 times more sensitive than H280 (Δ*mre11rad50*) or H364 (Δ*hef*). These data suggest that the Mre11 complex is also involved in MMC induced ICL repair. In addition, Hef and Mre11Rad50 are involved in two different pathways.

The double deletion strain H721 (Δ*fen1* Δ*mre11rad50*) is about 10 times more sensitive than single deletion strain H204 (Δ*mre11rad50*) or H720 (Δ*fen1*) (Figure 4.16 B). Therefore, Fen1 and Mre11Rad50 are also involved in two different pathways of MMC induced DNA damage repair.

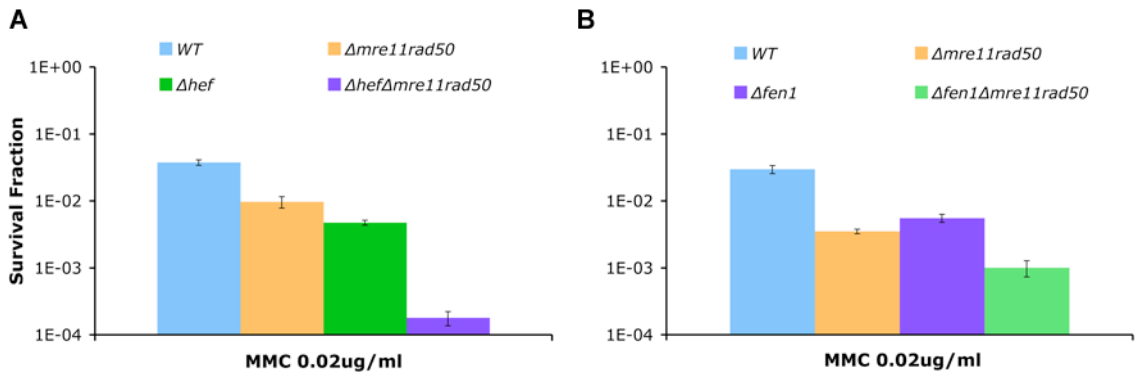

Figure 4.16 MMC sensitivity of *hef*, *fen1* and *mre11rad50* deletion mutants.

(A) Comparison of survival fractions of H195 (*hef*+ *mre11rad50*+), H280 (Δ*mre11rad50*), H364 (Δ*hef*) and H782 (Δ*hef* Δ*mre11rad50*) following MMC treatment. (B) Comparison of survival fractions of H115 (*fen1*+ *mre11rad50*+), H204 (Δ*mre11rad50*), H720 (Δ*fen1*) and H721 (Δ*fen1* Δ*mre11rad50*) following MMC treatment. All data points are calculated as the mean value of three trials. Error bars are based on standard error. Only relevant genotypes are shown.

PolX, PolY and Fen1

H648 (Δ*polX*), H734 (Δ*polY*) and H736 (Δ*polX* Δ*polY*) are as resistant as H115 (*polX*+ *polY*+) (Figure 4.17 A). Therefore, both PolX and PolY are not essential in ICL repair. However, PolX seems to be involved in the ICL repair in the absence of Fen1. This is suggested by the fact that H722 (Δ *fen1* Δ*polX*) is about 10 times more sensitive than H720 (Δ*fen1*) (Figure 4.17 B).

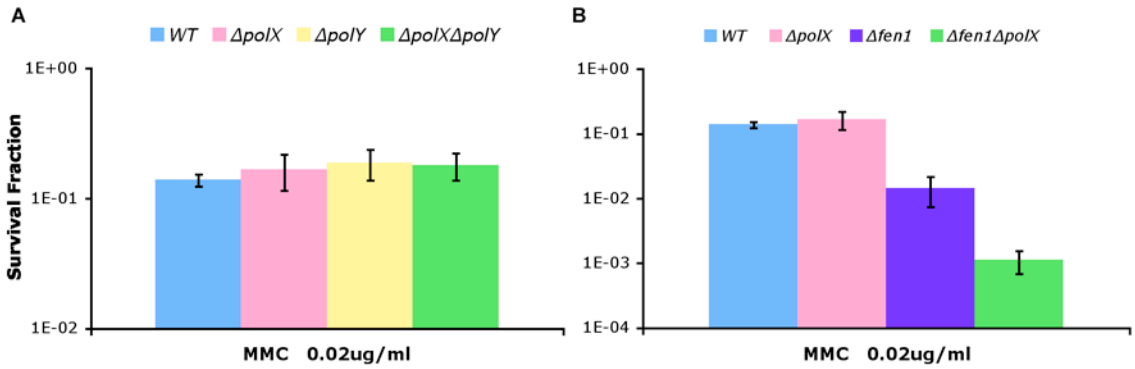

Figure 4.17 MMC sensitivity of *polX*, *polY* and *fen1* deletion mutants.

(A) Survival fractions of H115 (*polX*+ *polY*+), H648 (Δ*polX*), H734 (Δ*polY*) and H736 (Δ*polX* Δ*polY*) following MMC treatment are compared. (B) Survival fractions of H115 (*fen1*+ *polX*+), H648 (Δ*polX*), H720 (Δ*fen1*) and H722 (Δ*fen1* Δ*polX*) MMC treatment are compared. All data points are calculated as the mean value of three trials. Error bars are based on standard error. Only relevant genotypes are shown.

fen1* deletion mutants with a suppressor *sfnA

Two strains with a spontaneous suppressor of *fen1* (*sfnA*), H823 (Δ*fen1 sfnA*) and H859 (Δ*fen1*::*trpA sfnA*), were isolated on the basis of MMC resistance (Figure 4.18 A) and normal growth (Table 3.2). In contrast, H522 (Δ*fen1*::*trpA*) appeared to be more sensitive to MMC (Figure 4.18 A) and grow slower than H195 (wild-type) (Table 3.2). To determine whether *sfnA* also suppresses aspects of the Δ*fen1* phenotype other than slow growth rate and MMC sensitivity, UV irradiation survival assays were carried out on the same group of strains. However, H522 (Δ*fen1*::*trpA*), H823 (Δ*fen1 sfnA*) and H859 (Δ*fen1*::*trpA sfnA*) are all moderately sensitive to UV and showed very similar survival fractions (data not shown).

Fen1 was shown to be required for the Hef dependent ICL repair pathway (Figure 4.12). Fen1 and Hef might have overlapping functions for the repair of MMC induced DNA damage repair. To determine whether the transcription of *hef* was affected in mutants with the suppressor *sfnA*, RNA samples were extracted from cells in the late exponential phase (OD_{650}≈0.7) and RT-PCR was used to measure transcript levels of *hef* with a pair of primers hef-RTF/hef-RTR. As a control, the transcript level of *rpoA* was also measured by RT-PCR with primers rpoA-RTF/rpoA-RTR. *rpoA* encodes an RNA polymerase subunit. The transcript level of this gene is only related to the growth phase of the cell (Haldenby, 2007). The transcript levels of *rpoA* in the tested strains were similar, as predicted (Figure 4.18 B). This was also true for *hef* transcript levels, suggesting that the expression of *hef* is not affected by the Δ*fen1* suppressor *sfnA*.

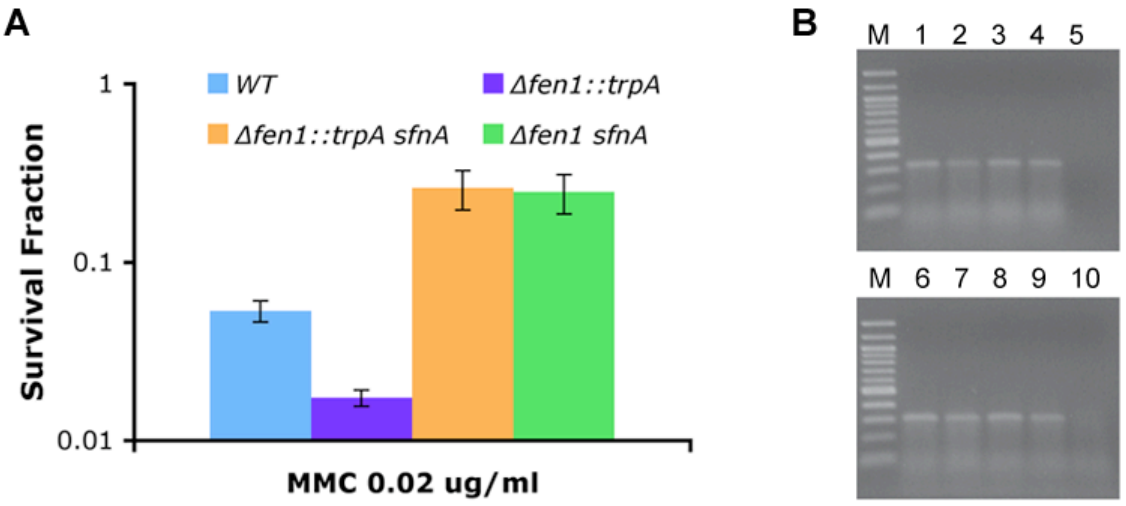

Figure 4.18 MMC sensitivity of *fen1* deletion mutants and transcript analysis of *hef*.

(A) Survival fractions of H195 (wild-type), H522 (Δ*fen1*::*trpA*), H823 (Δ*fen1*) and H859 (Δ*fen1 sfnA*) following MMC treatment are compared. All data points are calculated as the mean value of three trials. Error bars are based on standard error. Only relevant genotypes are shown. (B) Transcript levels of *rpoA* and *hef*. Lane M, size marker (from top to bottom): 10, 8, 6, 5, 4, 3, 2 1.5 1 and 0.5 kb. Lanes 1-5 show RT-PCR products amplified with rpoA-RTF/rpoA-RTR. Lanes 6-10 show RT-PCR products amplified with hef-RTF/hef-RTR. Lane 5 is the no RNA control and lane 10 is the no reverse transcription control.

4.4.3 Discussion

MMC is a natural antibiotic from *Streptomyces caespitosis* used to treat a variety of tumours. MMC forms adducts at the N-2 and N-7 of guanine, intrastrand cross-links, and interstrand cross-links (ICLs) between the N-2 of guanines at the d(CpG) sequences (Kumar et al., 1995; Paz et al., 2004). *H. volcanii* has a genome with a high G+C content of approximately 65%, compared to about 40% in the case of the human genome (Charlebois et al., 1991; Lander et al., 2001). Therefore, MMC can efficiently induce ICLs and lead to severe sensitivity in *H. volcanii*. Epistasis analysis suggests that the repair for MMC induced DNA damage is complicated in *H. volcanii*. Like in eukaryotes, the repair of ICLs involves multiple overlapping and redundant pathways in *H. volcanii* (Figure 4.19).

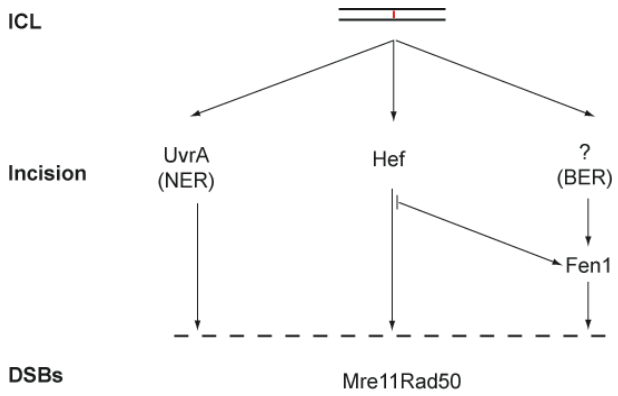

Figure 4.19 Possible pathways for the MMC induced ICL repair in *H. volcanii.*

MMC induced ICLs can be repaired by several pathways in *H. volcanii.* UvrA is supposed to be involved in NER pathway. Fen1 is involved in a Hef and UvrA independent pathway, which might be base excision repair (BER). Fen1 also has overlapping functions with Hef in a different pathway. The nicked DNA that generated by BER, NER or some other repair proteins can be transformed into DSBs via DNA replication-dependent fork breakage. Once DSBs are formed, homologous recombination takes part in the repair. The Mre11Rad50 complex is involved in this process.

The role of UvrA, Hef and Fen1 in the repair of MMC induced ICLs

UvrA and Hef were shown to be involved in two different pathways. From the results of the UV tests, it is speculated that the UvrABC system carries out a functional NER in

H. volcanii. Like in bacteria, the UvrABC system might also be involved in the repair of MMC induced DNA damage in *H. volcanii*. In both *E. coli* and eukaryotes, 6-4PPs are removed much faster than CPDs, indicating that the efficiency of lesion recognition is directly related to the conformation change of the DNA helix (Thoma, 1999). Compared to other ICL inducing agents such as psoralens, platinum compounds and nitrogen mustards, MMC induced ICL cause relatively little DNA distortion, which could be an important factor to affect the detection by the UvrABC system (Dronkert and Kanaar, 2001; Noll et al., 2006).

On the other hand, ICLs block DNA replication and transcription. The stalled replication fork or transcription machinery might offer an alternative way to detect MMC induced ICLs. Archaeal genomes lack homologues of the transcription-coupling factors (Mfd in bacteria, Rad28 and Rad26 in yeast, CSA and CSB in mammals). However, biochemical studies with the archaeal members of the XPF/Mus81 family have shown that Hef from *P. furiosus* and XPF from *S. solfataricus* have substrate specificities more similar to the Mus81 complexes than XPF-ERCC1 (Komori et al., 2002; Roberts and White, 2005b). Both archaeal proteins cleave replication fork structures in preference to splayed-arm DNA. Hef might cleave on the leading strand template of a replication fork blocked at a MMC induced ICL. Subsequently, DSBs are formed and DNA replication could restart by homologous recombination, which appears to be highly efficient in *H. volcanii*.

Fen1 is involved in two pathways. One is the Hef dependent pathway, the other is distinct from both the UvrA and Hef involved pathways. From the results of UV, H_2O_2 and MMS tests, it is plausible to speculate that Fen1 is involved in the BER pathway in *H. volcanii.* MMC is a bifunctional agent and can form monoadduct at the N-2 of guanine (Warren et al., 1998). In some conditions, the monoadduct can alkylate the guanine on the opposite strand of DNA to produce an ICL. From the current data, it is not clear that the Fen1 dependent pathway deals with monoadducts and/or ICLs. It has been reported that psoralen induced monoadducts are substrates for a human DNA glycosylase NEIL1, indicating that BER can provide an alternative to NER for the repair of bulky DNA adducts (Couve-Privat et al., 2007). DNA polymerase β deficient mouse fibroblasts have also been shown to be highly sensitive to MMC (Ochs Sobol Wilson 1999). More recently, 3-methyladenine DNA glycosylase has been found to be important for the resistance of mouse embryonic stem cells to psoralen induced ICLs

(Maor-Shoshani et al., 2008). Therefore, BER might be directly involved in the repair of ICLs induced by some agents. Alternatively, BER might repair cross-linking agents induced monoadducts, block the formation of ICLs and consequently contribute to the overall resistance to ICL agents.

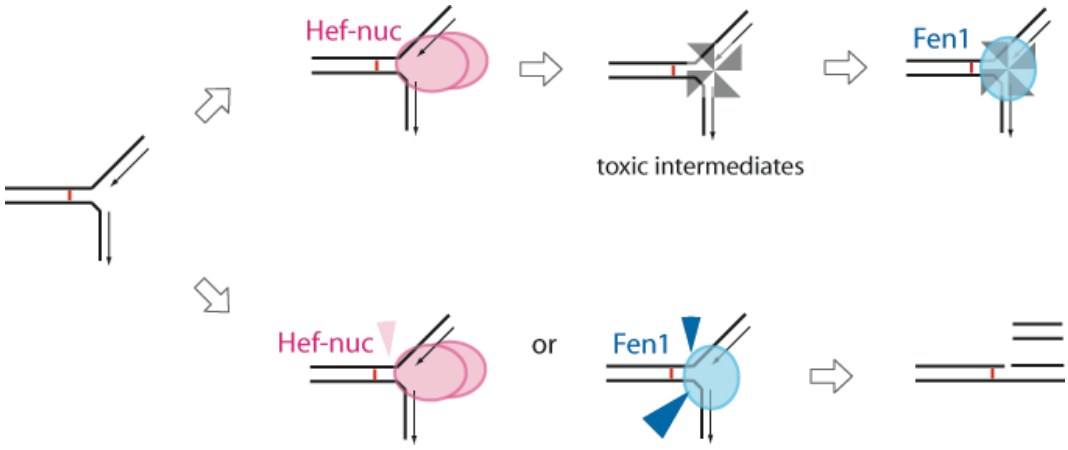

Figure 4.20 Possible pathways for the MMC induced ICL repair in *H. volcanii.*

MMC induced ICLs block DNA replication. In the absence of Hef helicase domain, Hef nuclease activity might generate some toxic intermediates that require Fen1 for further processing. Alternatively, Hef nuclease domain alone can cleave the leading strand template near the branch point with very low efficiency. Fen1 can cleave the blocked DNA replication fork with the preference of the lagging strand template. Thus, Fen1 might have overlapping functions with Hef in the processing of stalled replication forks to initiate homologous recombination repair.

Notably, cells with double deletion of Fen1 and the Hef helicase domain appeared to be more sensitive to MMC than cells with double deletion of Fen1 and Hef. Biochemical studies have shown that the nuclease domain of Hef from euryarchaeon *P. furiosus* can recognize flap or forked DNA substrate independently, and the coexistence of Hef helicase domain does not disturb the substrate specificity or the cleavage site of the Hef nuclease domain (Komori et al., 2004). However, the nuclease activity can be dramatically stimulated by the helicase activity, which can migrate the branch point close to the 5'-end of the nascent lagging strand. There are at least two possibilities to explain the observed severe phenotype of the Fen1 and Hef helicase deletion mutant (Figure 4.20). The Hef nuclease activity alone might generate some toxic intermediates

in vivo, which need to be further processed by Fen1 in *H. volcanii*. Alternatively, the Hef nuclease domain could bind the ICL stalled replication fork but cleave poorly without the helicase domain. As a consequence, Fen1 is required to resolve the situation. In support of the latter proposal, human Fen1 has been reported to possess a gap endonuclease (GEN) activity, which is possibly involved in the resolution of stalled replication forks (Zheng et al., 2005). The GEN activity specifically cleaves DNA replication-fork-like structures at the ssDNA region on either the lagging strand or the leading strand template. Moreover, GEN cleavage of the lagging strand template is about threefold more efficient than that of the leading strand template. Therefore, Hef and Fen1 might have overlapping functions in processing ICL stalled replication forks.

sfnA can suppress the MMC phenotype of _fen1_ deletion mutants

A spontaneous suppressor mutation *sfnA* appears to suppress the MMC sensitivity and slow growth, but not the UV sensitive phenotype of *fen1* deletion mutants. The suppression might be due to the up-regulation of a gene that has overlapping functions with *fen1*. Hef deletion mutants also have a phenotype of moderately slow growth. In addition, epistasis analysis showed that Hef and Fen1 have overlapping functions in MMC induced ICL repair. However, the results of RT-PCR showed that the transcript levels of *hef* were normal in the mutants with *sfnA*. Genetic studies have shown that deletion of *rad27*, the *fen1* homologue in yeast, leads to lethality in combination with a deletion of *pol3* exonulcease, or either the *RAD51* or *RAD52* epistasis group of genes (Tishkoff et al., 1997b; Symington, 1998; Jin et al., 2001). These data suggest that some backup pathways exist for the functions of Fen1. It might be compensatory mutation in other genes, such as nucleases or recombination proteins, to confer normal growth and MMC resistance to *fen1* deletion mutants. Alternatively, *sfnA* might be an activator of a cryptic gene.

The Mre11Rad50 complex is involved in MMC induced ICLs repair

In the absence of *hef* or *fen1*, deletion of *mre11rad50* led to increased MMC sensitivity, suggesting that the Mre11 complex is involved in a different pathway from those where Hef or Fen1 are involved. The Mre11Rad50 complex has been known to deal with DSBs (Lee and Paull, 2005). DSBs have been observed after introduction of ICLs in yeast and mammalian cells (Lehoczky et al., 2007). Using pulsed-field electrophoresis, we failed to identify MMC induced DSBs in *H. volcanii*, suggesting that DSBs might be transient intermediates. The UvrABC system or some other nuclease could cleave

around the ICLs, and the subsequent collapse of the replication fork would generate DSBs. In the presence of homologous DNA, HR can repair ICLs (Noll et al., 2006). *H. volcanii* has at least 10 copies of the genome per cell, indicating that intact homologous DNA might be available throughout the cell circle (Breuert et al., 2006). Therefore, HR might also be involved in ICL repair in *H. volcanii*. Consistent with this speculation, the *radA* deletion strain is severely sensitive to MMC, with the survival fraction of 10^{-7} in the presence of 0.02 μg/ml MMC (Haldenby, 2007).

TLS may be involved in ICL repair as a minor pathway

In bacteria and eukaryotes, translesion synthesis is used as a minor way for the repair of ICLs. In HR deficient strains of *E. coli*, DNA polymerase II cooperate with NER to bypass nitrogen mustard introduced ICLs (Berardini et al., 1999). More recently, Pol IV, a member of Y family DNA polymerase, has been demonstrated to bypass N2-N2-guanine ICLs (Kumari et al., 2008). In G1 phase yeast cells, the combination of NER and polζ has been shown to be the only pathway of ICL repair (Sarkar et al., 2006). Recently, it has been demonstrated that human Polκ, also a member of the Y family of DNA polymerase, can catalyze accurate incorporation opposite MMC cross-linked guanine and replicate beyond the lesion (Ohmori et al., 2004; Minko et al., 2008). In addition, both cell survival and chromosomal stability have been found to be adversely affected in Polκ depleted cells following MMC exposure, suggesting a role for Polκ in the processing of MMC induced ICLs.

The deletion mutants of *polX* and/or *polY* exhibited normal MMC resistance. However, in the absence of Fen1, deletion of *polX* appeared to further decrease the survival fraction. From the results of the H_2O_2 test, it is speculated that PolX from *H. volcanii* is an error prone polymerase for the repair of oxidative DNA damage. Therefore, TLS seems to be involved in the repair of MMC induced DNA damage as a minor pathway in *H. volcanii*. It would be interesting to examine the fidelity of this minor pathway.

Chapter V: End-joining and Recombination Tests

5.1 Introduction

The experiments described in this chapter aim to elucidate the role of the three proteins, Hef, Fen1 and UvrD, in DNA end–joining and homologous recombination. In addition, the effect of altering the ratio of crossover and non-crossover recombination in deletion mutants is described.

The transformation of *H. volcanii* with plasmid DNA is a multi-step process. The process of transformation itself could significantly affect cell survival. The surface protein layer encapsulating *H.volcanii* is called the S-layer. As a necessary step of transformation, the S-layer has to be removed from the cells by chelation of Mg^{2+} with EDTA (Charlebois et al., 1987). After this treatment, cells form spheroplasts, which are more susceptible to lysis. Some strains could be more sensitive to lysis than others so this factor is taken into account by measuring the viable cell count following the transformation procedure, so that any recombination events can be measured relative to the cell viability. Secondly, the plasmid DNA must then enter the cell. It cannot simply be assumed that the frequency of DNA uptake is equal in all strains. Any reduction in the efficiency of DNA uptake and transformation efficiency could be misinterpreted as a reduction in the frequency of end-joining or recombination. Finally, if the plasmid cannot replicate *in vivo*, it is only at this stage that the recombinogenic ability of the strain is tested by integration of the plasmid onto the chromosome at regions of homology. Thus, to measure the recombination efficiency of a strain, it is necessary to first determine the efficiency of DNA uptake for each strain assayed.

Four strains were used in the assays in this chapter. H195 was used as the wild–type control; H364, H522 and H518 were daughter strains derived from H195 but with *hef*, *fen1* and *uvrD* deletion, respectively. The viable cell count following the transformation suggested that these four strains are not sensitive to the process of transformation. Therefore the ratios of viable cell count between these strains were presumed to be the same before and after the transformation (Table 3.2).

An assay to determine the DNA uptake efficiency of each strain was carried out. This was achieved by transforming cells with 1 μg of the replicative plasmid pTA277. pTA277 contains the selectable marker *pyrE2*, a uracil biosynthesis gene (Allers et al.,

2004). Transformants were obtained on selective media (Hv-Ca + Trp + Thy, tryptophan and thymidine were supplemented as strains used in this chapter are Δ*trpA* and Δ*hdrB*). Transformation frequency is defined as the ratio of transformants per μg DNA to the total viable count. The relative transformation efficiency of each deletion strain was demonstrated by comparing transformation frequencies between the deletion strain and the wild-type strain, i.e.

$$\text{Relative transformation efficiency} = \frac{\text{Transformation frequency } \Delta}{\text{Transformation frequency WT}}$$

$$= \frac{\text{Transformants per μg DNA } \Delta \text{ / Viable cell count } \Delta}{\text{Transformants per μg DNA WT / Viable cell count WT}}$$

In addition to the *pyrE2* gene, pTA277 contains *ori-pHV2*, a *H. volcanii* origin of replication present on the plasmid pHV2 (Charlebois et al., 1987). The presence of this origin actually prevents the integration of pTA277 onto the chromosome at regions of homology, as this origin is not tolerated on the chromosome by *H. volcanii* (T. Allers, unpublished data). This effectively ensures that all factors associated with recombination are eliminated from this assay and any *ura*$^+$ colonies observed following growth on selective media would be due solely to the transformation of the plasmid DNA. The relative transformation efficiency of each strain can then be used to correct any results obtained from the recombination assays in this chapter, thus providing a true value of the frequency of recombination. I.e.

$$\text{True event frequency} = \frac{\text{Observed event frequency}}{\text{Transformation efficiency}}$$

5.2 Results

5.2.1 Transformation efficiency with pTA277

Generally, transformation with circular DNA is efficient in *H. volcanii*, i.e. around 10^6 transformants per μg DNA (Table 5.1). Both the transformation efficiencies of H364 (Δ*hef*) and H522 (Δ*fen1*) were shown to be about 79% of that of H195. The transformation efficiency of H518 (Δ*uvrD*) was lower, at about 75% of the transformation efficiency of H195 (wild-type).

Due to the limited differences between the transformation efficiencies of deletion strains and the wild-type strain, paired T tests were carried out to test the hypothesis that the

transformation efficiency of each deletion strain was lower than that of the wild-type strain. The *p* values of these tests are reported in Table 5.1. The T test results showed that there is no significant difference between the transformation efficiency of the deletion strains and that of the wild-type strain, since the *p* values are all more than 0.05. Therefore, the ability of DNA uptake in H364 (Δ*hef*), H522 (Δ*fen1*) and H518 (Δ*uvrD*) are assumed to be similar to that of H195 (wild-type).

Strain	Viable cell count relative to *wt*	Transformation frequency (transformants / μg DNA)	Tranformation efficiency relative to *wt* [a]	
wt	1.0	1.7E+6 ± 3.7E+5	1.0	
Δ*hef*	0.96	1.3E+6 ± 3.6E+5	0.79 ± 0.13	(*p* = 0.069)
Δ*fen1*	0.93	1.1E+6 ± 2.5E+5	0.79 ± 0.23	(*p* = 0.20)
Δ*uvrD*	1.1	1.3E+6 ± 5.2E+5	0.75 ± 0.18	(*p* = 0.10)

Table 5.1 Transformation frequency and efficiency with circular pTA277.

The transformation frequency of H195 (wild-type), H364 (Δ*hef*), H522 (Δ*fen1*) and H518 (Δ*uvrD*) were measured as transformants obtained after transformation with 1 μg DNA. The relative transformation efficiencies were calculated. The means and standard errors of 10 independent experiments are reported, except for H518 (Δ*uvrD*) where 8 independent experiments were done. [a] Significant differences compared to wild-type were calculated by T test and the *p* values are shown.

5.2.2 End-joining and recombination assay

pTA277 is a replicative plasmid containing a pHV2 origin, a *pyrE2* marker and a functional β-galactosidase gene *bgaHa*, within which there is a *Bst*BI site. In strains with the *bgaHa-Bb* allele such as H195, H364, H522 and H518, a 26 bp oligonucleotide is inserted at the *Bst*BI site of *bgaHa*. Consequently, the *bgaHa* gene is inactivated and an *Nco*I site replaces the original *Bst*BI site. pTA277 was digested by *Bst*BI and gel purified. The linear DNA was used to transform H195 (wild-type), H364 (Δ*hef*), H522 (Δ*fen1*) and H518 (Δ*uvrD*). *pyrE2*$^+$ transformants were selected on media lacking uracil (Hv-Ca + Trp + Thy).

There are three types of events that can lead to *pyrE2*$^+$ transformants (Figure 5.1). Firstly, cells may undergo accurate end-joining of the linear pTA277 and become

pyrE2^{+} *bgHa*$^{+}$. Secondly, cells may process the DNA ends, ligate the plasmid through inaccurate end-joining and become *pyrE2*$^{+}$ *bgHa*$^{-}$. Thirdly, cells may restore the circular plasmid DNA through homologous recombination and become *pyrE2*$^{+}$ *bgaHa-Bb*. *H. volcanii* lacks the activity of β-galactosidase and produces a characteristic pink pigment in the laboratory (Holmes and Dyall-Smith, 2000a). Only the colonies with the *bgaHa*$^{+}$ gene, which is a functional recombinant β-galactosidase gene, show blue in the presence of X-gal. Therefore, after transformation with linear pTA277, only those cells that have undergone accurate end-joining show blue in the presence of X-gal. To distinguish between accurate end-joining and homologous recombination, PCR was carried out. PBSF2 and PBSR3 are a pair of PCR primers that bind the flanking sequences of the *bgaHa* gene on pTA277. *Nco*I digestion on the PCR product results in DNA fragments of 2.62 and 0.66 kb for homologous recombination events, while other signs are distinguished as inaccurate end-joining (Figure 5.2).

Compared to the transformation frequency with circular pTA277 (Table 5.1), the transformation frequency with linear pTA277/*Bst*BI was approximately 3 orders lower in all tested strains, i.e. around 10^3 transformants per μg DNA (Table 5.2). Assuming that the abilities of uptake of circular and linear DNA are the same in each strain, the frequency of plasmid repair can be calculated as the ratio of transformation frequency transformed with linear DNA, relative to uncut DNA, i.e.

$$\text{Frequency of plasmid repair} = \frac{\text{pTA277/}\textit{Bst}\text{BI transformation frequency}}{\text{Uncut pTA277transformation frequency}}$$

As table 5.2 shows, H195 (wild-type), H522 (Δ*fen1*) and H518 (Δ*uvrD*) have very similar frequencies of plasmid repair, with means of 2.2E-3, 2.1E-3 and 2.2E-3, respectively. The plasmid repair frequency of H364 (Δ*hef*) appeared to be much lower, with a mean value of 1.4E-3, which is about 60% of the frequency of H195 (wild-type). A paired T test was carried out to test the hypothesis that the plasmid repair frequency of H364 (Δ*hef*) was lower than that of the H195 (wild-type). The T test results showed that there is a significant difference between the frequencies of these two strains, since the *p* value (0.021) is less than 0.05. Therefore, it is concluded that the frequency of plasmid repair in H364 (Δ*hef*) is lower than that of H195 (wild-type).

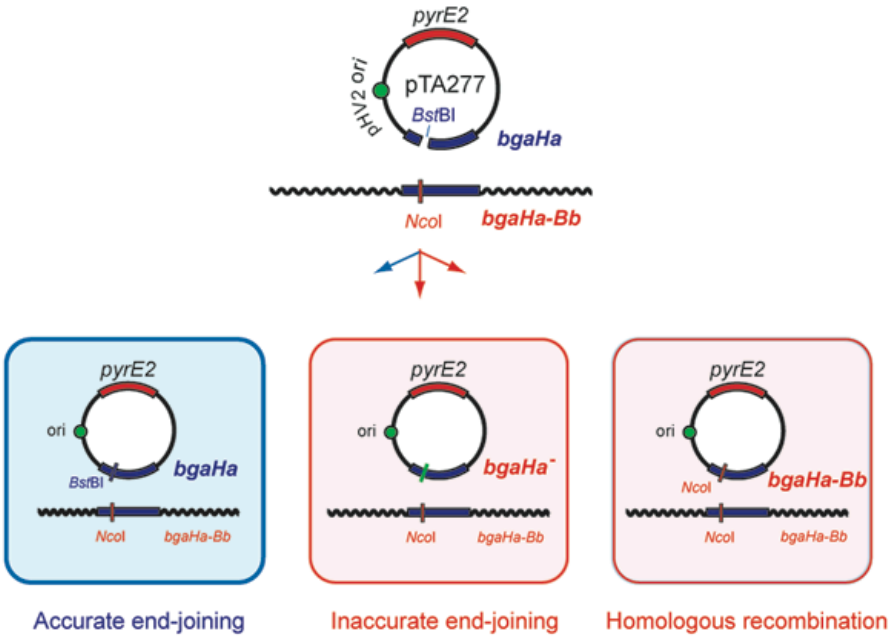

Figure 5.1 Schematic of pTA277/BstBI transformation.

pTA277 is a replicative plasmid containing a pHV2 origin, a *pyrE2* marker and a functional β-galactosidase gene *bgaHa,* which harbours a *Bst*BI site. Linear pTA277 digested by *Bst*BI is used to transform *pyrE2*$^-$ *bgHa-Bb* strains. *pyrE2*$^+$ transformants are selected on media lacking uracil (Hv-Ca + Trp + Thy). Either colonies have undergone accurate end-joining of the linear plasmid DNA and become *pyrE2*$^+$ *bgHa*$^+$, or have ligated the plasmid through inaccurate end-joining and become *pyrE2*$^+$ *bgHa*$^-$, or have repaired the DSB through homologous recombination and become *pyrE2*$^+$ *bgHa-Bb*. Only the colonies with the *bgaHa*$^+$ gene show blue in the presence of X-gal (accurate NHEJ). The other two events, inaccurate end-joining and homologous recombination, lead to red colonies that do not stain with X-gal.

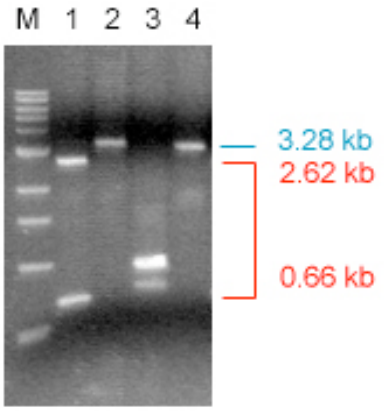

Figure 5.2 Electrophoresis of *Nco*I digested red colony PCR product.

M, size marker (from top to bottom): 10, 8, 6, 5, 4, 3, 2, 1.5, 1 and 0.5 kb. pTA277 plasmid DNA was used to amplify the 3.28 kb *bgaHa* region as a control (lane 2). Lanes 1, 3 and 4 were *Nco*I digested colony PCR products of pTA277/*Bst*BI transformants. If the colony had undergone homologous recombination, there should be two DNA fragments, 2.62 kb and 0.66 kb (lane 1). In lane 3 and 4, the unexpected electrophoresis patterns suggest the colonies had undergone inaccurate end-joining.

Strain	pTA277/*Bst*BI transformation frequenncy (transformants / μg DNA)	Frequency of plasmid repair
wt	2.3E+3 ± 2.7E+2	2.2E-3 ± 5.5E-4
Δ*hef*	8.6E+2 ± 1.2E+2	1.4E-3 ± 4.3E-4 (p = 0.021) [a]
Δ*fen1*	9.8E+2 ± 1.3E+2	2.1E-3 ± 9.6E-4
Δ*uvrD*	1.8E+3 ± 2.2E+2	2.2E-3 ± 4.7E-4

Table 5.2 Analysis of tranformation with pTA277/*Bst*BI.

The transformation efficiency of H195 (wild-type), H364 (Δ*hef*), H522 (Δ*fen1*) and H518 (Δ*uvrD*) were measured as transformants obtained after transformation with 1 μg DNA. The frequency of plasmid repair was calculated as the transformation efficiency with pTA277/*Bst*BI, relative to that with uncut pTA277. The means and standard errors of 10 independent experiments are reported, except that for H518 (Δ*uvrD*), where 8 independent experiments were carried out. [a] Significant difference compared to wild type was calculated by T test and the *p* value is shown.

In the presence of X-gal, blue or red colonies after transformation with pTA277/*Bst*BI indicates which events have taken place in the transformants (Figure 5.1). In all tested strains, most of the colonies turned out to be blue, suggesting that correct end-joining is the dominant event after the transformation with pTA277/*Bst*BI (Table 5.3 and Figure 5.3). H195 (wild-type), H522 (Δ*fen1*) and H518 (Δ*uvrD*) showed similar frequencies of correct end-joining, with means of 2.1E-3, 2.0E-3 and 2.0E-3, respectively. H364 (Δ*hef*) showed a much lower frequency of correct end-joining, with a mean value of 1.3E-3. A paired T test was carried out to test the hypotheses that the correct end-joining frequency of H364 (Δ*hef*) was lower than that of the H195 (wild-type). The *p* value (0.020) is less than 0.05, suggesting that there is a significant difference between the frequencies of these two strains. Therefore, it is concluded the frequency of correct end-joining in H364 (Δ*hef*) is lower than that of H195 (wild-type). From the data, the frequency of accurate end-joining in H364 (Δ*hef*) is about 60% of that of H195 (wild-type).

In the tested strains, less than 10% of transformants failed to stain with X-gal (red colonies), suggesting that incorrect end-joining and homologous recombination are minor events after transformation of pTA277/*Bst*BI (Table 5.3 and figure 5.3). H195 (wild-type) and H364 (Δ*hef*) showed similar frequencies of red colonies, with means of

7.6E-5 and 7.9E-5, respectively. H522 (Δ*fen1*) and H518 (Δ*uvrD*) showed a higher frequency of red colonies, with means of 1.4E-4 and 1.1E-4 respectively. Paired T tests were carried out to test the hypothesis that the red colony frequency of each deletion strain was higher than that of H195 (wild-type). The T test results showed that there is no significant difference between each deletion strain and the wild-type strain, since the *p* values are all more than 0.05. Therefore, it is concluded that the frequencies of incorrect end-joining and homologous recombination in H364 (Δ*hef*), H522 (Δ*fen1*) and H518 (Δ*uvrD*) are similar to that of H195 (wild-type).

Strain	Frequency of plasmid repair [a]	
	Blue colony (Correct end-joining)	Red colony (Incorrect end-joining & HR)
wt	2.1E-3 ± 5.4E-4	7.6E-5 ± 1.7E-5
Δ*hef*	1.3E-3 ± 4.2E-4 ($p = 0.020$)	7.9E-5 ± 2.8E-5 ($p = 0.45$)
Δ*fen1*	2.0E-3 ± 8.9E-4 ($p = 0.41$)	1.4E-4 ± 6.8E-5 ($p = 0.18$)
Δ*uvrD*	2.0E-3 ± 4.3E-4 ($p = 0.39$)	1.1E-4 ± 3.9E-5 ($p = 0.19$)

Table 5.3 Analysis of the frequency of circular plasmid restoration.

The transformation efficiencies of H195 (wild-type), H364 (Δ*hef*), H522 (Δ*fen1*) and H518 (Δ*uvrD*) were measured as transformants obtained after transformation with 1 µg DNA. The means and standard errors of 10 independent experiments are reported, except for H518 (Δ*uvrD*) where 8 independent experiments were done. [a] Significant differences compared to wild type were calculated by T test and the *p* values are shown.

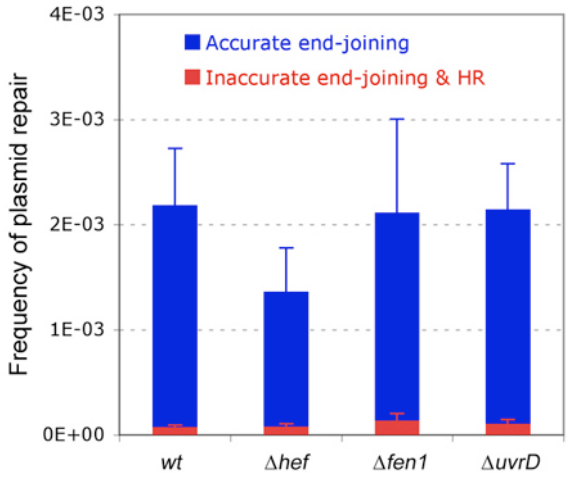

Figure 5.3 Analysis of plasmid repair.

Plasmid repair frequencies of H195 (wild-type), H364 (Δ*hef*), H522 (Δ*fen1*) and H518 (Δ*uvrD*) are shown. The frequencies of plasmid repair by accurate end-joining and by inaccurate end-joining/homologous recombination are shown in blue and red, respectively. Data are from Table 5.3.

To analyse the events that gave rise to the red colonies, PCR and *Nco*I digestion were carried out. As Table 5.4 shows, H195 (wild-type) and H364 (Δ*hef*) showed similar distributions of inaccurate end-joining and homologous recombination, i.e. 66% vs. 34% in H195 (wild-type) and 67% vs 33% in H364 (Δ*hef*). H518 (Δ*uvrD*) showed equal amount of inaccurate end-joining and homologous recombination. Compared to H195 (wild-type), H522 (Δ*fen1*) showed a lower percentage of inaccurate end-joining and higher percentage of homologous recombination, i.e. 36% vs. 64%. Due to the limited number of red colonies obtained from each independent experiment, it is hard to draw a conclusion about the role of Hef in inaccurate end-joining, or about whether the observed changes of distribution in H522 (Δ*fen1*) and H518 (Δ*uvrD*) are due to the deletion of *fen1* or *uvrD*.

Red colonies	H195 *wt*	H364 Δ*hef*	H522 Δ*fen1*	H518 Δ*uvrD*
Inaccurate end-joining	66% 37/56	67% 38/57	36% 8/22	50% 19/38
Homologous recombination	34% 19/56	33% 19/57	64% 14/22	50% 19/38

Table 5.4 Analysis of red colonies.

The percentage of inaccurate end-joining and that of homologous recombination are shown individually in red. The number of samples that were identified to have undergone inaccurate end-joining and homologous recombination are shown in black, followed by the total number of samples.

5.2.3 Non-crossover and crossover recombination assay

The plasmid utilised in this experiment was pTA168, containing a *pyrE2* marker and a mutant allele of the leucine biosynthesis gene, *leuB* (Allers et al., 2004). This particular allele (*leuB-Aa2*) contains an oligonucleotide insertion towards the 5' of the gene. Strain H195 and its derivative strains, including H364, H522 and H518 contain a different *leuB* allele (*leuB-Ag1*) in place of the wild-type copy. This mutant allele has a similar oligonucleotide insertion but towards the 3' end of the gene.

H195 (wild-type), H364 (Δ*hef*), H522 (Δ*fen1*) and H518 (Δ*uvrD*) were transformed with 100 ng pTA168. All transformants were plated on media lacking leucine (Hv-Min + Trp + Thy + Ura. Tryptophan, thymidine and uracil were supplemented as strains used are Δ*trpA* Δ*hdrB* Δ*pyrE2*), therefore selecting for *leuB*$^+$ cells. *leuB*$^+$ cells may arise by two ways. Firstly, the plasmid and chromosomal *leuB* alleles could undergo

crossover recombination between the two oligonucleotide insertions, resulting in two chromosomal *leuB* alleles: *leuB-Aa2-Ag*1 and wildtype *leuB*. The integrant strain would be both *ura*$^{+}$ (*pyrE2*$^{+}$) and prototrophic for leucine (*leuB*$^{+}$) (Figure 5.4). Secondly, the plasmid-borne *leuB-Aa2* sequence could be used as a template to convert the chromosomal *leuB-Ag1* allele to wild-type *leuB*. The strain would then be *leuB*$^{+}$ but *ura*$^{-}$, since the plasmid carrying the *pyrE2* marker was not integrated (Figure 5.4).

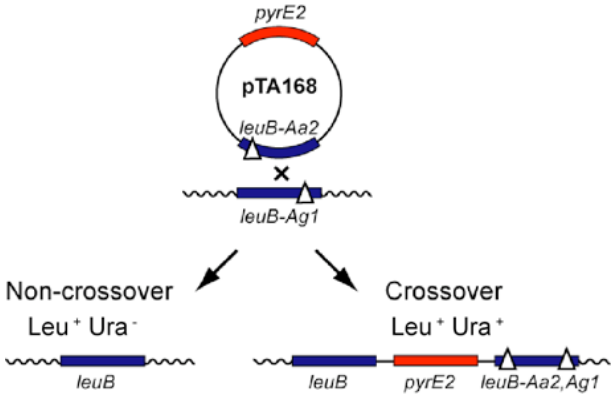

Figure 5.4 Schematic of non-crossover recombination assay.

An integrative plasmid containing *pyrE2* and a mutant *leuB* allele (pTA168) is used to transform ura- leu- (i.e. *leuB-Ag1*) strains. Following selection for Leu+ colonies by plating on media lacking leucine (Hv-Min + Trp + Thy + Ura), colonies have either undergone gene conversion of the chromosomal mutant *leuB* allele and become *leuB*$^{+}$ *ura*$^{-}$ (non-crossover recombination) or have integrated the plasmid onto the chromosome at the *leuB* locus, becoming both *leuB*$^{+}$ and *ura*$^{+}$ (crossover recombination). These two events can be distinguished by patching of Leu+ colonies on media lacking uracil (Hv-Min + Trp + Thy). Cells that grow on this media are crossover recombinants.

The total recombination frequency is defined as the ratio of the number of *leuB*$^{+}$ recombinants per μg DNA to the total viable count. The relative recombination efficiency of each deletion strain was calculated by comparing total recombination frequencies between the deletion strain and the wild-type strain, i.e.

$$\text{Relative recombination efficiency} = \frac{\text{Total recombination frequency } \Delta}{\text{Total recombination frequency WT}}$$

$$= \frac{\textit{LeuB}^{+} \text{ recombinants per μg DNA } \Delta \text{ / Viable cell count } \Delta}{\textit{LeuB}^{+} \text{ recombinants per μg DNA WT / Viable cell count WT}}$$

When *leuB*$^+$ colonies were visible after 7 days growth at 45°C, they were patched onto media that lacks uracil (Hv-Min + Trp + Thy). On this selective media, only crossover recombinants (*leuB*$^+$ *ura*$^+$) will grow. The frequency of crossover and non-crossover recombination can then be calculated by multiplying the total frequency of recombination by the fraction of colonies that grew on plates as described above, i.e.

Non-crossover frequency = Total recombination frequency (*leuB*$^+$) × % (*leuB*$^+$ *ura*$^-$)

Crossover frequency = Total recombination frequency (*leuB*$^+$) × % (*leuB*$^+$ *ura*$^+$)

The recombination frequencies and relative recombination efficiencies are shown in Table 5.5. The relative recombination efficiency of H364 (Δ*hef*) was shown to be significantly lower than that of H195 (wild-type), with the value of 0.44. H518 (Δ*uvrD*) showed a very similar recombination efficiency to that of H195 (wild-type) as the value was 1.0, and H522 (Δ*fen1*) showed 20% higher recombination frequency than that of H195. Paired T tests were carried out to test the hypothesis that the relative recombination frequencies of H522 (Δ*fen1*) and H518 (Δ*uvrD*) were higher than that of H195 (wild-type). The T test results showed that there is no significant difference between the values of the deletion strains and that of the wild-type strain, since the *p* values are both more than 0.05. Therefore, the recombination frequency of H522 (Δ*fen1*) and H518 (Δ*uvrD*) are concluded to be similar to that of H195 (wild-type).

Strain	Recombination frequency (*leuB*$^+$ recombinants/μg DNA)	Recombination efficiency relative to *wt* [a]	
wt	2.5E+3 ± 4.6E+2	1.0	
Δ*hef*	1.1E+3 ± 2.5E+2	0.44 ± 0.082	(p = 3.5E-5)
Δ*fen1*	3.0E+3 ± 8.0E+2	1.2 ± 0.21	(p = 0.18)
Δ*uvrD*	2.0E+3 ± 4.4E+2	1.0 ± 0.25	(p = 0.45)

Table 5.5 Recombination frequencies and efficiencies with pTA168.

The recombination frequencies of H195 (wild-type), H364 (Δ*hef*), H522 (Δ*fen1*) and H518 (Δ*uvrD*) were measured as *leuB*$^+$ transformants obtained after transformation with 1 μg DNA. Relative recombination efficiencies were calculated. The means and standard errors of recombination efficiency and frequency from 10 independent experiments are reported. [a] Significant differences compared to wild type were calculated by T test and the *p* values are shown.

leuB$^+$ colonies were patched onto selective media to distinguish crossover and non-crossover recombination. The data are presented in Table 5.6. H364 (Δ*hef*) showed much lower relative efficiencies of both non-crossover and crossover recombination compared with those of H195 (wild-type), with the values of 0.37 and 0.66, respectively. These data suggests that Hef is involved in both non-crossover and crossover recombination. In the absence of Hef, non-crossover recombination is affected more severely compared to crossover recombination.

Strain	Non-crossover		Crossover	
	Percentage [a]	Efficiency relative to *wt*	Percentage	Efficiency relative to *wt*
wt	77 %	1.0	23 %	1.0
Δ*hef*	65 % (p=4.9E-5)	0.37	35 %	0.66
Δ*fen1*	72 % (p=0.038)	0.93	28 %	1.2
Δ*uvrD*	76 % (p=0.35)	0.99	24 %	1.0

Table 5.6 Crossover and non-crossover recombination.

The percentages of crossover and non-crossover recombination in H195 (wild-type), H364 (Δ*hef*), H522 (Δ*fen1*) and H518 (Δ*uvrD*) were measured and analysed. The relative efficiencies were calculated. The means and standard errors of 8 independent experiments are reported. [a] Significant differences compared to wild type were calculated by T test and the p values are shown.

As shown previously, the total recombination frequency (including both non-crossover and crossover recombination) of H522 (Δ*fen1*) was similar to that of the wild-type strain H195 (Table 5.5). H522 (Δ*fen1*) showed a slightly lower percentage of non-crossover recombination to that of H195 (wild-type), i.e. 72.03% vs. 77.08%. A paired T test shows the difference between the percentage of non-crossover (or crossover) recombination of H522 (Δ*fen1*) and that of H195 (wild-type) is significant, as the p value (0.038) is less than 0.05. Therefore, Fen1 does not affect the total recombination frequency, but does affect the proportion of cells that undergo non-crossover and crossover recombination. In the absence of Fen1, the frequency of non-crossover recombination is slightly decreased and accordingly, the frequency of crossover recombination is slightly increased.

Table 5.6 shows that H518 (Δ*uvrD*) has very similar frequencies of both recombination events to those of H195 (wild-type), i.e. relative non-crossover efficiency of 0.99 and relative crossover efficiency of 1.03. Therefore, deletion of *uvrD* does not affect non-crossover or crossover recombination.

5.3 Discussion

Recombination Substrates

The transformation process for *H. volcanii* is practical as the frequency of transformation with circular DNA is approximately 10^6 transformants/μg DNA. The strains used in this research have a similar ability of taking in DNA since they showed a similar transformation frequency with a replicative plasmid pTA277. Recombination frequency between linear plasmid and chromosome was approximately two orders lower than that between circular plasmid and chromosome in the tested strains. These observations are in contrast to recombination in yeast, where recombination frequencies between plasmid and chromosome are highly elevated if the plasmid DNA is first linearised. It is possible that double strand breaks, even with 'clean' ends, are not the primary substrate for homologous recombination in *H. volcanii*. Data elsewhere shows that Mre11Rad50 is responsible for inhibiting homologous recombination at DSBs in *H. volcanii* (Stéphane Delmas and Thorsten Allers, unpublished data).

Hef is important for end-joining and homologous recombination.

Archaeal Hef, like its eukaryal homologue Mus81, has been shown to prefer 3'-flap, nicked Holliday junction and fork structured DNA substrates (Ciccia et al., 2008). Recently, two different groups have reported that Sgs1 and Mus81-Mms4 collaborate to ensure proper recombination metabolism during meiosis in *S. cerevisiae* (Jessop and Lichten, 2008; Oh et al., 2008). Meiotic homologous recombination is initiated by DNA double stranded breaks, catalysed by the Spo11 nuclease (Keeney, 2001). Strand exchange with a homologous chromosome forms joint molecule (JM) intermediates from which repair synthesis can rescue. Repair of these DSBs produces heteroduplex DNA-containing recombinant products: crossover, with a reciprocal exchange of chromosome arms, and non-crossover, with only a local alteration of DNA. Unregulated crossover can cause instability of the genome, such as chromosome rearrangements and missegregation (Richardson et al., 2004). Sgs1 limits the formation of aberrant joint

molecule recombination intermediates and Mus81-Mms4 promotes the resolution of joint molecules (Jessop and Lichten, 2008; Oh et al., 2008).

H. volcanii harbours multiple copies of the genome, i.e. about 18 copies/cell during the exponential phase and 10 at the stationary phase (Breuert et al., 2006). It is highly possible that aberrant joint molecules can be generated during homologous recombination. On the other hand, *H. volcanii* exhibits efficient homologous recombination, suggesting toxic intermediates can be resolved efficiently. Following the deletion of the *hef* gene in *H. volcanii*, the relative efficiency of homologous recombination is decreased to about 44%. Further analysis showed that both the relative efficiencies of non-crossover recombination and crossover recombination were reduced, to 36% and 65%, respectively. These data suggest that Hef might resolve aberrant homologous recombination intermediates and affect both non-crossover and crossover, in a similar way to its homologue Mus81. Notably, the non-crossover recombination appears to be more dependent on Hef than the crossover recombination.

In a different assay, the efficiency of accurate end-joining was reduced to about 60% relative to wild-type in the absence of *hef*. In this assay, *Bst*BI linearised plasmid DNA with complementary ends was used to examine the end-joining ability of cells. The majority of the complementary ends were joined by simple ligation in both the wild-type strain and the *hef* deletion mutant. Therefore, Hef might be invovled in broken DNA end protection and/or alignment.

Fen1 might play a role in regulating the ratio of non-crossover to crossover recombination

Deletion of Fen1 showed no effect on the frequency of accurate end-joining. Considering the DNA substrates used to examine the end-joining ability, Fen1 may not be required to process the complementary DNA ends to facilitate end-joining. However, eukaryal Fen1 has been implied in nonhomologous end-joining by creating blunt ended double strands (Wu et al., 1999b; Liang et al., 2005). Using substrates with more complicated DNA ends might disclose the role of Fen1 in nonhomologous end-joining in *H. volcanii.*

In the absence of Fen1, the total frequency of homologous recombination was similar to that of the wild-type strain. However, FEN1 has been reported to remove heterologous sequences at DNA damage sites and facilitate DNA repair by homologous recombination in eukaryotic cells (Kikuchi et al., 2005). A possible interpretation of this

discrepancy is that intact circular plasmid DNA was used in our homologous recombination tests. Nevertheless, Fen1 appeared to affect homologous recombination in a way that is different from that of Hef. The ratio of non-crossover recombination frequency to crossover recombination frequency appeared to be decreased. The changes were subtle, suggesting that Fen1 might process some recombination intermediates and has a slight preference for non-crossover events.

UvrD

The deletion of *uvrD* from *H. volcanii* was shown to have no effect on the frequencies of accurate end-joining or homologous recombination. UvrD has been reported to be able to reverse recombination intermediates *in vivo* and *in vitro* (Zieg et al., 1978; Morel et al., 1993; Bierne et al., 1997; Petranovic et al., 2001; Veaute et al., 2005). In bacteria, inactivation of UvrD causes a hyper-recombination phenotype. UvrD has an important role in restarting stalled replication forks and facilitates this process by displacing the RecA protein from DNA (Flores et al., 2005; Veaute et al., 2005). The anti-recombination role has also been suggested to be associated with non-replication events, such as RecBCD-dependent recombination during Hfr conjugation and certain RecFOR-dependent recombination events (Zieg et al., 1978; Bierne et al., 1997). The plasmid DNA used in this project might not be the preferred substrate for UvrD therefore, limiting the study of the *in vivo* function of UvrD. Alternatively, UvrD might have a different role in *H. volcanii.*

Chapter VI: Screen for Inducible Promoter

6.1 Introduction

Interest in the Archaea has grown steadily since being recognised as the third domain of life (Woese et al., 1990). A controlled system, where gene expression can be turned on or off by simple manipulation of growth conditions, would be valuable. Such a system would enable the construction of conditional lethal mutants in essential genes, as well as permitting the controlled over-production of archaeal proteins in their native host. Tools for the genetic manipulation of *H. volcanii* are better developed than those for most Archaea (Allers et al., 2004; Allers and Mevarech, 2005). We have therefore set out to identify promoters with a wide dynamic range of expression in this organism. The recently screened tryptophan-inducible promoter has been successfully used to analyse an essential chaperone gene *cct1* (Large et al., 2007) (Manuscript in Appendix). The work presented here is not the major part of this PhD project and will not be discussed in chapter VII. It is, however, included because the inducible promoter is promising to study some essential genes, for example *hel308a*, in *H. volcanii.*

6.2 Isolation of succinate-inducible promoter

H. volcanii is capable of growth on defined media using a single carbon source (Mevarech and Werczberger, 1985; Kauri et al., 1990). We hypothesised that gene expression in *H. volcanii* is regulated in response to specific sugars, akin to the arabinose-inducible *araBAD* promoter of *E. coli* (Guzman et al., 1995). To screen for sugar-inducible promoters we constructed the plasmid pTA425 (See Figure 6.1), which features a promoter-less *pyrE2* reporter gene for uracil biosynthesis (Bitan-Banin et al., 2003) that is insulated from read-through transcription by a terminator sequence (previously identified upstream of the L11e ribosomal gene of *H. volcanii*, (Shimmin and Dennis, 1996)). A partial *Aci*I digest of genomic DNA from *H. volcanii* Δ*pyrE2* Δ*trpA* strain H53 (Allers et al., 2004) was size-selected and fragments of ~500 bp were inserted into pTA425 between the terminator and *pyrE2* gene. The library was used to transform H53 and selection was carried out on minimal agar containing 0.5% of either glucose, glycerol, succinate or lactate. Since minimal media lacks uracil, only cells harbouring a pTA425 derivative with a promoter upstream of *pyrE2* will grow.

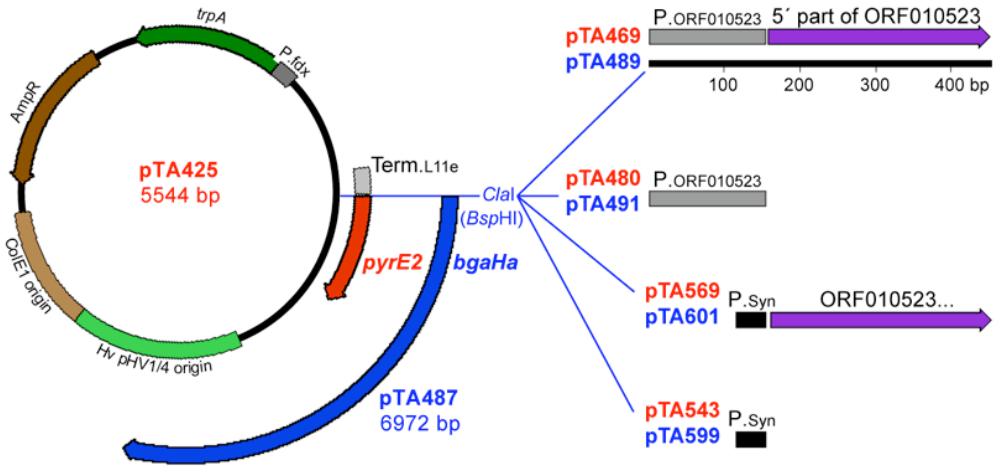

Figure 6.1 Isolation and further construction of succinate-inducible promoter.

pTA425 is a promoter-screen plasmid that is capable of replication in *H. volcanii* using the pHV1/4 origin (Norais et al., 2007b), and is selectable using the *trpA* marker (Allers et al., 2004). Potential promoters are inserted at the *Cla*I site located between a promoter-less *pyrE2* gene (Bitan-Banin et al., 2003) and a transcription terminator (Term.$_{L11e}$, derived from L11e ribosomal protein gene) (Shimmin and Dennis, 1996). pTA487 is based on pTA425, but features a *bgaHa* b-galactosidase reporter gene instead of *pyrE2*. The succinate-inducible/amino acid-repressible 454 bp *Aci*I fragment isolated from a genomic library was cloned in pTA469 and pTA489 (*pyrE2* and *bgaHa* reporters, respectively), while the 157 bp region upstream of ORF010523 was cloned in pTA480 and pTA491. To increase gene expression, the native promoter was replaced by a synthetic sequence (P.$_{Syn}$) based on the consensus tRNA promoter. This fusion construct was cloned in pTA569 and pTA601 (*pyrE2* and *bgaHa* reporters, respectively), while the synthetic promoter by itself was cloned in pTA543 and pTA599.

We obtained ~10^5 transformants per µg DNA, and these were subjected to a secondary screen on Hv-Ca (casamino acids) agar, to select for conditions under which promoters would be tightly repressed. One promising candidate emerged that grew on Hv-Min$_{suc}$ (minimal media + 0.5% succinic acid) but not on any other carbon source tested. Furthermore, the candidate failed to grow on Hv-Ca, regardless of whether succinate was added. Thus, the putative promoter is induced specifically by succinate and repressed by (cas) amino acids. Sequence analysis of the plasmid pTA469 (See Figure

6.1) revealed that the insert was a 454 bp *Aci*I fragment (bp 816,925 – 817,378 of the main chromosome). It comprised of 297 bp of the 5' part of ORF010523 (annotated as branched-chain amino acid ABC transporter amino acid binding protein), and 157 bp of the upstream sequence that should contain the succinate-inducible promoter.

6.3 Characterisation of succinate-inducible promoter

To evaluate the promoter, we used the *bgaHa* β-galactosidase reporter gene construct pTA487 and the Δ*pyrE2* Δ*trpA* Δ*bgaHv* strain H557 (Figure 6.1) (Holmes and Dyall-Smith, 2000b; Large et al., 2007). When the *Aci*I genomic DNA fragment from pTA469 was cloned in pTA489, very little blue staining was observed with Xgal (Figure 6.2). To confirm that this promoter was not particularly strong, the 157 bp region upstream of ORF010523 was analysed separately (Figure 6.1). The *bgaHa* plasmid pTA491 demonstrated that this region is a weak promoter and the *pyrE2* plasmid pTA480 indicated it is not repressible by amino acids (Figure 6.2). This suggests that control sequences responsible for repression by amino acids are located in the first 297 bp of ORF010523.

We therefore generated a fusion construct consisting of the 5' part of ORF010523, downstream of a 43 bp strong synthetic promoter (*p.syn*) based on the *H. volcanii* consensus tRNA promoter sequence (C. Daniels, personal communication). The fusion construct was inserted upstream of *pyrE2* to generate pTA569, or upstream of *bgaHa* to generate pTA601 (Figure 1A). Transformants containing pTA569 could grow on Hv-Min_{suc} but not Hv-Ca media, and cells containing pTA601 showed *bgaHa* expression only on Hv-Min_{suc} (Figure 1B). Control plasmids pTA543 and pTA569 contained the synthetic promoter only, and exhibited strong expression of *pyrE2* or *bgaHa*, respectively, on both Hv-Min_{suc} and Hv-Ca media (Figure 6.2).

We were able to confirm that critical regulatory sequences reside in the 5' part of ORF010523. However, the level of expression promoted by pTA601 was not particularly high, suggesting that the fusion construct was either suboptimally configured or that we had not determined the correct conditions for induction. A further disadvantage of this promoter is that induction by succinate requires the use of defined media and thus far, attempts to develop a minimal broth for *H. volcanii* have met with little success. Therefore, use of a succinate-inducible promoter would be limited to solid media.

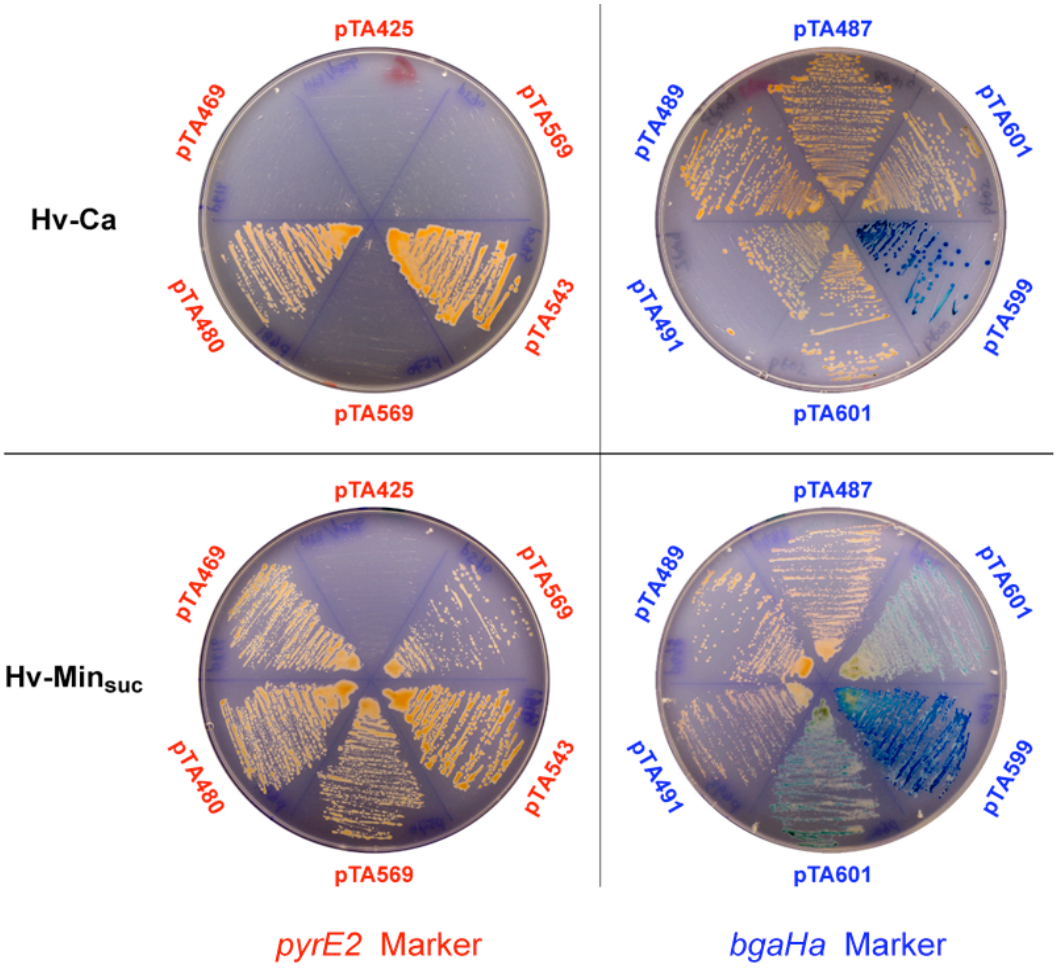

Figure 6.2 Character of different promoter constructions.

H. volcanii H53 (Δ*pyrE2* Δ*trpA*, left column) or H557 (Δ*pyrE2* Δ*trpA* Δ*bgaHv*, right column) were transformed with the plasmids described in Figure 6.1 and streaked on Hv-Ca (top row) or Hv-Min$_{suc}$ agar (bottom row). Colonies with *bgaHa* plasmids were sprayed with Xgal (right column). The fusion construct in pTA569 and pTA601, consisting of the synthetic promoter linked to the 5' part of ORF010523, confers succinate-inducible and amino acid-repressible gene expression.

6.4 Application of tryptophan-inducible promoter

Tryptophan is the most costly amino acid for the cell to synthesize. Therefore, tryptophan-regulated promoters might be good candidates. From Jörg Soppa's lab, microarray analysis of *H. volcanii* gene expression in the presence and absence of tryptophan identified a tryptophanase gene *tna* that showed strong induction in the presence of tryptophan (Large et al., 2007). The *tna* transcript level can increase more than 50-fold within 5 min by the induction of tryptophan. Most importantly, the *tna*

gene is hardly expressed in glucose medium, particularly when the promoter is on the chromosome. This indicates that the promoter would be ideally used as a molecular genetic tool to drive the regulated expression of other genes.

Large and colleagues confirmed the restricted regulation of the *tna* promoter (*p.tna*) by studying the expression of three independent reporter genes (*pyrE2*, *bgaHa* and *cct1*), which were fused downstream of the promoter. They also successfully constructed a conditional mutant of the essential *cct1* gene (in the absence of *cct2*) (Large et al., 2007). Thus, the *tna* promoter will be very promising for investigating some essential gene function in *H. volcanii* and potentially in other halophilic archaea.

Figure 6.3 shows three examples of using the promoter to construct a conditional mutant. In all strategies, the L11e terminator is inserted directly upstream of *p.tna* to block read-through transcription (Shimmin and Dennis, 1996). Firstly, the native promoter of the target gene can be replaced with *p.tna* simply by a *pyrE2* marked plasmid integration (Figure 6.3 A). This method leads to a 5' truncated gene with its native promoter and a full-length gene under *p.tna*. Secondly, the replacement of the native promoter with *p.tna* can be achieved by a pop-in pop-out (Figure 6.3 B). This strategy may be very useful to investigate some genes with functions related to the locus on the chromosome, since it aims at a cleaner replacement of the native promoter of the target gene compared to the first strategy. Thirdly, the target gene under *p.tna* can be inserted at the locus of some other gene already known to be non-essential, for example *pyrE2*. The target gene is then deleted from the original locus by a standard pop-in pop-out (Figure 6.3 C). To study an unknown gene, the pop-in pop-out system is normally carried out first and has been proven to be very efficient at knocking out non-essential genes in *H. volcanii*. For some essential genes that cannot be knocked out by this system, to construct a conditional mutant by the indirect strategy, the only extra construction required is to insert the entire gene coding sequence between the *tna* promoter and the *pyrE2* downstream region on the insertion plasmid.

Application of the *tna* promoter brings the possibility of constructing a conditional mutant in any gene. A successful construction enables further complementation studies with homologues to the gene of interest. In addition, the *tna* promoter is also useful to regulate the expression of some proteins that cause cell damage such as lysis or inclusion bodies, by growing cells to high density in media without tryptophan and then inducing with tryptophan late in a proper cell phase to allow reasonably high production of the protein.

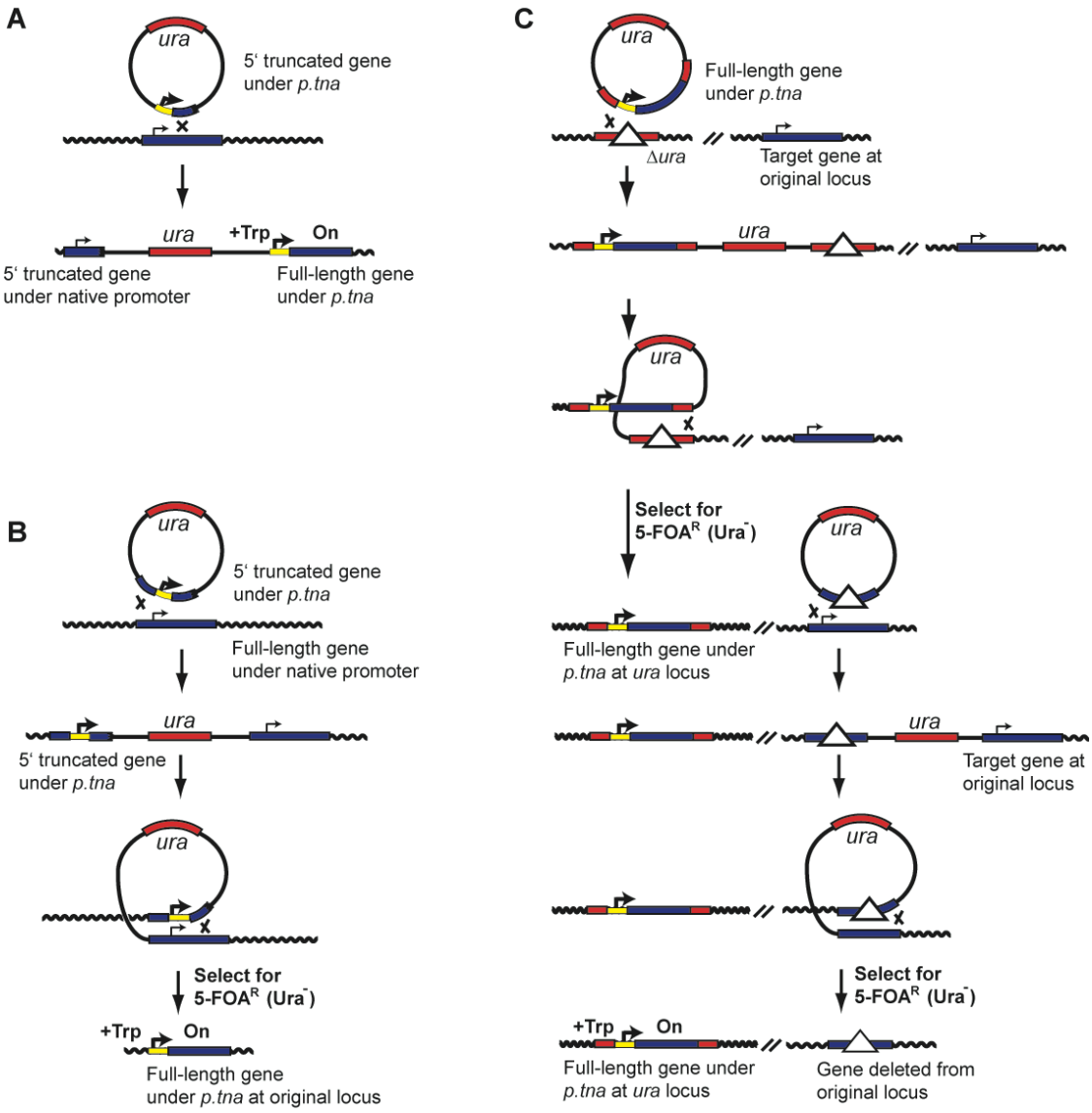

Figure 6.3 Construction of conditional mutant with tryptophan inducible promoter.

Figure 6.3 Construction of conditional mutant with tryptophan inducible promoter.

(A) The N-terminal part of the target gene under the promoter of *tna* gene (*p.tna*) is inserted into a plasmid with the auxotrophic marker *pyrE2* for uracil biosynthesis. Circular DNA is used to transform the *pyrE2*$^-$ strain and uracil prototrophic tansformants (*pyrE2*$^+$) are selected at the presence of tryptophan. Integration of the plasmid leads to a 5' truncated gene with its native promoter and a full-length gene under *p.tna*. (B) The N-terminal part of the target gene and its upstream region is inserted into a plasmid with the *pyrE2* marker. On this plasmid, the native promoter of the target gene is replaced by *p.tna.* Circular DNA is used to transform the *pyrE2*$^-$ strain and *pyrE2*$^+$ integrants are selected. Intramolecular recombinants that have lost the plasmid are counter-selected on plates containing tryptophan and 5-fluoroorotic acid (5-FOA), which is converted to toxic 5-fluorouracil in *pyrE2*$^+$ (but not *pyrE2*$^-$) cells. (C) The entire target gene under *p.tna* is first inserted at the *pyrE2* locus on the chromosome of the *pyrE2*$^-$ strain by the pop-in pop-out method. Then the target gene is deleted from its original locus by another round of pop-in pop-out, using a *pyrE2* marked plasmid with gene deletion construction.

Chapter VII: Conclusions and Future Perspectives

7.1 Conclusions

Biochemical and structural studies on archaeal Hef and Fen1 proteins have been reported in the past few years, but not genetic studies. In the studies described here, deletion mutants were constructed in *H. volcanii* and genetic data on the *in vivo* functions of Hef and Fen1 have been obtained. To clarify which repair pathway these two structure-specific endonucleases might be involved in, the genetic studies were also carried out on other proteins, such as UvrA, UvrD, PolX, PolY and Mre11Rad50. The major results are summarized in Table 7.1 and Table 7.2.

	Δhef	*Δhef-hel*	*Δhef-nuc*	*Δfen1*	*ΔuvrA*	*ΔuvrD*	*ΔpolX*	*ΔpolY*	*Δmre11rad50*
Growth	slightly slow	slightly slow	normal	slightly slow	normal	normal			±[a]
UV	normal	normal	normal	slightly sensitive	**Very sensitive**	normal			resistant
γ radiation	normal	normal	normal						
Phleomycin	resistant			resistant					resistant
H_2O_2	resistant	resistant	normal	**Very sensitive**	normal	normal	±[b]	normal	resistant
MMS	normal			**Very sensitive**	normal				
MMC	sensitive	sensitive	sensitive	sensitive	sensitive	normal	±[b]	normal	sensitive
End-joining	decreased			normal		normal			
Crossover	decreased			±[c]		normal			
Non-crossover	decreased			±[c]		normal			

Table 7.1 The phenotypes of mutants in the principal genes studied in this project.

[a] More obviously observed in strain with *hef* or *fen1* deletion. [b] Observed in the strain with *fen1* deletion. [a] and [b], also see Table 7.2. [c] The total efficiency of crossover and non-crossover recombination was normal in the absent of *fen1*, but the ratio of non-crossover recombination to crossover recombination appeared to be affected.

	Δ*hef*	Δ*fen1*
Δ*fen1*	Slower growth than Δ*hef* or Δ*fen1* Intermediate H_2O_2 sensitivity between Δ*hef* or Δ*fen1* More sensitive to MMC than Δ*hef* or Δ*fen1*	
Δ*uvrA*	More sensitive to MMC than Δ*hef* or Δ*uvrA*	More sensitive to MMC than Δ*fen1* or Δ*uvrA* More sensitive to UV than Δ*fen1* or Δ*uvrA*
Δ*mre11rad50*	Slower growth than Δ*hef* or Δ*mre11rad50* More resistant to H_2O_2 than Δ*hef* or Δ*mre11rad501* More sensitive to MMC than Δ*hef* or Δ*mre11rad50*	Slower growth than Δ*fen1* or Δ*mre11rad50* Intermediate H_2O_2 sensitivity between Δ*fen1* or Δ*mre11rad50* More sensitive to MMC than Δ*fen1* or Δ*mre11rad50*
Δ*polX*	Not determined	More sensitive to H_2O_2 than Δ*fen1* More sensitive to MMC than Δ*fen1*

Table 7.2 Synthetic phenotypes of mutants in the principal genes studied in the project.

Genetic analysis of Hef

hef deletion strains are not sensitive to UV irradiation. Therefore, unlike its eukaryotic homologue XPF/Rad1, the role of Hef is not significant for the repair of UV induced DNA damage.

In the absence of Hef or the Hef helicase domain, cells are slightly slow growing, while deficiency of Hef nuclease activity has no significant effect on normal growth. For the repair of H_2O_2 induced DNA damage, deletion of Hef or the Hef helicase domain confers cell resistance, while deletion of the Hef nuclease domain does not. In addition, mutants with Hef or Hef helicase domain deletion are more sensitive to mitomycin C than mutants with Hef nuclease domain deletion. Taken together, the Hef helicase activity is very important *in vivo.* This activity may be required for the Hef nuclease activity on some structure-specific intermediates. In the absence of Hef nuclease domain, the Hef helicase activity may cooperate with some other nuclease activity to maintain normal growth and genome integrity.

hef deletion mutants are more resistant to high doses of phleomycin than the wild-type. HR is the major pathway to repair DSBs in *H. volcanii*. Hef may be involved in NHEJ, which has lower fidelity than HR for the repair of DSBs. The deficient NHEJ in *hef* deletion mutants may increase the resistance at high doses of phleomycin by HR instead. In addition, using a plasmid repair assay, *hef* deletion mutants showed significant decrease of DSB repair by accurate end-joining. The plasmid DNA

substrates used in this assay have complementary ends, which can be simply ligated. Therefore, Hef might be involved in DNA end protection and/or alignment.

Hef also affects the efficiency of HR. Using a plasmid × chromosome assay, *hef* deletion cells were shown to be deficient for non-crossover recombination and to a lesser extent, crossover recombination. Recently, Mus81-Mms4 has been reported to promote the resolution of joint molecules during meiosis in yeast (Jessop and Lichten, 2008; Oh et al., 2008). Hef may resolve aberrant homologous recombination intermediates and affect both non-crossover and crossover recombination, in a similar way to its homologue Mus81.

Genetics analysis of Fen1

fen1 deletion mutants have a moderate UV sensitive phenotype, suggesting Fen1 is involved a minor pathway for UV induced DNA damage. By contrast, Fen1 is involved in the major pathway of oxidative and methylated DNA damage repair, since Δ*fen1* strains are very sensitive to H_2O_2 and MMS. Fen1 might also have a role in DNA replication, since Δ*fen1* strains grow slower than wild-type strains. Taken together, Fen1 from *H. volcanii*, like its eukaryal homologue FEN1/Rad27 may be responsible for the lagging strand maturation and play an important role in base excision repair.

Fen1 has been shown to be involved in two pathways for the repair of MMC induced DNA damage. Firstly, Fen1 has overlapping functions with Hef in one pathway. This may be due to the gap endonuclease activity of Fen1 in the processing of stalled replication forks to initiate homologous recombination. The other Fen1-dependent pathway may be base excision repair, which may be involved in the repair of MMC induced monoadducts and /or ICLs.

fen1 deletion mutants are more resistant to high doses of phleomycin than the wild-type. Fen1 may be responsible for the processing of some NHEJ intermediates. For the repair of DSBs, NHEJ has lower fidelity than HR and may accumulate lethal mutations. *fen1* deletion mutants may benefit from the deficient NHEJ at high doses of phleomycin by HR. However, using a plasmid repair assay, wild-type and *fen1* deletion cells showed no significant difference of DSB repair by accurate end-joining. In this assay, the plasmid DNA substrates have complementary ends, which may not require Fen1 for processing.

Using a plasmid × chromosome assay, we show that Fen1 does not affect the total recombination efficiency. Instead, Fen1 may regulate the ratio of non-crossover recombination to crossover recombination, with a slight preference for non-crossover recombination.

Finally, a spontaneous suppressor *sfnA* was obtained. Interestingly, *sfnA* can suppress the slow growth and MMC sensitivity, but not the UV sensitivity of *fen1* deletion mutants. Further analysis after the isolation of this suppressor would help us to understand more about the *in vivo* functions of Fen1.

NER in *H. volcanii*

Like most archaea, *H. volcanii* has homologues of some eukaryal NER proteins, including the helicases XPB and XPD, the single-stranded DNA binding protein RPA, and the nucleases XPF and XPG/Fen1. However, archaea lack obvious homologues of the eukaryal damage recognition proteins (Rad14 and Rad4 in yeast, XPA and XPC in mammals) and transcription-coupling factors (Rad28 and Rad26 in yeast, CSA and CSB in mammals) (Kelman and White, 2005). In addition, although there is some evidence that XPB from crenarchaeon *Archaeoglobus fulgidus* can unwind duplex DNA containing a UV photoproduct (Fan et al., 2006), *H*. volcanii mutants with deletion of *xpb* also appeared to have no defect after UV exposure (Michelle Hawkins, unpublished data). The results of this study clearly show that the role of Hef is not significant and Fen1 is involved in a minor pathway for the repair of UV induced DNA damage. By contrast, UvrA is a crucial factor.

The haloarchaeal *uvrA* gene probably encodes a protein that performs NER like its homologue in bacteria. The *uvrA*, *uvrB*, and *uvrC* genes in another halophilic archaea *Halobacterium sp.*NRC-1 have been reported to be required for UV induced DNA damage repair (Crowley et al., 2006). It has been suggested that the bacterial NER system was laterally transferred into archaea as the homologues of Uvr proteins have mainly been found in mesophilic methanogens and halophiles (McCready and Marcello, 2003; White, 2003). However, the UvrABC system in archaea is not simply transferred from bacteria as an integral unit. It is instead composed of genes transferred from different bacteria. Phylogenetic analysis has shown that individual Uvr genes in archaea come from diverse bacterial groups (Crowley et al., 2006). For example, the UvrA from *H. volcanii* and some other haloarchaeal species are most related to the UvrA from

bacteria *Thermus thermophilus* and *Thermus aquaticus*, while this is not true for UvrB, UvrC or UvrD.

Bacterial UvrD is a helicase with 3'-5' polarity, which is required for the displacement of DNA strands cleaved in NER (Sancar, 1996). In *E. coli*, *uvrD* mutants have been shown to be UV and ICL agent sensitive (Ogawa et al., 1968; Yoakum and Cole, 1977). Unlike in bacteria, the *uvrD* deletion mutants in *H. volcanii* appeared to be as resistant as wild-type strains to UV and MMC. Beside ORF01543_uvrD, another ORF encoding a functional UvrD homologue might exist in the genome of *H. volcanii*, but has not been annotated. However, DNA helicases are ubiquitous. There are several ORFs that have been annotated as helicases in *H. volcanii*. More likely, some redundancy of function occurs, for example with XPB. Eukaryotic XPB is a helicase with the same polarity as that of UvrD (Hwang et al., 1996). Further epistasis analysis is needed to examine the role of UvrD and XPB in *H. volcanii.*

7.2 Future perspectives

Identify the role of MMR factors in ICL repair

Our studies suggest that homologous recombination might be the major pathway for MMC induced DNA damage, while several pathways might act during the early stages of ICL repair, such as UvrA and Fen1 dependent pathways. The double deletion mutant of UvrA and Fen1 was viable in the presence of 0.02 μg/ml MMC and showed a survival fraction around 10^{-5}, which is about 100 times higher than that of the *radA* and *radB* deletion mutants. These data indicate that beside the UvrA- and Fen1-dependent pathways, there may be some other pathway to carry out the cleavage around MMC induced ICLs.

Recent studies have shown that MMR proteins are required for ICL repair. Human MutSβ (MSH2 and MSH3) binds to psoralen-induced ICLs and is required for the incisions proximal to a psoralen induced ICL (Zhang et al., 2002; Zhang et al., 2007a). In addition, biochemical studies of reconstituted human and yeast MMR have demonstrated a latent endonuclease activity within MutLα, which is capable of cleaving on either side of a mismatch (Kadyrov et al., 2006; Kadyrov et al., 2007). The endonuclease activity site of eukaryal MutLα includes a conserved metal binding motif, $DQHA(X)_2E(X)_4E$, within the COOH-terminus of human PMS2. The genome of *H. volcanii* encodes four homologues of MutS (MutS-1, MutS-2, MutS2-1, MutS2-2) and

two homologues of MutL (MutL-1, MutL-2). MutS-1, MutS-2, MutL-1 and MutL-2 have been shown to be involved in mismatch repair (Thorsten Allers, unpublished paper). Interestingly, the motif important for the endonuclease activity of eukaryal MutLα is also conserved in the two MutL homologues in *H. volcanii* (Figure 7.1). It is possible that the MMR proteins might carry out the single-stranded nicking that initiate ICL repair in *H. volcanii.*

S. cerevisiae	Pms1	699	IVDQHASDEKYNFETLQ 715
H. sapiens	PMS2	701	IVDQHATDEKYNFEMLQ 717
M. musculus	Pms2	698	LVDQHAADEKYNFEMLQ 714
H. volcanii	MutL-1	555	LVDQHAADERVNYERLR 571
H. volcanii	MutL-2	391	VVDQHAAHERINYERLR 407
	Consensus		-VDQHA--E--N-E-L-

Figure 7.1 Alignments about the DQHA(X)$_2$E(X)$_4$E motif of yeast Pms1, human PMS2, mouse Pms2, MutL-1 and MutL-2 from *H. volcanii.*

Identify the locus of suppressor *sfnA*

Two methods can be used to identify the locus of the suppressor mutation. The first method is to generate a plasmid library containing genomic DNA from the *sfnA* strain H823. As the genome of H823 contains *sfnA* and H522 does not, library DNA can be used to transform the latter in an attempt to confer suppression on H522. MMC plates can be used to screen for transformed H522 cells that had acquired *sfnA*, as they would survive better and grow faster than H522 cells without *sfnA*. Plasmid DNA can then be extracted from candidate survivors and the library fragment contained in the multiple cloning site can be sequenced to identify *sfnA*. However, this strategy relies on that *sfnA* being a dominant mutation with a low spontaneous mutation rate.

The genome project of *H. volcanii* is nearly finished and most of the DNA sequence is available. As genome sequencing techniques develop, they are becoming more affordable. The second method is to sequence the genome of H823 and compare it with the genome sequence of the standard strain. Direct sequencing may be quicker to screen out some candidates with mutated genes, but cloning and transformation of *fen1* deletion strains are required to further confirm the mutation is the suppressor of *fen1* deletion.

References

Aas, P.A., Otterlei, M., Falnes, P.O., Vagbo, C.B., Skorpen, F., Akbari, M., Sundheim, O., Bjoras, M., Slupphaug, G., Seeberg, E. and Krokan, H.E.: Human and bacterial oxidative demethylases repair alkylation damage in both RNA and DNA. Nature 421 (2003) 859-63.

Abe, H., Wada, M., Kohno, K. and Kuwano, M.: Altered drug sensitivities to anticancer agents in radiation-sensitive DNA repair deficient yeast mutants. Anticancer Res 14 (1994) 1807-10.

Aboussekhra, A., Chanet, R., Adjiri, A. and Fabre, F.: Semidominant suppressors of Srs2 helicase mutations of Saccharomyces cerevisiae map in the RAD51 gene, whose sequence predicts a protein with similarities to procaryotic RecA proteins. Mol Cell Biol 12 (1992) 3224-34.

Abraham, R.T.: Cell cycle checkpoint signaling through the ATM and ATR kinases. Genes Dev 15 (2001) 2177-96.

Abraham, R.T.: Checkpoint signalling: focusing on 53BP1. Nat Cell Biol 4 (2002) E277-9.

Acharya, S., Wilson, T., Gradia, S., Kane, M.F., Guerrette, S., Marsischky, G.T., Kolodner, R. and Fishel, R.: hMSH2 forms specific mispair-binding complexes with hMSH3 and hMSH6. Proc Natl Acad Sci U S A 93 (1996) 13629-34.

Adair, G.M., Rolig, R.L., Moore-Faver, D., Zabelshansky, M., Wilson, J.H. and Nairn, R.S.: Role of ERCC1 in removal of long non-homologous tails during targeted homologous recombination. Embo J 19 (2000) 5552-61.

Ahnesorg, P., Smith, P. and Jackson, S.P.: XLF interacts with the XRCC4-DNA ligase IV complex to promote DNA nonhomologous end-joining. Cell 124 (2006) 301-13.

Al-Minawi, A.Z., Saleh-Gohari, N. and Helleday, T.: The ERCC1/XPF endonuclease is required for efficient single-strand annealing and gene conversion in mammalian cells. Nucleic Acids Res 36 (2008) 1-9.

Allers, T. and Mevarech, M.: Archaeal genetics - the third way. Nat Rev Genet 6 (2005) 58-73.

Allers, T., Ngo, H.P., Mevarech, M. and Lloyd, R.G.: Development of additional selectable markers for the halophilic archaeon Haloferax volcanii based on the leuB and trpA genes. Appl Environ Microbiol 70 (2004) 943-53.

Altshuler, M.: Recovery of DNA replication in UV-damaged Escherichia coli. Mutat Res 294 (1993) 91-100.

Anderson, D.E., Trujillo, K.M., Sung, P. and Erickson, H.P.: Structure of the Rad50 x Mre11 DNA repair complex from Saccharomyces cerevisiae by electron microscopy. J Biol Chem 276 (2001) 37027-33.

Anderson, D.G. and Kowalczykowski, S.C.: The translocating RecBCD enzyme stimulates recombination by directing RecA protein onto ssDNA in a chi-regulated manner. Cell 90 (1997) 77-86.

Aoufouchi, S., Flatter, E., Dahan, A., Faili, A., Bertocci, B., Storck, S., Delbos, F., Cocea, L., Gupta, N., Weill, J.C. and Reynaud, C.A.: Two novel human and mouse DNA polymerases of the polX family. Nucleic Acids Res 28 (2000) 3684-93.

Aravind, L. and Koonin, E.V.: Prokaryotic homologs of the eukaryotic DNA-end-binding protein Ku, novel domains in the Ku protein and prediction of a prokaryotic double-strand break repair system. Genome Res 11 (2001) 1365-74.

Aravind, L., Walker, D.R. and Koonin, E.V.: Conserved domains in DNA repair proteins and evolution of repair systems. Nucleic Acids Res 27 (1999) 1223-42.

Ariza, A., Richard, D.J., White, M.F. and Bond, C.S.: Conformational flexibility revealed by the crystal structure of a crenarchaeal RadA. Nucleic Acids Res 33 (2005) 1465-73.

Assenmacher, N. and Hopfner, K.P.: MRE11/RAD50/NBS1: complex activities. Chromosoma 113 (2004) 157-66.

Augusto-Pinto, L., da Silva, C.G., Lopes Dde, O., Machado-Silva, A. and Machado, C.R.: Escherichia coli as a model system to study DNA repair genes of eukaryotic organisms. Genet Mol Res 2 (2003) 77-91.

Aylon, Y. and Kupiec, M.: The checkpoint protein Rad24 of Saccharomyces cerevisiae is involved in processing double-strand break ends and in recombination partner choice. Mol Cell Biol 23 (2003) 6585-96.

Bae, S.H. and Seo, Y.S.: Characterization of the enzymatic properties of the yeast dna2 Helicase/endonuclease suggests a new model for Okazaki fragment processing. J Biol Chem 275 (2000) 38022-31.

Bai, Y. and Symington, L.S.: A Rad52 homolog is required for RAD51-independent mitotic recombination in Saccharomyces cerevisiae. Genes Dev 10 (1996) 2025-37.

Baker, S.M., Plug, A.W., Prolla, T.A., Bronner, C.E., Harris, A.C., Yao, X., Christie, D.M., Monell, C., Arnheim, N., Bradley, A., Ashley, T. and Liskay, R.M.: Involvement of mouse Mlh1 in DNA mismatch repair and meiotic crossing over. Nat Genet 13 (1996) 336-42.
Bambara, R.A., Murante, R.S. and Henricksen, L.A.: Enzymes and reactions at the eukaryotic DNA replication fork. J Biol Chem 272 (1997) 4647-50.
Ban, N., Nissen, P., Hansen, J., Moore, P.B. and Steitz, T.A.: The complete atomic structure of the large ribosomal subunit at 2.4 A resolution. Science 289 (2000) 905-20.
Bankmann, M., Prakash, L. and Prakash, S.: Yeast RAD14 and human xeroderma pigmentosum group A DNA-repair genes encode homologous proteins. Nature 355 (1992) 555-8.
Barber, L.J., Ward, T.A., Hartley, J.A. and McHugh, P.J.: DNA interstrand cross-link repair in the Saccharomyces cerevisiae cell cycle: overlapping roles for PSO2 (SNM1) with MutS factors and EXO1 during S phase. Mol Cell Biol 25 (2005) 2297-309.
Barbour, L. and Xiao, W.: Regulation of alternative replication bypass pathways at stalled replication forks and its effects on genome stability: a yeast model. Mutat Res 532 (2003) 137-55.
Barnes, D.E., Stamp, G., Rosewell, I., Denzel, A. and Lindahl, T.: Targeted disruption of the gene encoding DNA ligase IV leads to lethality in embryonic mice. Curr Biol 8 (1998) 1395-8.
Barns, S.M., Delwiche, C.F., Palmer, J.D. and Pace, N.R.: Perspectives on archaeal diversity, thermophily and monophyly from environmental rRNA sequences. Proc Natl Acad Sci U S A 93 (1996) 9188-93.
Bassing, C.H., Swat, W. and Alt, F.W.: The mechanism and regulation of chromosomal V(D)J recombination. Cell 109 Suppl (2002) S45-55.
Bastin-Shanower, S.A., Fricke, W.M., Mullen, J.R. and Brill, S.J.: The mechanism of Mus81-Mms4 cleavage site selection distinguishes it from the homologous endonuclease Rad1-Rad10. Mol Cell Biol 23 (2003) 3487-96.
Bates, G. and Lehrach, H.: Trinucleotide repeat expansions and human genetic disease. Bioessays 16 (1994) 277-84.
Batty, D.P. and Wood, R.D.: Damage recognition in nucleotide excision repair of DNA. Gene 241 (2000) 193-204.
Bebenek, K., Garcia-Diaz, M., Patishall, S.R. and Kunkel, T.A.: Biochemical properties of Saccharomyces cerevisiae DNA polymerase IV. J Biol Chem 280 (2005) 20051-8.
Bebenek, K. and Kunkel, T.A.: Functions of DNA polymerases. Adv Protein Chem 69 (2004) 137-65.
Beernink, H.T. and Morrical, S.W.: RMPs: recombination/replication mediator proteins. Trends Biochem Sci 24 (1999) 385-9.
Belay, N., Sparling, R. and Daniels, L.: Dinitrogen fixation by a thermophilic methanogenic bacterium. Nature 312 (1984) 286-8.
Bell, S.D. and Jackson, S.P.: Mechanism and regulation of transcription in archaea. Curr Opin Microbiol 4 (2001) 208-13.
Bennett, C.B., Lewis, L.K., Karthikeyan, G., Lobachev, K.S., Jin, Y.H., Sterling, J.F., Snipe, J.R. and Resnick, M.A.: Genes required for ionizing radiation resistance in yeast. Nat Genet 29 (2001) 426-34.
Bentley, S.D., Chater, K.F., Cerdeno-Tarraga, A.M., et al.: Complete genome sequence of the model actinomycete Streptomyces coelicolor A3(2). Nature 417 (2002) 141-7.
Beranek, D.T.: Distribution of methyl and ethyl adducts following alkylation with monofunctional alkylating agents. Mutat Res 231 (1990) 11-30.
Berardini, M., Foster, P.L. and Loechler, E.L.: DNA polymerase II (polB) is involved in a new DNA repair pathway for DNA interstrand cross-links in Escherichia coli. J Bacteriol 181 (1999) 2878-82.
Bessho, T., Mu, D. and Sancar, A.: Initiation of DNA interstrand cross-link repair in humans: the nucleotide excision repair system makes dual incisions 5' to the cross-linked base and removes a 22- to 28-nucleotide-long damage-free strand. Mol Cell Biol 17 (1997a) 6822-30.
Bessho, T., Sancar, A., Thompson, L.H. and Thelen, M.P.: Reconstitution of human excision nuclease with recombinant XPF-ERCC1 complex. J Biol Chem 272 (1997b) 3833-7.
Bhatia, P.K., Verhage, R.A., Brouwer, J. and Friedberg, E.C.: Molecular cloning and characterization of Saccharomyces cerevisiae RAD28, the yeast homolog of the human Cockayne syndrome A (CSA) gene. J Bacteriol 178 (1996) 5977-88.
Bianco, P.R., Tracy, R.B. and Kowalczykowski, S.C.: DNA strand exchange proteins: a biochemical and physical comparison. Front Biosci 3 (1998) D570-603.
Bierne, H., Seigneur, M., Ehrlich, S.D. and Michel, B.: uvrD mutations enhance tandem repeat deletion in the Escherichia coli chromosome via SOS induction of the RecF recombination pathway. Mol Microbiol 26 (1997) 557-67.

Bishop, D.K.: RecA homologs Dmc1 and Rad51 interact to form multiple nuclear complexes prior to meiotic chromosome synapsis. Cell 79 (1994) 1081-92.
Bishop, D.K., Park, D., Xu, L. and Kleckner, N.: DMC1: a meiosis-specific yeast homolog of E. coli recA required for recombination, synaptonemal complex formation, and cell cycle progression. Cell 69 (1992) 439-56.
Bitan-Banin, G., Ortenberg, R. and Mevarech, M.: Development of a gene knockout system for the halophilic archaeon Haloferax volcanii by use of the pyrE gene. J Bacteriol 185 (2003) 772-8.
Blaseio, U. and Pfeifer, F.: Transformation of Halobacterium halobium: development of vectors and investigation of gas vesicle synthesis. Proc Natl Acad Sci U S A 87 (1990) 6772-6.
Blunt, T., Finnie, N.J., Taccioli, G.E., Smith, G.C., Demengeot, J., Gottlieb, T.M., Mizuta, R., Varghese, A.J., Alt, F.W., Jeggo, P.A. and et al.: Defective DNA-dependent protein kinase activity is linked to V(D)J recombination and DNA repair defects associated with the murine scid mutation. Cell 80 (1995) 813-23.
Blunt, T., Gell, D., Fox, M., Taccioli, G.E., Lehmann, A.R., Jackson, S.P. and Jeggo, P.A.: Identification of a nonsense mutation in the carboxyl-terminal region of DNA-dependent protein kinase catalytic subunit in the scid mouse. Proc Natl Acad Sci U S A 93 (1996) 10285-90.
Boddy, M.N., Gaillard, P.H., McDonald, W.H., Shanahan, P., Yates, J.R., 3rd and Russell, P.: Mus81-Eme1 are essential components of a Holliday junction resolvase. Cell 107 (2001) 537-48.
Boddy, M.N., Lopez-Girona, A., Shanahan, P., Interthal, H., Heyer, W.D. and Russell, P.: Damage tolerance protein Mus81 associates with the FHA1 domain of checkpoint kinase Cds1. Mol Cell Biol 20 (2000) 8758-66.
Boiteux, S. and Guillet, M.: Abasic sites in DNA: repair and biological consequences in Saccharomyces cerevisiae. DNA Repair (Amst) 3 (2004) 1-12.
Bolt, E.L., Lloyd, R.G. and Sharples, G.J.: Genetic analysis of an archaeal Holliday junction resolvase in Escherichia coli. J Mol Biol 310 (2001) 577-89.
Bork, J.M., Cox, M.M. and Inman, R.B.: The RecOR proteins modulate RecA protein function at 5' ends of single-stranded DNA. Embo J 20 (2001) 7313-22.
Botchan, M., Stringer, J., Mitchison, T. and Sambrook, J.: Integration and excision of SV40 DNA from the chromosome of a transformed cell. Cell 20 (1980) 143-52.
Boule, J.B., Rougeon, F. and Papanicolaou, C.: Terminal deoxynucleotidyl transferase indiscriminately incorporates ribonucleotides and deoxyribonucleotides. J Biol Chem 276 (2001) 31388-93.
Boulton, S.J. and Jackson, S.P.: Identification of a Saccharomyces cerevisiae Ku80 homologue: roles in DNA double strand break rejoining and in telomeric maintenance. Nucleic Acids Res 24 (1996) 4639-48.
Boulton, S.J. and Jackson, S.P.: Components of the Ku-dependent non-homologous end-joining pathway are involved in telomeric length maintenance and telomeric silencing. Embo J 17 (1998) 1819-28.
Bowater, R. and Doherty, A.J.: Making ends meet: repairing breaks in bacterial DNA by non-homologous end-joining. PLoS Genet 2 (2006) e8.
Boyd, J.B., Sakaguchi, K. and Harris, P.V.: mus308 mutants of Drosophila exhibit hypersensitivity to DNA cross-linking agents and are defective in a deoxyribonuclease. Genetics 125 (1990) 813-9.
Brendel, M., Bonatto, D., Strauss, M., Revers, L.F., Pungartnik, C., Saffi, J. and Henriques, J.A.: Role of PSO genes in repair of DNA damage of Saccharomyces cerevisiae. Mutat Res 544 (2003) 179-93.
Bressan, D.A., Baxter, B.K. and Petrini, J.H.: The Mre11-Rad50-Xrs2 protein complex facilitates homologous recombination-based double-strand break repair in Saccharomyces cerevisiae. Mol Cell Biol 19 (1999) 7681-7.
Breuert, S., Allers, T., Spohn, G. and Soppa, J.: Regulated polyploidy in halophilic archaea. PLoS ONE 1 (2006) e92.
Brochier-Armanet, C., Boussau, B., Gribaldo, S. and Forterre, P.: Mesophilic Crenarchaeota: proposal for a third archaeal phylum, the Thaumarchaeota. Nat Rev Microbiol 6 (2008) 245-52.
Brosh, R.M., Jr., von Kobbe, C., Sommers, J.A., Karmakar, P., Opresko, P.L., Piotrowski, J., Dianova, I., Dianov, G.L. and Bohr, V.A.: Werner syndrome protein interacts with human flap endonuclease 1 and stimulates its cleavage activity. Embo J 20 (2001) 5791-801.
Bruand, C. and Ehrlich, S.D.: UvrD-dependent replication of rolling-circle plasmids in Escherichia coli. Mol Microbiol 35 (2000) 204-10.
Buck, D., Malivert, L., de Chasseval, R., Barraud, A., Fondaneche, M.C., Sanal, O., Plebani, A., Stephan, J.L., Hufnagel, M., le Deist, F., Fischer, A., Durandy, A., de Villartay, J.P. and Revy, P.: Cernunnos, a novel nonhomologous end-joining factor, is mutated in human immunodeficiency with microcephaly. Cell 124 (2006) 287-99.
Budd, M.E. and Campbell, J.L.: A yeast replicative helicase, Dna2 helicase, interacts with yeast FEN-1 nuclease in carrying out its essential function. Mol Cell Biol 17 (1997) 2136-42.

Buermeyer, A.B., Deschenes, S.M., Baker, S.M. and Liskay, R.M.: Mammalian DNA mismatch repair. Annu Rev Genet 33 (1999) 533-64.
Burdett, V., Baitinger, C., Viswanathan, M., Lovett, S.T. and Modrich, P.: In vivo requirement for RecJ, ExoVII, ExoI, and ExoX in methyl-directed mismatch repair. Proc Natl Acad Sci U S A 98 (2001) 6765-70.
Buttner, K., Nehring, S. and Hopfner, K.P.: Structural basis for DNA duplex separation by a superfamily-2 helicase. Nat Struct Mol Biol 14 (2007) 647-52.
Cadet, J., Sage, E. and Douki, T.: Ultraviolet radiation-mediated damage to cellular DNA. Mutat Res 571 (2005) 3-17.
Cadman, C.J., Matson, S.W. and McGlynn, P.: Unwinding of forked DNA structures by UvrD. J Mol Biol 362 (2006) 18-25.
Callebaut, I., Moshous, D., Mornon, J.P. and de Villartay, J.P.: Metallo-beta-lactamase fold within nucleic acids processing enzymes: the beta-CASP family. Nucleic Acids Res 30 (2002) 3592-601.
Carlioz, A. and Touati, D.: Isolation of superoxide dismutase mutants in Escherichia coli: is superoxide dismutase necessary for aerobic life? Embo J 5 (1986) 623-30.
Caron, P.R., Kushner, S.R. and Grossman, L.: Involvement of helicase II (uvrD gene product) and DNA polymerase I in excision mediated by the uvrABC protein complex. Proc Natl Acad Sci U S A 82 (1985) 4925-9.
Carpousis, A.J.: Degradation of targeted mRNAs in Escherichia coli: regulation by a small antisense RNA. Genes Dev 17 (2003) 2351-5.
Carr, A.M., Schmidt, H., Kirchhoff, S., Muriel, W.J., Sheldrick, K.S., Griffiths, D.J., Basmacioglu, C.N., Subramani, S., Clegg, M., Nasim, A. and et al.: The rad16 gene of Schizosaccharomyces pombe: a homolog of the RAD1 gene of Saccharomyces cerevisiae. Mol Cell Biol 14 (1994) 2029-40.
Chaganti, R.S., Schonberg, S. and German, J.: A manyfold increase in sister chromatid exchanges in Bloom's syndrome lymphocytes. Proc Natl Acad Sci U S A 71 (1974) 4508-12.
Chan, D.W., Chen, B.P., Prithivirajsingh, S., Kurimasa, A., Story, M.D., Qin, J. and Chen, D.J.: Autophosphorylation of the DNA-dependent protein kinase catalytic subunit is required for rejoining of DNA double-strand breaks. Genes Dev 16 (2002) 2333-8.
Chang, J.H., Kim, J.J., Choi, J.M., Lee, J.H. and Cho, Y.: Crystal structure of the Mus81-Eme1 complex. Genes Dev 22 (2008) 1093-106.
Chapelle, F.H., O'Neill, K., Bradley, P.M., Methe, B.A., Ciufo, S.A., Knobel, L.L. and Lovley, D.R.: A hydrogen-based subsurface microbial community dominated by methanogens. Nature 415 (2002) 312-5.
Chappell, C., Hanakahi, L.A., Karimi-Busheri, F., Weinfeld, M. and West, S.C.: Involvement of human polynucleotide kinase in double-strand break repair by non-homologous end joining. Embo J 21 (2002) 2827-32.
Charlebois, R.L., Lam, W.L., Cline, S.W. and Doolittle, W.F.: Characterization of pHV2 from Halobacterium volcanii and its use in demonstrating transformation of an archaebacterium. Proc Natl Acad Sci U S A 84 (1987) 8530-4.
Charlebois, R.L., Schalkwyk, L.C., Hofman, J.D. and Doolittle, W.F.: Detailed physical map and set of overlapping clones covering the genome of the archaebacterium Haloferax volcanii DS2. J Mol Biol 222 (1991) 509-24.
Chase, J.W. and Richardson, C.C.: Exonuclease VII of Escherichia coli. Mechanism of action. J Biol Chem 249 (1974) 4553-61.
Chen, C., Merrill, B.J., Lau, P.J., Holm, C. and Kolodner, R.D.: Saccharomyces cerevisiae pol30 (proliferating cell nuclear antigen) mutations impair replication fidelity and mismatch repair. Mol Cell Biol 19 (1999a) 7801-15.
Chen, C.F., Chen, P.L., Zhong, Q., Sharp, Z.D. and Lee, W.H.: Expression of BRC repeats in breast cancer cells disrupts the BRCA2-Rad51 complex and leads to radiation hypersensitivity and loss of G(2)/M checkpoint control. J Biol Chem 274 (1999b) 32931-5.
Chen, L., Trujillo, K., Ramos, W., Sung, P. and Tomkinson, A.E.: Promotion of Dnl4-catalyzed DNA end-joining by the Rad50/Mre11/Xrs2 and Hdf1/Hdf2 complexes. Mol Cell 8 (2001a) 1105-15.
Chen, X.B., Melchionna, R., Denis, C.M., Gaillard, P.H., Blasina, A., Van de Weyer, I., Boddy, M.N., Russell, P., Vialard, J. and McGowan, C.H.: Human Mus81-associated endonuclease cleaves Holliday junctions in vitro. Mol Cell 8 (2001b) 1117-27.
Chen, Z., Xu, X.S., Harrison, J. and Wang, G.: Defining the function of xeroderma pigmentosum group F protein in psoralen interstrand cross-link-mediated DNA repair and mutagenesis. Biochem J 379 (2004) 71-8.
Chi, N.W. and Kolodner, R.D.: The effect of DNA mismatches on the ATPase activity of MSH1, a protein in yeast mitochondria that recognizes DNA mismatches. J Biol Chem 269 (1994) 29993-7.

Ciccia, A., Constantinou, A. and West, S.C.: Identification and characterization of the human mus81-eme1 endonuclease. J Biol Chem 278 (2003) 25172-8.
Ciccia, A., Ling, C., Coulthard, R., Yan, Z., Xue, Y., Meetei, A.R., Laghmani el, H., Joenje, H., McDonald, N., de Winter, J.P., Wang, W. and West, S.C.: Identification of FAAP24, a Fanconi anemia core complex protein that interacts with FANCM. Mol Cell 25 (2007) 331-43.
Ciccia, A., McDonald, N. and West, S.C.: Structural and Functional Relationships of the XPF/MUS81 Family of Proteins. Annu Rev Biochem 77 (2008) 259-287.
Clark, A.B., Valle, F., Drotschmann, K., Gary, R.K. and Kunkel, T.A.: Functional interaction of proliferating cell nuclear antigen with MSH2-MSH6 and MSH2-MSH3 complexes. J Biol Chem 275 (2000) 36498-501.
Clarke, A.A., Marsh, J.C., Gordon-Smith, E.C. and Rutherford, T.R.: Molecular genetics and Fanconi anaemia: new insights into old problems. Br J Haematol 103 (1998) 287-96.
Clarkson, S.G.: The XPG story. Biochimie 85 (2003) 1113-21.
Clerici, M., Mantiero, D., Lucchini, G. and Longhese, M.P.: The Saccharomyces cerevisiae Sae2 protein promotes resection and bridging of double strand break ends. J Biol Chem 280 (2005) 38631-8.
Cline, S.W., Lam, W.L., Charlebois, R.L., Schalkwyk, L.C. and Doolittle, W.F.: Transformation methods for halophilic archaebacteria. Can J Microbiol 35 (1989) 148-52.
Clingen, P.H., Arlett, C.F., Hartley, J.A. and Parris, C.N.: Chemosensitivity of primary human fibroblasts with defective unhooking of DNA interstrand cross-links. Exp Cell Res 313 (2007) 753-60.
Cloud, K.G., Shen, B., Strniste, G.F. and Park, M.S.: XPG protein has a structure-specific endonuclease activity. Mutat Res 347 (1995) 55-60.
Colaiacovo, M.P., Paques, F. and Haber, J.E.: Removal of one nonhomologous DNA end during gene conversion by a RAD1- and MSH2-independent pathway. Genetics 151 (1999) 1409-23.
Connelly, J.C., de Leau, E.S. and Leach, D.R.: DNA cleavage and degradation by the SbcCD protein complex from Escherichia coli. Nucleic Acids Res 27 (1999) 1039-46.
Connelly, J.C., de Leau, E.S., Okely, E.A. and Leach, D.R.: Overexpression, purification, and characterization of the SbcCD protein from Escherichia coli. J Biol Chem 272 (1997) 19819-26.
Constantinesco, F., Forterre, P., Koonin, E.V., Aravind, L. and Elie, C.: A bipolar DNA helicase gene, herA, clusters with rad50, mre11 and nurA genes in thermophilic archaea. Nucleic Acids Res 32 (2004) 1439-47.
Constantinou, A., Chen, X.B., McGowan, C.H. and West, S.C.: Holliday junction resolution in human cells: two junction endonucleases with distinct substrate specificities. Embo J 21 (2002) 5577-85.
Corry, P.M. and Cole, A.: Radiation-induced double-strand scission of the DNA of mammalian metaphase chromosomes. Radiat Res 36 (1968) 528-43.
Costa, R.M., Chigancas, V., Galhardo Rda, S., Carvalho, H. and Menck, C.F.: The eukaryotic nucleotide excision repair pathway. Biochimie 85 (2003) 1083-99.
Courcelle, J., Crowley, D.J. and Hanawalt, P.C.: Recovery of DNA replication in UV-irradiated Escherichia coli requires both excision repair and recF protein function. J Bacteriol 181 (1999) 916-22.
Couve-Privat, S., Mace, G., Rosselli, F. and Saparbaev, M.K.: Psoralen-induced DNA adducts are substrates for the base excision repair pathway in human cells. Nucleic Acids Res 35 (2007) 5672-82.
Crowley, D.J., Boubriak, I., Berquist, B.R., Clark, M., Richard, E., Sullivan, L., DasSarma, S. and McCready, S.: The uvrA, uvrB and uvrC genes are required for repair of ultraviolet light induced DNA photoproducts in Halobacterium sp. NRC-1. Saline Systems 2 (2006) 11.
Cunningham, R.P., Saporito, S.M., Spitzer, S.G. and Weiss, B.: Endonuclease IV (nfo) mutant of Escherichia coli. J Bacteriol 168 (1986) 1120-7.
D'Amours, D. and Jackson, S.P.: The Mre11 complex: at the crossroads of dna repair and checkpoint signalling. Nat Rev Mol Cell Biol 3 (2002) 317-27.
Daley, J.M., Laan, R.L., Suresh, A. and Wilson, T.E.: DNA joint dependence of pol X family polymerase action in nonhomologous end joining. J Biol Chem 280 (2005a) 29030-7.
Daley, J.M., Palmbos, P.L., Wu, D. and Wilson, T.E.: Nonhomologous end joining in yeast. Annu Rev Genet 39 (2005b) 431-51.
Damia, G., Guidi, G. and D'Incalci, M.: Expression of genes involved in nucleotide excision repair and sensitivity to cisplatin and melphalan in human cancer cell lines. Eur J Cancer 34 (1998) 1783-8.
Damia, G., Imperatori, L., Stefanini, M. and D'Incalci, M.: Sensitivity of CHO mutant cell lines with specific defects in nucleotide excision repair to different anti-cancer agents. Int J Cancer 66 (1996) 779-83.
Daniels, D.S., Woo, T.T., Luu, K.X., Noll, D.M., Clarke, N.D., Pegg, A.E. and Tainer, J.A.: DNA binding and nucleotide flipping by the human DNA repair protein AGT. Nat Struct Mol Biol 11 (2004) 714-20.

Danska, J.S., Holland, D.P., Mariathasan, S., Williams, K.M. and Guidos, C.J.: Biochemical and genetic defects in the DNA-dependent protein kinase in murine scid lymphocytes. Mol Cell Biol 16 (1996) 5507-17.
David, S.S., O'Shea, V.L. and Kundu, S.: Base-excision repair of oxidative DNA damage. Nature 447 (2007) 941-50.
Davies, A.A., Friedberg, E.C., Tomkinson, A.E., Wood, R.D. and West, S.C.: Role of the Rad1 and Rad10 proteins in nucleotide excision repair and recombination. J Biol Chem 270 (1995) 24638-41.
Davies, O.R. and Pellegrini, L.: Interaction with the BRCA2 C terminus protects RAD51-DNA filaments from disassembly by BRC repeats. Nat Struct Mol Biol 14 (2007) 475-83.
de Boer, J. and Hoeijmakers, J.H.: Nucleotide excision repair and human syndromes. Carcinogenesis 21 (2000) 453-60.
de Jager, M., van Noort, J., van Gent, D.C., Dekker, C., Kanaar, R. and Wyman, C.: Human Rad50/Mre11 is a flexible complex that can tether DNA ends. Mol Cell 8 (2001) 1129-35.
de Jong, M.M., Hofstra, R.M., Kooi, K.A., Westra, J.L., Berends, M.J., Wu, Y., Hollema, H., van der Sluis, T., van der Graaf, W.T., de Vries, E.G., Schaapveld, M., Sijmons, R.H., te Meerman, G.J. and Kleibeuker, J.H.: No association between two MLH3 variants (S845G and P844L)and colorectal cancer risk. Cancer Genet Cytogenet 152 (2004) 70-1.
De la Torre, C., Pincheira, J. and Lopez-Saez, J.F.: Human syndromes with genomic instability and multiprotein machines that repair DNA double-strand breaks. Histol Histopathol 18 (2003) 225-43.
de Laat, W.L., Appeldoorn, E., Jaspers, N.G. and Hoeijmakers, J.H.: DNA structural elements required for ERCC1-XPF endonuclease activity. J Biol Chem 273 (1998a) 7835-42.
de Laat, W.L., Sijbers, A.M., Odijk, H., Jaspers, N.G. and Hoeijmakers, J.H.: Mapping of interaction domains between human repair proteins ERCC1 and XPF. Nucleic Acids Res 26 (1998b) 4146-52.
de los Santos, T., Loidl, J., Larkin, B. and Hollingsworth, N.M.: A role for MMS4 in the processing of recombination intermediates during meiosis in Saccharomyces cerevisiae. Genetics 159 (2001) 1511-25.
De Silva, I.U., McHugh, P.J., Clingen, P.H. and Hartley, J.A.: Defining the roles of nucleotide excision repair and recombination in the repair of DNA interstrand cross-links in mammalian cells. Mol Cell Biol 20 (2000) 7980-90.
De Silva, I.U., McHugh, P.J., Clingen, P.H. and Hartley, J.A.: Defects in interstrand cross-link uncoupling do not account for the extreme sensitivity of ERCC1 and XPF cells to cisplatin. Nucleic Acids Res 30 (2002) 3848-56.
Debrauwere, H., Loeillet, S., Lin, W., Lopes, J. and Nicolas, A.: Links between replication and recombination in Saccharomyces cerevisiae: a hypersensitive requirement for homologous recombination in the absence of Rad27 activity. Proc Natl Acad Sci U S A 98 (2001) 8263-9.
Della, M., Palmbos, P.L., Tseng, H.M., Tonkin, L.M., Daley, J.M., Topper, L.M., Pitcher, R.S., Tomkinson, A.E., Wilson, T.E. and Doherty, A.J.: Mycobacterial Ku and ligase proteins constitute a two-component NHEJ repair machine. Science 306 (2004) 683-5.
DellaVecchia, M.J., Croteau, D.L., Skorvaga, M., Dezhurov, S.V., Lavrik, O.I. and Van Houten, B.: Analyzing the handoff of DNA from UvrA to UvrB utilizing DNA-protein photoaffinity labeling. J Biol Chem 279 (2004) 45245-56.
DeLong, E.F. and Pace, N.R.: Environmental diversity of bacteria and archaea. Syst Biol 50 (2001) 470-8.
Demple, B. and Linn, S.: DNA N-glycosylases and UV repair. Nature 287 (1980) 203-8.
Demuth, I., Digweed, M. and Concannon, P.: Human SNM1B is required for normal cellular response to both DNA interstrand crosslink-inducing agents and ionizing radiation. Oncogene 23 (2004) 8611-8.
Deshpande, R.A. and Wilson, T.E.: Modes of interaction among yeast Nej1, Lif1 and Dnl4 proteins and comparison to human XLF, XRCC4 and Lig4. DNA Repair (Amst) 6 (2007) 1507-16.
Dillingham, M.S., Spies, M. and Kowalczykowski, S.C.: RecBCD enzyme is a bipolar DNA helicase. Nature 423 (2003) 893-7.
Ding, Q., Bramble, L., Yuzbasiyan-Gurkan, V., Bell, T. and Meek, K.: DNA-PKcs mutations in dogs and horses: allele frequency and association with neoplasia. Gene 283 (2002) 263-9.
Ding, Q., Reddy, Y.V., Wang, W., Woods, T., Douglas, P., Ramsden, D.A., Lees-Miller, S.P. and Meek, K.: Autophosphorylation of the catalytic subunit of the DNA-dependent protein kinase is required for efficient end processing during DNA double-strand break repair. Mol Cell Biol 23 (2003) 5836-48.
DiRuggiero, J., Brown, J.R., Bogert, A.P. and Robb, F.T.: DNA repair systems in archaea: mementos from the last universal common ancestor? J Mol Evol 49 (1999) 474-84.
Doe, C.L., Ahn, J.S., Dixon, J. and Whitby, M.C.: Mus81-Eme1 and Rqh1 involvement in processing stalled and collapsed replication forks. J Biol Chem 277 (2002) 32753-9.

Doherty, A.J., Jackson, S.P. and Weller, G.R.: Identification of bacterial homologues of the Ku DNA repair proteins. FEBS Lett 500 (2001) 186-8.
Doherty, A.J., Serpell, L.C. and Ponting, C.P.: The helix-hairpin-helix DNA-binding motif: a structural basis for non-sequence-specific recognition of DNA. Nucleic Acids Res 24 (1996) 2488-97.
Dore, A.S., Furnham, N., Davies, O.R., Sibanda, B.L., Chirgadze, D.Y., Jackson, S.P., Pellegrini, L. and Blundell, T.L.: Structure of an Xrcc4-DNA ligase IV yeast ortholog complex reveals a novel BRCT interaction mode. DNA Repair (Amst) 5 (2006a) 362-8.
Dore, A.S., Kilkenny, M.L., Jones, S.A., Oliver, A.W., Roe, S.M., Bell, S.D. and Pearl, L.H.: Structure of an archaeal PCNA1-PCNA2-FEN1 complex: elucidating PCNA subunit and client enzyme specificity. Nucleic Acids Res 34 (2006b) 4515-26.
Drablos, F., Feyzi, E., Aas, P.A., Vaagbo, C.B., Kavli, B., Bratlie, M.S., Pena-Diaz, J., Otterlei, M., Slupphaug, G. and Krokan, H.E.: Alkylation damage in DNA and RNA--repair mechanisms and medical significance. DNA Repair (Amst) 3 (2004) 1389-407.
Drapkin, R., Reardon, J.T., Ansari, A., Huang, J.C., Zawel, L., Ahn, K., Sancar, A. and Reinberg, D.: Dual role of TFIIH in DNA excision repair and in transcription by RNA polymerase II. Nature 368 (1994) 769-72.
Dray, E., Siaud, N., Dubois, E. and Doutriaux, M.P.: Interaction between Arabidopsis Brca2 and its partners Rad51, Dmc1, and Dss1. Plant Physiol 140 (2006) 1059-69.
Dronkert, M.L., de Wit, J., Boeve, M., Vasconcelos, M.L., van Steeg, H., Tan, T.L., Hoeijmakers, J.H. and Kanaar, R.: Disruption of mouse SNM1 causes increased sensitivity to the DNA interstrand cross-linking agent mitomycin C. Mol Cell Biol 20 (2000) 4553-61.
Dronkert, M.L. and Kanaar, R.: Repair of DNA interstrand cross-links. Mutat Res 486 (2001) 217-47.
Dudasova, Z., Dudas, A. and Chovanec, M.: Non-homologous end-joining factors of Saccharomyces cerevisiae. FEMS Microbiol Rev 28 (2004) 581-601.
Dudley, D.D., Chaudhuri, J., Bassing, C.H. and Alt, F.W.: Mechanism and control of V(D)J recombination versus class switch recombination: similarities and differences. Adv Immunol 86 (2005) 43-112.
Duncan, T., Trewick, S.C., Koivisto, P., Bates, P.A., Lindahl, T. and Sedgwick, B.: Reversal of DNA alkylation damage by two human dioxygenases. Proc Natl Acad Sci U S A 99 (2002) 16660-5.
Durant, S.T., Morris, M.M., Illand, M., McKay, H.J., McCormick, C., Hirst, G.L., Borts, R.H. and Brown, R.: Dependence on RAD52 and RAD1 for anticancer drug resistance mediated by inactivation of mismatch repair genes. Curr Biol 9 (1999) 51-4.
Dzantiev, L., Constantin, N., Genschel, J., Iyer, R.R., Burgers, P.M. and Modrich, P.: A defined human system that supports bidirectional mismatch-provoked excision. Mol Cell 15 (2004) 31-41.
Ehmsen, K.T. and Heyer, W.D.: Saccharomyces cerevisiae Mus81-Mms4 is a catalytic, DNA structure-selective endonuclease. Nucleic Acids Res 36 (2008) 2182-95.
Eisen, J.A. and Hanawalt, P.C.: A phylogenomic study of DNA repair genes, proteins, and processes. Mutat Res 435 (1999) 171-213.
Eki, T., Okumura, K., Shiratori, A., Abe, M., Nogami, M., Taguchi, H., Shibata, T., Murakami, Y. and Hanaoka, F.: Assignment of the closest human homologue (DNA2L:KIAA0083) of the yeast Dna2 helicase gene to chromosome band 10q21.3-q22.1. Genomics 37 (1996) 408-10.
Engels, W.R., Johnson-Schlitz, D.M., Eggleston, W.B. and Sved, J.: High-frequency P element loss in Drosophila is homolog dependent. Cell 62 (1990) 515-25.
Enzlin, J.H. and Scharer, O.D.: The active site of the DNA repair endonuclease XPF-ERCC1 forms a highly conserved nuclease motif. Embo J 21 (2002) 2045-53.
Esashi, F., Christ, N., Gannon, J., Liu, Y., Hunt, T., Jasin, M. and West, S.C.: CDK-dependent phosphorylation of BRCA2 as a regulatory mechanism for recombinational repair. Nature 434 (2005) 598-604.
Evans, E., Fellows, J., Coffer, A. and Wood, R.D.: Open complex formation around a lesion during nucleotide excision repair provides a structure for cleavage by human XPG protein. Embo J 16 (1997a) 625-38.
Evans, E., Moggs, J.G., Hwang, J.R., Egly, J.M. and Wood, R.D.: Mechanism of open complex and dual incision formation by human nucleotide excision repair factors. Embo J 16 (1997b) 6559-73.
Fan, L., Arvai, A.S., Cooper, P.K., Iwai, S., Hanaoka, F. and Tainer, J.A.: Conserved XPB core structure and motifs for DNA unwinding: implications for pathway selection of transcription or excision repair. Mol Cell 22 (2006) 27-37.
Feldmann, H., Driller, L., Meier, B., Mages, G., Kellermann, J. and Winnacker, E.L.: HDF2, the second subunit of the Ku homologue from Saccharomyces cerevisiae. J Biol Chem 271 (1996) 27765-9.

Fiorentini, P., Huang, K.N., Tishkoff, D.X., Kolodner, R.D. and Symington, L.S.: Exonuclease I of Saccharomyces cerevisiae functions in mitotic recombination in vivo and in vitro. Mol Cell Biol 17 (1997) 2764-73.
Flores, M.J., Sanchez, N. and Michel, B.: A fork-clearing role for UvrD. Mol Microbiol 57 (2005) 1664-75.
Flores-Rozas, H. and Kolodner, R.D.: The Saccharomyces cerevisiae MLH3 gene functions in MSH3-dependent suppression of frameshift mutations. Proc Natl Acad Sci U S A 95 (1998) 12404-9.
Formosa, T. and Alberts, B.M.: Purification and characterization of the T4 bacteriophage uvsX protein. J Biol Chem 261 (1986) 6107-18.
Forterre, P. and Philippe, H.: The last universal common ancestor (LUCA), simple or complex? Biol Bull 196 (1999) 373-5; discussion 375-7.
Fortin, G.S. and Symington, L.S.: Mutations in yeast Rad51 that partially bypass the requirement for Rad55 and Rad57 in DNA repair by increasing the stability of Rad51-DNA complexes. Embo J 21 (2002) 3160-70.
Fortini, P., Pascucci, B., Parlanti, E., D'Errico, M., Simonelli, V. and Dogliotti, E.: The base excision repair: mechanisms and its relevance for cancer susceptibility. Biochimie 85 (2003) 1053-71.
Fousteri, M. and Mullenders, L.H.: Transcription-coupled nucleotide excision repair in mammalian cells: molecular mechanisms and biological effects. Cell Res 18 (2008) 73-84.
Fousteri, M., Vermeulen, W., van Zeeland, A.A. and Mullenders, L.H.: Cockayne syndrome A and B proteins differentially regulate recruitment of chromatin remodeling and repair factors to stalled RNA polymerase II in vivo. Mol Cell 23 (2006) 471-82.
Franca, M.B., Panek, A.D. and Eleutherio, E.C.: Oxidative stress and its effects during dehydration. Comp Biochem Physiol A Mol Integr Physiol 146 (2007) 621-31.
Frank, K.M., Sekiguchi, J.M., Seidl, K.J., Swat, W., Rathbun, G.A., Cheng, H.L., Davidson, L., Kangaloo, L. and Alt, F.W.: Late embryonic lethality and impaired V(D)J recombination in mice lacking DNA ligase IV. Nature 396 (1998) 173-7.
Frank-Vaillant, M. and Marcand, S.: NHEJ regulation by mating type is exercised through a novel protein, Lif2p, essential to the ligase IV pathway. Genes Dev 15 (2001) 3005-12.
Freisinger, E., Grollman, A.P., Miller, H. and Kisker, C.: Lesion (in)tolerance reveals insights into DNA replication fidelity. Embo J 23 (2004) 1494-505.
Fridovich, I.: The biology of oxygen radicals. Science 201 (1978) 875-80.
Fridovich, I.: Superoxide radical and superoxide dismutases. Annu Rev Biochem 64 (1995) 97-112.
Friedberg, E.C.: DNA damage and repair. Nature 421 (2003) 436-40.
Friedberg, E.C., Bardwell, A.J., Bardwell, L., Feaver, W.J., Kornberg, R.D., Svejstrup, J.Q., Tomkinson, A.E. and Wang, Z.: Nucleotide excision repair in the yeast Saccharomyces cerevisiae: its relationship to specialized mitotic recombination and RNA polymerase II basal transcription. Philos Trans R Soc Lond B Biol Sci 347 (1995a) 63-8.
Friedberg, E.C., Lehmann, A.R. and Fuchs, R.P.: Trading places: how do DNA polymerases switch during translesion DNA synthesis? Mol Cell 18 (2005) 499-505.
Friedberg, E.C., Walker, G.C., Wood, R.D., Schultz, R.A. and Ellenberger, T.: DNA repair and mutagenesis. ASM Press, Washington DC, 1995b.
Friedrich-Heineken, E., Henneke, G., Ferrari, E. and Hubscher, U.: The acetylatable lysines of human Fen1 are important for endo- and exonuclease activities. J Mol Biol 328 (2003) 73-84.
Friedrich-Heineken, E., Toueille, M., Tannler, B., Burki, C., Ferrari, E., Hottiger, M.O. and Hubscher, U.: The two DNA clamps Rad9/Rad1/Hus1 complex and proliferating cell nuclear antigen differentially regulate flap endonuclease 1 activity. J Mol Biol 353 (2005) 980-9.
Fujikane, R., Komori, K., Shinagawa, H. and Ishino, Y.: Identification of a novel helicase activity unwinding branched DNAs from the hyperthermophilic archaeon, Pyrococcus furiosus. J Biol Chem 280 (2005) 12351-8.
Fujimori, A., Tachiiri, S., Sonoda, E., Thompson, L.H., Dhar, P.K., Hiraoka, M., Takeda, S., Zhang, Y., Reth, M. and Takata, M.: Rad52 partially substitutes for the Rad51 paralog XRCC3 in maintaining chromosomal integrity in vertebrate cells. Embo J 20 (2001) 5513-20.
Fujimoto, M., Matsumoto, N., Tsujita, T., Tomita, H., Kondo, S., Miyake, N., Nakano, M. and Niikawa, N.: Characterization of the promoter region, first ten exons and nine intron-exon boundaries of the DNA-dependent protein kinase catalytic subunit gene, DNA-PKcs (XRCC7). DNA Res 4 (1997) 151-4.
Furuse, M., Nagase, Y., Tsubouchi, H., Murakami-Murofushi, K., Shibata, T. and Ohta, K.: Distinct roles of two separable in vitro activities of yeast Mre11 in mitotic and meiotic recombination. Embo J 17 (1998) 6412-25.

Fuss, J.O. and Cooper, P.K.: DNA repair: dynamic defenders against cancer and aging. PLoS Biol 4 (2006) e203.
Galli, A. and Schiestl, R.H.: Effects of DNA double-strand and single-strand breaks on intrachromosomal recombination events in cell-cycle-arrested yeast cells. Genetics 149 (1998) 1235-50.
Game, J.C. and Mortimer, R.K.: A genetic study of x-ray sensitive mutants in yeast. Mutat Res 24 (1974) 281-92.
Gangloff, S., Soustelle, C. and Fabre, F.: Homologous recombination is responsible for cell death in the absence of the Sgs1 and Srs2 helicases. Nat Genet 25 (2000) 192-4.
Gao, Y., Chaudhuri, J., Zhu, C., Davidson, L., Weaver, D.T. and Alt, F.W.: A targeted DNA-PKcs-null mutation reveals DNA-PK-independent functions for KU in V(D)J recombination. Immunity 9 (1998a) 367-76.
Gao, Y., Sun, Y., Frank, K.M., Dikkes, P., Fujiwara, Y., Seidl, K.J., Sekiguchi, J.M., Rathbun, G.A., Swat, W., Wang, J., Bronson, R.T., Malynn, B.A., Bryans, M., Zhu, C., Chaudhuri, J., Davidson, L., Ferrini, R., Stamato, T., Orkin, S.H., Greenberg, M.E. and Alt, F.W.: A critical role for DNA end-joining proteins in both lymphogenesis and neurogenesis. Cell 95 (1998b) 891-902.
Gary, R., Park, M.S., Nolan, J.P., Cornelius, H.L., Kozyreva, O.G., Tran, H.T., Lobachev, K.S., Resnick, M.A. and Gordenin, D.A.: A novel role in DNA metabolism for the binding of Fen1/Rad27 to PCNA and implications for genetic risk. Mol Cell Biol 19 (1999) 5373-82.
Gasior, S.L., Olivares, H., Ear, U., Hari, D.M., Weichselbaum, R. and Bishop, D.K.: Assembly of RecA-like recombinases: distinct roles for mediator proteins in mitosis and meiosis. Proc Natl Acad Sci U S A 98 (2001) 8411-8.
Gasior, S.L., Wong, A.K., Kora, Y., Shinohara, A. and Bishop, D.K.: Rad52 associates with RPA and functions with rad55 and rad57 to assemble meiotic recombination complexes. Genes Dev 12 (1998) 2208-21.
Gatignol, A., Dassain, M. and Tiraby, G.: Cloning of Saccharomyces cerevisiae promoters using a probe vector based on phleomycin resistance. Gene 91 (1990) 35-41.
Gaudier, M., Schuwirth, B.S., Westcott, S.L. and Wigley, D.B.: Structural basis of DNA replication origin recognition by an ORC protein. Science 317 (2007) 1213-6.
Geacintov, N.E., Broyde, S., Buterin, T., Naegeli, H., Wu, M., Yan, S. and Patel, D.J.: Thermodynamic and structural factors in the removal of bulky DNA adducts by the nucleotide excision repair machinery. Biopolymers 65 (2002) 202-10.
Gellert, M.: V(D)J recombination: RAG proteins, repair factors, and regulation. Annu Rev Biochem 71 (2002) 101-32.
Genschel, J., Bazemore, L.R. and Modrich, P.: Human exonuclease I is required for 5' and 3' mismatch repair. J Biol Chem 277 (2002) 13302-11.
Genschel, J. and Modrich, P.: Analysis of the excision step in human DNA mismatch repair. Methods Enzymol 408 (2006) 273-84.
Gibbs, P.E., McGregor, W.G., Maher, V.M., Nisson, P. and Lawrence, C.W.: A human homolog of the Saccharomyces cerevisiae REV3 gene, which encodes the catalytic subunit of DNA polymerase zeta. Proc Natl Acad Sci U S A 95 (1998) 6876-80.
Gillette, T.G., Yu, S., Zhou, Z., Waters, R., Johnston, S.A. and Reed, S.H.: Distinct functions of the ubiquitin-proteasome pathway influence nucleotide excision repair. Embo J 25 (2006) 2529-38.
Girard, P.M. and Boiteux, S.: Repair of oxidized DNA bases in the yeast Saccharomyces cerevisiae. Biochimie 79 (1997) 559-66.
Gong, C., Bongiorno, P., Martins, A., Stephanou, N.C., Zhu, H., Shuman, S. and Glickman, M.S.: Mechanism of nonhomologous end-joining in mycobacteria: a low-fidelity repair system driven by Ku, ligase D and ligase C. Nat Struct Mol Biol 12 (2005) 304-12.
Gong, C., Martins, A., Bongiorno, P., Glickman, M. and Shuman, S.: Biochemical and genetic analysis of the four DNA ligases of mycobacteria. J Biol Chem 279 (2004) 20594-606.
Goodman, M.F.: Error-prone repair DNA polymerases in prokaryotes and eukaryotes. Annu Rev Biochem 71 (2002) 17-50.
Grabowski, B. and Kelman, Z.: Archeal DNA replication: eukaryal proteins in a bacterial context. Annu Rev Microbiol 57 (2003) 487-516.
Graves, R.J., Felzenszwalb, I., Laval, J. and O'Connor, T.R.: Excision of 5'-terminal deoxyribose phosphate from damaged DNA is catalyzed by the Fpg protein of Escherichia coli. J Biol Chem 267 (1992) 14429-35.
Gregor, D. and Pfeifer, F.: In vivo analyses of constitutive and regulated promoters in halophilic archaea. Microbiology 151 (2005) 25-33.
Gribaldo, S. and Brochier-Armanet, C.: The origin and evolution of Archaea: a state of the art. Philos Trans R Soc Lond B Biol Sci 361 (2006) 1007-22.

Grilley, M., Welsh, K.M., Su, S.S. and Modrich, P.: Isolation and characterization of the Escherichia coli mutL gene product. J Biol Chem 264 (1989) 1000-4.
Grombacher, T., Tomicic, M., Digweed, M. and Kaina, B.: Overexpression of cDNA encoding FANCC, SPHAR, MPG, SNM1 or HA 3611 does not render CHO cells more resistant to DNA crosslinking agents. Anticancer Res 19 (1999) 1729-35.
Grossmann, K.F., Ward, A.M., Matkovic, M.E., Folias, A.E. and Moses, R.E.: S. cerevisiae has three pathways for DNA interstrand crosslink repair. Mutat Res 487 (2001) 73-83.
Grossmann, K.F., Ward, A.M. and Moses, R.E.: Saccharomyces cerevisiae lacking Snm1, Rev3 or Rad51 have a normal S-phase but arrest permanently in G2 after cisplatin treatment. Mutat Res 461 (2000) 1-13.
Gu, L., Hong, Y., McCulloch, S., Watanabe, H. and Li, G.M.: ATP-dependent interaction of human mismatch repair proteins and dual role of PCNA in mismatch repair. Nucleic Acids Res 26 (1998) 1173-8.
Gu, L., Huang, S.M. and Sander, M.: Drosophila Rrp1 complements E. coli xth nfo mutants: protection against both oxidative and alkylation-induced DNA damage. Nucleic Acids Res 21 (1993) 4788-95.
Gu, Y., Sekiguchi, J., Gao, Y., Dikkes, P., Frank, K., Ferguson, D., Hasty, P., Chun, J. and Alt, F.W.: Defective embryonic neurogenesis in Ku-deficient but not DNA-dependent protein kinase catalytic subunit-deficient mice. Proc Natl Acad Sci U S A 97 (2000) 2668-73.
Gudmundsdottir, K., Lord, C.J., Witt, E., Tutt, A.N. and Ashworth, A.: DSS1 is required for RAD51 focus formation and genomic stability in mammalian cells. EMBO Rep 5 (2004) 989-93.
Guo, S. and Kemphues, K.J.: par-1, a gene required for establishing polarity in C. elegans embryos, encodes a putative Ser/Thr kinase that is asymmetrically distributed. Cell 81 (1995) 611-20.
Guo, S., Presnell, S.R., Yuan, F., Zhang, Y., Gu, L. and Li, G.M.: Differential requirement for proliferating cell nuclear antigen in 5' and 3' nick-directed excision in human mismatch repair. J Biol Chem 279 (2004) 16912-7.
Gupta, R., Sharma, S., Sommers, J.A., Kenny, M.K., Cantor, S.B. and Brosh, R.M., Jr.: FANCJ (BACH1) helicase forms DNA damage inducible foci with replication protein A and interacts physically and functionally with the single-stranded DNA-binding protein. Blood 110 (2007) 2390-8.
Guy, C.P. and Bolt, E.L.: Archaeal Hel308 helicase targets replication forks in vivo and in vitro and unwinds lagging strands. Nucleic Acids Res 33 (2005) 3678-90.
Guy, C.P., Haldenby, S., Brindley, A., Walsh, D.A., Briggs, G.S., Warren, M.J., Allers, T. and Bolt, E.L.: Interactions of RadB, a DNA repair protein in archaea, with DNA and ATP. J Mol Biol 358 (2006) 46-56.
Guzder, S.N., Sung, P., Prakash, L. and Prakash, S.: The DNA-dependent ATPase activity of yeast nucleotide excision repair factor 4 and its role in DNA damage recognition. J Biol Chem 273 (1998) 6292-6.
Guzder, S.N., Torres-Ramos, C., Johnson, R.E., Haracska, L., Prakash, L. and Prakash, S.: Requirement of yeast Rad1-Rad10 nuclease for the removal of 3'-blocked termini from DNA strand breaks induced by reactive oxygen species. Genes Dev 18 (2004) 2283-91.
Guzman, L.M., Belin, D., Carson, M.J. and Beckwith, J.: Tight regulation, modulation, and high-level expression by vectors containing the arabinose PBAD promoter. J Bacteriol 177 (1995) 4121-30.
Habraken, Y., Sung, P., Prakash, S. and Prakash, L.: Transcription factor TFIIH and DNA endonuclease Rad2 constitute yeast nucleotide excision repair factor 3: implications for nucleotide excision repair and Cockayne syndrome. Proc Natl Acad Sci U S A 93 (1996) 10718-22.
Habu, T., Taki, T., West, A., Nishimune, Y. and Morita, T.: The mouse and human homologs of DMC1, the yeast meiosis-specific homologous recombination gene, have a common unique form of exon-skipped transcript in meiosis. Nucleic Acids Res 24 (1996) 470-7.
Haldenby, S.T.: Genetic analysis of RadB, a paralogue of the archaeal Rad51/RecA homologue, RadA. University of Nottingham, 2007.
Hamilton, K.K., Kim, P.M. and Doetsch, P.W.: A eukaryotic DNA glycosylase/lyase recognizing ultraviolet light-induced pyrimidine dimers. Nature 356 (1992) 725-8.
Hanada, K., Budzowska, M., Modesti, M., Maas, A., Wyman, C., Essers, J. and Kanaar, R.: The structure-specific endonuclease Mus81-Eme1 promotes conversion of interstrand DNA crosslinks into double-strands breaks. Embo J 25 (2006) 4921-32.
Hanakahi, L.A., Bartlet-Jones, M., Chappell, C., Pappin, D. and West, S.C.: Binding of inositol phosphate to DNA-PK and stimulation of double-strand break repair. Cell 102 (2000) 721-9.
Hanawalt, P.C.: Subpathways of nucleotide excision repair and their regulation. Oncogene 21 (2002) 8949-56.
Handa, N., Ohashi, S., Kusano, K. and Kobayashi, I.: Chi-star, a chi-related 11-mer sequence partially active in an E. coli recC1004 strain. Genes Cells 2 (1997) 525-36.

Hang, H., Hager, D.N., Goriparthi, L., Hopkins, K.M., Shih, H. and Lieberman, H.B.: Schizosaccharomyces pombe rad23 is allelic with swi10, a mating-type switching/radioresistance gene that shares sequence homology with human and mouse ERCC1. Gene 170 (1996) 113-7.
Harfe, B.D., Minesinger, B.K. and Jinks-Robertson, S.: Discrete in vivo roles for the MutL homologs Mlh2p and Mlh3p in the removal of frameshift intermediates in budding yeast. Curr Biol 10 (2000) 145-8.
Harfst, E., Cooper, S., Neubauer, S., Distel, L. and Grawunder, U.: Normal V(D)J recombination in cells from patients with Nijmegen breakage syndrome. Mol Immunol 37 (2000) 915-29.
Harrington, J.J. and Lieber, M.R.: Functional domains within FEN-1 and RAD2 define a family of structure-specific endonucleases: implications for nucleotide excision repair. Genes Dev 8 (1994a) 1344-55.
Harrington, J.J. and Lieber, M.R.: The characterization of a mammalian DNA structure-specific endonuclease. Embo J 13 (1994b) 1235-46.
Harris, P.V., Mazina, O.M., Leonhardt, E.A., Case, R.B., Boyd, J.B. and Burtis, K.C.: Molecular cloning of Drosophila mus308, a gene involved in DNA cross-link repair with homology to prokaryotic DNA polymerase I genes. Mol Cell Biol 16 (1996) 5764-71.
Hartley, K.O., Gell, D., Smith, G.C., Zhang, H., Divecha, N., Connelly, M.A., Admon, A., Lees-Miller, S.P., Anderson, C.W. and Jackson, S.P.: DNA-dependent protein kinase catalytic subunit: a relative of phosphatidylinositol 3-kinase and the ataxia telangiectasia gene product. Cell 82 (1995) 849-56.
Haseltine, C.A. and Kowalczykowski, S.C.: A distinctive single-strand DNA-binding protein from the Archaeon Sulfolobus solfataricus. Mol Microbiol 43 (2002) 1505-15.
Haseltine, W.A., Gordon, L.K., Lindan, C.P., Grafstrom, R.H., Shaper, N.L. and Grossman, L.: Cleavage of pyrimidine dimers in specific DNA sequences by a pyrimidine dimer DNA-glycosylase of M. luteus. Nature 285 (1980) 634-41.
Hatahet, Z., Kow, Y.W., Purmal, A.A., Cunningham, R.P. and Wallace, S.S.: New substrates for old enzymes. 5-Hydroxy-2'-deoxycytidine and 5-hydroxy-2'-deoxyuridine are substrates for Escherichia coli endonuclease III and formamidopyrimidine DNA N-glycosylase, while 5-hydroxy-2'-deoxyuridine is a substrate for uracil DNA N-glycosylase. J Biol Chem 269 (1994) 18814-20.
Hayase, A., Takagi, M., Miyazaki, T., Oshiumi, H., Shinohara, M. and Shinohara, A.: A protein complex containing Mei5 and Sae3 promotes the assembly of the meiosis-specific RecA homolog Dmc1. Cell 119 (2004) 927-40.
Hazrati, A., Ramis-Castelltort, M., Sarkar, S., Barber, L.J., Schofield, C.J., Hartley, J.A. and McHugh, P.J.: Human SNM1A suppresses the DNA repair defects of yeast pso2 mutants. DNA Repair (Amst) 7 (2008) 230-8.
Heelis, P.F., Kim, S.T., Okamura, T. and Sancar, A.: The photo repair of pyrimidine dimers by DNA photolyase and model systems. J Photochem Photobiol B 17 (1993) 219-28.
Hefferin, M.L. and Tomkinson, A.E.: Mechanism of DNA double-strand break repair by non-homologous end joining. DNA Repair (Amst) 4 (2005) 639-48.
Hegde, S.P., Qin, M.H., Li, X.H., Atkinson, M.A., Clark, A.J., Rajagopalan, M. and Madiraju, M.V.: Interactions of RecF protein with RecO, RecR, and single-stranded DNA binding proteins reveal roles for the RecF-RecO-RecR complex in DNA repair and recombination. Proc Natl Acad Sci U S A 93 (1996) 14468-73.
Helleday, T., Lo, J., van Gent, D.C. and Engelward, B.P.: DNA double-strand break repair: from mechanistic understanding to cancer treatment. DNA Repair (Amst) 6 (2007) 923-35.
Henderson, D.S., Bailey, D.A., Sinclair, D.A. and Grigliatti, T.A.: Isolation and characterization of second chromosome mutagen-sensitive mutations in Drosophila melanogaster. Mutat Res 177 (1987) 83-93.
Henneke, G., Koundrioukoff, S. and Hubscher, U.: Phosphorylation of human Fen1 by cyclin-dependent kinase modulates its role in replication fork regulation. Oncogene 22 (2003) 4301-13.
Henner, W.D., Grunberg, S.M. and Haseltine, W.A.: Sites and structure of gamma radiation-induced DNA strand breaks. J Biol Chem 257 (1982) 11750-4.
Henriques, J.A. and Moustacchi, E.: Isolation and characterization of pso mutants sensitive to photo-addition of psoralen derivatives in Saccharomyces cerevisiae. Genetics 95 (1980) 273-88.
Herrmann, G., Lindahl, T. and Schar, P.: Saccharomyces cerevisiae LIF1: a function involved in DNA double-strand break repair related to mammalian XRCC4. Embo J 17 (1998) 4188-98.
Heyer, W.D., Ehmsen, K.T. and Solinger, J.A.: Holliday junctions in the eukaryotic nucleus: resolution in sight? Trends Biochem Sci 28 (2003) 548-57.
Hickson, I.D.: RecQ helicases: caretakers of the genome. Nat Rev Cancer 3 (2003) 169-78.

Hienonen, T., Laiho, P., Salovaara, R., Mecklin, J.P., Jarvinen, H., Sistonen, P., Peltomaki, P., Lehtonen, R., Nupponen, N.N., Launonen, V., Karhu, A. and Aaltonen, L.A.: Little evidence for involvement of MLH3 in colorectal cancer predisposition. Int J Cancer 106 (2003) 292-6.

Hirashima, A., Sawaki, S., Inokuchi, Y. and Inouye, M.: Engineering of the mRNA-interfering complementary RNA immune system against viral infection. Proc Natl Acad Sci U S A 83 (1986) 7726-30.

Hoare, S., Zou, Y., Purohit, V., Krishnasamy, R., Skorvaga, M., Van Houten, B., Geacintov, N.E. and Basu, A.K.: Differential incision of bulky carcinogen-DNA adducts by the UvrABC nuclease: comparison of incision rates and the interactions of Uvr subunits with lesions of different structures. Biochemistry 39 (2000) 12252-61.

Hoege, C., Pfander, B., Moldovan, G.L., Pyrowolakis, G. and Jentsch, S.: RAD6-dependent DNA repair is linked to modification of PCNA by ubiquitin and SUMO. Nature 419 (2002) 135-41.

Hoeijmakers, J.H.: Genome maintenance mechanisms for preventing cancer. Nature 411 (2001) 366-74.

Hogg, M., Wallace, S.S. and Doublie, S.: Crystallographic snapshots of a replicative DNA polymerase encountering an abasic site. Embo J 23 (2004) 1483-93.

Hohn, M.J., Hedlund, B.P. and Huber, H.: Detection of 16S rDNA sequences representing the novel phylum "Nanoarchaeota": indication for a wide distribution in high temperature biotopes. Syst Appl Microbiol 25 (2002) 551-4.

Hollingsworth, N.M. and Brill, S.J.: The Mus81 solution to resolution: generating meiotic crossovers without Holliday junctions. Genes Dev 18 (2004) 117-25.

Holmes, A. and Haber, J.E.: Physical monitoring of HO-induced homologous recombination. Methods Mol Biol 113 (1999) 403-15.

Holmes, M.L. and Dyall-Smith, M.L.: Sequence and expression of a halobacterial beta-galactosidase gene. Mol Microbiol 36 (2000a) 114-22.

Holmes, M.L. and Dyall-Smith, M.L.: Sequence and expression of a halobacterial beta-galactosidase gene. Mol Microbiol 36 (2000b) 114-122.

Hopfner, K.P., Craig, L., Moncalian, G., Zinkel, R.A., Usui, T., Owen, B.A., Karcher, A., Henderson, B., Bodmer, J.L., McMurray, C.T., Carney, J.P., Petrini, J.H. and Tainer, J.A.: The Rad50 zinc-hook is a structure joining Mre11 complexes in DNA recombination and repair. Nature 418 (2002) 562-6.

Hopfner, K.P., Karcher, A., Craig, L., Woo, T.T., Carney, J.P. and Tainer, J.A.: Structural biochemistry and interaction architecture of the DNA double-strand break repair Mre11 nuclease and Rad50-ATPase. Cell 105 (2001) 473-85.

Hopfner, K.P., Karcher, A., Shin, D., Fairley, C., Tainer, J.A. and Carney, J.P.: Mre11 and Rad50 from Pyrococcus furiosus: cloning and biochemical characterization reveal an evolutionarily conserved multiprotein machine. J Bacteriol 182 (2000a) 6036-41.

Hopfner, K.P., Karcher, A., Shin, D.S., Craig, L., Arthur, L.M., Carney, J.P. and Tainer, J.A.: Structural biology of Rad50 ATPase: ATP-driven conformational control in DNA double-strand break repair and the ABC-ATPase superfamily. Cell 101 (2000b) 789-800.

Hopkins, B.B. and Paull, T.T.: The P. furiosus mre11/rad50 complex promotes 5' strand resection at a DNA double-strand break. Cell 135 (2008) 250-60.

Hosfield, D.J., Frank, G., Weng, Y., Tainer, J.A. and Shen, B.: Newly discovered archaebacterial flap endonucleases show a structure-specific mechanism for DNA substrate binding and catalysis resembling human flap endonuclease-1. J Biol Chem 273 (1998a) 27154-61.

Hosfield, D.J., Mol, C.D., Shen, B. and Tainer, J.A.: Structure of the DNA repair and replication endonuclease and exonuclease FEN-1: coupling DNA and PCNA binding to FEN-1 activity. Cell 95 (1998b) 135-46.

Howard-Flanders, P., Boyce, R.P. and Theriot, L.: Three loci in Escherichia coli K-12 that control the excision of pyrimidine dimers and certain other mutagen products from DNA. Genetics 53 (1966) 1119-36.

Huang, C.H., Mirabelli, C.K., Jan, Y. and Crooke, S.T.: Single-strand and double-strand deoxyribonucleic acid breaks produced by several bleomycin analogues. Biochemistry 20 (1981) 233-8.

Huang, J. and Dynan, W.S.: Reconstitution of the mammalian DNA double-strand break end-joining reaction reveals a requirement for an Mre11/Rad50/NBS1-containing fraction. Nucleic Acids Res 30 (2002) 667-74.

Huber, H., Hohn, M.J., Rachel, R., Fuchs, T., Wimmer, V.C. and Stetter, K.O.: A new phylum of Archaea represented by a nanosized hyperthermophilic symbiont. Nature 417 (2002) 63-7.

Huber, R., Huber, H. and Stetter, K.O.: Towards the ecology of hyperthermophiles: biotopes, new isolation strategies and novel metabolic properties. FEMS Microbiol Rev 24 (2000) 615-23.

Hubscher, U., Maga, G. and Spadari, S.: Eukaryotic DNA polymerases. Annu Rev Biochem 71 (2002) 133-63.
Hubscher, U., Nasheuer, H.P. and Syvaoja, J.E.: Eukaryotic DNA polymerases, a growing family. Trends Biochem Sci 25 (2000) 143-7.
Husain, I., Van Houten, B., Thomas, D.C., Abdel-Monem, M. and Sancar, A.: Effect of DNA polymerase I and DNA helicase II on the turnover rate of UvrABC excision nuclease. Proc Natl Acad Sci U S A 82 (1985) 6774-8.
Hwang, J.R., Moncollin, V., Vermeulen, W., Seroz, T., van Vuuren, H., Hoeijmakers, J.H. and Egly, J.M.: A 3' --> 5' XPB helicase defect in repair/transcription factor TFIIH of xeroderma pigmentosum group B affects both DNA repair and transcription. J Biol Chem 271 (1996) 15898-904.
Imamura, K., Fukunaga, K., Kawarabayasi, Y. and Ishino, Y.: Specific interactions of three proliferating cell nuclear antigens with replication-related proteins in Aeropyrum pernix. Mol Microbiol 64 (2007) 308-18.
Inamdar, K.V., Pouliot, J.J., Zhou, T., Lees-Miller, S.P., Rasouli-Nia, A. and Povirk, L.F.: Conversion of phosphoglycolate to phosphate termini on 3' overhangs of DNA double strand breaks by the human tyrosyl-DNA phosphodiesterase hTdp1. J Biol Chem 277 (2002) 27162-8.
Interthal, H. and Heyer, W.D.: MUS81 encodes a novel helix-hairpin-helix protein involved in the response to UV- and methylation-induced DNA damage in Saccharomyces cerevisiae. Mol Gen Genet 263 (2000) 812-27.
Ionov, Y., Peinado, M.A., Malkhosyan, S., Shibata, D. and Perucho, M.: Ubiquitous somatic mutations in simple repeated sequences reveal a new mechanism for colonic carcinogenesis. Nature 363 (1993) 558-61.
Ira, G., Malkova, A., Liberi, G., Foiani, M. and Haber, J.E.: Srs2 and Sgs1-Top3 suppress crossovers during double-strand break repair in yeast. Cell 115 (2003) 401-11.
Ishimi, Y., Claude, A., Bullock, P. and Hurwitz, J.: Complete enzymatic synthesis of DNA containing the SV40 origin of replication. J Biol Chem 263 (1988) 19723-33.
Ivanov, E.L. and Haber, J.E.: RAD1 and RAD10, but not other excision repair genes, are required for double-strand break-induced recombination in Saccharomyces cerevisiae. Mol Cell Biol 15 (1995) 2245-51.
Ivanov, E.L., Sugawara, N., Fishman-Lobell, J. and Haber, J.E.: Genetic requirements for the single-strand annealing pathway of double-strand break repair in Saccharomyces cerevisiae. Genetics 142 (1996) 693-704.
Ivanov, E.L., Sugawara, N., White, C.I., Fabre, F. and Haber, J.E.: Mutations in XRS2 and RAD50 delay but do not prevent mating-type switching in Saccharomyces cerevisiae. Mol Cell Biol 14 (1994) 3414-25.
Iwabuchi, K., Bartel, P.L., Li, B., Marraccino, R. and Fields, S.: Two cellular proteins that bind to wild-type but not mutant p53. Proc Natl Acad Sci U S A 91 (1994) 6098-102.
Iwabuchi, K., Basu, B.P., Kysela, B., Kurihara, T., Shibata, M., Guan, D., Cao, Y., Hamada, T., Imamura, K., Jeggo, P.A., Date, T. and Doherty, A.J.: Potential role for 53BP1 in DNA end-joining repair through direct interaction with DNA. J Biol Chem 278 (2003) 36487-95.
Iwasaki, H., Takahagi, M., Shiba, T., Nakata, A. and Shinagawa, H.: Escherichia coli RuvC protein is an endonuclease that resolves the Holliday structure. Embo J 10 (1991) 4381-9.
Iyer, N., Reagan, M.S., Wu, K.J., Canagarajah, B. and Friedberg, E.C.: Interactions involving the human RNA polymerase II transcription/nucleotide excision repair complex TFIIH, the nucleotide excision repair protein XPG, and Cockayne syndrome group B (CSB) protein. Biochemistry 35 (1996) 2157-67.
Iyer, R.R., Pluciennik, A., Burdett, V. and Modrich, P.L.: DNA mismatch repair: functions and mechanisms. Chem Rev 106 (2006) 302-23.
Jachymczyk, W.J., von Borstel, R.C., Mowat, M.R. and Hastings, P.J.: Repair of interstrand cross-links in DNA of Saccharomyces cerevisiae requires two systems for DNA repair: the RAD3 system and the RAD51 system. Mol Gen Genet 182 (1981) 196-205.
Jasin, M.: Homologous repair of DNA damage and tumorigenesis: the BRCA connection. Oncogene 21 (2002) 8981-93.
Jaspers, N.G., Raams, A., Silengo, M.C., Wijgers, N., Niedernhofer, L.J., Robinson, A.R., Giglia-Mari, G., Hoogstraten, D., Kleijer, W.J., Hoeijmakers, J.H. and Vermeulen, W.: First reported patient with human ERCC1 deficiency has cerebro-oculo-facio-skeletal syndrome with a mild defect in nucleotide excision repair and severe developmental failure. Am J Hum Genet 80 (2007) 457-66.
Jessop, L. and Lichten, M.: Mus81/Mms4 endonuclease and Sgs1 helicase collaborate to ensure proper recombination intermediate metabolism during meiosis. Mol Cell 31 (2008) 313-23.

Ji, X.: The mechanism of RNase III action: how dicer dices. Curr Top Microbiol Immunol 320 (2008) 99-116.

Jilani, A., Ramotar, D., Slack, C., Ong, C., Yang, X.M., Scherer, S.W. and Lasko, D.D.: Molecular cloning of the human gene, PNKP, encoding a polynucleotide kinase 3'-phosphatase and evidence for its role in repair of DNA strand breaks caused by oxidative damage. J Biol Chem 274 (1999) 24176-86.

Jin, Y.H., Obert, R., Burgers, P.M., Kunkel, T.A., Resnick, M.A. and Gordenin, D.A.: The 3'-->5' exonuclease of DNA polymerase delta can substitute for the 5' flap endonuclease Rad27/Fen1 in processing Okazaki fragments and preventing genome instability. Proc Natl Acad Sci U S A 98 (2001) 5122-7.

Johnson, A.W. and Demple, B.: Yeast DNA 3'-repair diesterase is the major cellular apurinic/apyrimidinic endonuclease: substrate specificity and kinetics. J Biol Chem 263 (1988) 18017-22.

Johnson, R.E., Kovvali, G.K., Guzder, S.N., Amin, N.S., Holm, C., Habraken, Y., Sung, P., Prakash, L. and Prakash, S.: Evidence for involvement of yeast proliferating cell nuclear antigen in DNA mismatch repair. J Biol Chem 271 (1996) 27987-90.

Kadyrov, F.A., Dzantiev, L., Constantin, N. and Modrich, P.: Endonucleolytic function of MutLalpha in human mismatch repair. Cell 126 (2006) 297-308.

Kadyrov, F.A., Holmes, S.F., Arana, M.E., Lukianova, O.A., O'Donnell, M., Kunkel, T.A. and Modrich, P.: Saccharomyces cerevisiae MutLalpha is a mismatch repair endonuclease. J Biol Chem 282 (2007) 37181-90.

Kaiser, M.W., Lyamicheva, N., Ma, W., Miller, C., Neri, B., Fors, L. and Lyamichev, V.I.: A comparison of eubacterial and archaeal structure-specific 5'-exonucleases. J Biol Chem 274 (1999) 21387-94.

Kamiuchi, S., Saijo, M., Citterio, E., de Jager, M., Hoeijmakers, J.H. and Tanaka, K.: Translocation of Cockayne syndrome group A protein to the nuclear matrix: possible relevance to transcription-coupled DNA repair. Proc Natl Acad Sci U S A 99 (2002) 201-6.

Kanaar, R., Troelstra, C., Swagemakers, S.M., Essers, J., Smit, B., Franssen, J.H., Pastink, A., Bezzubova, O.Y., Buerstedde, J.M., Clever, B., Heyer, W.D. and Hoeijmakers, J.H.: Human and mouse homologs of the Saccharomyces cerevisiae RAD54 DNA repair gene: evidence for functional conservation. Curr Biol 6 (1996) 828-38.

Kandler, O. and Konig, H.: Chemical composition of the peptidoglycan-free cell walls of methanogenic bacteria. Arch Microbiol 118 (1978) 141-52.

Kao, H.I., Henricksen, L.A., Liu, Y. and Bambara, R.A.: Cleavage specificity of Saccharomyces cerevisiae flap endonuclease 1 suggests a double-flap structure as the cellular substrate. J Biol Chem 277 (2002) 14379-89.

Kao, H.I., Veeraraghavan, J., Polaczek, P., Campbell, J.L. and Bambara, R.A.: On the roles of Saccharomyces cerevisiae Dna2p and Flap endonuclease 1 in Okazaki fragment processing. J Biol Chem 279 (2004) 15014-24.

Karimi-Busheri, F., Daly, G., Robins, P., Canas, B., Pappin, D.J., Sgouros, J., Miller, G.G., Fakhrai, H., Davis, E.M., Le Beau, M.M. and Weinfeld, M.: Molecular characterization of a human DNA kinase. J Biol Chem 274 (1999) 24187-94.

Karmakar, P., Piotrowski, J., Brosh, R.M., Jr., Sommers, J.A., Miller, S.P., Cheng, W.H., Snowden, C.M., Ramsden, D.A. and Bohr, V.A.: Werner protein is a target of DNA-dependent protein kinase in vivo and in vitro, and its catalytic activities are regulated by phosphorylation. J Biol Chem 277 (2002a) 18291-302.

Karmakar, P., Snowden, C.M., Ramsden, D.A. and Bohr, V.A.: Ku heterodimer binds to both ends of the Werner protein and functional interaction occurs at the Werner N-terminus. Nucleic Acids Res 30 (2002b) 3583-91.

Karran, P., Lindahl, T., Ofsteng, I., Evensen, G.B. and Seeberg, E.: Escherichia coli mutants deficient in 3-methyladenine-DNA glycosylase. J Mol Biol 140 (1980) 101-27.

Kates, M.: Biology of halophilic bacteria, Part II. Membrane lipids of extreme halophiles: biosynthesis, function and evolutionary significance. Experientia 49 (1993) 1027-36.

Kauri, T., Wallace, R. and Kushner, D.J.: Nutrition of the halophilic archaebacterium, *Haloferax volcanii*. System. Appl. Microbiol. 13 (1990) 14-18.

Keeney, S.: Mechanism and control of meiotic recombination initiation. Curr Top Dev Biol 52 (2001) 1-53.

Kelly, T.J., Simancek, P. and Brush, G.S.: Identification and characterization of a single-stranded DNA-binding protein from the archaeon Methanococcus jannaschii. Proc Natl Acad Sci U S A 95 (1998) 14634-9.

Kelman, Z.: PCNA: structure, functions and interactions. Oncogene 14 (1997) 629-40.

Kelman, Z. and White, M.F.: Archaeal DNA replication and repair. Curr Opin Microbiol 8 (2005) 669-76.
Kempf, B. and Bremer, E.: Uptake and synthesis of compatible solutes as microbial stress responses to high-osmolality environments. Arch Microbiol 170 (1998) 319-30.
Kennedy, R.D. and D'Andrea, A.D.: The Fanconi Anemia/BRCA pathway: new faces in the crowd. Genes Dev 19 (2005) 2925-40.
Keszenman, D.J., Salvo, V.A. and Nunes, E.: Effects of bleomycin on growth kinetics and survival of Saccharomyces cerevisiae: a model of repair pathways. J Bacteriol 174 (1992) 3125-32.
Kienker, L.J., Shin, E.K. and Meek, K.: Both V(D)J recombination and radioresistance require DNA-PK kinase activity, though minimal levels suffice for V(D)J recombination. Nucleic Acids Res 28 (2000) 2752-61.
Kikuchi, K., Taniguchi, Y., Hatanaka, A., Sonoda, E., Hochegger, H., Adachi, N., Matsuzaki, Y., Koyama, H., van Gent, D.C., Jasin, M. and Takeda, S.: Fen-1 facilitates homologous recombination by removing divergent sequences at DNA break ends. Mol Cell Biol 25 (2005) 6948-55.
Kim, C.Y., Park, M.S. and Dyer, R.B.: Human flap endonuclease-1: conformational change upon binding to the flap DNA substrate and location of the Mg2+ binding site. Biochemistry 40 (2001) 3208-14.
Kim, C.Y., Shen, B., Park, M.S. and Olah, G.A.: Structural changes measured by X-ray scattering from human flap endonuclease-1 complexed with Mg2+ and flap DNA substrate. J Biol Chem 274 (1999) 1233-9.
Kim, J.M., Kee, Y., Gurtan, A. and D'Andrea, A.D.: Cell cycle dependent chromatin loading of the fanconi anemia core complex by FANCM/FAAP24. Blood (2008).
Kim, K., Biade, S. and Matsumoto, Y.: Involvement of flap endonuclease 1 in base excision DNA repair. J Biol Chem 273 (1998) 8842-8.
Kirchgessner, C.U., Patil, C.K., Evans, J.W., Cuomo, C.A., Fried, L.M., Carter, T., Oettinger, M.A. and Brown, J.M.: DNA-dependent kinase (p350) as a candidate gene for the murine SCID defect. Science 267 (1995) 1178-83.
Kirkpatrick, D.T.: Roles of the DNA mismatch repair and nucleotide excision repair proteins during meiosis. Cell Mol Life Sci 55 (1999) 437-49.
Klungland, A., Hoss, M., Gunz, D., Constantinou, A., Clarkson, S.G., Doetsch, P.W., Bolton, P.H., Wood, R.D. and Lindahl, T.: Base excision repair of oxidative DNA damage activated by XPG protein. Mol Cell 3 (1999) 33-42.
Kneitz, B., Cohen, P.E., Avdievich, E., Zhu, L., Kane, M.F., Hou, H., Jr., Kolodner, R.D., Kucherlapati, R., Pollard, J.W. and Edelmann, W.: MutS homolog 4 localization to meiotic chromosomes is required for chromosome pairing during meiosis in male and female mice. Genes Dev 14 (2000) 1085-97.
Kobayashi, J., Antoccia, A., Tauchi, H., Matsuura, S. and Komatsu, K.: NBS1 and its functional role in the DNA damage response. DNA Repair (Amst) 3 (2004) 855-61.
Kobayashi, N., Agematsu, K., Sugita, K., Sako, M., Nonoyama, S., Yachie, A., Kumaki, S., Tsuchiya, S., Ochs, H.D., Sugita, K., Fukushima, Y. and Komiyama, A.: Novel Artemis gene mutations of radiosensitive severe combined immunodeficiency in Japanese families. Hum Genet 112 (2003) 348-52.
Koch, C.A., Agyei, R., Galicia, S., Metalnikov, P., O'Donnell, P., Starostine, A., Weinfeld, M. and Durocher, D.: Xrcc4 physically links DNA end processing by polynucleotide kinase to DNA ligation by DNA ligase IV. Embo J 23 (2004) 3874-85.
Kojic, M., Yang, H., Kostrub, C.F., Pavletich, N.P. and Holloman, W.K.: The BRCA2-interacting protein DSS1 is vital for DNA repair, recombination, and genome stability in Ustilago maydis. Mol Cell 12 (2003) 1043-9.
Koken, M.H., Reynolds, P., Jaspers-Dekker, I., Prakash, L., Prakash, S., Bootsma, D. and Hoeijmakers, J.H.: Structural and functional conservation of two human homologs of the yeast DNA repair gene RAD6. Proc Natl Acad Sci U S A 88 (1991) 8865-9.
Kokoska, R.J., Stefanovic, L., Tran, H.T., Resnick, M.A., Gordenin, D.A. and Petes, T.D.: Destabilization of yeast micro- and minisatellite DNA sequences by mutations affecting a nuclease involved in Okazaki fragment processing (rad27) and DNA polymerase delta (pol3-t). Mol Cell Biol 18 (1998) 2779-88.
Kolodner, R.: Biochemistry and genetics of eukaryotic mismatch repair. Genes Dev 10 (1996) 1433-42.
Kolodner, R.D. and Marsischky, G.T.: Eukaryotic DNA mismatch repair. Curr Opin Genet Dev 9 (1999) 89-96.
Komori, K., Fujikane, R., Shinagawa, H. and Ishino, Y.: Novel endonuclease in Archaea cleaving DNA with various branched structure. Genes Genet Syst 77 (2002) 227-41.

Komori, K., Hidaka, M., Horiuchi, T., Fujikane, R., Shinagawa, H. and Ishino, Y.: Cooperation of the N-terminal Helicase and C-terminal endonuclease activities of Archaeal Hef protein in processing stalled replication forks. J Biol Chem 279 (2004) 53175-85.
Komori, K. and Ishino, Y.: Replication protein A in Pyrococcus furiosus is involved in homologous DNA recombination. J Biol Chem 276 (2001) 25654-60.
Komori, K., Miyata, T., Daiyasu, H., Toh, H., Shinagawa, H. and Ishino, Y.: Domain analysis of an archaeal RadA protein for the strand exchange activity. J Biol Chem 275 (2000a) 33791-7.
Komori, K., Miyata, T., DiRuggiero, J., Holley-Shanks, R., Hayashi, I., Cann, I.K., Mayanagi, K., Shinagawa, H. and Ishino, Y.: Both RadA and RadB are involved in homologous recombination in Pyrococcus furiosus. J Biol Chem 275 (2000b) 33782-90.
Komori, K., Sakae, S., Shinagawa, H., Morikawa, K. and Ishino, Y.: A Holliday junction resolvase from Pyrococcus furiosus: functional similarity to Escherichia coli RuvC provides evidence for conserved mechanism of homologous recombination in Bacteria, Eukarya, and Archaea. Proc Natl Acad Sci U S A 96 (1999) 8873-8.
Kottemann, M., Kish, A., Iloanusi, C., Bjork, S. and DiRuggiero, J.: Physiological responses of the halophilic archaeon Halobacterium sp. strain NRC1 to desiccation and gamma irradiation. Extremophiles 9 (2005) 219-27.
Kowalczykowski, S.C.: Initiation of genetic recombination and recombination-dependent replication. Trends Biochem Sci 25 (2000) 156-65.
Kozak, M.: Point mutations define a sequence flanking the AUG initiator codon that modulates translation by eukaryotic ribosomes. Cell 44 (1986) 283-92.
Kraus, E., Leung, W.Y. and Haber, J.E.: Break-induced replication: a review and an example in budding yeast. Proc Natl Acad Sci U S A 98 (2001) 8255-62.
Krejci, L., Van Komen, S., Li, Y., Villemain, J., Reddy, M.S., Klein, H., Ellenberger, T. and Sung, P.: DNA helicase Srs2 disrupts the Rad51 presynaptic filament. Nature 423 (2003) 305-9.
Krishna, S., Wagener, B.M., Liu, H.P., Lo, Y.C., Sterk, R., Petrini, J.H. and Nickoloff, J.A.: Mre11 and Ku regulation of double-strand break repair by gene conversion and break-induced replication. DNA Repair (Amst) 6 (2007) 797-808.
Krogh, B.O. and Symington, L.S.: Recombination proteins in yeast. Annu Rev Genet 38 (2004) 233-71.
Krokan, H.E., Nilsen, H., Skorpen, F., Otterlei, M. and Slupphaug, G.: Base excision repair of DNA in mammalian cells. FEBS Lett 476 (2000) 73-7.
Kucherlapati, M., Yang, K., Kuraguchi, M., Zhao, J., Lia, M., Heyer, J., Kane, M.F., Fan, K., Russell, R., Brown, A.M., Kneitz, B., Edelmann, W., Kolodner, R.D., Lipkin, M. and Kucherlapati, R.: Haploinsufficiency of Flap endonuclease (Fen1) leads to rapid tumor progression. Proc Natl Acad Sci U S A 99 (2002) 9924-9.
Kumar, G.S., He, Q.Y., Behr-Ventura, D. and Tomasz, M.: Binding of 2,7-diaminomitosene to DNA: model for the precovalent recognition of DNA by activated mitomycin C. Biochemistry 34 (1995) 2662-71.
Kumaresan, K.R. and Lambert, M.W.: Fanconi anemia, complementation group A, cells are defective in ability to produce incisions at sites of psoralen interstrand cross-links. Carcinogenesis 21 (2000) 741-51.
Kumaresan, K.R., Sridharan, D.M., McMahon, L.W. and Lambert, M.W.: Deficiency in incisions produced by XPF at the site of a DNA interstrand cross-link in Fanconi anemia cells. Biochemistry 46 (2007) 14359-68.
Kumari, A., Minko, I.G., Harbut, M.B., Finkel, S.E., Goodman, M.F. and Lloyd, R.S.: Replication bypass of interstrand cross-link intermediates by Escherichia coli DNA polymerase IV. J Biol Chem (2008).
Kunkel, T.A.: The mutational specificity of DNA polymerase-beta during in vitro DNA synthesis. Production of frameshift, base substitution, and deletion mutations. J Biol Chem 260 (1985) 5787-96.
Kunkel, T.A.: DNA replication fidelity. J Biol Chem 279 (2004) 16895-8.
Kunkel, T.A. and Loeb, L.A.: Fidelity of mammalian DNA polymerases. Science 213 (1981) 765-7.
Kuraoka, I., Kobertz, W.R., Ariza, R.R., Biggerstaff, M., Essigmann, J.M. and Wood, R.D.: Repair of an interstrand DNA cross-link initiated by ERCC1-XPF repair/recombination nuclease. J Biol Chem 275 (2000) 26632-6.
Kurimasa, A., Kumano, S., Boubnov, N.V., Story, M.D., Tung, C.S., Peterson, S.R. and Chen, D.J.: Requirement for the kinase activity of human DNA-dependent protein kinase catalytic subunit in DNA strand break rejoining. Mol Cell Biol 19 (1999) 3877-84.
Kusser, A.G., Bertero, M.G., Naji, S., Becker, T., Thomm, M., Beckmann, R. and Cramer, P.: Structure of an archaeal RNA polymerase. J Mol Biol 376 (2008) 303-7.
Kvaratskhelia, M., Wardleworth, B.N. and White, M.F.: Multiple Holliday junction resolving enzyme activities in the Crenarchaeota and Euryarchaeota. FEBS Lett 491 (2001) 243-6.

Kyrpides, N.C. and Ouzounis, C.A.: Transcription in archaea. Proc Natl Acad Sci U S A 96 (1999) 8545-50.
Lahue, R.S., Au, K.G. and Modrich, P.: DNA mismatch correction in a defined system. Science 245 (1989) 160-4.
Lam, W.L., Cohen, A., Tsouluhas, D. and Doolittle, W.F.: Genes for tryptophan biosynthesis in the archaebacterium Haloferax volcanii. Proc Natl Acad Sci U S A 87 (1990) 6614-8.
Lander, E.S., Linton, L.M., Birren, B., et al.: Initial sequencing and analysis of the human genome. Nature 409 (2001) 860-921.
Lao, J.P., Oh, S.D., Shinohara, M., Shinohara, A. and Hunter, N.: Rad52 promotes postinvasion steps of meiotic double-strand-break repair. Mol Cell 29 (2008) 517-24.
Lao-Sirieix, S.H., Pellegrini, L. and Bell, S.D.: The promiscuous primase. Trends Genet 21 (2005) 568-72.
Large, A., Stamme, C., Lange, C., Duan, Z., Allers, T., Soppa, J. and Lund, P.A.: Characterization of a tightly controlled promoter of the halophilic archaeon Haloferax volcanii and its use in the analysis of the essential cct1 gene. Mol Microbiol 66 (2007) 1092-106.
Larsen, E., Gran, C., Saether, B.E., Seeberg, E. and Klungland, A.: Proliferation failure and gamma radiation sensitivity of Fen1 null mutant mice at the blastocyst stage. Mol Cell Biol 23 (2003) 5346-53.
Lau, P.J., Flores-Rozas, H. and Kolodner, R.D.: Isolation and characterization of new proliferating cell nuclear antigen (POL30) mutator mutants that are defective in DNA mismatch repair. Mol Cell Biol 22 (2002) 6669-80.
Laurencon, A., Orme, C.M., Peters, H.K., Boulton, C.L., Vladar, E.K., Langley, S.A., Bakis, E.P., Harris, D.T., Harris, N.J., Wayson, S.M., Hawley, R.S. and Burtis, K.C.: A large-scale screen for mutagen-sensitive loci in Drosophila. Genetics 167 (2004) 217-31.
Lawley, P.D.: Mutagens as carcinogens: development of current concepts. Mutat Res 213 (1989) 3-25.
Le Page, F., Kwoh, E.E., Avrutskaya, A., Gentil, A., Leadon, S.A., Sarasin, A. and Cooper, P.K.: Transcription-coupled repair of 8-oxoguanine: requirement for XPG, TFIIH, and CSB and implications for Cockayne syndrome. Cell 101 (2000) 159-71.
Lee, B.I. and Wilson, D.M., 3rd: The RAD2 domain of human exonuclease 1 exhibits 5' to 3' exonuclease and flap structure-specific endonuclease activities. J Biol Chem 274 (1999) 37763-9.
Lee, J.H. and Paull, T.T.: ATM activation by DNA double-strand breaks through the Mre11-Rad50-Nbs1 complex. Science 308 (2005) 551-4.
Lee, K. and Lee, S.E.: Saccharomyces cerevisiae Sae2- and Tel1-dependent single-strand DNA formation at DNA break promotes microhomology-mediated end joining. Genetics 176 (2007) 2003-14.
Lee, K.J., Huang, J., Takeda, Y. and Dynan, W.S.: DNA ligase IV and XRCC4 form a stable mixed tetramer that functions synergistically with other repair factors in a cell-free end-joining system. J Biol Chem 275 (2000) 34787-96.
Lee, S.K., Yu, S.L., Prakash, L. and Prakash, S.: Requirement of yeast RAD2, a homolog of human XPG gene, for efficient RNA polymerase II transcription. implications for Cockayne syndrome. Cell 109 (2002) 823-34.
Lees-Miller, S.P. and Meek, K.: Repair of DNA double strand breaks by non-homologous end joining. Biochimie 85 (2003) 1161-73.
Lehman, I.R. and Nussbaum, A.L.: The Deoxyribonucleases of Escherichia Coli. V. on the Specificity of Exonuclease I (Phosphodiesterase). J Biol Chem 239 (1964) 2628-36.
Lehmann, A.R.: DNA repair-deficient diseases, xeroderma pigmentosum, Cockayne syndrome and trichothiodystrophy. Biochimie 85 (2003) 1101-11.
Lehoczky, P., McHugh, P.J. and Chovanec, M.: DNA interstrand cross-link repair in Saccharomyces cerevisiae. FEMS Microbiol Rev 31 (2007) 109-33.
Leipe, D.D., Aravind, L. and Koonin, E.V.: Did DNA replication evolve twice independently? Nucleic Acids Res 27 (1999) 3389-401.
Lestini, R. and Michel, B.: UvrD controls the access of recombination proteins to blocked replication forks. Embo J 26 (2007) 3804-14.
Levitus, M., Waisfisz, Q., Godthelp, B.C., de Vries, Y., Hussain, S., Wiegant, W.W., Elghalbzouri-Maghrani, E., Steltenpool, J., Rooimans, M.A., Pals, G., Arwert, F., Mathew, C.G., Zdzienicka, M.Z., Hiom, K., De Winter, J.P. and Joenje, H.: The DNA helicase BRIP1 is defective in Fanconi anemia complementation group J. Nat Genet 37 (2005) 934-5.
Li, B. and Comai, L.: Requirements for the nucleolytic processing of DNA ends by the Werner syndrome protein-Ku70/80 complex. J Biol Chem 276 (2001) 9896-902.

Li, L., Moshous, D., Zhou, Y., Wang, J., Xie, G., Salido, E., Hu, D., de Villartay, J.P. and Cowan, M.J.: A founder mutation in Artemis, an SNM1-like protein, causes SCID in Athabascan-speaking Native Americans. J Immunol 168 (2002) 6323-9.
Li, L., Peterson, C.A., Lu, X., Wei, P. and Legerski, R.J.: Interstrand cross-links induce DNA synthesis in damaged and undamaged plasmids in mammalian cell extracts. Mol Cell Biol 19 (1999) 5619-30.
Li, T.K. and Liu, L.F.: Tumor cell death induced by topoisomerase-targeting drugs. Annu Rev Pharmacol Toxicol 41 (2001) 53-77.
Li, X., Hejna, J. and Moses, R.E.: The yeast Snm1 protein is a DNA 5'-exonuclease. DNA Repair (Amst) 4 (2005) 163-70.
Li, X. and Heyer, W.D.: Homologous recombination in DNA repair and DNA damage tolerance. Cell Res 18 (2008) 99-113.
Li, X. and Moses, R.E.: The beta-lactamase motif in Snm1 is required for repair of DNA double-strand breaks caused by interstrand crosslinks in S. cerevisiae. DNA Repair (Amst) 2 (2003) 121-9.
Li, Z., Lu, S., Hou, G., Ma, X., Sheng, D., Ni, J. and Shen, Y.: Hjm/Hel308A DNA helicase from Sulfolobus tokodaii promotes replication fork regression and interacts with Hjc endonuclease in vitro. J Bacteriol 190 (2008) 3006-17.
Liang, F., Romanienko, P.J., Weaver, D.T., Jeggo, P.A. and Jasin, M.: Chromosomal double-strand break repair in Ku80-deficient cells. Proc Natl Acad Sci U S A 93 (1996) 8929-33.
Liang, L., Deng, L., Chen, Y., Li, G.C., Shao, C. and Tischfield, J.A.: Modulation of DNA end joining by nuclear proteins. J Biol Chem 280 (2005) 31442-9.
Lieber, M.R.: The FEN-1 family of structure-specific nucleases in eukaryotic DNA replication, recombination and repair. Bioessays 19 (1997) 233-40.
Lieber, M.R., Ma, Y., Pannicke, U. and Schwarz, K.: The mechanism of vertebrate nonhomologous DNA end joining and its role in V(D)J recombination. DNA Repair (Amst) 3 (2004) 817-26.
Limoli, C.L., Giedzinski, E., Bonner, W.M. and Cleaver, J.E.: UV-induced replication arrest in the xeroderma pigmentosum variant leads to DNA double-strand breaks, gamma -H2AX formation, and Mre11 relocalization. Proc Natl Acad Sci U S A 99 (2002) 233-8.
Lin, F.L., Sperle, K. and Sternberg, N.: Model for homologous recombination during transfer of DNA into mouse L cells: role for DNA ends in the recombination process. Mol Cell Biol 4 (1984) 1020-34.
Lin, F.L., Sperle, K. and Sternberg, N.: Intermolecular recombination between DNAs introduced into mouse L cells is mediated by a nonconservative pathway that leads to crossover products. Mol Cell Biol 10 (1990a) 103-12.
Lin, F.L., Sperle, K. and Sternberg, N.: Repair of double-stranded DNA breaks by homologous DNA fragments during transfer of DNA into mouse L cells. Mol Cell Biol 10 (1990b) 113-9.
Lin, J.J., Phillips, A.M., Hearst, J.E. and Sancar, A.: Active site of (A)BC excinuclease. II. Binding, bending, and catalysis mutants of UvrB reveal a direct role in 3' and an indirect role in 5' incision. J Biol Chem 267 (1992) 17693-700.
Lin, J.J. and Sancar, A.: Active site of (A)BC excinuclease. I. Evidence for 5' incision by UvrC through a catalytic site involving Asp399, Asp438, Asp466, and His538 residues. J Biol Chem 267 (1992) 17688-92.
Lindahl, T.: An N-glycosidase from Escherichia coli that releases free uracil from DNA containing deaminated cytosine residues. Proc Natl Acad Sci U S A 71 (1974) 3649-53.
Lindahl, T.: Keynote: past, present, and future aspects of base excision repair. Prog Nucleic Acid Res Mol Biol 68 (2001) xvii-xxx.
Lindahl, T. and Wood, R.D.: Quality control by DNA repair. Science 286 (1999) 1897-905.
Linding, R., Russell, R.B., Neduva, V. and Gibson, T.J.: GlobPlot: Exploring protein sequences for globularity and disorder. Nucleic Acids Res 31 (2003) 3701-8.
Lipkin, S.M., Wang, V., Jacoby, R., Banerjee-Basu, S., Baxevanis, A.D., Lynch, H.T., Elliott, R.M. and Collins, F.S.: MLH3: a DNA mismatch repair gene associated with mammalian microsatellite instability. Nat Genet 24 (2000) 27-35.
Liu, H.X., Zhou, X.L., Liu, T., Werelius, B., Lindmark, G., Dahl, N. and Lindblom, A.: The role of hMLH3 in familial colorectal cancer. Cancer Res 63 (2003) 1894-9.
Liu, L. and Gerson, S.L.: Targeted modulation of MGMT: clinical implications. Clin Cancer Res 12 (2006) 328-31.
Liu, Y., Kao, H.I. and Bambara, R.A.: Flap endonuclease 1: a central component of DNA metabolism. Annu Rev Biochem 73 (2004a) 589-615.
Liu, Y., Masson, J.Y., Shah, R., O'Regan, P. and West, S.C.: RAD51C is required for Holliday junction processing in mammalian cells. Science 303 (2004b) 243-6.
Liu, Y., Stasiak, A.Z., Masson, J.Y., McIlwraith, M.J., Stasiak, A. and West, S.C.: Conformational changes modulate the activity of human RAD51 protein. J Mol Biol 337 (2004c) 817-27.

Liu, Y., Zhang, H., Veeraraghavan, J., Bambara, R.A. and Freudenreich, C.H.: Saccharomyces cerevisiae flap endonuclease 1 uses flap equilibration to maintain triplet repeat stability. Mol Cell Biol 24 (2004d) 4049-64.
Lo, Y.C., Paffett, K.S., Amit, O., Clikeman, J.A., Sterk, R., Brenneman, M.A. and Nickoloff, J.A.: Sgs1 regulates gene conversion tract lengths and crossovers independently of its helicase activity. Mol Cell Biol 26 (2006) 4086-94.
Lobachev, K.S., Gordenin, D.A. and Resnick, M.A.: The Mre11 complex is required for repair of hairpin-capped double-strand breaks and prevention of chromosome rearrangements. Cell 108 (2002) 183-93.
Loewen, P.C. and Triggs, B.L.: Genetic mapping of katF, a locus that with katE affects the synthesis of a second catalase species in Escherichia coli. J Bacteriol 160 (1984) 668-75.
Londei, P.: Evolution of translational initiation: new insights from the archaea. FEMS Microbiol Rev 29 (2005) 185-200.
Lopez de Saro, F.J., Marinus, M.G., Modrich, P. and O'Donnell, M.: The beta sliding clamp binds to multiple sites within MutL and MutS. J Biol Chem 281 (2006) 14340-9.
Lopez de Saro, F.J. and O'Donnell, M.: Interaction of the beta sliding clamp with MutS, ligase, and DNA polymerase I. Proc Natl Acad Sci U S A 98 (2001) 8376-80.
Lovett, S.T. and Kolodner, R.D.: Identification and purification of a single-stranded-DNA-specific exonuclease encoded by the recJ gene of Escherichia coli. Proc Natl Acad Sci U S A 86 (1989) 2627-31.
Lu, H., Guo, X., Meng, X., Liu, J., Allen, C., Wray, J., Nickoloff, J.A. and Shen, Z.: The BRCA2-interacting protein BCCIP functions in RAD51 and BRCA2 focus formation and homologous recombinational repair. Mol Cell Biol 25 (2005) 1949-57.
Lundgren, M., Andersson, A., Chen, L., Nilsson, P. and Bernander, R.: Three replication origins in Sulfolobus species: synchronous initiation of chromosome replication and asynchronous termination. Proc Natl Acad Sci U S A 101 (2004) 7046-51.
Lushchak, V.I.: Budding yeast Saccharomyces cerevisiae as a model to study oxidative modification of proteins in eukaryotes. Acta Biochim Pol 53 (2006) 679-84.
Lyons, S.M. and Schendel, P.F.: Kinetics of methylation in Escherichia coli K-12. J Bacteriol 159 (1984) 421-3.
Ma, C. and Simons, R.W.: The IS10 antisense RNA blocks ribosome binding at the transposase translation initiation site. Embo J 9 (1990) 1267-74.
Ma, J.L., Kim, E.M., Haber, J.E. and Lee, S.E.: Yeast Mre11 and Rad1 proteins define a Ku-independent mechanism to repair double-strand breaks lacking overlapping end sequences. Mol Cell Biol 23 (2003) 8820-8.
Ma, Y., Lu, H., Tippin, B., Goodman, M.F., Shimazaki, N., Koiwai, O., Hsieh, C.L., Schwarz, K. and Lieber, M.R.: A biochemically defined system for mammalian nonhomologous DNA end joining. Mol Cell 16 (2004) 701-13.
Ma, Y., Pannicke, U., Schwarz, K. and Lieber, M.R.: Hairpin opening and overhang processing by an Artemis/DNA-dependent protein kinase complex in nonhomologous end joining and V(D)J recombination. Cell 108 (2002) 781-94.
Magana-Schwencke, N., Henriques, J.A., Chanet, R. and Moustacchi, E.: The fate of 8-methoxypsoralen photoinduced crosslinks in nuclear and mitochondrial yeast DNA: comparison of wild-type and repair-deficient strains. Proc Natl Acad Sci U S A 79 (1982) 1722-6.
Mages, G.J., Feldmann, H.M. and Winnacker, E.L.: Involvement of the Saccharomyces cerevisiae HDF1 gene in DNA double-strand break repair and recombination. J Biol Chem 271 (1996) 7910-5.
Mahajan, K.N., Gangi-Peterson, L., Sorscher, D.H., Wang, J., Gathy, K.N., Mahajan, N.P., Reeves, W.H. and Mitchell, B.S.: Association of terminal deoxynucleotidyl transferase with Ku. Proc Natl Acad Sci U S A 96 (1999) 13926-31.
Mahajan, K.N., Nick McElhinny, S.A., Mitchell, B.S. and Ramsden, D.A.: Association of DNA polymerase mu (pol mu) with Ku and ligase IV: role for pol mu in end-joining double-strand break repair. Mol Cell Biol 22 (2002) 5194-202.
Malmgren, C., Engdahl, H.M., Romby, P. and Wagner, E.G.: An antisense/target RNA duplex or a strong intramolecular RNA structure 5' of a translation initiation signal blocks ribosome binding: the case of plasmid R1. Rna 2 (1996) 1022-32.
Mansilla-Soto, J. and Cortes, P.: VDJ recombination: Artemis and its in vivo role in hairpin opening. J Exp Med 197 (2003) 543-7.
Maor-Shoshani, A., Meira, L.B., Yang, X. and Samson, L.D.: 3-Methyladenine DNA glycosylase is important for cellular resistance to psoralen interstrand cross-links. DNA Repair (Amst) 7 (2008) 1399-406.

Mari, P.O., Florea, B.I., Persengiev, S.P., Verkaik, N.S., Bruggenwirth, H.T., Modesti, M., Giglia-Mari, G., Bezstarosti, K., Demmers, J.A., Luider, T.M., Houtsmuller, A.B. and van Gent, D.C.: Dynamic assembly of end-joining complexes requires interaction between Ku70/80 and XRCC4. Proc Natl Acad Sci U S A 103 (2006) 18597-602.

Marini, F. and Wood, R.D.: A human DNA helicase homologous to the DNA cross-link sensitivity protein Mus308. J Biol Chem 277 (2002) 8716-23.

Marnett, L.J.: Oxyradicals and DNA damage. Carcinogenesis 21 (2000) 361-70.

Marti, T.M., Kunz, C. and Fleck, O.: DNA mismatch repair and mutation avoidance pathways. J Cell Physiol 191 (2002) 28-41.

Martin, E.L., Reinhardt, R.L., Baum, L.L., Becker, M.R., Shaffer, J.J. and Kokjohn, T.A.: The effects of ultraviolet radiation on the moderate halophile Halomonas elongata and the extreme halophile Halobacterium salinarum. Can J Microbiol 46 (2000) 180-7.

Martin, S.G., Laroche, T., Suka, N., Grunstein, M. and Gasser, S.M.: Relocalization of telomeric Ku and SIR proteins in response to DNA strand breaks in yeast. Cell 97 (1999) 621-33.

Maryon, E. and Carroll, D.: Characterization of recombination intermediates from DNA injected into Xenopus laevis oocytes: evidence for a nonconservative mechanism of homologous recombination. Mol Cell Biol 11 (1991a) 3278-87.

Maryon, E. and Carroll, D.: Involvement of single-stranded tails in homologous recombination of DNA injected into Xenopus laevis oocyte nuclei. Mol Cell Biol 11 (1991b) 3268-77.

Maser, R.S., Mirzoeva, O.K., Wells, J., Olivares, H., Williams, B.R., Zinkel, R.A., Farnham, P.J. and Petrini, J.H.: Mre11 complex and DNA replication: linkage to E2F and sites of DNA synthesis. Mol Cell Biol 21 (2001) 6006-16.

Masson, J.Y., Tarsounas, M.C., Stasiak, A.Z., Stasiak, A., Shah, R., McIlwraith, M.J., Benson, F.E. and West, S.C.: Identification and purification of two distinct complexes containing the five RAD51 paralogs. Genes Dev 15 (2001) 3296-307.

Masuda, K., Ouchida, R., Hikida, M., Kurosaki, T., Yokoi, M., Masutani, C., Seki, M., Wood, R.D., Hanaoka, F. and J, O.W.: DNA polymerases eta and theta function in the same genetic pathway to generate mutations at A/T during somatic hypermutation of Ig genes. J Biol Chem 282 (2007) 17387-94.

Masuda-Sasa, T., Imamura, O. and Campbell, J.L.: Biochemical analysis of human Dna2. Nucleic Acids Res 34 (2006) 1865-75.

Masutani, C., Sugasawa, K., Yanagisawa, J., Sonoyama, T., Ui, M., Enomoto, T., Takio, K., Tanaka, K., van der Spek, P.J., Bootsma, D. and et al.: Purification and cloning of a nucleotide excision repair complex involving the xeroderma pigmentosum group C protein and a human homologue of yeast RAD23. Embo J 13 (1994) 1831-43.

Matson, S.W.: Escherichia coli helicase II (urvD gene product) translocates unidirectionally in a 3' to 5' direction. J Biol Chem 261 (1986) 10169-75.

Matsunaga, F., Forterre, P., Ishino, Y. and Myllykallio, H.: In vivo interactions of archaeal Cdc6/Orc1 and minichromosome maintenance proteins with the replication origin. Proc Natl Acad Sci U S A 98 (2001) 11152-7.

Matsunaga, F., Norais, C., Forterre, P. and Myllykallio, H.: Identification of short 'eukaryotic' Okazaki fragments synthesized from a prokaryotic replication origin. EMBO Rep 4 (2003) 154-8.

Matsuzaki, Y., Adachi, N. and Koyama, H.: Vertebrate cells lacking FEN-1 endonuclease are viable but hypersensitive to methylating agents and H2O2. Nucleic Acids Res 30 (2002) 3273-7.

Mattimore, V. and Battista, J.R.: Radioresistance of Deinococcus radiodurans: functions necessary to survive ionizing radiation are also necessary to survive prolonged desiccation. J Bacteriol 178 (1996) 633-7.

Mazina, O.M., Mazin, A.V., Nakagawa, T., Kolodner, R.D. and Kowalczykowski, S.C.: Saccharomyces cerevisiae Mer3 helicase stimulates 3'-5' heteroduplex extension by Rad51; implications for crossover control in meiotic recombination. Cell 117 (2004) 47-56.

Mazloum, N., Zhou, Q. and Holloman, W.K.: DNA binding, annealing, and strand exchange activities of Brh2 protein from Ustilago maydis. Biochemistry 46 (2007) 7163-73.

Mazo, A., Hodgson, J.W., Petruk, S., Sedkov, Y. and Brock, H.W.: Transcriptional interference: an unexpected layer of complexity in gene regulation. J Cell Sci 120 (2007) 2755-61.

McCaffrey, R., St Johnston, D. and Gonzalez-Reyes, A.: Drosophila mus301/spindle-C encodes a helicase with an essential role in double-strand DNA break repair and meiotic progression. Genetics 174 (2006) 1273-85.

McCready, S. and Marcello, L.: Repair of UV damage in Halobacterium salinarum. Biochem Soc Trans 31 (2003) 694-8.

McCready, S.J., Osman, F. and Yasui, A.: Repair of UV damage in the fission yeast Schizosaccharomyces pombe. Mutat Res 451 (2000) 197-210.
McCutchen-Maloney, S.L., Giannecchini, C.A., Hwang, M.H. and Thelen, M.P.: Domain mapping of the DNA binding, endonuclease, and ERCC1 binding properties of the human DNA repair protein XPF. Biochemistry 38 (1999) 9417-25.
McDonald, J.P., Rapic-Otrin, V., Epstein, J.A., Broughton, B.C., Wang, X., Lehmann, A.R., Wolgemuth, D.J. and Woodgate, R.: Novel human and mouse homologs of Saccharomyces cerevisiae DNA polymerase eta. Genomics 60 (1999) 20-30.
McGlynn, P., Mahdi, A.A. and Lloyd, R.G.: Characterisation of the catalytically active form of RecG helicase. Nucleic Acids Res 28 (2000) 2324-32.
McHugh, P.J., Gill, R.D., Waters, R. and Hartley, J.A.: Excision repair of nitrogen mustard-DNA adducts in Saccharomyces cerevisiae. Nucleic Acids Res 27 (1999) 3259-66.
McHugh, P.J., Sones, W.R. and Hartley, J.A.: Repair of intermediate structures produced at DNA interstrand cross-links in Saccharomyces cerevisiae. Mol Cell Biol 20 (2000) 3425-33.
McHugh, P.J., Spanswick, V.J. and Hartley, J.A.: Repair of DNA interstrand crosslinks: molecular mechanisms and clinical relevance. Lancet Oncol 2 (2001) 483-90.
McInnis, M., O'Neill, G., Fossum, K. and Reagan, M.S.: Epistatic analysis of the roles of the RAD27 and POL4 gene products in DNA base excision repair in S. cerevisiae. DNA Repair (Amst) 1 (2002) 311-5.
McWhir, J., Selfridge, J., Harrison, D.J., Squires, S. and Melton, D.W.: Mice with DNA repair gene (ERCC-1) deficiency have elevated levels of p53, liver nuclear abnormalities and die before weaning. Nat Genet 5 (1993) 217-24.
Mechanic, L.E., Frankel, B.A. and Matson, S.W.: Escherichia coli MutL loads DNA helicase II onto DNA. J Biol Chem 275 (2000) 38337-46.
Meek, K., Kienker, L., Dallas, C., Wang, W., Dark, M.J., Venta, P.J., Huie, M.L., Hirschhorn, R. and Bell, T.: SCID in Jack Russell terriers: a new animal model of DNA-PKcs deficiency. J Immunol 167 (2001) 2142-50.
Meetei, A.R., Medhurst, A.L., Ling, C., Xue, Y., Singh, T.R., Bier, P., Steltenpool, J., Stone, S., Dokal, I., Mathew, C.G., Hoatlin, M., Joenje, H., de Winter, J.P. and Wang, W.: A human ortholog of archaeal DNA repair protein Hef is defective in Fanconi anemia complementation group M. Nat Genet 37 (2005) 958-63.
Merlo, A., Mabry, M., Gabrielson, E., Vollmer, R., Baylin, S.B. and Sidransky, D.: Frequent microsatellite instability in primary small cell lung cancer. Cancer Res 54 (1994) 2098-101.
Mevarech, M. and Werczberger, R.: Genetic transfer in *Halobacterium volcanii*. J Bacteriol 162 (1985) 461-2.
Mickelsen, S., Snyder, C., Trujillo, K., Bogue, M., Roth, D.B. and Meek, K.: Modulation of terminal deoxynucleotidyltransferase activity by the DNA-dependent protein kinase. J Immunol 163 (1999) 834-43.
Miller, R.D., Hogg, J., Ozaki, J.H., Gell, D., Jackson, S.P. and Riblet, R.: Gene for the catalytic subunit of mouse DNA-dependent protein kinase maps to the scid locus. Proc Natl Acad Sci U S A 92 (1995) 10792-5.
Miller, R.D., Prakash, L. and Prakash, S.: Defective excision of pyrimidine dimers and interstrand DNA crosslinks in rad7 and rad23 mutants of Saccharomyces cerevisiae. Mol Gen Genet 188 (1982a) 235-9.
Miller, R.D., Prakash, L. and Prakash, S.: Genetic control of excision of Saccharomyces cerevisiae interstrand DNA cross-links induced by psoralen plus near-UV light. Mol Cell Biol 2 (1982b) 939-48.
Mills, K.D., Sinclair, D.A. and Guarente, L.: MEC1-dependent redistribution of the Sir3 silencing protein from telomeres to DNA double-strand breaks. Cell 97 (1999) 609-20.
Milne, G.T., Jin, S., Shannon, K.B. and Weaver, D.T.: Mutations in two Ku homologs define a DNA end-joining repair pathway in Saccharomyces cerevisiae. Mol Cell Biol 16 (1996) 4189-98.
Minko, I.G., Harbut, M.B., Kozekov, I.D., Kozekova, A., Jakobs, P.M., Olson, S.B., Moses, R.E., Harris, T.M., Rizzo, C.J. and Lloyd, R.S.: Role for DNA polymerase kappa in the processing of N2-N2-guanine interstrand cross-links. J Biol Chem 283 (2008) 17075-82.
Mishina, Y., Duguid, E.M. and He, C.: Direct reversal of DNA alkylation damage. Chem Rev 106 (2006) 215-32.
Missura, M., Buterin, T., Hindges, R., Hubscher, U., Kasparkova, J., Brabec, V. and Naegeli, H.: Double-check probing of DNA bending and unwinding by XPA-RPA: an architectural function in DNA repair. Embo J 20 (2001) 3554-64.

Mocquet, V., Laine, J.P., Riedl, T., Yajin, Z., Lee, M.Y. and Egly, J.M.: Sequential recruitment of the repair factors during NER: the role of XPG in initiating the resynthesis step. Embo J 27 (2008) 155-67.
Modesti, M., Hesse, J.E. and Gellert, M.: DNA binding of Xrcc4 protein is associated with V(D)J recombination but not with stimulation of DNA ligase IV activity. Embo J 18 (1999) 2008-18.
Modrich, P.: Methyl-directed DNA mismatch correction. J Biol Chem 264 (1989) 6597-600.
Modrich, P. and Lahue, R.: Mismatch repair in replication fidelity, genetic recombination, and cancer biology. Annu Rev Biochem 65 (1996) 101-33.
Moens, S. and Vanderleyden, J.: Glycoproteins in prokaryotes. Arch Microbiol 168 (1997) 169-75.
Moldovan, G.L., Pfander, B. and Jentsch, S.: PCNA, the maestro of the replication fork. Cell 129 (2007) 665-79.
Moolenaar, G.F., Moorman, C. and Goosen, N.: Role of the Escherichia coli nucleotide excision repair proteins in DNA replication. J Bacteriol 182 (2000) 5706-14.
Moolenaar, G.F., van Rossum-Fikkert, S., van Kesteren, M. and Goosen, N.: Cho, a second endonuclease involved in Escherichia coli nucleotide excision repair. Proc Natl Acad Sci U S A 99 (2002) 1467-72.
Moore, C.W.: Responses of radiation-sensitive mutants of Saccharomyces cerevisiae to lethal effects of bleomycin. Mutat Res 51 (1978) 165-80.
Moore, J.K. and Haber, J.E.: Capture of retrotransposon DNA at the sites of chromosomal double-strand breaks. Nature 383 (1996) 644-6.
Morales, J.C., Xia, Z., Lu, T., Aldrich, M.B., Wang, B., Rosales, C., Kellems, R.E., Hittelman, W.N., Elledge, S.J. and Carpenter, P.B.: Role for the BRCA1 C-terminal repeats (BRCT) protein 53BP1 in maintaining genomic stability. J Biol Chem 278 (2003) 14971-7.
Moreau, S., Ferguson, J.R. and Symington, L.S.: The nuclease activity of Mre11 is required for meiosis but not for mating type switching, end joining, or telomere maintenance. Mol Cell Biol 19 (1999) 556-66.
Morel, P., Hejna, J.A., Ehrlich, S.D. and Cassuto, E.: Antipairing and strand transferase activities of E. coli helicase II (UvrD). Nucleic Acids Res 21 (1993) 3205-9.
Morimatsu, K. and Kowalczykowski, S.C.: RecFOR proteins load RecA protein onto gapped DNA to accelerate DNA strand exchange: a universal step of recombinational repair. Mol Cell 11 (2003) 1337-47.
Mortensen, U.H., Bendixen, C., Sunjevaric, I. and Rothstein, R.: DNA strand annealing is promoted by the yeast Rad52 protein. Proc Natl Acad Sci U S A 93 (1996) 10729-34.
Moser, J., Kool, H., Giakzidis, I., Caldecott, K., Mullenders, L.H. and Fousteri, M.I.: Sealing of chromosomal DNA nicks during nucleotide excision repair requires XRCC1 and DNA ligase III alpha in a cell-cycle-specific manner. Mol Cell 27 (2007) 311-23.
Moshous, D., Callebaut, I., de Chasseval, R., Corneo, B., Cavazzana-Calvo, M., Le Deist, F., Tezcan, I., Sanal, O., Bertrand, Y., Philippe, N., Fischer, A. and de Villartay, J.P.: Artemis, a novel DNA double-strand break repair/V(D)J recombination protein, is mutated in human severe combined immune deficiency. Cell 105 (2001) 177-86.
Moynahan, M.E.: The cancer connection: BRCA1 and BRCA2 tumor suppression in mice and humans. Oncogene 21 (2002) 8994-9007.
Moynahan, M.E., Pierce, A.J. and Jasin, M.: BRCA2 is required for homology-directed repair of chromosomal breaks. Mol Cell 7 (2001) 263-72.
Mu, D., Bessho, T., Nechev, L.V., Chen, D.J., Harris, T.M., Hearst, J.E. and Sancar, A.: DNA interstrand cross-links induce futile repair synthesis in mammalian cell extracts. Mol Cell Biol 20 (2000) 2446-54.
Mu, D., Hsu, D.S. and Sancar, A.: Reaction mechanism of human DNA repair excision nuclease. J Biol Chem 271 (1996) 8285-94.
Mu, D., Wakasugi, M., Hsu, D.S. and Sancar, A.: Characterization of reaction intermediates of human excision repair nuclease. J Biol Chem 272 (1997) 28971-9.
Mullakhanbhai, M.F. and Larsen, H.: Halobacterium volcanii spec. nov., a Dead Sea halobacterium with a moderate salt requirement. Arch Microbiol 104 (1975) 207-14.
Mullen, J.R., Kaliraman, V., Ibrahim, S.S. and Brill, S.J.: Requirement for three novel protein complexes in the absence of the Sgs1 DNA helicase in Saccharomyces cerevisiae. Genetics 157 (2001) 103-18.
Mulsant, P., Gatignol, A., Dalens, M. and Tiraby, G.: Phleomycin resistance as a dominant selectable marker in CHO cells. Somat Cell Mol Genet 14 (1988) 243-52.
Murakumo, Y., Roth, T., Ishii, H., Rasio, D., Numata, S., Croce, C.M. and Fishel, R.: A human REV7 homolog that interacts with the polymerase zeta catalytic subunit hREV3 and the spindle assembly checkpoint protein hMAD2. J Biol Chem 275 (2000) 4391-7.

Murante, R.S., Huang, L., Turchi, J.J. and Bambara, R.A.: The calf 5'- to 3'-exonuclease is also an endonuclease with both activities dependent on primers annealed upstream of the point of cleavage. J Biol Chem 269 (1994) 1191-6.
Murray, D., Vallee-Lucic, L., Rosenberg, E. and Andersson, B.: Sensitivity of nucleotide excision repair-deficient human cells to ionizing radiation and cyclophosphamide. Anticancer Res 22 (2002) 21-6.
Murray, J.M., Tavassoli, M., al-Harithy, R., Sheldrick, K.S., Lehmann, A.R., Carr, A.M. and Watts, F.Z.: Structural and functional conservation of the human homolog of the Schizosaccharomyces pombe rad2 gene, which is required for chromosome segregation and recovery from DNA damage. Mol Cell Biol 14 (1994) 4878-88.
Myllykallio, H., Lopez, P., Lopez-Garcia, P., Heilig, R., Saurin, W., Zivanovic, Y., Philippe, H. and Forterre, P.: Bacterial mode of replication with eukaryotic-like machinery in a hyperthermophilic archaeon. Science 288 (2000) 2212-5.
Nakagawa, T., Datta, A. and Kolodner, R.D.: Multiple functions of MutS- and MutL-related heterocomplexes. Proc Natl Acad Sci U S A 96 (1999) 14186-8.
Nakagawa, T., Flores-Rozas, H. and Kolodner, R.D.: The MER3 helicase involved in meiotic crossing over is stimulated by single-stranded DNA-binding proteins and unwinds DNA in the 3' to 5' direction. J Biol Chem 276 (2001) 31487-93.
Nakagawa, T. and Ogawa, H.: The Saccharomyces cerevisiae MER3 gene, encoding a novel helicase-like protein, is required for crossover control in meiosis. Embo J 18 (1999) 5714-23.
Nassif, N., Penney, J., Pal, S., Engels, W.R. and Gloor, G.B.: Efficient copying of nonhomologous sequences from ectopic sites via P-element-induced gap repair. Mol Cell Biol 14 (1994) 1613-25.
Negritto, M.C., Qiu, J., Ratay, D.O., Shen, B. and Bailis, A.M.: Novel function of Rad27 (FEN-1) in restricting short-sequence recombination. Mol Cell Biol 21 (2001) 2349-58.
New, J.H., Sugiyama, T., Zaitseva, E. and Kowalczykowski, S.C.: Rad52 protein stimulates DNA strand exchange by Rad51 and replication protein A. Nature 391 (1998) 407-10.
Newman, M., Murray-Rust, J., Lally, J., Rudolf, J., Fadden, A., Knowles, P.P., White, M.F. and McDonald, N.Q.: Structure of an XPF endonuclease with and without DNA suggests a model for substrate recognition. Embo J 24 (2005) 895-905.
Nicholson, W.L., Munakata, N., Horneck, G., Melosh, H.J. and Setlow, P.: Resistance of Bacillus endospores to extreme terrestrial and extraterrestrial environments. Microbiol Mol Biol Rev 64 (2000) 548-72.
Nick McElhinny, S.A., Havener, J.M., Garcia-Diaz, M., Juarez, R., Bebenek, K., Kee, B.L., Blanco, L., Kunkel, T.A. and Ramsden, D.A.: A gradient of template dependence defines distinct biological roles for family X polymerases in nonhomologous end joining. Mol Cell 19 (2005) 357-66.
Nick McElhinny, S.A., Snowden, C.M., McCarville, J. and Ramsden, D.A.: Ku recruits the XRCC4-ligase IV complex to DNA ends. Mol Cell Biol 20 (2000) 2996-3003.
Niedernhofer, L.J.: The Fanconi anemia signalosome anchor. Mol Cell 25 (2007) 487-90.
Niedernhofer, L.J., Essers, J., Weeda, G., Beverloo, B., de Wit, J., Muijtjens, M., Odijk, H., Hoeijmakers, J.H. and Kanaar, R.: The structure-specific endonuclease Ercc1-Xpf is required for targeted gene replacement in embryonic stem cells. Embo J 20 (2001) 6540-9.
Niedernhofer, L.J., Odijk, H., Budzowska, M., van Drunen, E., Maas, A., Theil, A.F., de Wit, J., Jaspers, N.G., Beverloo, H.B., Hoeijmakers, J.H. and Kanaar, R.: The structure-specific endonuclease Ercc1-Xpf is required to resolve DNA interstrand cross-link-induced double-strand breaks. Mol Cell Biol 24 (2004) 5776-87.
Nishino, T., Komori, K., Ishino, Y. and Morikawa, K.: Dissection of the regional roles of the archaeal Holliday junction resolvase Hjc by structural and mutational analyses. J Biol Chem 276 (2001a) 35735-40.
Nishino, T., Komori, K., Ishino, Y. and Morikawa, K.: X-ray and biochemical anatomy of an archaeal XPF/Rad1/Mus81 family nuclease: similarity between its endonuclease domain and restriction enzymes. Structure 11 (2003) 445-57.
Nishino, T., Komori, K., Ishino, Y. and Morikawa, K.: Structural and functional analyses of an archaeal XPF/Rad1/Mus81 nuclease: asymmetric DNA binding and cleavage mechanisms. Structure 13 (2005a) 1183-92.
Nishino, T., Komori, K., Tsuchiya, D., Ishino, Y. and Morikawa, K.: Crystal structure of the archaeal holliday junction resolvase Hjc and implications for DNA recognition. Structure 9 (2001b) 197-204.
Nishino, T., Komori, K., Tsuchiya, D., Ishino, Y. and Morikawa, K.: Crystal structure and functional implications of Pyrococcus furiosus hef helicase domain involved in branched DNA processing. Structure 13 (2005b) 143-53.
Noll, D.M., Mason, T.M. and Miller, P.S.: Formation and repair of interstrand cross-links in DNA. Chem Rev 106 (2006) 277-301.

Norais, C., Hawkins, M., Hartman, A.L., Eisen, J.A., Myllykallio, H. and Allers, T.: Genetic and physical mapping of DNA replication origins in Haloferax volcanii. PLoS Genet 3 (2007a) e77.
Norais, C., Hawkins, M., Hartman, A.L., Eisen, J.A., Myllykallio, H. and Allers, T.: Genetic and physical mapping of DNA replication origins in *Haloferax volcanii*. PLoS Genet (Submitted) (2007b).
Nordstrom, K., Wagner, E.G., Persson, C., Blomberg, P. and Ohman, M.: Translational control by antisense RNA in control of plasmid replication. Gene 72 (1988) 237-40.
Nouspikel, T., Lalle, P., Leadon, S.A., Cooper, P.K. and Clarkson, S.G.: A common mutational pattern in Cockayne syndrome patients from xeroderma pigmentosum group G: implications for a second XPG function. Proc Natl Acad Sci U S A 94 (1997) 3116-21.
O'Donovan, A., Scherly, D., Clarkson, S.G. and Wood, R.D.: Isolation of active recombinant XPG protein, a human DNA repair endonuclease. J Biol Chem 269 (1994) 15965-8.
Ogawa, H., Shimada, K. and Tomizawa, J.: Studies on radiation-sensitive mutants of E. coli. I. Mutants defective in the repair synthesis. Mol Gen Genet 101 (1968) 227-44.
Ogawa, T., Yu, X., Shinohara, A. and Egelman, E.H.: Similarity of the yeast RAD51 filament to the bacterial RecA filament. Science 259 (1993) 1896-9.
Ogrunc, M., Becker, D.F., Ragsdale, S.W. and Sancar, A.: Nucleotide excision repair in the third kingdom. J Bacteriol 180 (1998) 5796-8.
Ogrunc, M. and Sancar, A.: Identification and characterization of human MUS81-MMS4 structure-specific endonuclease. J Biol Chem 278 (2003) 21715-20.
Oh, E.Y. and Grossman, L.: The effect of Escherichia coli Uvr protein binding on the topology of supercoiled DNA. Nucleic Acids Res 14 (1986) 8557-71.
Oh, S.D., Lao, J.P., Hwang, P.Y., Taylor, A.F., Smith, G.R. and Hunter, N.: BLM ortholog, Sgs1, prevents aberrant crossing-over by suppressing formation of multichromatid joint molecules. Cell 130 (2007) 259-72.
Oh, S.D., Lao, J.P., Taylor, A.F., Smith, G.R. and Hunter, N.: RecQ helicase, Sgs1, and XPF family endonuclease, Mus81-Mms4, resolve aberrant joint molecules during meiotic recombination. Mol Cell 31 (2008) 324-36.
Ohmori, H., Ohashi, E. and Ogi, T.: Mammalian Pol kappa: regulation of its expression and lesion substrates. Adv Protein Chem 69 (2004) 265-78.
Okano, S., Kanno, S., Nakajima, S. and Yasui, A.: Cellular responses and repair of single-strand breaks introduced by UV damage endonuclease in mammalian cells. J Biol Chem 275 (2000) 32635-41.
Olsen, G.J. and Woese, C.R.: Lessons from an Archaeal genome: what are we learning from Methanococcus jannaschii? Trends Genet 12 (1996) 377-9.
Ophir, T. and Gutnick, D.L.: A Role for Exopolysaccharides in the Protection of Microorganisms from Desiccation. Appl Environ Microbiol 60 (1994) 740-745.
Oren, A.: Bioenergetic aspects of halophilism. Microbiol Mol Biol Rev 63 (1999) 334-48.
Orren, D.K., Machwe, A., Karmakar, P., Piotrowski, J., Cooper, M.P. and Bohr, V.A.: A functional interaction of Ku with Werner exonuclease facilitates digestion of damaged DNA. Nucleic Acids Res 29 (2001) 1926-34.
Orren, D.K. and Sancar, A.: Formation and enzymatic properties of the UvrB.DNA complex. J Biol Chem 265 (1990) 15796-803.
Ortenberg, R., Rozenblatt-Rosen, O. and Mevarech, M.: The extremely halophilic archaeon Haloferax volcanii has two very different dihydrofolate reductases. Mol Microbiol 35 (2000) 1493-505.
Osman, F., Dixon, J., Barr, A.R. and Whitby, M.C.: The F-Box DNA helicase Fbh1 prevents Rhp51-dependent recombination without mediator proteins. Mol Cell Biol 25 (2005) 8084-96.
Osman, F., Dixon, J., Doe, C.L. and Whitby, M.C.: Generating crossovers by resolution of nicked Holliday junctions: a role for Mus81-Eme1 in meiosis. Mol Cell 12 (2003) 761-74.
Otterlei, M., Kavli, B., Standal, R., Skjelbred, C., Bharati, S. and Krokan, H.E.: Repair of chromosomal abasic sites in vivo involves at least three different repair pathways. Embo J 19 (2000) 5542-51.
Otto, C.J., Almqvist, E., Hayden, M.R. and Andrew, S.E.: The "flap" endonuclease gene FEN1 is excluded as a candidate gene implicated in the CAG repeat expansion underlying Huntington disease. Clin Genet 59 (2001) 122-7.
Ouhammouch, M.: Transcriptional regulation in Archaea. Curr Opin Genet Dev 14 (2004) 133-8.
Palmbos, P.L., Daley, J.M. and Wilson, T.E.: Mutations of the Yku80 C terminus and Xrs2 FHA domain specifically block yeast nonhomologous end joining. Mol Cell Biol 25 (2005) 10782-90.
Palombo, F., Iaccarino, I., Nakajima, E., Ikejima, M., Shimada, T. and Jiricny, J.: hMutSbeta, a heterodimer of hMSH2 and hMSH3, binds to insertion/deletion loops in DNA. Curr Biol 6 (1996) 1181-4.

Papadopoulos, N., Nicolaides, N.C., Wei, Y.F., Ruben, S.M., Carter, K.C., Rosen, C.A., Haseltine, W.A., Fleischmann, R.D., Fraser, C.M., Adams, M.D. and et al.: Mutation of a mutL homolog in hereditary colon cancer. Science 263 (1994) 1625-9.

Papouli, E., Chen, S., Davies, A.A., Huttner, D., Krejci, L., Sung, P. and Ulrich, H.D.: Crosstalk between SUMO and ubiquitin on PCNA is mediated by recruitment of the helicase Srs2p. Mol Cell 19 (2005) 123-33.

Paques, F. and Haber, J.E.: Two pathways for removal of nonhomologous DNA ends during double-strand break repair in Saccharomyces cerevisiae. Mol Cell Biol 17 (1997) 6765-71.

Paques, F. and Haber, J.E.: Multiple pathways of recombination induced by double-strand breaks in Saccharomyces cerevisiae. Microbiol Mol Biol Rev 63 (1999) 349-404.

Parenteau, J. and Wellinger, R.J.: Differential processing of leading- and lagging-strand ends at Saccharomyces cerevisiae telomeres revealed by the absence of Rad27p nuclease. Genetics 162 (2002) 1583-94.

Park, E., Guzder, S.N., Koken, M.H., Jaspers-Dekker, I., Weeda, G., Hoeijmakers, J.H., Prakash, S. and Prakash, L.: RAD25 (SSL2), the yeast homolog of the human xeroderma pigmentosum group B DNA repair gene, is essential for viability. Proc Natl Acad Sci U S A 89 (1992) 11416-20.

Park, S.G., Cha, M.K., Jeong, W. and Kim, I.H.: Distinct physiological functions of thiol peroxidase isoenzymes in Saccharomyces cerevisiae. J Biol Chem 275 (2000) 5723-32.

Parker, B.O. and Marinus, M.G.: Repair of DNA heteroduplexes containing small heterologous sequences in Escherichia coli. Proc Natl Acad Sci U S A 89 (1992) 1730-4.

Parrish, J.Z., Yang, C., Shen, B. and Xue, D.: CRN-1, a Caenorhabditis elegans FEN-1 homologue, cooperates with CPS-6/EndoG to promote apoptotic DNA degradation. Embo J 22 (2003) 3451-60.

Parsons, C.A., Stasiak, A. and West, S.C.: The E.coli RuvAB proteins branch migrate Holliday junctions through heterologous DNA sequences in a reaction facilitated by SSB. Embo J 14 (1995) 5736-44.

Pastink, A., Eeken, J.C. and Lohman, P.H.: Genomic integrity and the repair of double-strand DNA breaks. Mutat Res 480-481 (2001) 37-50.

Pastwa, E. and Blasiak, J.: Non-homologous DNA end joining. Acta Biochim Pol 50 (2003) 891-908.

Patel, K.J. and Joenje, H.: Fanconi anemia and DNA replication repair. DNA Repair (Amst) 6 (2007) 885-90.

Paull, T.T. and Gellert, M.: The 3' to 5' exonuclease activity of Mre 11 facilitates repair of DNA double-strand breaks. Mol Cell 1 (1998) 969-79.

Paulson, H.L. and Fischbeck, K.H.: Trinucleotide repeats in neurogenetic disorders. Annu Rev Neurosci 19 (1996) 79-107.

Paz, M.M., Kumar, G.S., Glover, M., Waring, M.J. and Tomasz, M.: Mitomycin dimers: polyfunctional cross-linkers of DNA. J Med Chem 47 (2004) 3308-19.

Pederson, T.: RNA interference and mRNA silencing, 2004: how far will they reach? Mol Biol Cell 15 (2004) 407-10.

Pellegrini, L. and Venkitaraman, A.: Emerging functions of BRCA2 in DNA recombination. Trends Biochem Sci 29 (2004) 310-6.

Pellegrini, L., Yu, D.S., Lo, T., Anand, S., Lee, M., Blundell, T.L. and Venkitaraman, A.R.: Insights into DNA recombination from the structure of a RAD51-BRCA2 complex. Nature 420 (2002) 287-93.

Perez, P., Tiraby, G., Kallerhoff, J. and Perret, J.: Phleomycin resistance as a dominant selectable marker for plant cell transformation. Plant Mol Biol 13 (1989) 365-73.

Perry, J.J., Yannone, S.M., Holden, L.G., Hitomi, C., Asaithamby, A., Han, S., Cooper, P.K., Chen, D.J. and Tainer, J.A.: WRN exonuclease structure and molecular mechanism imply an editing role in DNA end processing. Nat Struct Mol Biol 13 (2006) 414-22.

Petranovic, M., Zahradka, K., Zahradka, D., Petranovic, D., Nagy, B., Salaj-Smic, E. and Petranovic, D.: Genetic evidence that the elevated levels of Escherichia coli helicase II antagonize recombinational DNA repair. Biochimie 83 (2001) 1041-7.

Petukhova, G., Stratton, S. and Sung, P.: Catalysis of homologous DNA pairing by yeast Rad51 and Rad54 proteins. Nature 393 (1998) 91-4.

Petukhova, G., Stratton, S.A. and Sung, P.: Single strand DNA binding and annealing activities in the yeast recombination factor Rad59. J Biol Chem 274 (1999) 33839-42.

Petukhova, G., Sung, P. and Klein, H.: Promotion of Rad51-dependent D-loop formation by yeast recombination factor Rdh54/Tid1. Genes Dev 14 (2000) 2206-15.

Pfander, B., Moldovan, G.L., Sacher, M., Hoege, C. and Jentsch, S.: SUMO-modified PCNA recruits Srs2 to prevent recombination during S phase. Nature 436 (2005) 428-33.

Pitcher, R.S., Brissett, N.C. and Doherty, A.J.: Nonhomologous end-joining in bacteria: a microbial perspective. Annu Rev Microbiol 61 (2007) 259-82.

Pitcher, R.S., Tonkin, L.M., Green, A.J. and Doherty, A.J.: Domain structure of a NHEJ DNA repair ligase from Mycobacterium tuberculosis. J Mol Biol 351 (2005) 531-44.
Plank, J.L., Wu, J. and Hsieh, T.S.: Topoisomerase IIIalpha and Bloom's helicase can resolve a mobile double Holliday junction substrate through convergent branch migration. Proc Natl Acad Sci U S A 103 (2006) 11118-23.
Poltoratsky, V.P., Shi, X., York, J.D., Lieber, M.R. and Carter, T.H.: Human DNA-activated protein kinase (DNA-PK) is homologous to phosphatidylinositol kinases. J Immunol 155 (1995) 4529-33.
Popoff, S.C., Spira, A.I., Johnson, A.W. and Demple, B.: Yeast structural gene (APN1) for the major apurinic endonuclease: homology to Escherichia coli endonuclease IV. Proc Natl Acad Sci U S A 87 (1990) 4193-7.
Potts, M.: Desiccation tolerance of prokaryotes. Microbiol Rev 58 (1994) 755-805.
Povirk, L.F.: DNA damage and mutagenesis by radiomimetic DNA-cleaving agents: bleomycin, neocarzinostatin and other enediynes. Mutat Res 355 (1996) 71-89.
Povirk, L.F., Hogan, M., Dattagupta, N. and Buechner, M.: Copper(II).bleomycin, iron(III).bleomycin, and copper(II).phleomycin: comparative study of deoxyribonucleic acid binding. Biochemistry 20 (1981) 665-71.
Prakash, L.: Defective thymine dimer excision in radiation-sensitive mutants rad10 and rad16 of Saccharomyces cerevisiae. Mol Gen Genet 152 (1977) 125-8.
Prakash, L. and Prakash, S.: Isolation and characterization of MMS-sensitive mutants of Saccharomyces cerevisiae. Genetics 86 (1977) 33-55.
Prakash, L. and Prakash, S.: Three additional genes involved in pyrimidine dimer removal in Saccharomyces cerevisiae: RAD7, RAD14 and MMS19. Mol Gen Genet 176 (1979) 351-9.
Prakash, S. and Prakash, L.: Nucleotide excision repair in yeast. Mutat Res 451 (2000) 13-24.
Prasad, A., Wallace, S.S. and Pederson, D.S.: Initiation of base excision repair of oxidative lesions in nucleosomes by the human, bifunctional DNA glycosylase NTH1. Mol Cell Biol 27 (2007) 8442-53.
Prasad, R., Widen, S.G., Singhal, R.K., Watkins, J., Prakash, L. and Wilson, S.H.: Yeast open reading frame YCR14C encodes a DNA beta-polymerase-like enzyme. Nucleic Acids Res 21 (1993) 5301-7.
Prolla, T.A., Pang, Q., Alani, E., Kolodner, R.D. and Liskay, R.M.: MLH1, PMS1, and MSH2 interactions during the initiation of DNA mismatch repair in yeast. Science 265 (1994) 1091-3.
Pukkila, P.J., Peterson, J., Herman, G., Modrich, P. and Meselson, M.: Effects of high levels of DNA adenine methylation on methyl-directed mismatch repair in Escherichia coli. Genetics 104 (1983) 571-82.
Puyet, A., Greenberg, B. and Lacks, S.A.: The exoA gene of Streptococcus pneumoniae and its product, a DNA exonuclease with apurinic endonuclease activity. J Bacteriol 171 (1989) 2278-86.
Quaiser, A., Constantinesco, F., White, M.F., Forterre, P. and Elie, C.: The Mre11 protein interacts with both Rad50 and the HerA bipolar helicase and is recruited to DNA following gamma irradiation in the archaeon Sulfolobus acidocaldarius. BMC Mol Biol 9 (2008) 25.
Raaphorst, G.P. and Kruuv, J.: Effect of salt solutions on radiosensitivity of mammalian cells. I. Specific ion effects. Int J Radiat Biol Relat Stud Phys Chem Med 32 (1977) 71-88.
Radany, E.H. and Friedberg, E.C.: A pyrimidine dimer-DNA glycosylase activity associated with the v gene product of bacterophage T4. Nature 286 (1980) 182-5.
Ragu, S., Faye, G., Iraqui, I., Masurel-Heneman, A., Kolodner, R.D. and Huang, M.E.: Oxygen metabolism and reactive oxygen species cause chromosomal rearrangements and cell death. Proc Natl Acad Sci U S A 104 (2007) 9747-52.
Ramotar, D., Popoff, S.C., Gralla, E.B. and Demple, B.: Cellular role of yeast Apn1 apurinic endonuclease/3'-diesterase: repair of oxidative and alkylation DNA damage and control of spontaneous mutation. Mol Cell Biol 11 (1991) 4537-44.
Raymond, A.C., Rideout, M.C., Staker, B., Hjerrild, K. and Burgin, A.B., Jr.: Analysis of human tyrosyl-DNA phosphodiesterase I catalytic residues. J Mol Biol 338 (2004) 895-906.
Raymond, A.C., Staker, B.L. and Burgin, A.B., Jr.: Substrate specificity of tyrosyl-DNA phosphodiesterase I (Tdp1). J Biol Chem 280 (2005) 22029-35.
Rayssiguier, C., Thaler, D.S. and Radman, M.: The barrier to recombination between Escherichia coli and Salmonella typhimurium is disrupted in mismatch-repair mutants. Nature 342 (1989) 396-401.
Reagan, M.S., Pittenger, C., Siede, W. and Friedberg, E.C.: Characterization of a mutant strain of Saccharomyces cerevisiae with a deletion of the RAD27 gene, a structural homolog of the RAD2 nucleotide excision repair gene. J Bacteriol 177 (1995) 364-71.
Reddy, Y.V., Ding, Q., Lees-Miller, S.P., Meek, K. and Ramsden, D.A.: Non-homologous end joining requires that the DNA-PK complex undergo an autophosphorylation-dependent rearrangement at DNA ends. J Biol Chem 279 (2004) 39408-13.

Reenan, R.A. and Kolodner, R.D.: Characterization of insertion mutations in the Saccharomyces cerevisiae MSH1 and MSH2 genes: evidence for separate mitochondrial and nuclear functions. Genetics 132 (1992) 975-85.
Reeve, J.N.: Archaeal chromatin and transcription. Mol Microbiol 48 (2003) 587-98.
Revy, P., Malivert, L. and de Villartay, J.P.: Cernunnos-XLF, a recently identified non-homologous end-joining factor required for the development of the immune system. Curr Opin Allergy Clin Immunol 6 (2006) 416-20.
Reynolds, R.J. and Friedberg, E.C.: Molecular mechanisms of pyrimidine dimer excision in Saccharomyces cerevisiae: incision of ultraviolet-irradiated deoxyribonucleic acid in vivo. J Bacteriol 146 (1981) 692-704.
Riballo, E., Kuhne, M., Rief, N., Doherty, A., Smith, G.C., Recio, M.J., Reis, C., Dahm, K., Fricke, A., Krempler, A., Parker, A.R., Jackson, S.P., Gennery, A., Jeggo, P.A. and Lobrich, M.: A pathway of double-strand break rejoining dependent upon ATM, Artemis, and proteins locating to gamma-H2AX foci. Mol Cell 16 (2004) 715-24.
Richards, J.D., Johnson, K.A., Liu, H., McRobbie, A.M., McMahon, S., Oke, M., Carter, L., Naismith, J.H. and White, M.F.: Structure of the DNA repair helicase hel308 reveals DNA binding and autoinhibitory domains. J Biol Chem 283 (2008) 5118-26.
Richardson, C., Horikoshi, N. and Pandita, T.K.: The role of the DNA double-strand break response network in meiosis. DNA Repair (Amst) 3 (2004) 1149-64.
Rijkers, T., Van Den Ouweland, J., Morolli, B., Rolink, A.G., Baarends, W.M., Van Sloun, P.P., Lohman, P.H. and Pastink, A.: Targeted inactivation of mouse RAD52 reduces homologous recombination but not resistance to ionizing radiation. Mol Cell Biol 18 (1998) 6423-9.
Roberts, J.A., Bell, S.D. and White, M.F.: An archaeal XPF repair endonuclease dependent on a heterotrimeric PCNA. Mol Microbiol 48 (2003) 361-71.
Roberts, J.A. and White, M.F.: An archaeal endonuclease displays key properties of both eukaryal XPF-ERCC1 and Mus81. J Biol Chem 280 (2005a) 5924-8.
Roberts, J.A. and White, M.F.: DNA end-directed and processive nuclease activities of the archaeal XPF enzyme. Nucleic Acids Res 33 (2005b) 6662-70.
Robinson, N.P., Dionne, I., Lundgren, M., Marsh, V.L., Bernander, R. and Bell, S.D.: Identification of two origins of replication in the single chromosome of the archaeon Sulfolobus solfataricus. Cell 116 (2004) 25-38.
Robson, C.N. and Hickson, I.D.: Isolation of cDNA clones encoding a human apurinic/apyrimidinic endonuclease that corrects DNA repair and mutagenesis defects in E. coli xth (exonuclease III) mutants. Nucleic Acids Res 19 (1991) 5519-23.
Rockmill, B., Fung, J.C., Branda, S.S. and Roeder, G.S.: The Sgs1 helicase regulates chromosome synapsis and meiotic crossing over. Curr Biol 13 (2003) 1954-62.
Rong, L. and Klein, H.L.: Purification and characterization of the SRS2 DNA helicase of the yeast Saccharomyces cerevisiae. J Biol Chem 268 (1993) 1252-9.
Rooney, S., Alt, F.W., Lombard, D., Whitlow, S., Eckersdorff, M., Fleming, J., Fugmann, S., Ferguson, D.O., Schatz, D.G. and Sekiguchi, J.: Defective DNA repair and increased genomic instability in Artemis-deficient murine cells. J Exp Med 197 (2003) 553-65.
Roseaulin, L., Yamada, Y., Tsutsui, Y., Russell, P., Iwasaki, H. and Arcangioli, B.: Mus81 is essential for sister chromatid recombination at broken replication forks. Embo J 27 (2008) 1378-87.
Rother, M. and Metcalf, W.W.: Genetic technologies for Archaea. Curr Opin Microbiol 8 (2005) 745-51.
Rothschild, L.J. and Mancinelli, R.L.: Life in extreme environments. Nature 409 (2001) 1092-101.
Ruhland, A., Kircher, M., Wilborn, F. and Brendel, M.: A yeast mutant specifically sensitive to bifunctional alkylation. Mutat Res 91 (1981) 457-62.
Saffran, W.A., Ahmed, S., Bellevue, S., Pereira, G., Patrick, T., Sanchez, W., Thomas, S., Alberti, M. and Hearst, J.E.: DNA repair defects channel interstrand DNA cross-links into alternate recombinational and error-prone repair pathways. J Biol Chem 279 (2004) 36462-9.
Saharia, A., Guittat, L., Crocker, S., Lim, A., Steffen, M., Kulkarni, S. and Stewart, S.A.: Flap endonuclease 1 contributes to telomere stability. Curr Biol 18 (2008) 496-500.
Sancar, A.: DNA excision repair. Annu Rev Biochem 65 (1996) 43-81.
Sander, M. and Ramotar, D.: Partial purification of Pde1 from Saccharomyces cerevisiae: enzymatic redundancy for the repair of 3'-terminal DNA lesions and abasic sites in yeast. Biochemistry 36 (1997) 6100-6.
Sandler, S.J. and Clark, A.J.: RecOR suppression of recF mutant phenotypes in Escherichia coli K-12. J Bacteriol 176 (1994) 3661-72.

Sandler, S.J., Hugenholtz, P., Schleper, C., DeLong, E.F., Pace, N.R. and Clark, A.J.: Diversity of radA genes from cultured and uncultured archaea: comparative analysis of putative RadA proteins and their use as a phylogenetic marker. J Bacteriol 181 (1999) 907-15.
Sandler, S.J., Satin, L.H., Samra, H.S. and Clark, A.J.: recA-like genes from three archaean species with putative protein products similar to Rad51 and Dmc1 proteins of the yeast Saccharomyces cerevisiae. Nucleic Acids Res 24 (1996) 2125-32.
Sanger, F., Nicklen, S. and Coulson, A.R.: DNA sequencing with chain-terminating inhibitors. Proc Natl Acad Sci U S A 74 (1977) 5463-7.
Santucci-Darmanin, S., Neyton, S., Lespinasse, F., Saunieres, A., Gaudray, P. and Paquis-Flucklinger, V.: The DNA mismatch-repair MLH3 protein interacts with MSH4 in meiotic cells, supporting a role for this MutL homolog in mammalian meiotic recombination. Hum Mol Genet 11 (2002) 1697-706.
Saparbaev, M., Prakash, L. and Prakash, S.: Requirement of mismatch repair genes MSH2 and MSH3 in the RAD1-RAD10 pathway of mitotic recombination in Saccharomyces cerevisiae. Genetics 142 (1996) 727-36.
Sargent, R.G., Brenneman, M.A. and Wilson, J.H.: Repair of site-specific double-strand breaks in a mammalian chromosome by homologous and illegitimate recombination. Mol Cell Biol 17 (1997) 267-77.
Sargent, R.G., Meservy, J.L., Perkins, B.D., Kilburn, A.E., Intody, Z., Adair, G.M., Nairn, R.S. and Wilson, J.H.: Role of the nucleotide excision repair gene ERCC1 in formation of recombination-dependent rearrangements in mammalian cells. Nucleic Acids Res 28 (2000) 3771-8.
Sarkar, S., Davies, A.A., Ulrich, H.D. and McHugh, P.J.: DNA interstrand crosslink repair during G1 involves nucleotide excision repair and DNA polymerase zeta. Embo J 25 (2006) 1285-94.
Sarker, A.H., Tsutakawa, S.E., Kostek, S., Ng, C., Shin, D.S., Peris, M., Campeau, E., Tainer, J.A., Nogales, E. and Cooper, P.K.: Recognition of RNA polymerase II and transcription bubbles by XPG, CSB, and TFIIH: insights for transcription-coupled repair and Cockayne Syndrome. Mol Cell 20 (2005) 187-98.
Savery, N.J.: The molecular mechanism of transcription-coupled DNA repair. Trends Microbiol 15 (2007) 326-33.
Savva, R., McAuley-Hecht, K., Brown, T. and Pearl, L.: The structural basis of specific base-excision repair by uracil-DNA glycosylase. Nature 373 (1995) 487-93.
Schild, D., Lio, Y.C., Collins, D.W., Tsomondo, T. and Chen, D.J.: Evidence for simultaneous protein interactions between human Rad51 paralogs. J Biol Chem 275 (2000) 16443-9.
Schlissel, M.S.: Does artemis end the hunt for the hairpin-opening activity in V(D)J recombination? Cell 109 (2002) 1-4.
Schmidt, H., Kapitza-Fecke, P., Stephen, E.R. and Gutz, H.: Some of the swi genes of Schizosaccharomyces pombe also have a function in the repair of radiation damage. Curr Genet 16 (1989) 89-94.
Schofield, M.J. and Hsieh, P.: DNA mismatch repair: molecular mechanisms and biological function. Annu Rev Microbiol 57 (2003) 579-608.
Sczakiel, G.: The design of antisense RNA. Antisense Nucleic Acid Drug Dev 7 (1997) 439-44.
Sedgwick, B.: Repairing DNA-methylation damage. Nat Rev Mol Cell Biol 5 (2004) 148-57.
Sedgwick, B., Bates, P.A., Paik, J., Jacobs, S.C. and Lindahl, T.: Repair of alkylated DNA: recent advances. DNA Repair (Amst) 6 (2007) 429-42.
Seeberg, E., Eide, L. and Bjoras, M.: The base excision repair pathway. Trends Biochem Sci 20 (1995) 391-7.
Seitz, E.M. and Kowalczykowski, S.C.: The DNA binding and pairing preferences of the archaeal RadA protein demonstrate a universal characteristic of DNA strand exchange proteins. Mol Microbiol 37 (2000) 555-60.
Sekelsky, J.J., McKim, K.S., Chin, G.M. and Hawley, R.S.: The Drosophila meiotic recombination gene mei-9 encodes a homologue of the yeast excision repair protein Rad1. Genetics 141 (1995) 619-27.
Seki, M., Gearhart, P.J. and Wood, R.D.: DNA polymerases and somatic hypermutation of immunoglobulin genes. EMBO Rep 6 (2005) 1143-8.
Seki, M., Marini, F. and Wood, R.D.: POLQ (Pol theta), a DNA polymerase and DNA-dependent ATPase in human cells. Nucleic Acids Res 31 (2003) 6117-26.
Seki, M., Masutani, C., Yang, L.W., Schuffert, A., Iwai, S., Bahar, I. and Wood, R.D.: High-efficiency bypass of DNA damage by human DNA polymerase Q. Embo J 23 (2004) 4484-94.
Selby, C.P., Witkin, E.M. and Sancar, A.: Escherichia coli mfd mutant deficient in "mutation frequency decline" lacks strand-specific repair: in vitro complementation with purified coupling factor. Proc Natl Acad Sci U S A 88 (1991) 11574-8.

Setlow, P.: Mechanisms for the prevention of damage to DNA in spores of Bacillus species. Annu Rev Microbiol 49 (1995) 29-54.
Setlow, R.B., Swenson, P.A. and Carrier, W.L.: Thymine Dimers and Inhibition of DNA Synthesis by Ultraviolet Irradiation of Cells. Science 142 (1963) 1464-6.
Sgouros, J., Gaillard, P.H. and Wood, R.D.: A relationship betweena DNA-repair/recombination nuclease family and archaeal helicases. Trends Biochem Sci 24 (1999) 95-7.
Shah, R., Bennett, R.J. and West, S.C.: Genetic recombination in E. coli: RuvC protein cleaves Holliday junctions at resolution hotspots in vitro. Cell 79 (1994) 853-64.
Shahmohammadi, H.R., Asgarani, E., Terato, H., Saito, T., Ohyama, Y., Gekko, K., Yamamoto, O. and Ide, H.: Protective roles of bacterioruberin and intracellular KCl in the resistance of Halobacterium salinarium against DNA-damaging agents. J Radiat Res (Tokyo) 39 (1998) 251-62.
Shao, X. and Grishin, N.V.: Common fold in helix-hairpin-helix proteins. Nucleic Acids Res 28 (2000) 2643-50.
Sharma, S., Otterlei, M., Sommers, J.A., Driscoll, H.C., Dianov, G.L., Kao, H.I., Bambara, R.A. and Brosh, R.M., Jr.: WRN helicase and FEN-1 form a complex upon replication arrest and together process branchmigrating DNA structures associated with the replication fork. Mol Biol Cell 15 (2004a) 734-50.
Sharma, S., Sommers, J.A., Gary, R.K., Friedrich-Heineken, E., Hubscher, U. and Brosh, R.M., Jr.: The interaction site of Flap Endonuclease-1 with WRN helicase suggests a coordination of WRN and PCNA. Nucleic Acids Res 33 (2005) 6769-81.
Sharma, S., Sommers, J.A., Wu, L., Bohr, V.A., Hickson, I.D. and Brosh, R.M., Jr.: Stimulation of flap endonuclease-1 by the Bloom's syndrome protein. J Biol Chem 279 (2004b) 9847-56.
Sharples, G.J., Ingleston, S.M. and Lloyd, R.G.: Holliday junction processing in bacteria: insights from the evolutionary conservation of RuvABC, RecG, and RusA. J Bacteriol 181 (1999) 5543-50.
Shen, B., Singh, P., Liu, R., Qiu, J., Zheng, L., Finger, L.D. and Alas, S.: Multiple but dissectible functions of FEN-1 nucleases in nucleic acid processing, genome stability and diseases. Bioessays 27 (2005) 717-29.
Shen, X., Jun, S., O'Neal, L.E., Sonoda, E., Bemark, M., Sale, J.E. and Li, L.: REV3 and REV1 play major roles in recombination-independent repair of DNA interstrand cross-links mediated by monoubiquitinated proliferating cell nuclear antigen (PCNA). J Biol Chem 281 (2006) 13869-72.
Shen, X., Xiao, H., Ranallo, R., Wu, W.H. and Wu, C.: Modulation of ATP-dependent chromatin-remodeling complexes by inositol polyphosphates. Science 299 (2003) 112-4.
Shi, Q., Thresher, R., Sancar, A. and Griffith, J.: Electron microscopic study of (A)BC excinuclease. DNA is sharply bent in the UvrB-DNA complex. J Mol Biol 226 (1992) 425-32.
Shibata, Y. and Nakamura, T.: Defective flap endonuclease 1 activity in mammalian cells is associated with impaired DNA repair and prolonged S phase delay. J Biol Chem 277 (2002) 746-54.
Shima, H., Suzuki, M. and Shinohara, M.: Isolation and characterization of novel xrs2 mutations in Saccharomyces cerevisiae. Genetics 170 (2005) 71-85.
Shimmin, L.C. and Dennis, P.P.: Conserved sequence elements involved in regulation of ribosomal protein gene expression in halophilic archaea. J Bacteriol 178 (1996) 4737-41.
Shin, D.S., Pellegrini, L., Daniels, D.S., Yelent, B., Craig, L., Bates, D., Yu, D.S., Shivji, M.K., Hitomi, C., Arvai, A.S., Volkmann, N., Tsuruta, H., Blundell, T.L., Venkitaraman, A.R. and Tainer, J.A.: Full-length archaeal Rad51 structure and mutants: mechanisms for RAD51 assembly and control by BRCA2. Embo J 22 (2003) 4566-76.
Shine, J. and Dalgarno, L.: The 3'-terminal sequence of Escherichia coli 16S ribosomal RNA: complementarity to nonsense triplets and ribosome binding sites. Proc Natl Acad Sci U S A 71 (1974) 1342-6.
Shinohara, A., Ogawa, H. and Ogawa, T.: Rad51 protein involved in repair and recombination in S. cerevisiae is a RecA-like protein. Cell 69 (1992) 457-70.
Shinohara, A. and Ogawa, T.: Stimulation by Rad52 of yeast Rad51-mediated recombination. Nature 391 (1998) 404-7.
Shinohara, A., Shinohara, M., Ohta, T., Matsuda, S. and Ogawa, T.: Rad52 forms ring structures and co-operates with RPA in single-strand DNA annealing. Genes Cells 3 (1998) 145-56.
Shiomi, N., Hayashi, E., Sasanuma, S., Mita, K. and Shiomi, T.: Disruption of Xpg increases spontaneous mutation frequency, particularly A:T to C:G transversion. Mutat Res 487 (2001) 127-35.
Shiomi, N., Kito, S., Oyama, M., Matsunaga, T., Harada, Y.N., Ikawa, M., Okabe, M. and Shiomi, T.: Identification of the XPG region that causes the onset of Cockayne syndrome by using Xpg mutant mice generated by the cDNA-mediated knock-in method. Mol Cell Biol 24 (2004) 3712-9.
Shrivastav, M., De Haro, L.P. and Nickoloff, J.A.: Regulation of DNA double-strand break repair pathway choice. Cell Res 18 (2008) 134-47.

Shuster, R.C. and Boyce, R.P.: The excision of thymine dimer from the DNA of UV-irradiated E. coli 15 T-A-U during thymine deprivation. Biochem Biophys Res Commun 16 (1964) 489-96.
Siaud, N., Dray, E., Gy, I., Gerard, E., Takvorian, N. and Doutriaux, M.P.: Brca2 is involved in meiosis in Arabidopsis thaliana as suggested by its interaction with Dmc1. Embo J 23 (2004) 1392-401.
Siede, W., Friedl, A.A., Dianova, I., Eckardt-Schupp, F. and Friedberg, E.C.: The Saccharomyces cerevisiae Ku autoantigen homologue affects radiosensitivity only in the absence of homologous recombination. Genetics 142 (1996) 91-102.
Signon, L., Malkova, A., Naylor, M.L., Klein, H. and Haber, J.E.: Genetic requirements for RAD51- and RAD54-independent break-induced replication repair of a chromosomal double-strand break. Mol Cell Biol 21 (2001) 2048-56.
Sijbers, A.M., van der Spek, P.J., Odijk, H., van den Berg, J., van Duin, M., Westerveld, A., Jaspers, N.G., Bootsma, D. and Hoeijmakers, J.H.: Mutational analysis of the human nucleotide excision repair gene ERCC1. Nucleic Acids Res 24 (1996) 3370-80.
Simons, R.W.: Naturally occurring antisense RNA control--a brief review. Gene 72 (1988) 35-44.
Singleton, S.F., Simonette, R.A., Sharma, N.C. and Roca, A.I.: Intein-mediated affinity-fusion purification of the Escherichia coli RecA protein. Protein Expr Purif 26 (2002) 476-88.
Sladek, F.M., Munn, M.M., Rupp, W.D. and Howard-Flanders, P.: In vitro repair of psoralen-DNA cross-links by RecA, UvrABC, and the 5'-exonuclease of DNA polymerase I. J Biol Chem 264 (1989) 6755-65.
Sleigh, M.J. and Grigg, G.W.: Sulphydryl-mediated DNA breakage by phlemomycin in Escherichia coli. Mutat Res 42 (1977) 181-90.
Slupphaug, G., Kavli, B. and Krokan, H.E.: The interacting pathways for prevention and repair of oxidative DNA damage. Mutat Res 531 (2003) 231-51.
Smirnova, M., Van Komen, S., Sung, P. and Klein, H.L.: Effects of tumor-associated mutations on Rad54 functions. J Biol Chem 279 (2004) 24081-8.
Smogorzewska, A., Matsuoka, S., Vinciguerra, P., McDonald, E.R., 3rd, Hurov, K.E., Luo, J., Ballif, B.A., Gygi, S.P., Hofmann, K., D'Andrea, A.D. and Elledge, S.J.: Identification of the FANCI protein, a monoubiquitinated FANCD2 paralog required for DNA repair. Cell 129 (2007) 289-301.
Snowden, T., Acharya, S., Butz, C., Berardini, M. and Fishel, R.: hMSH4-hMSH5 recognizes Holliday Junctions and forms a meiosis-specific sliding clamp that embraces homologous chromosomes. Mol Cell 15 (2004) 437-51.
Sonoda, E., Hochegger, H., Saberi, A., Taniguchi, Y. and Takeda, S.: Differential usage of non-homologous end-joining and homologous recombination in double strand break repair. DNA Repair (Amst) 5 (2006) 1021-9.
Soppa, J.: Basal and regulated transcription in archaea. Adv Appl Microbiol 50 (2001) 171-217.
Soppa, J.: From genomes to function: haloarchaea as model organisms. Microbiology 152 (2006) 585-90.
Steger, D.J., Haswell, E.S., Miller, A.L., Wente, S.R. and O'Shea, E.K.: Regulation of chromatin remodeling by inositol polyphosphates. Science 299 (2003) 114-6.
Storici, F., Henneke, G., Ferrari, E., Gordenin, D.A., Hubscher, U. and Resnick, M.A.: The flexible loop of human FEN1 endonuclease is required for flap cleavage during DNA replication and repair. Embo J 21 (2002) 5930-42.
Story, R.M., Weber, I.T. and Steitz, T.A.: The structure of the E. coli recA protein monomer and polymer. Nature 355 (1992) 318-25.
Strand, M., Earley, M.C., Crouse, G.F. and Petes, T.D.: Mutations in the MSH3 gene preferentially lead to deletions within tracts of simple repetitive DNA in Saccharomyces cerevisiae. Proc Natl Acad Sci U S A 92 (1995) 10418-21.
Strom, L. and Sjogren, C.: Chromosome segregation and double-strand break repair - a complex connection. Curr Opin Cell Biol 19 (2007) 344-9.
Su, S.S. and Modrich, P.: Escherichia coli mutS-encoded protein binds to mismatched DNA base pairs. Proc Natl Acad Sci U S A 83 (1986) 5057-61.
Sugawara, N. and Haber, J.E.: Characterization of double-strand break-induced recombination: homology requirements and single-stranded DNA formation. Mol Cell Biol 12 (1992) 563-75.
Sugawara, N., Ira, G. and Haber, J.E.: DNA length dependence of the single-strand annealing pathway and the role of Saccharomyces cerevisiae RAD59 in double-strand break repair. Mol Cell Biol 20 (2000) 5300-9.
Sugawara, N., Paques, F., Colaiacovo, M. and Haber, J.E.: Role of Saccharomyces cerevisiae Msh2 and Msh3 repair proteins in double-strand break-induced recombination. Proc Natl Acad Sci U S A 94 (1997) 9214-9.
Sugawara, N., Wang, X. and Haber, J.E.: In vivo roles of Rad52, Rad54, and Rad55 proteins in Rad51-mediated recombination. Mol Cell 12 (2003) 209-19.

Sugiyama, T., Kantake, N., Wu, Y. and Kowalczykowski, S.C.: Rad52-mediated DNA annealing after Rad51-mediated DNA strand exchange promotes second ssDNA capture. Embo J 25 (2006) 5539-48.
Sugiyama, T., New, J.H. and Kowalczykowski, S.C.: DNA annealing by RAD52 protein is stimulated by specific interaction with the complex of replication protein A and single-stranded DNA. Proc Natl Acad Sci U S A 95 (1998) 6049-54.
Sugiyama, T., Zaitseva, E.M. and Kowalczykowski, S.C.: A single-stranded DNA-binding protein is needed for efficient presynaptic complex formation by the Saccharomyces cerevisiae Rad51 protein. J Biol Chem 272 (1997) 7940-5.
Sung, P.: Catalysis of ATP-dependent homologous DNA pairing and strand exchange by yeast RAD51 protein. Science 265 (1994) 1241-3.
Sung, P.: Function of yeast Rad52 protein as a mediator between replication protein A and the Rad51 recombinase. J Biol Chem 272 (1997a) 28194-7.
Sung, P.: Yeast Rad55 and Rad57 proteins form a heterodimer that functions with replication protein A to promote DNA strand exchange by Rad51 recombinase. Genes Dev 11 (1997b) 1111-21.
Sung, P. and Klein, H.: Mechanism of homologous recombination: mediators and helicases take on regulatory functions. Nat Rev Mol Cell Biol 7 (2006) 739-50.
Symington, L.S.: Homologous recombination is required for the viability of rad27 mutants. Nucleic Acids Res 26 (1998) 5589-95.
Symington, L.S.: Role of RAD52 epistasis group genes in homologous recombination and double-strand break repair. Microbiol Mol Biol Rev 66 (2002) 630-70, table of contents.
Taddei, A., Gartenberg, M.R., Neumann, F.R., Hediger, F. and Gasser, S.M.: Multiple pathways tether telomeres and silent chromatin at the nuclear periphery: functional implications for sir-mediated repression. Novartis Found Symp 264 (2005) 140-56; discussion 156-65, 227-30.
Taddei, A., Hediger, F., Neumann, F.R., Bauer, C. and Gasser, S.M.: Separation of silencing from perinuclear anchoring functions in yeast Ku80, Sir4 and Esc1 proteins. Embo J 23 (2004) 1301-12.
Takao, M., Yonemasu, R., Yamamoto, K. and Yasui, A.: Characterization of a UV endonuclease gene from the fission yeast Schizosaccharomyces pombe and its bacterial homolog. Nucleic Acids Res 24 (1996) 1267-71.
Takata, M., Sasaki, M.S., Sonoda, E., Morrison, C., Hashimoto, M., Utsumi, H., Yamaguchi-Iwai, Y., Shinohara, A. and Takeda, S.: Homologous recombination and non-homologous end-joining pathways of DNA double-strand break repair have overlapping roles in the maintenance of chromosomal integrity in vertebrate cells. Embo J 17 (1998) 5497-508.
Tamaru, Y., Takani, Y., Yoshida, T. and Sakamoto, T.: Crucial role of extracellular polysaccharides in desiccation and freezing tolerance in the terrestrial cyanobacterium Nostoc commune. Appl Environ Microbiol 71 (2005) 7327-33.
Tang, J. and Chu, G.: Xeroderma pigmentosum complementation group E and UV-damaged DNA-binding protein. DNA Repair (Amst) 1 (2002) 601-16.
Tantin, D., Kansal, A. and Carey, M.: Recruitment of the putative transcription-repair coupling factor CSB/ERCC6 to RNA polymerase II elongation complexes. Mol Cell Biol 17 (1997) 6803-14.
Tarsounas, M., Davies, D. and West, S.C.: BRCA2-dependent and independent formation of RAD51 nuclear foci. Oncogene 22 (2003) 1115-23.
Tateishi, S., Sakuraba, Y., Masuyama, S., Inoue, H. and Yamaizumi, M.: Dysfunction of human Rad18 results in defective postreplication repair and hypersensitivity to multiple mutagens. Proc Natl Acad Sci U S A 97 (2000) 7927-32.
Tauchi, H., Kobayashi, J., Morishima, K., van Gent, D.C., Shiraishi, T., Verkaik, N.S., vanHeems, D., Ito, E., Nakamura, A., Sonoda, E., Takata, M., Takeda, S., Matsuura, S. and Komatsu, K.: Nbs1 is essential for DNA repair by homologous recombination in higher vertebrate cells. Nature 420 (2002) 93-8.
Thacker, J.: A surfeit of RAD51-like genes? Trends Genet 15 (1999) 166-8.
Thoma, F.: Light and dark in chromatin repair: repair of UV-induced DNA lesions by photolyase and nucleotide excision repair. Embo J 18 (1999) 6585-98.
Thompson, J.D., Higgins, D.G. and Gibson, T.J.: CLUSTAL W: improving the sensitivity of progressive multiple sequence alignment through sequence weighting, position-specific gap penalties and weight matrix choice. Nucleic Acids Res 22 (1994) 4673-80.
Thompson, L.H. and Schild, D.: Recombinational DNA repair and human disease. Mutat Res 509 (2002) 49-78.
Tian, M., Shinkura, R., Shinkura, N. and Alt, F.W.: Growth retardation, early death, and DNA repair defects in mice deficient for the nucleotide excision repair enzyme XPF. Mol Cell Biol 24 (2004) 1200-5.

Tishkoff, D.X., Boerger, A.L., Bertrand, P., Filosi, N., Gaida, G.M., Kane, M.F. and Kolodner, R.D.: Identification and characterization of Saccharomyces cerevisiae EXO1, a gene encoding an exonuclease that interacts with MSH2. Proc Natl Acad Sci U S A 94 (1997a) 7487-92.
Tishkoff, D.X., Filosi, N., Gaida, G.M. and Kolodner, R.D.: A novel mutation avoidance mechanism dependent on S. cerevisiae RAD27 is distinct from DNA mismatch repair. Cell 88 (1997b) 253-63.
Todo, T.: Functional diversity of the DNA photolyase/blue light receptor family. Mutat Res 434 (1999) 89-97.
Tomasz, M., Lipman, R., Chowdary, D., Pawlak, J., Verdine, G.L. and Nakanishi, K.: Isolation and structure of a covalent cross-link adduct between mitomycin C and DNA. Science 235 (1987) 1204-8.
Tremeau-Bravard, A., Riedl, T., Egly, J.M. and Dahmus, M.E.: Fate of RNA polymerase II stalled at a cisplatin lesion. J Biol Chem 279 (2004) 7751-9.
Truglio, J.J., Croteau, D.L., Van Houten, B. and Kisker, C.: Prokaryotic nucleotide excision repair: the UvrABC system. Chem Rev 106 (2006) 233-52.
Trujillo, K.M., Roh, D.H., Chen, L., Van Komen, S., Tomkinson, A. and Sung, P.: Yeast xrs2 binds DNA and helps target rad50 and mre11 to DNA ends. J Biol Chem 278 (2003) 48957-64.
Trujillo, K.M., Yuan, S.S., Lee, E.Y. and Sung, P.: Nuclease activities in a complex of human recombination and DNA repair factors Rad50, Mre11, and p95. J Biol Chem 273 (1998) 21447-50.
Tseng, H.M. and Tomkinson, A.E.: A physical and functional interaction between yeast Pol4 and Dnl4-Lif1 links DNA synthesis and ligation in nonhomologous end joining. J Biol Chem 277 (2002) 45630-7.
Tseng, H.M. and Tomkinson, A.E.: Processing and joining of DNA ends coordinated by interactions among Dnl4/Lif1, Pol4, and FEN-1. J Biol Chem 279 (2004) 47580-8.
Tsubouchi, H. and Roeder, G.S.: The budding yeast mei5 and sae3 proteins act together with dmc1 during meiotic recombination. Genetics 168 (2004) 1219-30.
Tsukamoto, Y., Mitsuoka, C., Terasawa, M., Ogawa, H. and Ogawa, T.: Xrs2p regulates Mre11p translocation to the nucleus and plays a role in telomere elongation and meiotic recombination. Mol Biol Cell 16 (2005) 597-608.
Tsukamoto, Y., Taggart, A.K. and Zakian, V.A.: The role of the Mre11-Rad50-Xrs2 complex in telomerase- mediated lengthening of Saccharomyces cerevisiae telomeres. Curr Biol 11 (2001) 1328-35.
Turchi, J.J. and Bambara, R.A.: Completion of mammalian lagging strand DNA replication using purified proteins. J Biol Chem 268 (1993) 15136-41.
Ueda, K. and Komano, T.: Sequence-specific DNA damage induced by reduced mitomycin C and 7-N-(p-hydroxyphenyl)mitomycin C. Nucleic Acids Res 12 (1984) 6673-83.
Ulmer, K.M., Gomez, R.F. and Sinskey, A.J.: Ionizing radiation damage to the folded chromosome of Escherichia coli K-12: repair of double-strand breaks in deoxyribonucleic acid. J Bacteriol 138 (1979) 486-91.
Ulrich, H.D.: The RAD6 pathway: control of DNA damage bypass and mutagenesis by ubiquitin and SUMO. Chembiochem 6 (2005) 1735-43.
Umar, A., Buermeyer, A.B., Simon, J.A., Thomas, D.C., Clark, A.B., Liskay, R.M. and Kunkel, T.A.: Requirement for PCNA in DNA mismatch repair at a step preceding DNA resynthesis. Cell 87 (1996) 65-73.
Usui, T., Ohta, T., Oshiumi, H., Tomizawa, J., Ogawa, H. and Ogawa, T.: Complex formation and functional versatility of Mre11 of budding yeast in recombination. Cell 95 (1998) 705-16.
Valencia, M., Bentele, M., Vaze, M.B., Herrmann, G., Kraus, E., Lee, S.E., Schar, P. and Haber, J.E.: NEJ1 controls non-homologous end joining in Saccharomyces cerevisiae. Nature 414 (2001) 666-9.
van de Vossenberg, J.L., Driessen, A.J. and Konings, W.N.: The essence of being extremophilic: the role of the unique archaeal membrane lipids. Extremophiles 2 (1998) 163-70.
van Gent, D.C. and van der Burg, M.: Non-homologous end-joining, a sticky affair. Oncogene 26 (2007) 7731-40.
van Gool, A.J., Citterio, E., Rademakers, S., van Os, R., Vermeulen, W., Constantinou, A., Egly, J.M., Bootsma, D. and Hoeijmakers, J.H.: The Cockayne syndrome B protein, involved in transcription-coupled DNA repair, resides in an RNA polymerase II-containing complex. Embo J 16 (1997) 5955-65.
van Gool, A.J., Hajibagheri, N.M., Stasiak, A. and West, S.C.: Assembly of the Escherichia coli RuvABC resolvasome directs the orientation of holliday junction resolution. Genes Dev 13 (1999) 1861-70.
van Gool, A.J., Verhage, R., Swagemakers, S.M., van de Putte, P., Brouwer, J., Troelstra, C., Bootsma, D. and Hoeijmakers, J.H.: RAD26, the functional S. cerevisiae homolog of the Cockayne syndrome B gene ERCC6. Embo J 13 (1994) 5361-9.

van Heemst, D., Brugmans, L., Verkaik, N.S. and van Gent, D.C.: End-joining of blunt DNA double-strand breaks in mammalian fibroblasts is precise and requires DNA-PK and XRCC4. DNA Repair (Amst) 3 (2004) 43-50.
van Hoffen, A., Natarajan, A.T., Mayne, L.V., van Zeeland, A.A., Mullenders, L.H. and Venema, J.: Deficient repair of the transcribed strand of active genes in Cockayne's syndrome cells. Nucleic Acids Res 21 (1993) 5890-5.
Van Houten, B.: Nucleotide excision repair in Escherichia coli. Microbiol Rev 54 (1990) 18-51.
Van Houten, B., Croteau, D.L., DellaVecchia, M.J., Wang, H. and Kisker, C.: 'Close-fitting sleeves': DNA damage recognition by the UvrABC nuclease system. Mutat Res 577 (2005) 92-117.
Van Houten, B., Gamper, H., Holbrook, S.R., Hearst, J.E. and Sancar, A.: Action mechanism of ABC excision nuclease on a DNA substrate containing a psoralen crosslink at a defined position. Proc Natl Acad Sci U S A 83 (1986) 8077-81.
Van Houten, B. and McCullough, A.: Nucleotide excision repair in E. coli. Ann N Y Acad Sci 726 (1994) 236-51.
van Noort, J., van Der Heijden, T., de Jager, M., Wyman, C., Kanaar, R. and Dekker, C.: The coiled-coil of the human Rad50 DNA repair protein contains specific segments of increased flexibility. Proc Natl Acad Sci U S A 100 (2003) 7581-6.
Vaze, M.B., Pellicioli, A., Lee, S.E., Ira, G., Liberi, G., Arbel-Eden, A., Foiani, M. and Haber, J.E.: Recovery from checkpoint-mediated arrest after repair of a double-strand break requires Srs2 helicase. Mol Cell 10 (2002) 373-85.
Veaute, X., Delmas, S., Selva, M., Jeusset, J., Le Cam, E., Matic, I., Fabre, F. and Petit, M.A.: UvrD helicase, unlike Rep helicase, dismantles RecA nucleoprotein filaments in Escherichia coli. Embo J 24 (2005) 180-9.
Veaute, X., Jeusset, J., Soustelle, C., Kowalczykowski, S.C., Le Cam, E. and Fabre, F.: The Srs2 helicase prevents recombination by disrupting Rad51 nucleoprotein filaments. Nature 423 (2003) 309-12.
Veenhuis, M., Salomons, F.A. and Van Der Klei, I.J.: Peroxisome biogenesis and degradation in yeast: a structure/function analysis. Microsc Res Tech 51 (2000) 584-600.
Venema, J., van Hoffen, A., Natarajan, A.T., van Zeeland, A.A. and Mullenders, L.H.: The residual repair capacity of xeroderma pigmentosum complementation group C fibroblasts is highly specific for transcriptionally active DNA. Nucleic Acids Res 18 (1990) 443-8.
Verhoeven, E.E., van Kesteren, M., Moolenaar, G.F., Visse, R. and Goosen, N.: Catalytic sites for 3' and 5' incision of Escherichia coli nucleotide excision repair are both located in UvrC. J Biol Chem 275 (2000) 5120-3.
Viswanathan, M., Burdett, V., Baitinger, C., Modrich, P. and Lovett, S.T.: Redundant exonuclease involvement in Escherichia coli methyl-directed mismatch repair. J Biol Chem 276 (2001) 31053-8.
Viswanathan, M. and Lovett, S.T.: Exonuclease X of Escherichia coli. A novel 3'-5' DNase and Dnaq superfamily member involved in DNA repair. J Biol Chem 274 (1999) 30094-100.
Voloshin, O.N., Wang, L. and Camerini-Otero, R.D.: Homologous DNA pairing promoted by a 20-amino acid peptide derived from RecA. Science 272 (1996) 868-72.
Vos, J.M.: Cis and trans mechanisms of DNA repair. Curr Opin Cell Biol 4 (1992) 385-95.
Wadsworth, R.I. and White, M.F.: Identification and properties of the crenarchaeal single-stranded DNA binding protein from Sulfolobus solfataricus. Nucleic Acids Res 29 (2001) 914-20.
Waga, S., Bauer, G. and Stillman, B.: Reconstitution of complete SV40 DNA replication with purified replication factors. J Biol Chem 269 (1994) 10923-34.
Wagner, R., Jr. and Meselson, M.: Repair tracts in mismatched DNA heteroduplexes. Proc Natl Acad Sci U S A 73 (1976) 4135-9.
Wakasugi, M., Reardon, J.T. and Sancar, A.: The non-catalytic function of XPG protein during dual incision in human nucleotide excision repair. J Biol Chem 272 (1997) 16030-4.
Walker, J.R., Corpina, R.A. and Goldberg, J.: Structure of the Ku heterodimer bound to DNA and its implications for double-strand break repair. Nature 412 (2001) 607-14.
Wang, B., Matsuoka, S., Carpenter, P.B. and Elledge, S.J.: 53BP1, a mediator of the DNA damage checkpoint. Science 298 (2002) 1435-8.
Wang, J.C.: Cellular roles of DNA topoisomerases: a molecular perspective. Nat Rev Mol Cell Biol 3 (2002) 430-40.
Wang, T.F., Kleckner, N. and Hunter, N.: Functional specificity of MutL homologs in yeast: evidence for three Mlh1-based heterocomplexes with distinct roles during meiosis in recombination and mismatch correction. Proc Natl Acad Sci U S A 96 (1999) 13914-9.
Wang, Z., Wu, X. and Friedberg, E.C.: DNA repair synthesis during base excision repair in vitro is catalyzed by DNA polymerase epsilon and is influenced by DNA polymerases alpha and delta in Saccharomyces cerevisiae. Mol Cell Biol 13 (1993) 1051-8.

Ward, J.F.: DNA damage produced by ionizing radiation in mammalian cells: identities, mechanisms of formation, and reparability. Prog Nucleic Acid Res Mol Biol 35 (1988) 95-125.
Warren, A.J., Maccubbin, A.E. and Hamilton, J.W.: Detection of mitomycin C-DNA adducts in vivo by 32P-postlabeling: time course for formation and removal of adducts and biochemical modulation. Cancer Res 58 (1998) 453-61.
Webb, B.L., Cox, M.M. and Inman, R.B.: Recombinational DNA repair: the RecF and RecR proteins limit the extension of RecA filaments beyond single-strand DNA gaps. Cell 91 (1997) 347-56.
Weber, C.A., Salazar, E.P., Stewart, S.A. and Thompson, L.H.: ERCC2: cDNA cloning and molecular characterization of a human nucleotide excision repair gene with high homology to yeast RAD3. Embo J 9 (1990) 1437-47.
Weller, G.R. and Doherty, A.J.: A family of DNA repair ligases in bacteria? FEBS Lett 505 (2001) 340-2.
Weller, G.R., Kysela, B., Roy, R., Tonkin, L.M., Scanlan, E., Della, M., Devine, S.K., Day, J.P., Wilkinson, A., d'Adda di Fagagna, F., Devine, K.M., Bowater, R.P., Jeggo, P.A., Jackson, S.P. and Doherty, A.J.: Identification of a DNA nonhomologous end-joining complex in bacteria. Science 297 (2002) 1686-9.
Welsh, K.M., Lu, A.L., Clark, S. and Modrich, P.: Isolation and characterization of the Escherichia coli mutH gene product. J Biol Chem 262 (1987) 15624-9.
Werner, A.: Natural antisense transcripts. RNA Biol 2 (2005) 53-62.
West, S.C.: Processing of recombination intermediates by the RuvABC proteins. Annu Rev Genet 31 (1997) 213-44.
West, S.C.: Molecular views of recombination proteins and their control. Nat Rev Mol Cell Biol 4 (2003) 435-45.
Whitby, M.C., Osman, F. and Dixon, J.: Cleavage of model replication forks by fission yeast Mus81-Eme1 and budding yeast Mus81-Mms4. J Biol Chem 278 (2003) 6928-35.
White, M.F.: Archaeal DNA repair: paradigms and puzzles. Biochem Soc Trans 31 (2003) 690-3.
White, O., Eisen, J.A., Heidelberg, J.F., et al.: Genome sequence of the radioresistant bacterium Deinococcus radiodurans R1. Science 286 (1999) 1571-7.
Wilcox, D.R. and Prakash, L.: Incision and postincision steps of pyrimidine dimer removal in excision-defective mutants of Saccharomyces cerevisiae. J Bacteriol 148 (1981) 618-23.
Wildenberg, J. and Meselson, M.: Mismatch repair in heteroduplex DNA. Proc Natl Acad Sci U S A 72 (1975) 2202-6.
Wiler, R., Leber, R., Moore, B.B., VanDyk, L.F., Perryman, L.E. and Meek, K.: Equine severe combined immunodeficiency: a defect in V(D)J recombination and DNA-dependent protein kinase activity. Proc Natl Acad Sci U S A 92 (1995) 11485-9.
Wilson, J.H., Berget, P.B. and Pipas, J.M.: Somatic cells efficiently join unrelated DNA segments end-to-end. Mol Cell Biol 2 (1982) 1258-69.
Wilson, T.E.: A genomics-based screen for yeast mutants with an altered recombination/end-joining repair ratio. Genetics 162 (2002) 677-88.
Wilson, T.E., Grawunder, U. and Lieber, M.R.: Yeast DNA ligase IV mediates non-homologous DNA end joining. Nature 388 (1997) 495-8.
Wilson, T.E. and Lieber, M.R.: Efficient processing of DNA ends during yeast nonhomologous end joining. Evidence for a DNA polymerase beta (Pol4)-dependent pathway. J Biol Chem 274 (1999) 23599-609.
Wilson, T.E., Topper, L.M. and Palmbos, P.L.: Non-homologous end-joining: bacteria join the chromosome breakdance. Trends Biochem Sci 28 (2003) 62-6.
Wiltzius, J.J., Hohl, M., Fleming, J.C. and Petrini, J.H.: The Rad50 hook domain is a critical determinant of Mre11 complex functions. Nat Struct Mol Biol 12 (2005) 403-7.
Winocour, E. and Keshet, I.: Indiscriminate recombination in simian virus 40-infected monkey cells. Proc Natl Acad Sci U S A 77 (1980) 4861-5.
Woese, C.R. and Fox, G.E.: Phylogenetic structure of the prokaryotic domain: the primary kingdoms. Proc Natl Acad Sci U S A 74 (1977) 5088-90.
Woese, C.R., Kandler, O. and Wheelis, M.L.: Towards a natural system of organisms: proposal for the domains Archaea, Bacteria, and Eucarya. Proc Natl Acad Sci U S A 87 (1990) 4576-9.
Wold, M.S.: Replication protein A: a heterotrimeric, single-stranded DNA-binding protein required for eukaryotic DNA metabolism. Annu Rev Biochem 66 (1997) 61-92.
Woods, W.G. and Dyall-Smith, M.L.: Construction and analysis of a recombination-deficient (radA) mutant of Haloferax volcanii. Mol Microbiol 23 (1997) 791-7.

Woudstra, E.C., Gilbert, C., Fellows, J., Jansen, L., Brouwer, J., Erdjument-Bromage, H., Tempst, P. and Svejstrup, J.Q.: A Rad26-Def1 complex coordinates repair and RNA pol II proteolysis in response to DNA damage. Nature 415 (2002) 929-33.
Wu, D., Topper, L.M. and Wilson, T.E.: Recruitment and Dissociation of Nonhomologous End Joining Proteins at a DNA Double-Strand Break in Saccharomyces cerevisiae. Genetics 178 (2008) 1237-49.
Wu, H.I., Brown, J.A., Dorie, M.J., Lazzeroni, L. and Brown, J.M.: Genome-wide identification of genes conferring resistance to the anticancer agents cisplatin, oxaliplatin, and mitomycin C. Cancer Res 64 (2004) 3940-8.
Wu, L., Bachrati, C.Z., Ou, J., Xu, C., Yin, J., Chang, M., Wang, W., Li, L., Brown, G.W. and Hickson, I.D.: BLAP75/RMI1 promotes the BLM-dependent dissolution of homologous recombination intermediates. Proc Natl Acad Sci U S A 103 (2006) 4068-73.
Wu, L. and Hickson, I.D.: The Bloom's syndrome helicase suppresses crossing over during homologous recombination. Nature 426 (2003) 870-4.
Wu, X., Braithwaite, E. and Wang, Z.: DNA ligation during excision repair in yeast cell-free extracts is specifically catalyzed by the CDC9 gene product. Biochemistry 38 (1999a) 2628-35.
Wu, X. and Wang, Z.: Relationships between yeast Rad27 and Apn1 in response to apurinic/apyrimidinic (AP) sites in DNA. Nucleic Acids Res 27 (1999) 956-62.
Wu, X., Wilson, T.E. and Lieber, M.R.: A role for FEN-1 in nonhomologous DNA end joining: the order of strand annealing and nucleolytic processing events. Proc Natl Acad Sci U S A 96 (1999b) 1303-8.
Wu, Y., Berends, M.J., Sijmons, R.H., Mensink, R.G., Verlind, E., Kooi, K.A., van der Sluis, T., Kempinga, C., van dDer Zee, A.G., Hollema, H., Buys, C.H., Kleibeuker, J.H. and Hofstra, R.M.: A role for MLH3 in hereditary nonpolyposis colorectal cancer. Nat Genet 29 (2001) 137-8.
Xia, B., Sheng, Q., Nakanishi, K., Ohashi, A., Wu, J., Christ, N., Liu, X., Jasin, M., Couch, F.J. and Livingston, D.M.: Control of BRCA2 cellular and clinical functions by a nuclear partner, PALB2. Mol Cell 22 (2006) 719-29.
Xia, F., Taghian, D.G., DeFrank, J.S., Zeng, Z.C., Willers, H., Iliakis, G. and Powell, S.N.: Deficiency of human BRCA2 leads to impaired homologous recombination but maintains normal nonhomologous end joining. Proc Natl Acad Sci U S A 98 (2001) 8644-9.
Xiao, W., Chow, B.L. and Milo, C.N.: Mms4, a putative transcriptional (co)activator, protects Saccharomyces cerevisiae cells from endogenous and environmental DNA damage. Mol Gen Genet 257 (1998a) 614-23.
Xiao, W., Chow, B.L. and Rathgeber, L.: The repair of DNA methylation damage in Saccharomyces cerevisiae. Curr Genet 30 (1996) 461-8.
Xiao, W., Lechler, T., Chow, B.L., Fontanie, T., Agustus, M., Carter, K.C. and Wei, Y.F.: Identification, chromosomal mapping and tissue-specific expression of hREV3 encoding a putative human DNA polymerase zeta. Carcinogenesis 19 (1998b) 945-9.
Xie, Y., Liu, Y., Argueso, J.L., Henricksen, L.A., Kao, H.I., Bambara, R.A. and Alani, E.: Identification of rad27 mutations that confer differential defects in mutation avoidance, repeat tract instability, and flap cleavage. Mol Cell Biol 21 (2001) 4889-99.
Xin, H., Lin, W., Sumanasekera, W., Zhang, Y., Wu, X. and Wang, Z.: The human RAD18 gene product interacts with HHR6A and HHR6B. Nucleic Acids Res 28 (2000) 2847-54.
Xu, Y., Grindley, N.D. and Joyce, C.M.: Coordination between the polymerase and 5'-nuclease components of DNA polymerase I of Escherichia coli. J Biol Chem 275 (2000) 20949-55.
Xue, Y., Li, Y., Guo, R., Ling, C. and Wang, W.: FANCM of the Fanconi anemia core complex is required for both monoubiquitination and DNA repair. Hum Mol Genet (2008).
Yajima, H., Takao, M., Yasuhira, S., Zhao, J.H., Ishii, C., Inoue, H. and Yasui, A.: A eukaryotic gene encoding an endonuclease that specifically repairs DNA damaged by ultraviolet light. Embo J 14 (1995) 2393-9.
Yamaguchi-Iwai, Y., Sonoda, E., Buerstedde, J.M., Bezzubova, O., Morrison, C., Takata, M., Shinohara, A. and Takeda, S.: Homologous recombination, but not DNA repair, is reduced in vertebrate cells deficient in RAD52. Mol Cell Biol 18 (1998) 6430-5.
Yang, H., Jeffrey, P.D., Miller, J., Kinnucan, E., Sun, Y., Thoma, N.H., Zheng, N., Chen, P.L., Lee, W.H. and Pavletich, N.P.: BRCA2 function in DNA binding and recombination from a BRCA2-DSS1-ssDNA structure. Science 297 (2002) 1837-48.
Yang, H., Li, Q., Fan, J., Holloman, W.K. and Pavletich, N.P.: The BRCA2 homologue Brh2 nucleates RAD51 filament formation at a dsDNA-ssDNA junction. Nature 433 (2005) 653-7.
Yannone, S.M., Roy, S., Chan, D.W., Murphy, M.B., Huang, S., Campisi, J. and Chen, D.J.: Werner syndrome protein is regulated and phosphorylated by DNA-dependent protein kinase. J Biol Chem 276 (2001) 38242-8.

Yoakum, G.H. and Cole, R.S.: Role of ATP in removal of psoralen cross-links from DNA of Escherichia coli permeabilized by treatment with toluene. J Biol Chem 252 (1977) 7023-30.
Yonemasu, R., McCready, S.J., Murray, J.M., Osman, F., Takao, M., Yamamoto, K., Lehmann, A.R. and Yasui, A.: Characterization of the alternative excision repair pathway of UV-damaged DNA in Schizosaccharomyces pombe. Nucleic Acids Res 25 (1997) 1553-8.
Yonetani, Y., Hochegger, H., Sonoda, E., Shinya, S., Yoshikawa, H., Takeda, S. and Yamazoe, M.: Differential and collaborative actions of Rad51 paralog proteins in cellular response to DNA damage. Nucleic Acids Res 33 (2005) 4544-52.
Yoon, J.H., Swiderski, P.M., Kaplan, B.E., Takao, M., Yasui, A., Shen, B. and Pfeifer, G.P.: Processing of UV damage in vitro by FEN-1 proteins as part of an alternative DNA excision repair pathway. Biochemistry 38 (1999) 4809-17.
Yoshimura, M., Kohzaki, M., Nakamura, J., Asagoshi, K., Sonoda, E., Hou, E., Prasad, R., Wilson, S.H., Tano, K., Yasui, A., Lan, L., Seki, M., Wood, R.D., Arakawa, H., Buerstedde, J.M., Hochegger, H., Okada, T., Hiraoka, M. and Takeda, S.: Vertebrate POLQ and POLbeta cooperate in base excision repair of oxidative DNA damage. Mol Cell 24 (2006) 115-25.
Yu, J., Marshall, K., Yamaguchi, M., Haber, J.E. and Weil, C.F.: Microhomology-dependent end joining and repair of transposon-induced DNA hairpins by host factors in Saccharomyces cerevisiae. Mol Cell Biol 24 (2004) 1351-64.
Zaitseva, E.M., Zaitsev, E.N. and Kowalczykowski, S.C.: The DNA binding properties of Saccharomyces cerevisiae Rad51 protein. J Biol Chem 274 (1999) 2907-15.
Zdraveski, Z.Z., Mello, J.A., Marinus, M.G. and Essigmann, J.M.: Multiple pathways of recombination define cellular responses to cisplatin. Chem Biol 7 (2000) 39-50.
Zerbib, D., Mezard, C., George, H. and West, S.C.: Coordinated actions of RuvABC in Holliday junction processing. J Mol Biol 281 (1998) 621-30.
Zhang, N., Liu, X., Li, L. and Legerski, R.: Double-strand breaks induce homologous recombinational repair of interstrand cross-links via cooperation of MSH2, ERCC1-XPF, REV3, and the Fanconi anemia pathway. DNA Repair (Amst) 6 (2007a) 1670-8.
Zhang, N., Lu, X., Zhang, X., Peterson, C.A. and Legerski, R.J.: hMutSbeta is required for the recognition and uncoupling of psoralen interstrand cross-links in vitro. Mol Cell Biol 22 (2002) 2388-97.
Zhang, N., Zhang, X., Peterson, C., Li, L. and Legerski, R.: Differential processing of UV mimetic and interstrand crosslink damage by XPF cell extracts. Nucleic Acids Res 28 (2000) 4800-4.
Zhang, S., Wei, T., Hou, G., Zhang, C., Liang, P., Ni, J., Sheng, D. and Shen, Y.: Archaeal DNA helicase HerA interacts with Mre11 homologue and unwinds blunt-ended double-stranded DNA and recombination intermediates. DNA Repair (Amst) 7 (2008) 380-91.
Zhang, Y., Hefferin, M.L., Chen, L., Shim, E.Y., Tseng, H.M., Kwon, Y., Sung, P., Lee, S.E. and Tomkinson, A.E.: Role of Dnl4-Lif1 in nonhomologous end-joining repair complex assembly and suppression of homologous recombination. Nat Struct Mol Biol 14 (2007b) 639-46.
Zhang, Y., Yuan, F., Presnell, S.R., Tian, K., Gao, Y., Tomkinson, A.E., Gu, L. and Li, G.M.: Reconstitution of 5'-directed human mismatch repair in a purified system. Cell 122 (2005) 693-705.
Zheng, L., Dai, H., Zhou, M., Li, M., Singh, P., Qiu, J., Tsark, W., Huang, Q., Kernstine, K., Zhang, X., Lin, D. and Shen, B.: Fen1 mutations result in autoimmunity, chronic inflammation and cancers. Nat Med 13 (2007) 812-9.
Zheng, L., Zhou, M., Chai, Q., Parrish, J., Xue, D., Patrick, S.M., Turchi, J.J., Yannone, S.M., Chen, D. and Shen, B.: Novel function of the flap endonuclease 1 complex in processing stalled DNA replication forks. EMBO Rep 6 (2005) 83-9.
Zhu, H. and Shuman, S.: A primer-dependent polymerase function of pseudomonas aeruginosa ATP-dependent DNA ligase (LigD). J Biol Chem 280 (2005) 418-27.
Zhu, H., Wang, L.K. and Shuman, S.: Essential constituents of the 3'-phosphoesterase domain of bacterial DNA ligase D, a nonhomologous end-joining enzyme. J Biol Chem 280 (2005) 33707-15.
Zhu, X.D., Niedernhofer, L., Kuster, B., Mann, M., Hoeijmakers, J.H. and de Lange, T.: ERCC1/XPF removes the 3' overhang from uncapped telomeres and represses formation of telomeric DNA-containing double minute chromosomes. Mol Cell 12 (2003) 1489-98.
Zieg, J., Maples, V.F. and Kushner, S.R.: Recombinant levels of Escherichia coli K-12 mutants deficient in various replication, recombination, or repair genes. J Bacteriol 134 (1978) 958-66.
Zou, Y. and Van Houten, B.: Strand opening by the UvrA(2)B complex allows dynamic recognition of DNA damage. Embo J 18 (1999) 4889-901.